AFIT/GNE/ENP/93M-6

CONSTRUCTION AND TESTING OF A NEUTRON AND GAMMA SPECTROMETRY SYSTEM USING PULSE SHAPE DISCRIMINATION WITH AN ORGANIC SCINTILLATOR

THESIS

Robert S. Pope, Second Lieutenant, USAF

AFIT/GNE/ENP/93M-6

Approved for public release; distribution unlimited

AFIT/GNE/ENP/93M-6

CONSTRUCTION AND TESTING OF A NEUTRON AND GAMMA SPECTROMETRY SYSTEM USING PULSE SHAPE DISCRIMINATION WITH AN ORGANIC SCINTILLATOR

THESIS

Presented to the Faculty of the School of Engineering

of the Air Force Institute of Technology

Air University

In Partial Fulfillment of the

Requirements for the Degree of

Master of Science

Robert S. Pope, B.S.

Second Lieutenant, USAF

March 1993

Acknowledgments

The contributions of many people have made this thesis possible. I would first like to thank my advisor, LtCol (Dr.) Richard Hartley, and committee members, Dr. Nolan Hertel and Dr. George John. LtCol Hartley provided a great deal of time and guidance throughout the course of this project, which began with my Research Apprenticeship work more than eight months ago. Dr. Hertel offered guidance with the PSD setup of the spectrometry system and provided many helpful suggestions on the modifications of FORIST and ZSHIFT. Dr. John, who taught the Nuclear Physics and Nucleonics Instrumentation courses at the Air Force Institute of Technology, provided me with the knowledge base necessary to begin this research project.

I would also like to thank Doug Burkholtz and Jack Phillips of the AFIT small computers section for all of their help with the VAX VMS mainframe. Additionally, I would like to thank my classmate, Capt Sean Miller, who worked with me during the Research Apprenticeship project and provided his encouragement and a listening ear throughout the thesis work. I would like to especially thank Bob Hendricks, the laboratory supervisor at the Air Force Nuclear Engineering Center, who provided invaluable support and assistance in the laboratory.

Finally, there are two literature sources which deserve special mention. I highly recommend the book Radiation Detection and Measurement by Glenn F. Knoll to anyone who plans to do an experimental thesis in the field of Nuclear Physics. While the literature search performed for this thesis was extensive, nearly all inquires began with Knoll. Additionally, the best periodical source of experimentally-oriented literature that was found during the course of this project was the journal Nuclear Instruments and Methods.

Table of Contents

List of Figures

Figure Page

List of Tables

Abstract

The goal of this thesis was to construct and test a neutron detection system to measure the energy spectrum of neutrons in the presence of gammas for neutrons in an energy range from 1 to 14 MeV. To accomplish this, a neutron spectrometer based on the process of pulse shape discrimination (PSD) was constructed, in which a xylene-based scintillator, NE-213, was used as the detector material. The primary neutron/gamma sources used were 78-mCi and 4.7-Ci ^{239}PuBe sources, while 4.7-μCi and 97.6-μCi ^{22}Na gamma sources were used for energy calibration and additional testing of the detector. Proton recoil spectra and Compton electron recoil spectra were unfolded with the neutron and gamma unfolding code FORIST to generate the incident neutron and gamma spectra, respectively. FORIST, which was written for a CDC computer, was modified to run on a VAX 6420.

The experimental spectra were compared to those in the scientific literature. It was found that the locations of the peaks in the ^{239}PuBe spectrum agreed with the literature to within 8.3%, the ^{239}PuBe gamma spectrum agreed to within 0.7%, while the ^{22}Na gamma spectrum agreed exactly. Uncertainties in the detection system and unfolding procedure are on the order of 5 to 10%, so these results are reasonable.

This thesis was written as a summary of the relevant literature and as a user's guide to the neutron spectrometer developed in this project. To this end, this paper first develops the theory of PSD techniques, computer unfolding, and energy calibration; then describes the hardware, software, and experimental procedures; and in the end presents the experimental results and compares them to the literature results as validation of the system.

CONSTRUCTION AND TESTING OF A NEUTRON AND GAMMA SPECTROMETRY SYSTEM USING PULSE SHAPE DISCRIMINATION WITH AN ORGANIC SCINTILLATOR

I. Introduction

Background

Neutron detection and spectrometry are very important to nuclear research, but because the neutron is an uncharged particle, detecting neutrons and measuring their energy is not a trivial task. Because the energy range of neutrons can cover 14 decades (10^{-6} to 10^{8} eV), many different neutron detection and spectrometry methods have been developed, most of which only cover a portion of the full neutron energy range.

Nearly all present neutron spectrometry methods are based on one of four general principles:

1. measurement of the energies of charged particles produced by neutron interactions, *e.g.*, nuclear emulsions, damage track detectors, recoil proton telescopes, proportional counters, sandwich spectrometers, lithium glass scintillators, and organic scintillators;
2. measurement of the flight time of neutrons over a given distance, *e.g.*, TOF spectrometers;
3. measurement of attenuation and moderation of neutrons in various

thicknesses of hydrogenous material, *e.g.*, Bonner spheres; and

4. measurement of activation or fission reactions in a set of detectors having different energy responses, *e.g.*, threshold detectors.

The approximate energy ranges covered by these different spectrometer types are shown in Figure 1 [8:95-96].

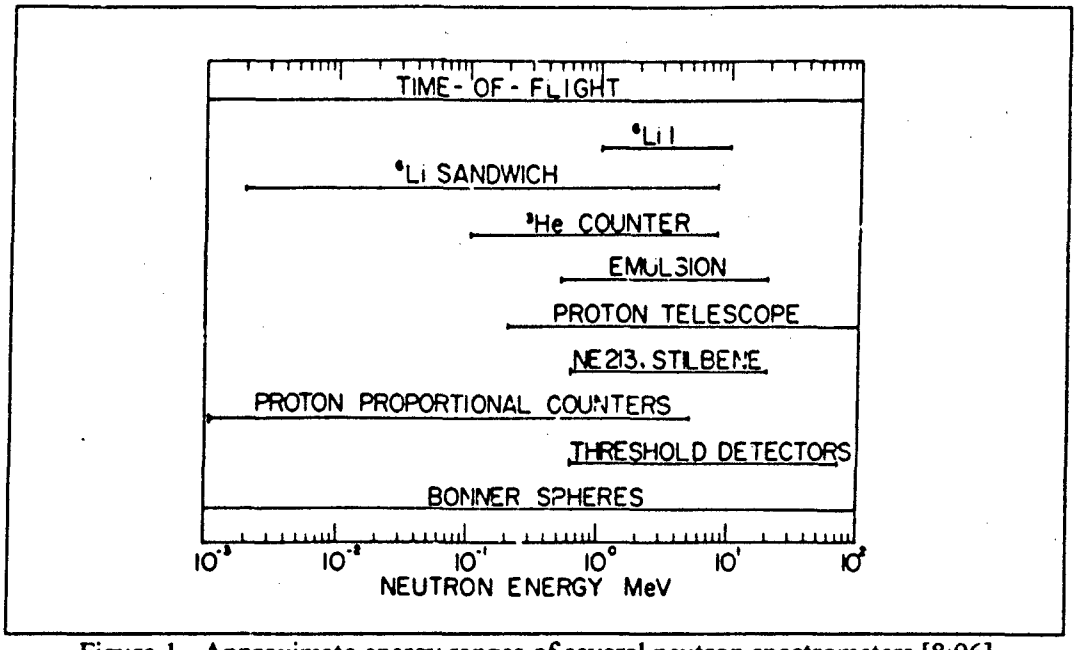

Figure 1. Approximate energy ranges of several neutron spectrometers [8:96]

The detector constructed for this research project operates on the first of the four principles: the measurement of the energies of charged particles produced by neutron and gamma interactions. The detection material is a xylene-based liquid organic scintillator, often called NE-213 in the literature. This organic scintillator detects both incoming neutrons and gammas. Neutron-gamma discrimination is accomplished by the method of pulse shape discrimination (PSD), which uses a timing circuit that operates on the

difference in the decay component of the output signal (the shape of the pulse) from neutrons and gammas. The timing information is then used to gate the energy information, so that the user can select whether the neutron or gamma energy is recorded. PSD is useful over the entire 1-to-14-MeV range of interest. Pulse shape discrimination is explained more fully in the "Theory" section.

The organic scintillator does not record the neutron and gamma energy spectra directly. Rather, incoming neutrons interact with the hydrogen nuclei in the scintillator to produce recoil protons, while the incoming gammas interact with atomic electrons to produce Compton recoil electrons. Re-creating the incoming neutron and gamma spectra requires unfolding the recoil spectra recorded by the detector. Unfolding is a mathematical operation in which the recoil information is placed into a vector and multiplied with an appropriate response matrix to yield a vector which contains the calculated incident neutron or gamma spectrum. Spectrum unfolding is discussed in detail in the "Theory" section. The FORIST (FERDOR with **O**ptimized **R**esolution using an **I**terative **S**moothing **T**echnique) [26:-] unfolding code, modified to run on the VAX 6420, is used to unfold the experimental recoil spectra recorded with the detector.

Scope

The type of detection system used in this project is not new. Verbinski *et al.* [29:-;6:-] did the definitive work with an NE-213 neutron spectrometer in 1968. In that work, Verbinski's team used monoenergetic neutron sources to construct the neutron response matrix for their detector. That response matrix forms the basis for the neutron response matrix used with FORIST. They also established protocols in equipment and procedure that many others subsequently followed so that Verbinski's response matrix would apply to their work. To be able to use the FORIST unfolding code, the detector

built for the Air Force Nuclear Engineering Center during this thesis project also follows Verbinski's protocols. A comparison of the two detectors is made in the "Description of Apparatus" section.

The focus of this thesis research is, then, not to develop a new kind of neutron spectrometer, but to construct and test an accepted spectrometer design and then to provide a complete user's manual for the system. To that end, this thesis completely describes the apparatus and computer codes used and then gives a complete procedure to follow in order to construct and use this system. A search of the literature indicated that, while this kind of spectrometer has been in use for more than twenty years, there was no complete guide for the system geared to the new user. The intent of this thesis is to provide such a manual.

Sequence of Presentation

The rest of this thesis is divided into five major sections. The first section discusses the general theory behind pulse shape discrimination and spectrum unfolding. The second section describes the apparatus and computer software used during this project. The third section presents a step-by-step guide to assembling and using the spectrometer constructed for this research, from initial setup through data collection and processing. The fourth section presents the experimental results from the project. These results include verification of the correct operation of the modified FORIST code and validation of the spectrometry sytstem. This validation was performed by comparing exprimental spectra from ^{239}PuBe and ^{22}Na to spectra from the literature. The fifth and final section summarizes the project and presents recommendations for future work with this detection system.

II. Theory

Pulse Shape Discrimination (PSD)

Organic scintillation detectors have been in use for more than forty years [4:477]. These detectors respond both to incident gammas and neutrons. Distinguishing between neutrons and gammas is the function of pulse shape discrimination (PSD). In order to explain PSD, one must first understand the response of organic scintillators, such as NE-213, to incident radiation. To that end, this section first describes how the uncharged neutrons and gammas are detected within the scintillator. It then presents a discussion of the scintillation mechanism in organic scintillation detectors, which is used to explain the theory of PSD.

Scintillation is the process in which incident ionizing radiation upon a material produces the emission of light. There are two types of scintillators: organic and inorganic. In general, inorganic scintillators are favored for gamma-ray spectroscopy because of their high-Z constituents. Though comparatively less efficient, organic scintillators are selected for fast neutron detection because of advantages in energy resolution and pulse shape discrimination. Organic scintillators are composed of compounds of hydrogen and carbon and are available in crystalline, plastic, or liquid form. The scintillator used in this project is a binary liquid scintillator in which a small quantity of fluor is dissolved in a large quantity of organic solvent (xylene). The organic solvent participates in the reactions with incident radiation and then transfers the resulting energy to the fluor, which then de-excites by emitting light [4:479].

Neutrons entering the scintillator interact by elastically scattering with hydrogen and carbon nuclei. This elastic scattering reaction transfers some or all of the incident

neutron's energy to the target nucleus, which then recoils. At neutron energies above about 8 MeV, $^{12}C(\alpha,n)$ reactions are also possible, which create multiple recoiling particles. The recoil nucleus or $^{12}C(\alpha,n)$ reaction products then collide with the fluor, transferring their excitation energy. The fluor subsequently de-excites by emitting light [4:485-486,17:530-540].

Gamma photons entering the scintillator interact, not with the scintillator nuclei, but with the atomic electrons. Due to the low-Z scintillator constituents, they interact almost entirely by Compton scatter. The Compton interaction creates a Compton recoil electron [17:54] that then transfers its energy to the fluor, which subsequently de-excites through fluorescence.

Organic scintillators have a molecular structure known as π-electron structure. This structure consists of planar molecules built up mainly from benzene rings. A key feature of the molecular structure is the presence of extended groupings of conjugated double bonds, based largely on linkages between unsaturated carbon atoms. This non-saturation implies that only two or three of the four valence electrons of carbon are strongly localized within the molecular structure. The remaining valance electrons are delocalized within the molecule and are not associated with any one particular atom. They occupy π-molecular orbitals which extend over the conjugated region. The π-electron states are of particular interest because transitions between these states lead to the luminescence observed in the scintillation process [4:479]. The π-electronic energy levels of such a molecule are illustrated in Figure 2.

Scintillation occurs in a molecule with π-electron structure in the following manner. In a molecule at thermal equilibrium, the electrons are in the lowest vibration state of the ground electronic state, S_{00}. Electrons are excited into a higher energy level when energy is absorbed by the molecule. They can be excited into one of the singlet states (spin 0) or into one of the triplet states (spin 1). The first subscript denotes a s

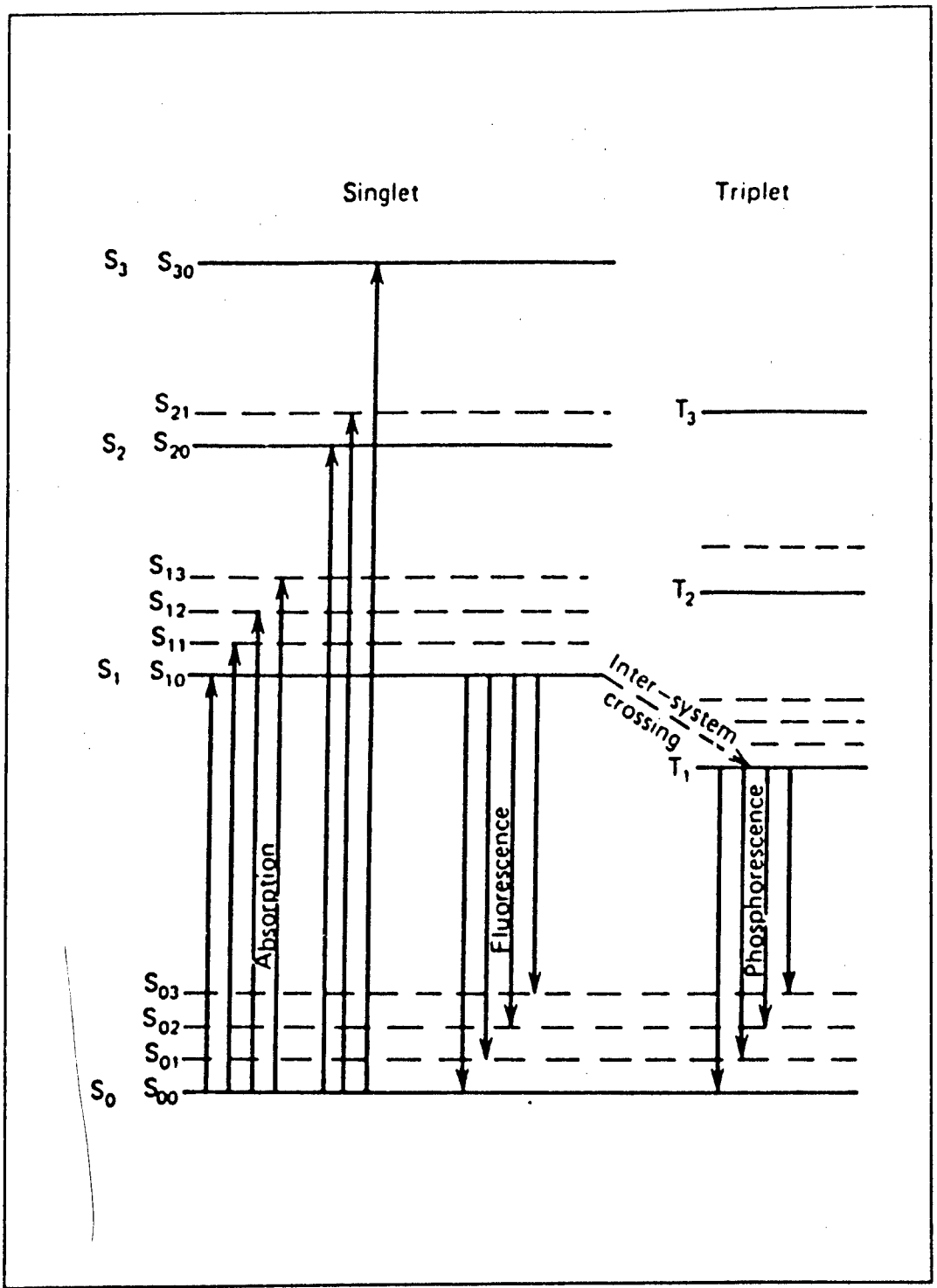

Figure 2. Energy levels of an organic molecule with π-electron structure [17:217]

quantum number and the second a vibrational quantum number. The energy of the S_1 state is approximately 3-4 eV above S_0 and the energy difference between higher states is generally smaller. The energy differences between vibrational states, S_{nn}, are on the order of 0.15 eV apart. Because this is relatively large compared to thermal temperatures (0.025 eV), nearly all molecules are in the S_{00} state at room temperature. [17:216-217]

When an energetic particle such as a recoil proton or Compton recoil electron collides with the fluor molecule, some of the kinetic energy is absorbed by the molecule. This is represented by the up arrows. Electrons which are excited into the higher singlet states quickly de-excite to the S_{10} level through radiationless internal conversions. Any electrons in S_1 above S_{10} are not in thermal equilibrium with their neighbors and also quickly lose the excess vibrational energy. The net effect of a single energetic particle passing through the material is to produce a large number of molecules with excited electrons all in the same energy state. The number of electrons in the higher energy state and the consequent fluorescence are proportional to the kinetic energy of the recoiling particle that passed through scintillating material [17:217]. The scintillating material is said to fluoresce when the electrons in the S_{10} state de-excite to the ground state or one of the ground vibrational states. These prompt decays are indicated by the down arrows in Figure 2. The time it takes for a material to fluoresce once it has been excited is on the order of a few nanoseconds [17:226].

Electrons which are excited through inter-system crossings to a triplet state must de-excite in a different manner. When electrons in the T_1 state de-excite to the ground state or one of the ground vibrational states, the light emitted in this delayed decay is called phosphorescence. However, a decay from the T_1 triplet state directly to the S_{00} ground state is not a quantum-mechanically-preferred mode of decay and hence contributes little to the light output [4:480]. The preferred mode of de-excitation for a molecule in a triplet state is to participate in a bimolecular interaction with another

molecule in the triplet state. Such an interaction places one molecule in the first singlet state (S_1) and the other in the ground state (S_0). The molecule in the S_1 state can then de-excite in the normal way, leading to delayed fluorescence, which takes on the order of a few hundred nanoseconds [17:227].

The majority of the light yield of the scintillator occurs in the prompt fluorescence component, but the delayed fluorescence component is significant because the fraction of light that appears in the delayed component depends on the nature of the exciting particle. The delayed fluorescence, then, provides the basis for pulse shape discrimination [17:226]. In general, as the mass of the incident particle increases, the number of fluor molecules de-exciting through delayed fluorescence also increases and hence increases the delayed component of the resulting pulse. This is shown in Figure 3. Pulse shape discrimination, therefore, enables the identity of an interacting particle to be determined, regardless of its energy.

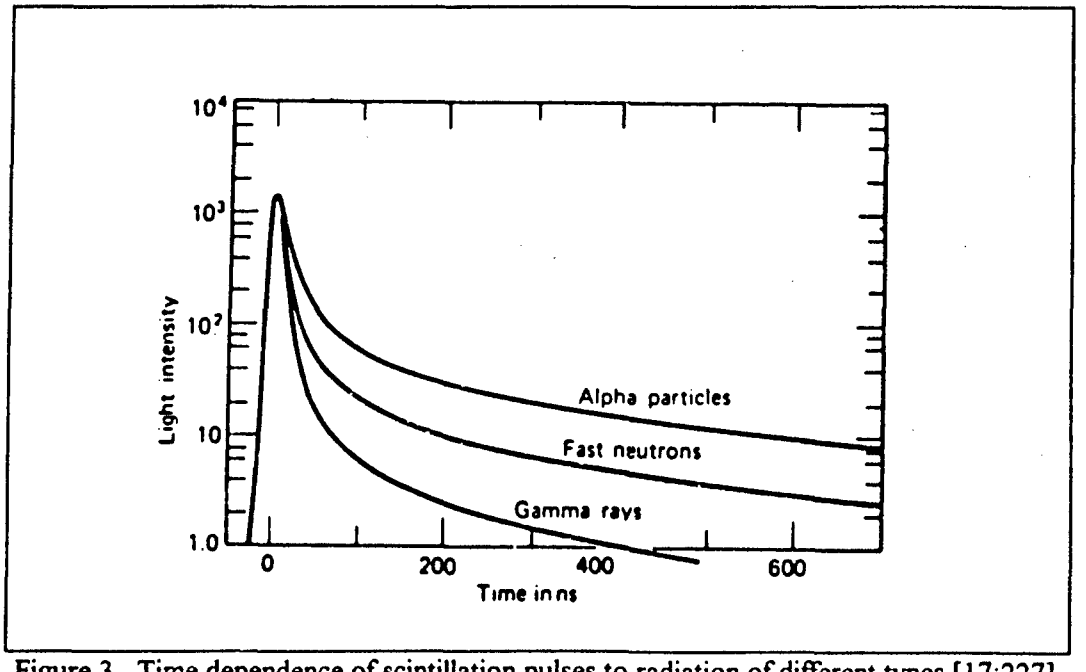

Figure 3. Time dependence of scintillation pulses to radiation of different types [17:227]

Spectrum Unfolding

The organic scintillation detector converts incident neutrons and gammas to recoil protons and Compton recoil electrons, respectively. It is the energy spectra of these recoil protons and electrons which are then recorded in the laboratory by the detection system. The process which attempts to reproduce the incident neutron and gamma spectra from the measured recoil spectra is called unfolding. To understand the unfolding process, one must first understand the relationship between the incident neutron and gamma energy and the resulting recoil spectra. After that, one can proceed to discuss the mathematical process by which the incident spectrum is extracted from the recoil spectrum.

As stated previously, neutrons entering the scintillator interact by scattering with hydrogen and carbon nuclei. The amount of energy a neutron can lose in a single collision, and thus impart to the recoil nucleus, is dependent upon the mass of the target nucleus. The recoil energy E_R,is given by [17:531]

$$E_R = \frac{4A}{(1+A)^2}(\cos^2\theta)E_n \qquad (1)$$

where θ is the scattering angle in the laboratory reference frame, A is the mass number of the target nucleus, and E_n is the energy of the incident neutron. If the target nucleus is initially at rest at the origin of the lab frame coordinates and the incident neutron is traveling from left to right along the negative x-axis, the scattering angle θ is measured between the positive x-axis and the outbound direction of the recoil nucleus. To maximize the energy deposited in the course of the fewest interactions, a nucleus with a mass close to that of the neutron is the preferred target. Since the mass of a hydrogen nucleus and a neutron differ by less than 0.2%, hydrogen makes an ideal target. It is possible for the

neutron to give up all of its energy to the recoil nucleus in a single collision with hydrogen when θ=0°, denoted by $E_{R\,max}$. This happens when the incident neutron stops and the recoil nucleus continues along the original path of the incident neutron. In the case where θ=0° recoil, Eq (1) simplifies to [17:531]:

$$E_{R\max} = \frac{4A}{(1+A)^2} E_n \tag{2}$$

The minimum recoil energy, on the other hand, occurs when the θ =90° and no energy is imparted to the target. With hydrogen as a target and assuming isotropic scattering in the center-of-mass reference frame, the energy spectrum of the recoil proton is ideally rectangular, as shown in Figure 4. In this figure, the probability of a neutron creating a recoil proton with a given energy, $P(E_p)$, is plotted vs. recoil proton energy, E_p. The maximum energy that a recoil proton can receive is equal to the energy of the incident neutron, E_n. This graph is a probability distribution function, so the area under the curve is 1.

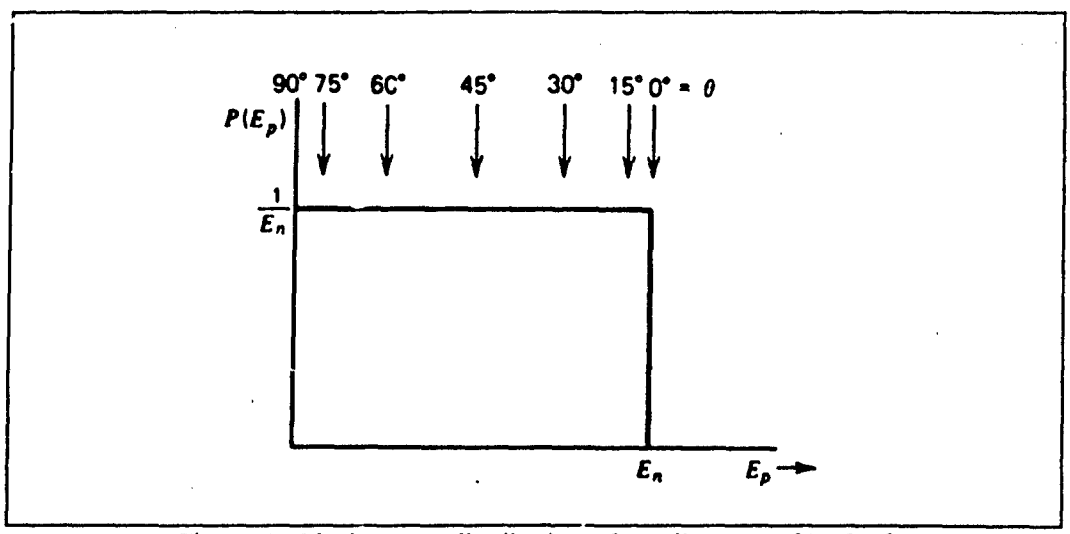

Figure 4. Ideal energy distribution of recoil protons [17:534]

The probability of a neutron creating a recoil proton of a given energy, $P(E_p)$, can also be expressed as the change in the number of recoil protons with changing recoil proton energy, dN/dE.

In a real organic scintillator, however, the ideal rectangular response of Figure 4 is complicated by the following factors:

1. scattering with carbon,
2. finite detector resolution,
3. nonlinear light output with energy,
4. edge effect,
5. multiple scattering with hydrogen, and
6. competing reactions at high neutron energies [17:538-542].

Carbon, the other constituent of organic scintillators (xylene is 45 atom% carbon), complicates things somewhat. Carbon has a mass number of 12, so by Eq. (2) a neutron can deposit up to 28% of its kinetic energy in a single elastic scatter with carbon. Thus, the maximum energy of a subsequent recoil proton from hydrogen after a collision with carbon varies between 72 and 100% of the original neutron energy. The energy deposited during the carbon scatter is not converted to light in the scintillator, so the incident neutron appears to have a lower kinetic energy than it actually had upon entering the scintillator. The effect of carbon scattering is shown in Figure 5. [17:540]

The finite resolution of the detector, due to sources of dispersion such as nonuniform light collection and photoelectron statistics, tends to wash out some of the distinct structure expected in the response function. This distorts the sharp edge of the distribution function at its maximum energy, E_p, as shown in Figure 6 [17:541].

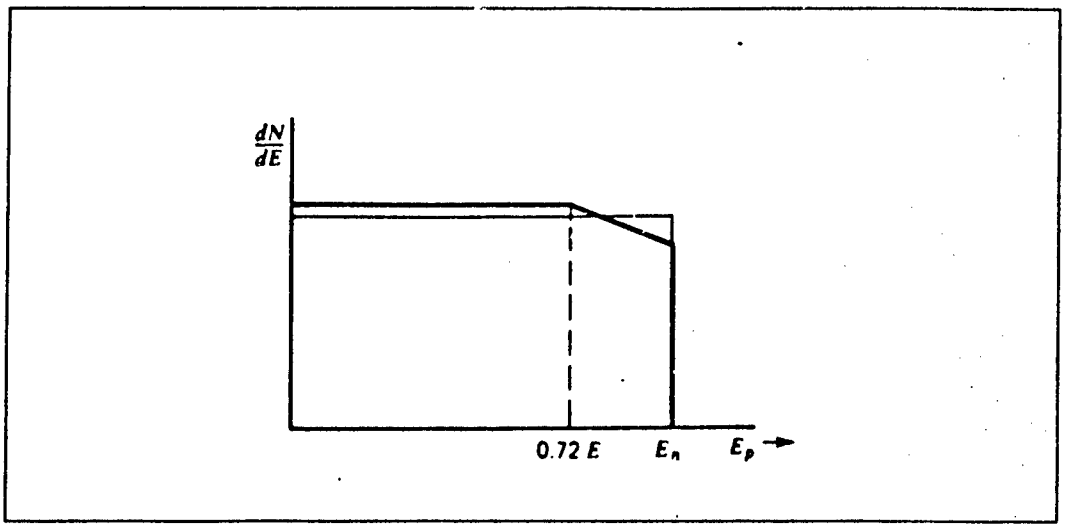

Figure 5. Distortion to the recoil proton response function due to scattering with carbon. The thin line represents the ideal rectangular distribution, while the thick line shows the effect of carbon scattering [17:540]

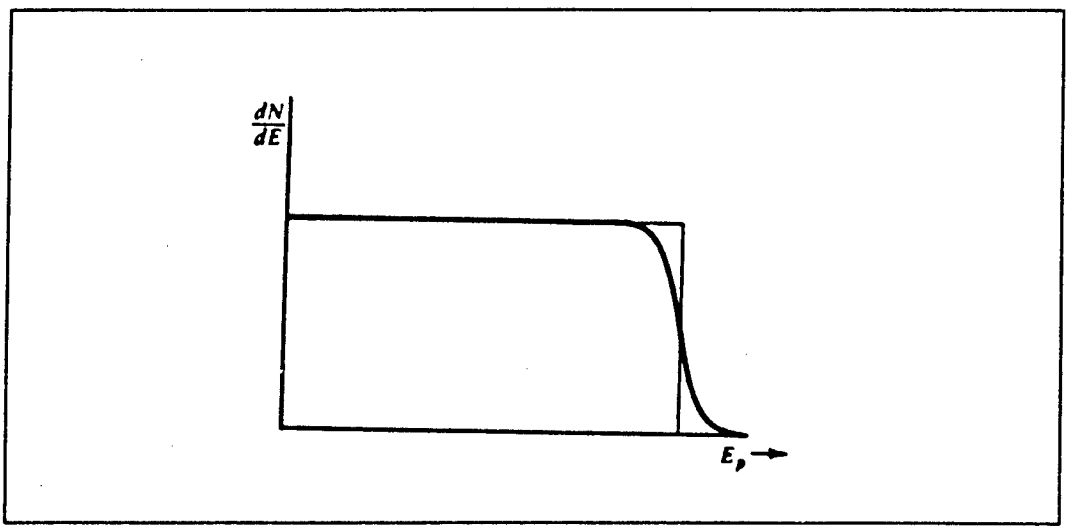

Figure 6. Distortion to the recoil proton response function due to finite detector resolution. The thin line represents the ideal rectangular distribution, while the thick line shows the effect of finite resolution [17:540]

The light output, H, from most organic scintillators is not linear with neutron energy, but is proportional to $kE^{3/2}$, where E is the energy of the incident neutron and k is

a constant of proportionality. This relation between H and E is shown in Figure 7(a). The change in light output with changing energy, then, is the derivative of this relation [17:538]:

$$\frac{dH}{dE} = \frac{3}{2} kE^{1/2} \tag{3}$$

which is shown in Figure 7(b). The distortion in the ideal recoil proton spectrum due to nonlinear response is expressed as the change in number of recoil protons with pulse height, which is [17:538]:

$$\frac{dN}{dH} = \frac{dN/dE}{dH/dE} = \frac{\text{constant}}{\frac{3}{2} kE^{1/2}} \tag{4}$$

Graphically, Eq. (4) represents the division of Figure 4 by Figure 7(b), which results in Figure 7(c).

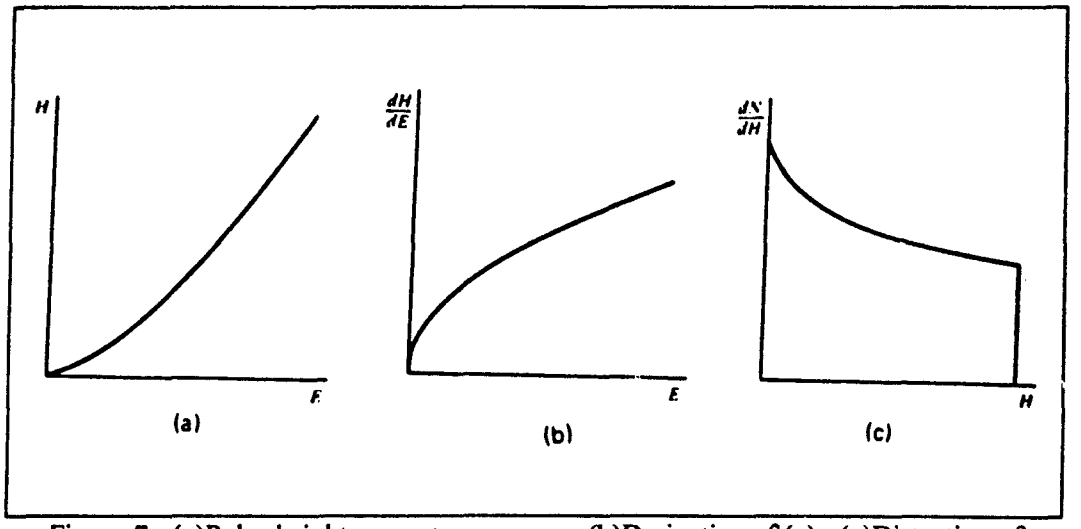

Figure 7. (a)Pulse height vs neutron energy; (b)Derivative of (a); (c)Distortion of rectangular proton recoil spectrum due to nonlinear response of scintillator [17:539]

Organic scintillators, however, do have a linear light output with increasing energy for gamma events. For this reason, spectrometry systems such as the one constructed for this research are energy calibrated with a gamma source of known energy, usually ^{22}Na [17:222].

Another factor which distorts the ideal rectangular recoil spectrum in an organic scintillator is edge effect. Edge effect occurs when either a small detector or high energy incident radiation results in incident particles exiting the detector after having deposited only part of their energy in the sensitive volume of the scintillator. This causes a shift of highly-energetic events toward lower pulse heights. The effect on the response function is to further increase the slope of the spectrum in Figure 7(c) [17:539].

An additional effect which distorts the response function is multiple scattering from hydrogen. In the ideal case, all of the energy from the neutron is transferred to a recoil proton in a single scatter. However, in practice it is possible for a neutron to scatter more than once with hydrogen nuclei before coming to rest in the detector or escaping from the scintillator. Because all such events usually happen within a very short time compared to the fluorescence time of the scintillator, the light from multiple scatters is summed into a single pulse whose amplitude is proportional to the total light output. The effect on the response function is to add events at large amplitudes at the expense of those at lower pulse heights, as shown in Figure 8 [17:539]. This figure represents the output from a multi-channel analyzer (MCA), which is used in the laboratory to view the pulse height spectrum of recoil protons. In this figure, dN/dH is equivalent to the number of counts per MCA channel, while the pulse height corresponding to the neutron, H, is equivalent to the channel number of the MCA.

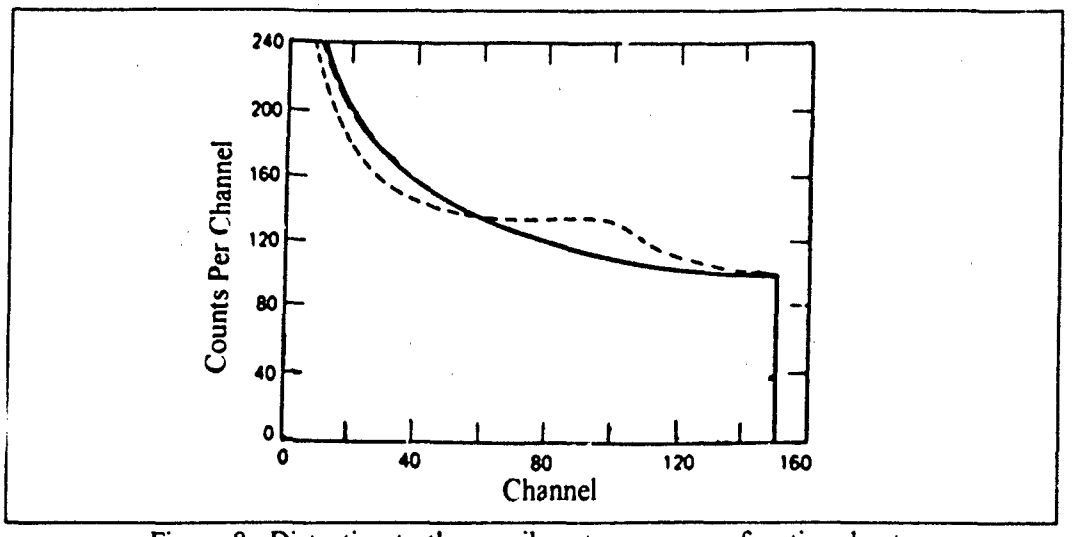

Figure 8. Distortion to the recoil proton response function due to multiple scatters with hydrogen (dotted line) [17:541]

As a final factor, once the neutron energy exceeds about 8 MeV, two additional competing reactions must be considered in the overall response of the scintillator. These reactions are: [17:542]

$$n + {}^{12}C + 6.17\ MeV \rightarrow \alpha + {}^{9}Be$$

and

$$n + {}^{12}C + 7.98\ MeV \rightarrow n' + 3\alpha$$

The effect of these alpha-producing reactions is to increase the detection efficiency of neutrons above the energy thresholds of these reactions [17:542].

The discussion up to this point has not considered the effect on the recoil proton spectrum due to many neutrons of different energies. As discussed previously, in the ideal case a recoil proton has an equal probability of receiving anywhere from none to all of a scattered neutron's kinetic energy. Ideally (ignoring the six distortions just discussed), the

measured recoil proton spectrum, $M(H_p)$, resulting from several monoenergetic neutrons will match the probability distribution function of Figure 4. For the same number of neutrons of any different neutron energy, we expect a rectangular response with a different height, but with the same area under the curve. If we were to measure neutrons of several discrete energies, each discrete energy group having the same number of neutrons, we would ideally expect a family of rectangular responses, $R(H_p,E_n)$, each with the same area, as shown in Figure 9.

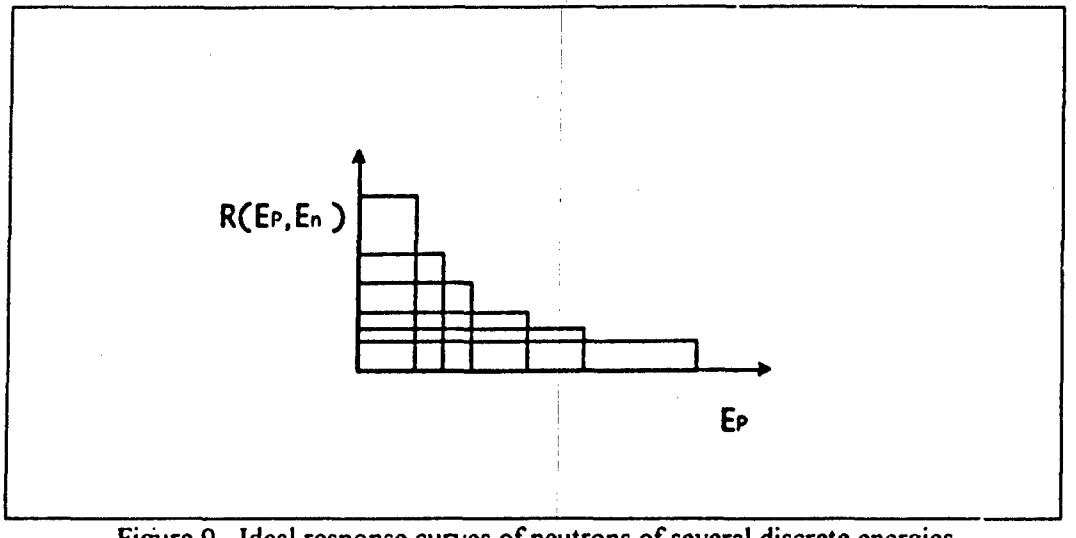

Figure 9. Ideal response curves of neutrons of several discrete energies

Therefore the response, $R(H_p,E_n)$, is the probability that a neutron with energy E_n will scatter once with a hydrogen nucleus and create a recoil proton of energy E_p, which will in turn produce a pulse of height H_p in the detection system. If every neutron that enters the scintillator interacts, then the following relationship holds for each response curve [5:85]:

$$\int_0^\infty R(H_p, E_n)\,dH_p = 1 \qquad (5)$$

The response function, $R(H_p,E_n)$, is ideally $1/E_n$ for $0 \leq Ep \leq En$ [5:85].

If the curves from Figure 9 are added together to simulate incident neutrons of several discrete energies, a plot of the total number of recoil protons, $M(H_p)$, for all of the discrete-energy neutrons that entered the scintillator volume is obtained, as shown in Figure 10.

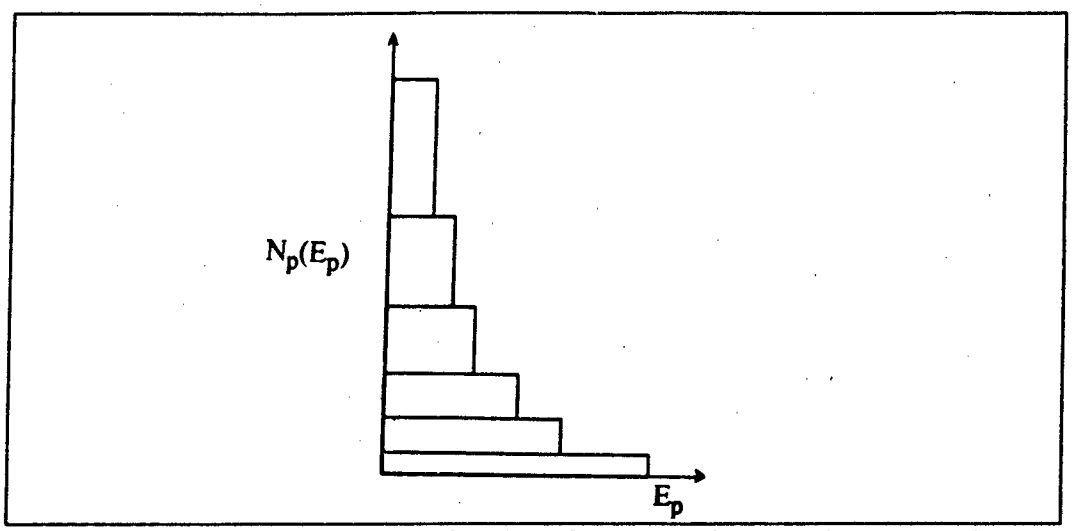

Figure 10. Total ideal response function of neutrons of several discrete energies

The measured recoil proton spectrum $M(H_p)$, is related to the true incident neutron spectrum, $T(E_n)$, as follows [17:672]:

$$M(H_p) = \frac{dN}{dH} = \int_0^{E_{n,max}} R(H_p, E_n) T(E_n) dE_n \qquad (6)$$

where $R(H_p,E_n)$ is called the response function or response matrix and is specific to the spectrometry system used. The response matrix accounts for the response of the detector

to incident neutrons of each energy E_n in terms of the pulse height of the corresponding recoil proton, H_p. Taken together, the term in the integral is the differential probability that a quantum of energy within dE_n about E_n leads to a pulse with amplitude within dH about H [17:672].

The summed response functions shown in Figure 10 still assume that the response of the detector to neutrons of each discrete energy is ideal and, therefore, rectangular. If all of the distortions to the ideal rectangular response are now considered, the recoil proton spectrum of a multi-energy neutron source, such as PuBe, becomes quite complicated. The response function of the detector used must be known with a high degree of accuracy to unfold recoil proton spectra and correctly reproduce the incident neutron spectrum from the measured recoil proton spectrum. For this reason, the response functions of a particular detector to monoenergetic neutrons of several different energies are either carefully measured in the laboratory or are calculated using a Monte Carlo code in which the detector has been carefully modeled. Verbinski *et al.* [29:8] measured the response of an NE-213 spectrometry system to monoenergetic neutrons at 20 energies between 0.2 and 20 MeV and compared these measurements to Monte Carlo calculations. These results form the basis for the neutron response matrix used by the FORIST unfolding code. For this reason, many neutron spectrometry experiments are now performed using the laboratory protocols of Verbinski *et al.* in order that FORIST and its neutron response matrix may be utilized.

The integral unfolding problem given in Eq (6) must be reduced to a matrix unfolding problem to solve it numerically. The matrix equation is [5:85;17:673]:

$$M(H_p)_i = \sum_j R(H_p, E_n)_{ij} T(E_n)_j \tag{7}$$

where M_i is the measured number of counts in the i^{th} channel of a multi-channel a
R_{ij} is the response matrix coupling the i^{th} pulse height interval with the j^{th} energy
and T_j is the true neutron intensity in the j^{th} energy interval [17:673]. M and T ar
vectors, while R is a square matrix [5:85]. The matrix R is upper triangular beca
recoil proton can not receive more energy than the incident neutron had before th
collision.

Eq (7) can be solved for the incident neutron spectrum, T, by multiplying t
sides of the equation by the inverse of R [15:4]:

$$T(E_n)_j = \sum_i R(H_p, E_n)^{-1}_{ji} M(H_p)_i$$

Problems occur, however, in the numerical solution because of round-off er o s.
the matrix inversion process, as well as uncertainties in the detector readings and in the
response matrix. These errors can produce large oscillations about the true spectrum in
the solution vector. In practice, errors in R and M are inevitable, and the more channels of
data that are used, the more likely it is for R is to be ill-conditioned and the system to
become unstable, so that small errors produce large changes in the output spectrum
[8:131]. Most unfolding methods, therefore, must have some means of limiting errors and
oscillations. Some strategies include forcing the solution vector, T, to be "near z
[15:5], or to have a certain degree of smoothness [8:131].

The unfolding of the incident gamma ray spectrum from the measured C
recoil electron spectrum proceeds in a very similar manner. The interaction proc
Compton scattering takes place between the incident gamma photon and an elec
scintillator. In Compton scattering, the incoming gamma is deflected through a
(in the lab frame) with respect to its original direction. The gamma transfers a p
its energy to the electron, which is assumed to be at rest initially. The energy tr sferred

from the gamma to the recoil electron is dependent upon the scattering angle as follows [17:53]:

$$E_e = \frac{\frac{E_\gamma^2}{m_e c^2}(1-\cos\theta)}{1+\frac{E_\gamma}{m_e c^2}(1-\cos\theta)} \tag{9}$$

where E_γ is the energy of the incident gamma, E_e is the energy of the resulting recoil electron, and $m_e c^2$ is the rest-mass energy of the electron (0.511 MeV). The maximum energy transferred to the electron occurs when θ=180°. Under normal circumstances, all scattering angles will occur in the detector. Therefore a continuum of energies can be transferred to the electron, ranging from zero up to the maximum predicted by Eq (9) [17:290-291]. For a monoenergetic gamma ray, the recoil electron energy distribution with scattering angle has the shape shown in Figure 11.

Note that there is some similarity between the energy distribution of recoil electrons in Figure 11 and the ideal distribution of recoil protons in Figure 4. Similarly, too, the ideal energy distribution of the recoil electrons suffers distortions due to factors such as the finite resolution of the detector. One important feature that the recoil electron spectrum does not experience is the nonlinear light collection with increasing energy observed with the recoil proton spectrum. This, coupled with the fact that the Compton edges, though smeared by the finite resolution of the detector, are identifiable in the recoil electron spectrum, makes gamma ray sources ideal for energy calibrating organic scintillation detectors. The exact theory and process of energy calibration are described in following sections.

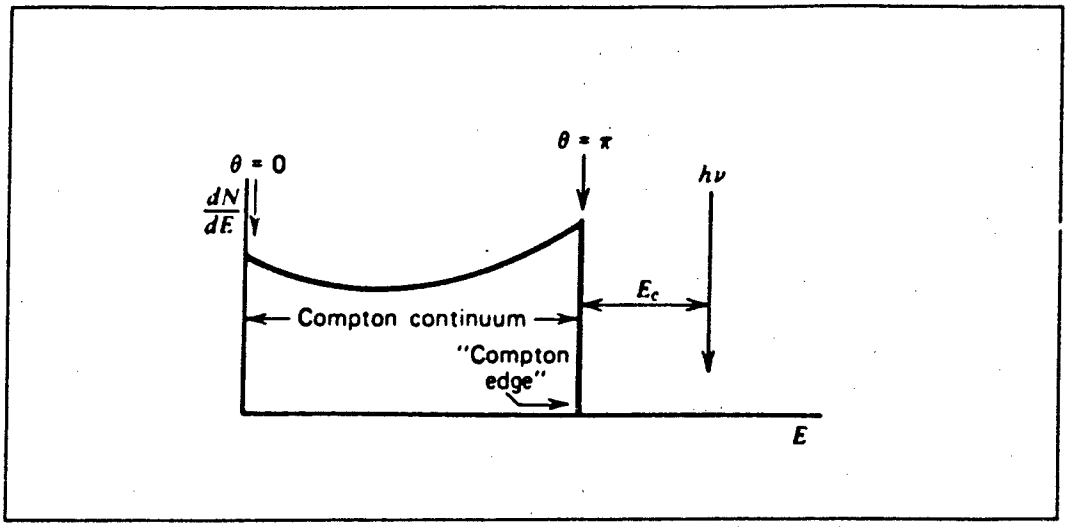

Figure 11. Energy distribution of Compton recoil electrons [17:291]

As with neutrons, the response of a detector to incident gamma rays can be either measured or calculated, yielding a gamma response matrix for the detector which allows the recoil electron spectra to be unfolded to reproduce the incident gamma spectra. Ingersoll and Wehring [13:551] used the NE-213 detector configuration of Verbinski *et al.* to measure the gamma ray response functions of the spectrometry system for 100 monoenergetic gamma rays from 2 to 11.5 MeV. These measurements were used to construct the gamma response matrix which is used with the FORIST code.

Energy Calibration

To unfold a recoil spectrum to yield the incident spectrum, the spectrometer must be energy-calibrated. Calibration is required both to assign an energy scale to the unfolded spectrum and to match the detector's response to the response matrices provided with FORIST.

The pulse height response of the scintillator is nonlinear for incident neutrons, but it is linear for incident gammas, so the easiest way to calibrate the detection system is to use a gamma source and to perform a linear fit to determine the calibration. A gamma source with at least two peaks of known energy is required. Following the protocols of Verbinski *et al.* [29:14], a ^{22}Na source, which has two gammas of energy 0.511 and 1.275 MeV, is used to calibrate the system. The maximum Compton recoil electron energies produced by these two gammas, calculated using Eq (9), are 0.341 and 1.062 MeV respectively. A ^{22}Na Compton recoil electron spectrum from the literature is shown in Figure 12.

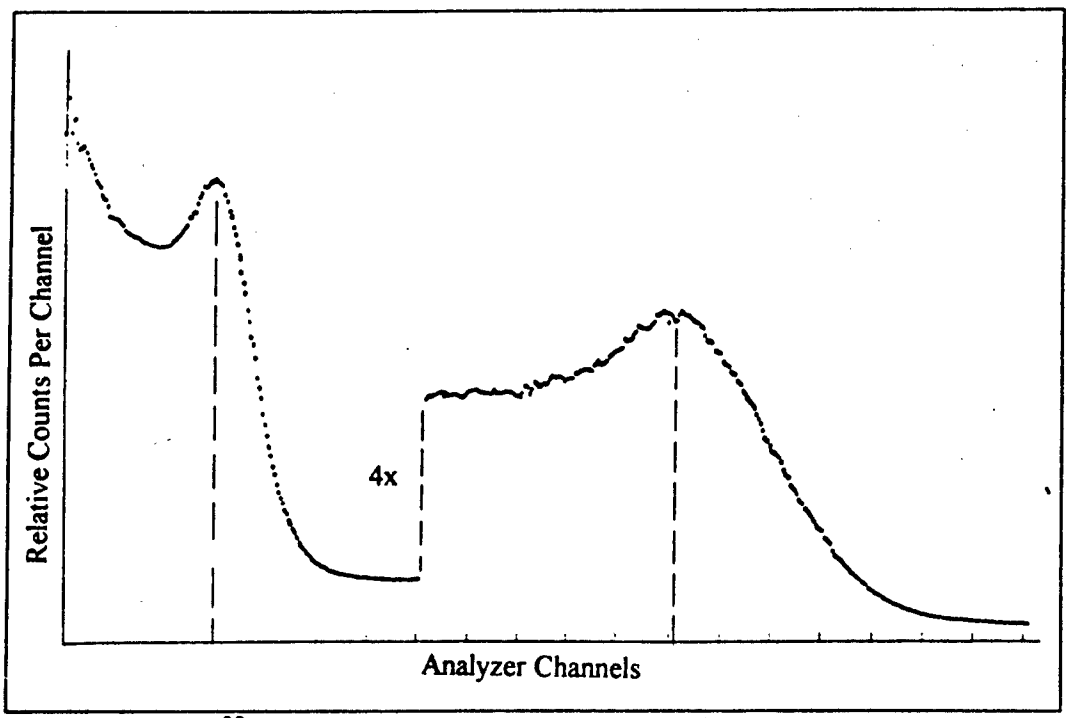

Figure 12. ^{22}Na Compton recoil electron spectrum from literature [18:523]

Verbinski *et al.*, in their calibration work, defined an energy unit called a "light unit" (lu). They defined 0.885 lu to be equal to the maximum recoil energy of the 1.275-MeV gamma from ^{22}Na, or equal to 1.062 MeV. [6:183] The FORIST unfolding code requires that the recoil spectra recorded in the lab be calibrated in terms of light units.

Because of the finite resolution of the detector, the Compton edge is not a sharp event, but is smeared over several MCA channels, as can be seen in Figure 12. Various researchers have differed in their choice of the location of the maximum recoil electron energy on these Compton edges, selecting either the peak, two-thirds height, or half-height [7:351;18:522]. The half-height is used for this thesis research because it consistently provides more accurate results [24:267;16:341].

The calibration is calculated as follows. The channel locations of the half-heights of the two Compton edges are used to define a line. First, the slope of the line is calculated using the equation:

$$m = \frac{y_2 - y_1}{x_2 - x_1} \tag{10}$$

where m is the slope of the line, (x_1,y_1) are the half-height channel location and maximum recoil electron energy of the first (0.511 MeV) gamma, and (x_2,y_2) are the half-height channel location and maximum recoil electron energy of the second gamma (1.275 MeV). Next, the y-intercept of the line is calculated using the equation:

$$b = y_2 - mx_2 \tag{11}$$

where b is the y-intercept of the line calculated in Eq (11), m is the slope calculated in

Eq (10), and (x_2,y_2) again correspond to the half-height channel location and maximum recoil electron energy of the second gamma. Third, the zero-intercept, which is the location where zero energy crosses the x-axis, is found using the equation:

$$z = -\frac{b}{m} \tag{12}$$

where z is the zero-intercept, while m and b are the slope and y-intercept calculated previously. Finally, the gain, in light units, is calculated for the system using the equation:

$$G = \frac{0.885}{x_2 - z} \tag{13}$$

where G is the gain, z is the zero intercept from Eq (12), x_2 is the channel location of the maximum recoil energy of the second gamma, and 0.885 is the light unit conversion factor of Verbinski *et al.* Detailed discussions of the calibration procedure and the gain and zero-intercept requirements of the FORIST code are presented the "Laboratory Procedure" section.

III. Description of Apparatus

The detector used in this research project is a xylene-based organic scintillator similar to the one used by Verbinski *et al.* This type and size of detector were chosen so that the FORIST unfolding code could be used to reproduce the incident neutron and gamma spectra from the recorded recoil proton and Compton electron spectra. This section first compares the detector used in this research to the one used by Verbinski *et al.* to show that the FORIST response matrices apply to the current detector. Next, it presents the electronics used in the laboratory to record the data, with an emphasis on the setup used to differentiate between neutron and gamma events on the basis of PSD. Following the discussion of the electronics, the requirement for and design of the shadow shield are discussed. Next, the radiation sources used during the course of this research are described. Finally, this section presents a brief description of all of the computer software used in conjunction with the spectrometry system, including the FORIST unfolding code.

Detector

The detector used in this research consists of a 5.0-cm by 5.0-cm cylindrical Bicron(BC)-501A liquid organic scintillator coupled to a Hamamatsu R329-02 photomultiplier tube (PMT) by means of a 1.6-cm thick clear plastic light pipe. Both the scintillator-light-pipe interface and the light-pipe-PMT interface are optically coupled with a Dow Corning transparent silicon fluid which has a kinematic viscosity of 2000 stokes. Aluminum foil is used as a reflective coating on the outside of the light pipe, and the entire

assembly is sealed with black electrical tape to eliminate light leaks. The PMT was then surrounded by a μ-metal shield to reduce magnetic interference. An equipment list is included in this thesis in Appendix A, while a diagram of the detector is shown in Figure 13.

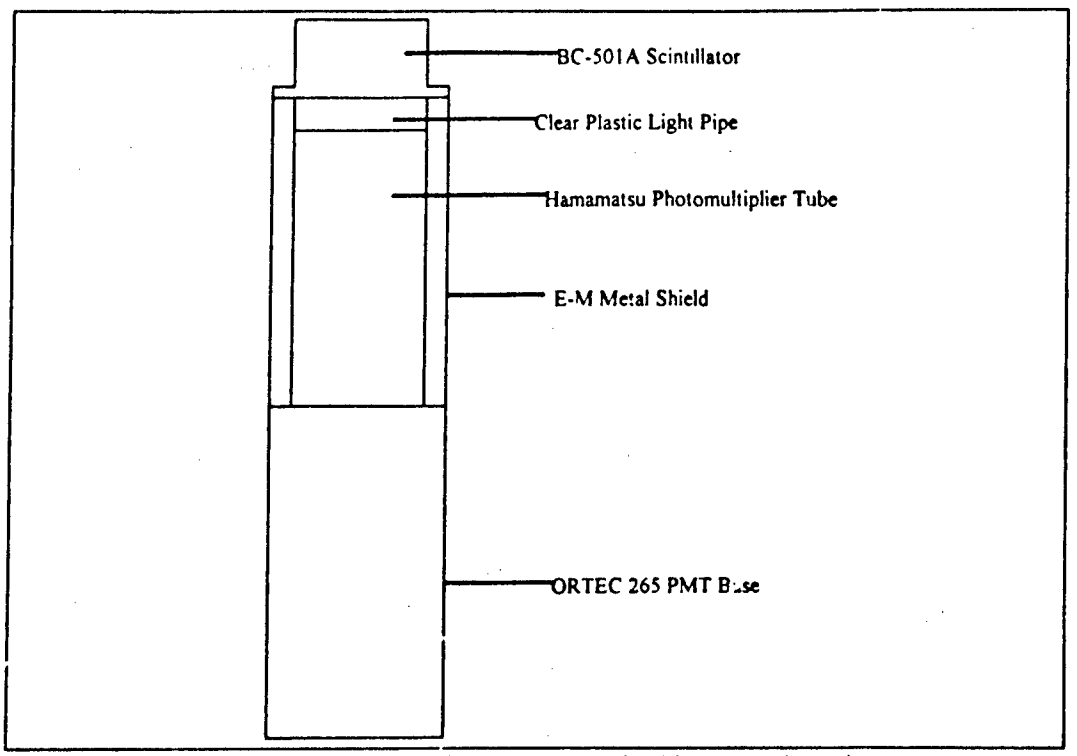

Figure 13. Diagram of detector used in this research project

The detector used by Verbinski *et al.* consisted of a 4.60-cm by 4.65-cm diameter NE-213 liquid organic scintillator mounted on a 0.63-cm thick clear plastic light pipe and coupled to an RCA-6810-A PMT. An aluminum foil reflector was used to cover the scintillator and light pipe [6:183].

The NE-213 liquid scintillator manufactured by Nuclear Enterprises and used in neutron spectrometry for many years is no longer available in the United States. An available substitute, and the one used in the detection system constructed for this project, is the BC-501A liquid scintillator manufactured by Bicron. A comparison of these two scintillators, shown in Table 1, shows that they are essentially identical.

Table 1. Comparison of NE-213 and BC-501A scintillators [17:221;3:1]

Property	NE-213	BC-501A
Light output, % anthracene	78	78
Density (g/cm^3)	0.874	0.874
Refractive Index	1.508	1.505
Wavelength of max emission (nm)	425	425
H/C (atomic ratio)	1.213	1.212

The cylindrical geometry of the NE-213 and BC-501A scintillators are the same, but there may be a small difference in the dimensions of the cylinder. The 5.0 by 5.0-cm dimensions reported for the scintillator used in the detection system in this thesis are the outer dimensions of the plastic-and-aluminum container in which the liquid scintillator is contained. Verbinski *et al.* do not mention whether their reported dimensions are the inner or outer measurements of their scintillator, but judging from the number of other researchers that have reported using a 5.0 by 5.0-cm scintillator in conjunction with the FORIST code [13:551;16:337], either Verbinski *et al.* probably reported the inner dimensions of their scintillator.

The light pipe used in the current detector is the same as Verbinski's except that it is 0.97 cm thicker than his. This slightly thicker dimension was chosen to allow the rim of

the BC-501A scintillator to sit directly on top of the μ-metal shield without cutting 0.97 cm from the top of the shield. The light pipe serves only to distribute the scintillator light more uniformly on the photocathode of the PMT , so the absence of a light pipe might be expected to affect the response, but the small difference in thickness should have a negligible effect on the response of the detector to incident radiation [17:242-246].

Finally, one must compare the parameters of the two photomultiplier tubes used, the RCA 6810-A of Verbinski *et al.* and the Hamamatsu R329-02 of the current detection system. The Hamamatsu tube used with the current detector configuration was marketed by Bicron as the properly-matched PMT for the BC-501A scintillator. The RCA 8610-A tube used by Verbinski *et al.* is no longer made, but the tube marketed by RCA as its replacement, the RCA 8575, has similar characteristics. The RCA and the Hamamatsu tubes are compared in Table 2. Both Verbinski's PMT and the tube used for this project are very well matched to the 425-nm wavelength of maximum emission of the scintillator, and both have response times appropriate to PSD. The selection of the Hamamatsu tube should allow the use of Verbinski's response functions with this detector.

Table 2. Comparison of RCA 8610-A and Hamamatsu R329-02 photomultiplier tubes [27:12-13;11:44-45]

Parameter	RCA 8610-A (8575)	Hamamatsu R329-02
Spectral Range (nm)	260 - 650	300 - 650
Peak Wavelength (nm)	420	420
Voltage Divider Stages	12	12
Maximum HV (V)	3000	2700
Diameter (mm)	51	51
Rise Time (ns)	2.8	2.6
Transit Time (ns)	37	48

Electronics

The electronics used in the spectrometry system constructed for this thesis can be divided into four subsystems: the detection subsystem, the PSD subsystem, the energy subsystem, and the output subsystem. The function of each of the four subsystems is discussed in turn though a detailed description of the operation of each electronic module is described in the "Experimental Procedure" section. A diagram of the spectrometry system's electronics is presented in Figure 14, and an equipment list is provided in Appendix A.

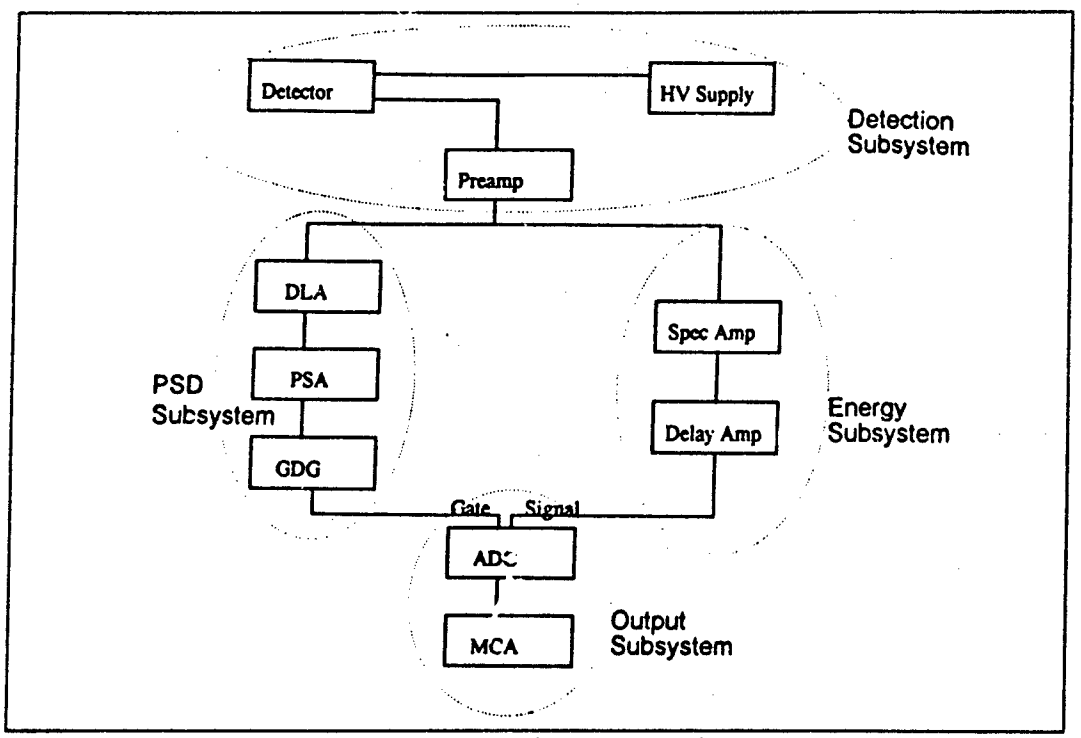

Figure 14. Block diagram of electronic equipment for spectrometry system

The function of the electronics in the detection subsystem is to provide the optimum signal from the scintillator for the PSD subsystem and the energy subsystem. This requires a fast, unsaturated signal to convey the PSD information and to properly convey the energy information. The electronics in the detection subsystem consist of the photomultiplier tube base, high voltage (HV) supply, and preamplifier.

The PMT base accepts the input from the HV supply and has BNC outputs for both the anode and the 9th dynode signal from the PMT. Many early researchers, including Verbinski *et al.*, took the output from a dynode for their energy signal and the output from both a later dynode and the anode for their PSD signal. This method usually required modifications to the PMT base and a number of complicated modules in the PSD subsystem [29:13]. This is no longer necessary since nuclear electronics have progressed since the original work, however. The electronic configuration chosen for the current research project was based on a setup suggested in the operating manual for an ORTEC model-460 delay-line amplifier [10:10]. In this new setup, both the timing and energy signals are taken from the 9th dynode. The advantages of this setup are that the PMT base does not have to be modified and the output is suitable for processing by simple sets of follow-on electronics in the timing and energy subsystems.

The HV supply provides the potential difference to the PMT necessary to accelerate the electrons from one dynode to the next. The HV supply must be chosen to properly match both the magnitude and polarity of the PMT's voltage requirements. For this system the HV supply provides negative high voltage to the photocathode.

The preamplifier serves as an intermediate amplification step in the system, which improves the signal-to-noise ratio and minimizes capacitive loading on the detector. The connection from the 9th dynode of the PMT base to the preamp must be transmitted on short a cable to minimize degradation of the signal. The output from the preamp can be transmitted over long lengths of 93Ω coaxial cable to allow the operator to locate the rest

of the electronics at a safe distance from the radiation sources. During this research, the operator's station was located approximately 4 meters from the detector and radiation sources.

The next subsystem to be discussed is the PSD subsystem. The function of the pulse shape discrimination, or timing, subsystem is to process the available pulse shape information produced by the organic scintillator and to use this information to establish a gate to select gamma or neutron events. The PSD subsystem chosen for this research consists of a delay line amplifier (DLA), a pulse shape analyzer (PSA), and a gate and delay generator (GDG).

The delay line amplifier takes the positive unipolar signal from the preamp and produces a double-delay-line shaped bipolar pulse with positive polarity leading [10:1]. Timing measurements are obtained from the zero crossover point of the bipolar pulse. Neutrons, which have a larger delayed fluorescence component in the scintillator than gammas, will produce pulses in the DLA which cross zero later than those pulses produced by gamma events. A sample output from the DLA is shown in Figure 20 of the "Experimental Procedure" section.

The pulse shape analyzer, the next module in the PSD subsystem, measures the fall time of an input pulse and generates a linear output pulse with an amplitude that is proportional to the fall time. A logic output pulse is also generated when the fall time of the input pulse lies between the upper- and lower-level discriminators of the PSA time window [9:1]. In the context of this spectrometry system, the PSA operates on the positive lobe of the bipolar output pulse from the DLA. The linear output pulse generated is suitable for input to an analog-to-digital converter (ADC) and multi-channel analyzer (MCA). This linear pulse provides a timing spectrum on the MCA which can be used to set the PSA time window to trigger a logic pulse only when a gamma event is detected by the scintillator. This logic pulse is then used as the basis for the gate between neutron and

gamma events. Sample outputs from the PSA are shown in Figures 21 and 22 of the "Experimental Procedure" section.

The gate and delay generator, the last module in the PSD subsystem, is used to shape the logic pulse output from the PSA in both amplitude and width to meet the specifications required by the ADC for a gate pulse. The logic output from the PSA is used as the input to the GDG, and the output from the GDG is used as the gate input to the ADC, which is the first module in the output subsystem. Sample outputs from the GDG are shown in Figures 23 and 24 of the "Experimental Procedure" section.

The third subsystem to be described is the energy subsystem. The function of the energy subsystem is to take the energy information from the detector and process it to meet the specifications required by the ADC for a signal pulse. The energy subsystem consists of an amplifier and a delay amplifier.

The amplifier increases the amplitudes of the pulses from the preamp to a magnitude suitable for the ADC. The gain of the amplifier is selected to match the gain settings required for the FORIST unfolding code. The specific gain settings are described later. A sample output from the amplifier is shown in Figure 24.

The delay amplifier is used to match a pulse from the energy subsystem with the corresponding pulse from the PSD subsystem. Because there are more modules in the PSD subsystem, the timing signal, without some way to delay the energy pulse, would reach the ADC later than the energy pulse. A delay of a few microseconds is required. An oscilloscope is used to view the outputs from the GDG and amplifier in order to adjust this delay. The output of the delay amp is then used as the signal input to the ADC. The gate and signal pulses are shown in Figure 24.

The fourth and final subsystem in the spectrometer is the output subsystem. The function of the output subsystem, which consists of the analog-to-digital converter (ADC) and multi-channel analyzer (MCA), is to use the PSD information to select only gamma or

neutron events and to then collect the corresponding Compton electron or recoil proton spectrum in the MCA.

The ADC receives the energy signal from the energy subsystem and is gated by the timing gate from the PSD subsystem. A switch on the ADC allows selection of gamma events, neutron events, or a combination of the two.

The MCA, which is a program running on a personal computer in the [illegible] of this spectrometry system, assigns the incoming energy pulses to bins, or channels, in direct proportion to the amplitude of the signal. The resulting recoil proton or Compton electron spectra recorded by the MCA are then saved to a floppy disk and later unfolded by the FORIST unfolding code to generate the incident neutron and gamma spectra.

Shadow Shield

To measure just those neutrons or gammas traveling directly from the source to the detector, the background contributions to the spectrum must be subtracted. The background spectrum results from neutrons and gammas from the source scattering off the floor, walls, and other scattering surfaces in the experimental area, as well as any radiation emitted by any other radioactive sources which may be in the area. To measure the background, or room return spectrum from the radiation source, a shadow shield is used to attenuate the direct source spectrum. The spectrum recorded with the shadow shield can then be subtracted from the spectrum of the direct source recorded without the shadow shield to reduce the room return contribution.

An effective shadow shield must completely obstruct the line of sight between the source and the detector, and must be composed of materials which are effective shields for gammas and neutrons. The shield assembled for this spectrometry system consists of 36

inches of paraffin followed by 4 inches of lead in a rectangular array of total dimensions 40" x 11" x 6". The 11" x 6" rectangle is the cross section along the axis between the source and detector, which is large enough to obstruct the line of sight.

The paraffin used in the shield, which is contained in two 18-inch long plywood boxes, was chosen because it is a hydrogenous material and, thus, and excellent neutron absorber. The 36 inches of paraffin between the source and detector provide 13 mean free paths of absorber for monoenergetic 14-MeV neutrons, and even more MFPs for neutrons of all lower energies. This means that the shield only passes 0.0023% of incident 14-MeV neutrons and even fewer neutrons of lower incident energies.

The lead used in the shield is composed of two 2-inch thick lead bricks. The 4 inches of lead between the source and detector provide 5.6 mean free paths of absorber for 10-MeV gammas, and even more MFPs for gammas of all lower energies. This means that the shield only passes 0.38% of incident 10-MeV gammas and even fewer gammas of lower incident energies.

The lead is placed behind the paraffin, as viewed from the source, to absorb any gammas made by (n,γ) events within the paraffin caused by the absorption of the high-energy incident neutrons [23:57-58]. There was no need for additional paraffin after the lead, as (γ,n) reactions in the lead are highly unlikely.

Radiation Sources

Four radioactive sources were used during the course of this research, two ^{239}PuBe sources and two ^{22}Na sources. The PuBe sources provide both neutrons and gammas, while the ^{22}Na provide only gammas. The four sources are:

1. PuBe #T022: 78 mCi, measured 22 September 1992;

2. PuBe #M-1170: 4.7 Ci, measured 22 September 1992;
3. ^{22}Na #217: 4.7 μCi, measured 22 September 1992; and
4. ^{22}Na #T028: 97.6 μCi, measured 1 October 1992.

The weaker of the two PuBe sources, #T022, was used during all of the setup and optimization of the spectrometer, as well as for most of the data runs, in order to limit the radiation exposure. The smaller of the two ^{22}Na sources, #217, was used as the gamma-only source throughout the setup and optimization work, as well as for nearly all of the energy calibration data runs. The large PuBe source, #M-1170, was used for only two data runs, in which a higher count rate was desired to improve the counting statistics. The large ^{22}Na source, #T028, was used only once in a data run to measure the ^{22}Na gamma spectrum with the spectrometry system. The #T028 source was also used to calibrate the spectrometer for that run only.

The ^{239}PuBe neutron/gamma sources were used for two reasons. First, they provide neutron and gamma spectra which are both well-characterized and within the detection range of the spectrometry system (1 to 14 MeV). Second, the sources are quite compact, making them easy to handle, store, and place in position in relation to the detector. The spectrum generated by the PuBe source is quite complicated, so a detailed discussion of the PuBe source is presented in Appendix B rather than here in the body of the thesis.

The ^{22}Na gamma sources were used in order to follow the convention of Verbinski *et al.* This simple source has gamma peaks at two energies: 0.511 MeV and 1.275 MeV.

Computer Software

The spectrometry system constructed for this research requires the use of four pieces of computer software. The most obvious, of course, is the FORIST unfolding code. Additionally, the system uses a program called ZSHIFT, which takes the recoil spectra recorded on the MCA, along with the appropriate calibration information, and prepares the input file for FORIST to read. The output file from FORIST is interpreted by a third program, called GRAPHICS.TK, which produces plots of the spectra of the incident neutrons and gammas. The fourth piece of software, called CALIBER.TK, generates the calibration information required by FORIST and ZSHIFT. FORIST and ZSHIFT are both written in FORTRAN and were modified to run on a VAX 6420 mainframe computer. The other two codes are written using a software package called "TK Solver Plus" [28:1], and are meant to run on any IBM-compatible personal computer. The four codes are presented in their entirety in Appendices C, D, E, and F, while instructions for using the codes are given in the "Experimental Procedure" section of this thesis. All of the code examples provided in the appendices correspond to the same data run (PuBe #M-1170 neutrons, run #9), so they may be studied as a set to see how the four codes work together.

IV. Experimental Procedure

This section is intended to be a user's guide to operating the spectrometry system constructed for this project, or even for the construction and use an identical system from scratch. This section first describes the arrangement of the equipment in the laboratory. Next, it describes how to set up and optimize the electronics. Then it describes, step by step, how to collect data using this spectrometer. Finally, it gives instructions for processing and unfolding the laboratory data to generate the spectrum of the incident radiation.

Laboratory Arrangement

The detector, source, and shadow shield (when used) are placed on a desk top in the configuration shown in Figure 15. The source-detector separation distance is 42 inches, or just 2 inches larger than the length of the shadow shield. This minimum distance was chosen because of the relative weakness of the small PuBe source (#T022), which would have required inordinately long counting times if the distance had been increased any further. The detector assembly is placed in a wooden cradle on top of a paraffin-filled 18" x 11" x 6" plywood box to raise the detector at least a small distance above the desktop. The detector is placed so that the radiation from the source is incident on the curved face of the detector, in accordance with the protocols of Verbinski *et al* [29:8]. The source under study is placed in a clip on a ring stand located at the source location and raised to the same height above the desktop as the detector. Between the source and detector (below the source-detector plane) are two more

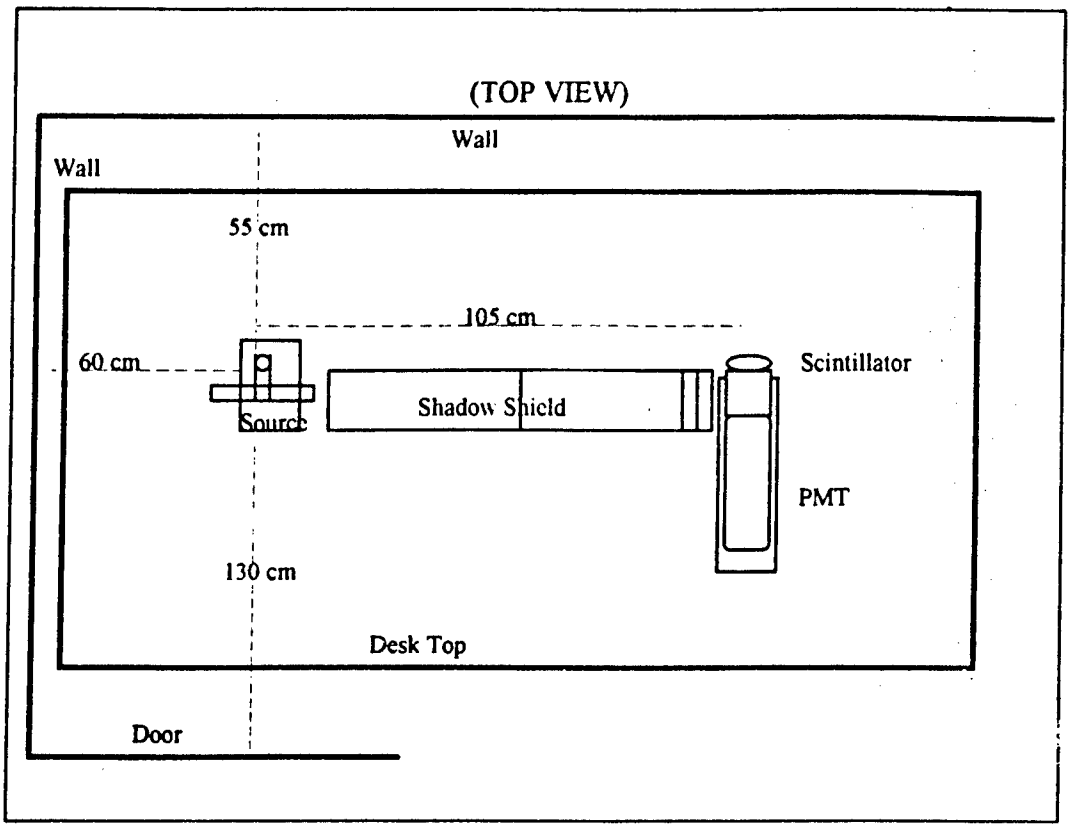

Figure 15. Laboratory arrangement of source, detector, and shadow shield

paraffin-filled plywood boxes, on which the shadow shield rests when it is in use. The nearest scattering surface (other than the plywood boxes) is the desktop, which is 18 inches below the source-detector plane. Two concrete walls and a metal door are also quite close to the source, as shown in Figure 15. This high-scattering geometry is not optimum for actually performing neutron spectrometry, but for original equipment setup and testing, the arrangement is adequate. The configuration is convenient to use during construction and testing because it can be easily varied on the desktop as improvements are made in the system. For radiation safety, the operator's station is located in another room, approximately 4 meters from the source.

Electronics: Set-up and Optimization

The setup and optimization of the electronics in the spectrometry system is accomplished in two parts. In the first part, the detection, PSD, and output subsystems are connected together and optimized for maximum pulse shape discrimination. This configuration is shown in Figure 16. In the second part of the setup process, the electronics are reconnected in the configuration shown previously in Figure 14. The two parts of the setup process are discussed sequentially.

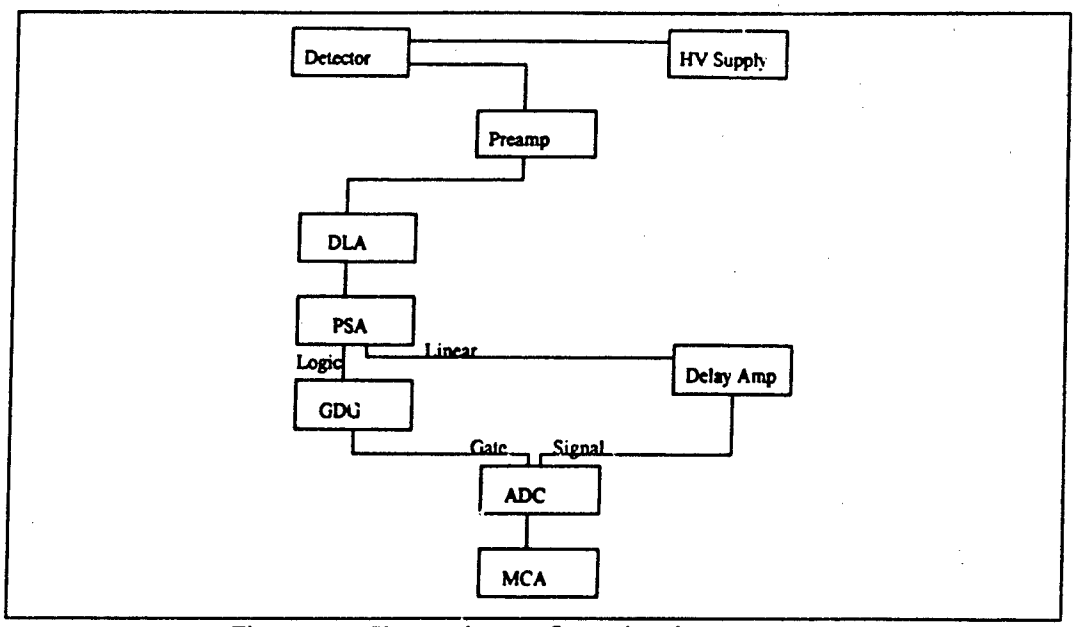

Figure 16. Electronics configuration for PSD work

Pulse Shape Discrimination (PSD). With the electronics configured as shown in Figure 16, the HV, preamp, DLA, and PSA are each optimized in turn. Optimization consists of observing the PSD picture on the MCA, shown in Figure 17, and adjusting the controls on each module to achieve the largest separation between the gamma and neutron peaks and to achieve the best resolution of the peaks as measured by the peak-to-valley ratios. The ADC and MCA are set to 1024 channels full scale for best resolution, and the ADC gate is not used. The linear output from the PSA is used as the signal input to the ADC.

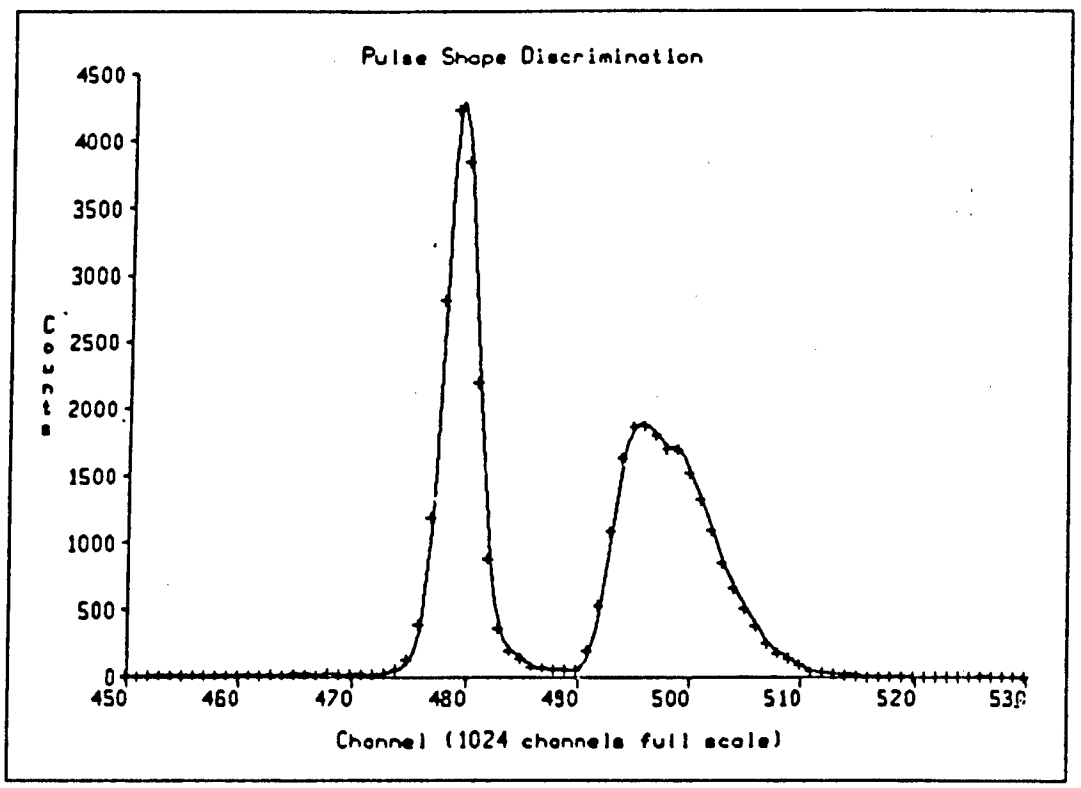

Figure 17. Experimentally-determined optimum PSD for this spectrometry system. The narrow peak at the left corresponds to gamma events, while the broader peak at the right corresponds to neutron events

The HV supply must be set to negative high voltage to correspond to the input voltage requirements of the PMT and PMT base. Keeping in mind that the maximum high voltage allowed for the tube is -2700 V, the HV is varied in increasing steps of 100 V, beginning at -1000 V. It is found that the PSD picture of Figure 17 is essentially impossible to see at -1000 V. It becomes progressively better from -1100 to -1300 V then begins to show anomalies at higher voltages. The optimum setting is -1300 V, as this setting achieved the best combination of peak separation (14 channels) and peak-to-valley ratios (γ-valley: 4.9, n-valley: 9.8). The value of the high voltage is read from the digital display on the HV supply rather than from the dial settings, under the assumption that the voltmeter is more accurate than the scale on the dials. The discrepancy between the two values is 35 V, with the display reading lower than the dials.

The only control that can be varied on the preamplifier is the input capacitance, which can be set to either 0, 100, 200, 500, or 1000 pf. Observing the PSD spectrum on the MCA for each of these settings, it is found that the spectrum becomes progressively worse with increasing capacitance, until the PSD spectrum is unintelligible at 1000 pf. The best resolution, then, is at 0 pf (γ-n sep: 14 ch, γ-valley ratio: 5.3 n-valley ratio: 10). The optimized output from the preamp, as viewed on the oscilloscope, looks like the plots shown in Figures 18 and 19. Figure 18 shows a collection of gamma and neutron event pulses of different amplitudes, while Figure 19 is a magnification of just one of these positive, unipolar pulses in which the detail of the pulse can be seen. These plots are direct screen dumps from the oscilloscope.

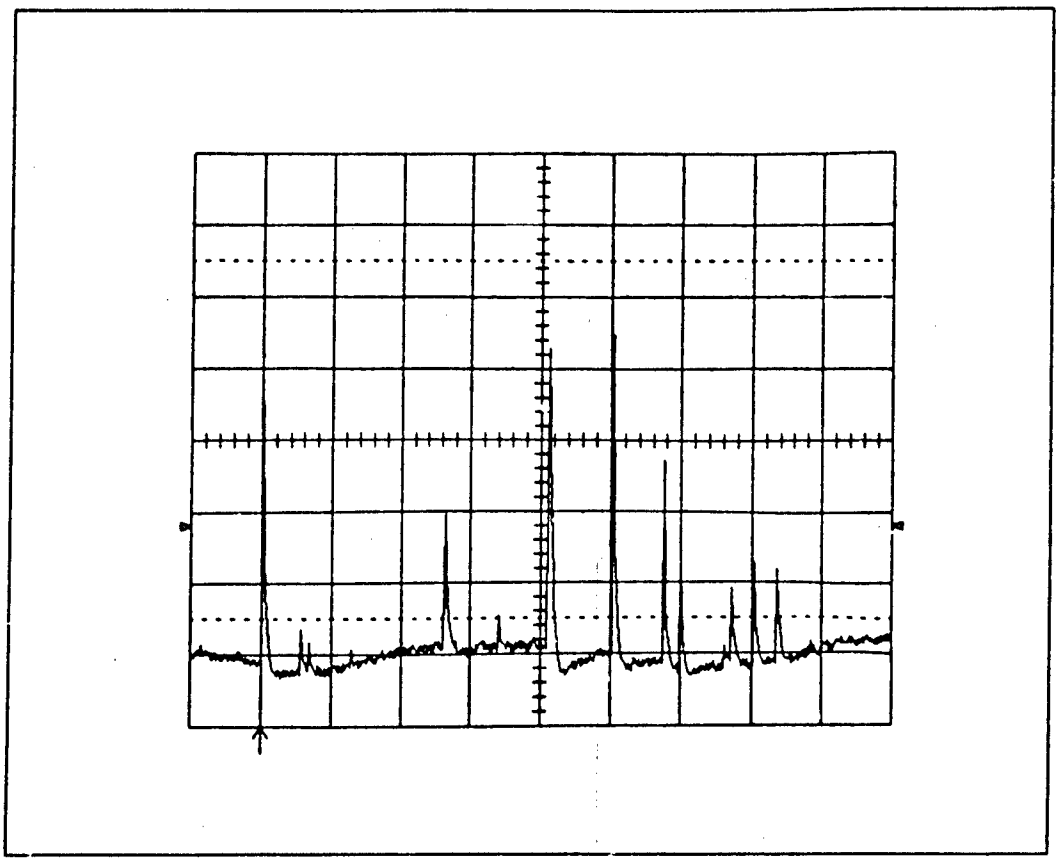

Figure 18. Oscilloscope trace of output from the preamp showing several signals from the PuBe #T022 γ/n source (vertical scale: 5 mV/div, horizontal scale: 1 ms/div)

The next module in line is the delay line amplifier. Several controls must be adjusted on the DLA. They are the input signal polarity, integration time, DC offset, pole zero, and gain. The input polarity switch must be set to positive to match the positive input signal from the preamp. An integration time of 0.25 μs is absolutely necessary to preserve the timing information. Setting the integration time to either 0.1 or 0.04 μsec distorts the DLA output into a square wave and results in no discernible PSD on the MCA. The correct setting of the DC offset, a ten-turn screw adjustment, is verified on the oscilloscope by setting the 0-V line of the DLA output to be the same as the grounded

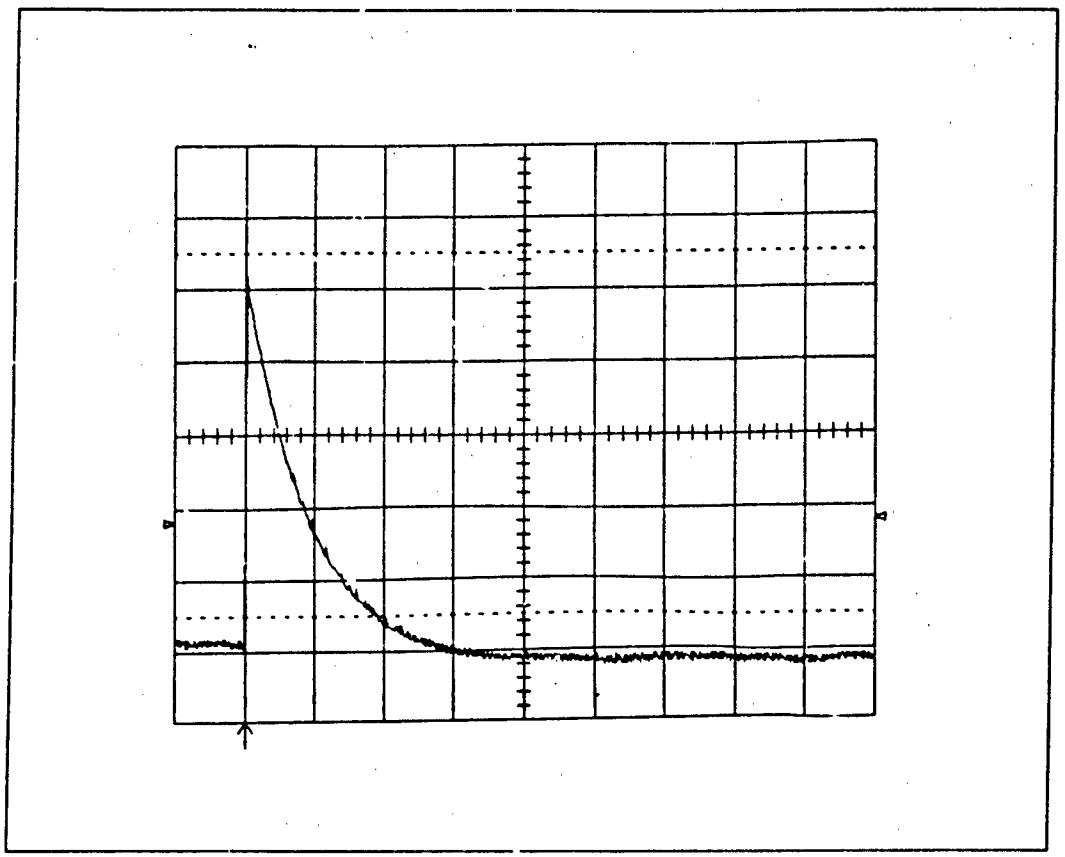

Figure 19. Oscilloscope trace of output from preamp showing single signal from PuBe #T022 with magnified horizontal scale to show detail of pulse (vertical scale: 5 mV/div, horizontal scale: 50 μs/div)

oscilloscope trace. The pole zero, another ten-turn screw adjustment, must also be adjusted by using the oscilloscope. The correct setting of the pole zero eliminates over- and under-shoot of the 0-V line at the end of the DLA output pulse. Finally, the DLA gain is adjusted by optimizing the PSD spectrum on the MCA. While PSD is discernible over a range of gains from 3 to 250, the optimum setting is found to be 15 (γ-n sep: 14 ch, γ-valley ratio: 5.0, n-valley ratio: 9.9). The oscilloscope trace of the optimized bipolar output from the DLA is shown in Figure 20.

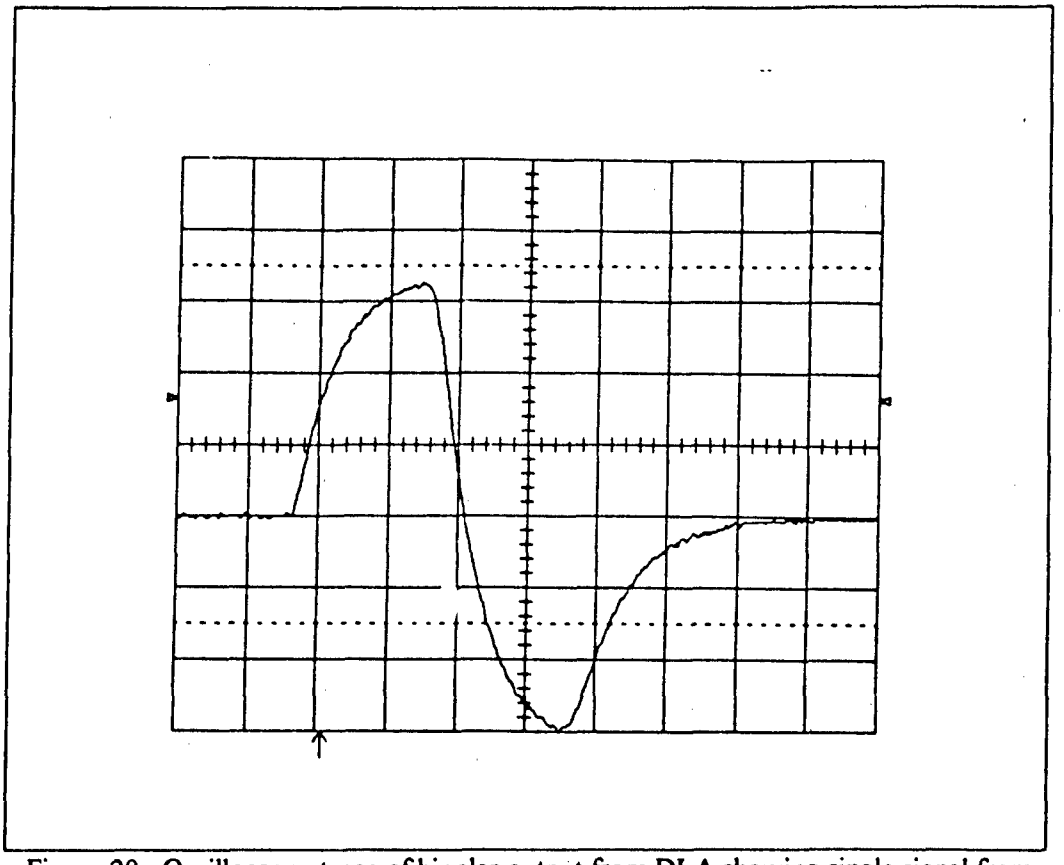

Figure 20. Oscilloscope trace of bipolar output from DLA showing single signal from PuBe #T022 (vertical scale: 0.1 V/div, horizontal scale: 0.5 μs/div)

The next module, which is the PSA, has settings for time range, input voltage discrimination, walk adjustment, and upper and lower level discriminators for the time window. The first thing to do is to set the full-scale time range from to 0.4 μs. This both expands the PSD picture and moves it toward the center of the MCA screen. Increasing the input discrimination makes the valley between the gamma and neutron peaks more prominent. Up to now, the input discrimination has been set at 0.2 V, but by raising this control to 0.7 V, the background and dead time are both lowered.

The walk adjustment of the PSA is very important. This control is a ten-turn screw with no scale on the module to indicate its position. It must be adjusted by

watching the PSD spectrum on the MCA. The optimum adjustment of this control is reached when the gamma and neutron peaks reach their maximum separation (γ-n sep: 17 ch, γ-valley ratio: 70, n-valley ratio: 31). Turning the screw in either direction from this optimum point will bring the peaks closer together, or even smear them together into a single peak. If no PSD is observed during the earlier stages of this optimization procedure, try adjusting this screw and then repeating the procedure with the previous modules. Oscilloscope traces of the linear output of the PSA, which is used as the signal input to the ADC when determining PSD, are shown in Figures 21 and 22.

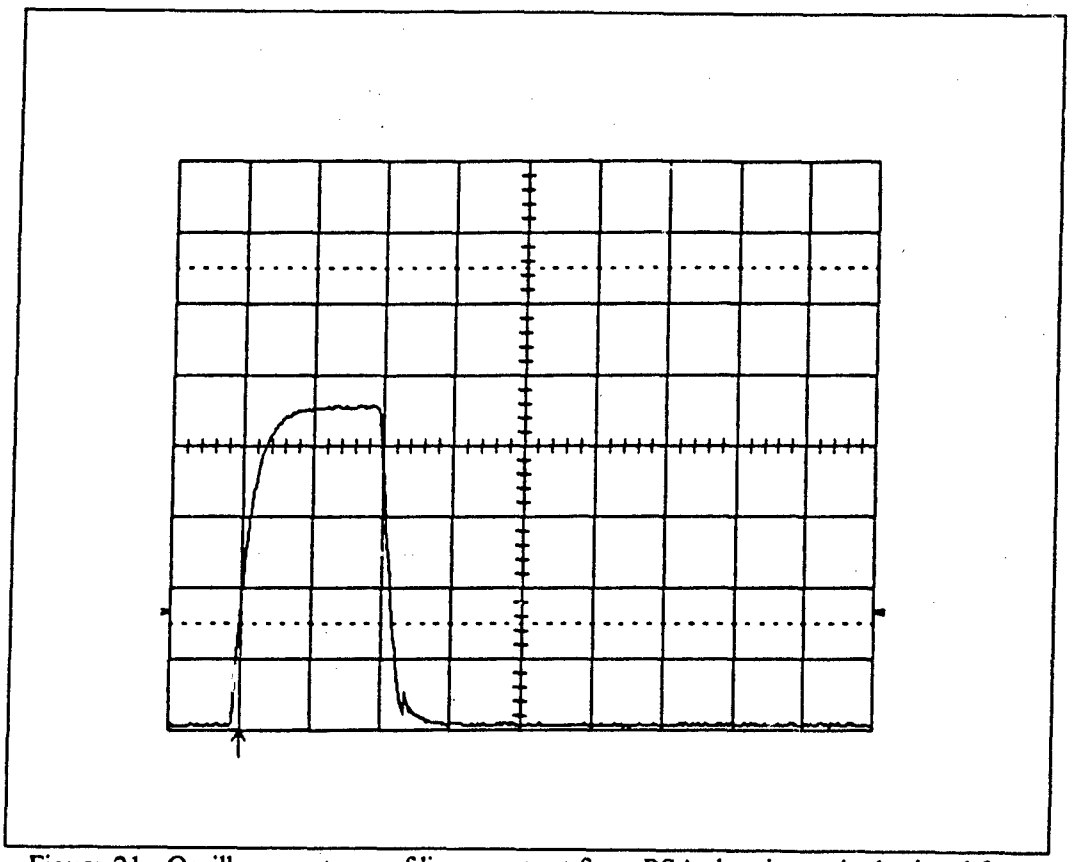

Figure 21. Oscilloscope trace of linear output from PSA showing a single signal from PuBe #T022 (vertical scale: 1 V/div, horizontal scale: 0.5 μs/div)

Figure 21 shows a single pulse, while Figure 22 uses a five-times compression feature of the oscilloscope to show five consecutive pulses on a compressed horizontal scale. The first four pulses of lower amplitude are gamma pulses, while the last, higher-amplitude pulse corresponds to a neutron event.

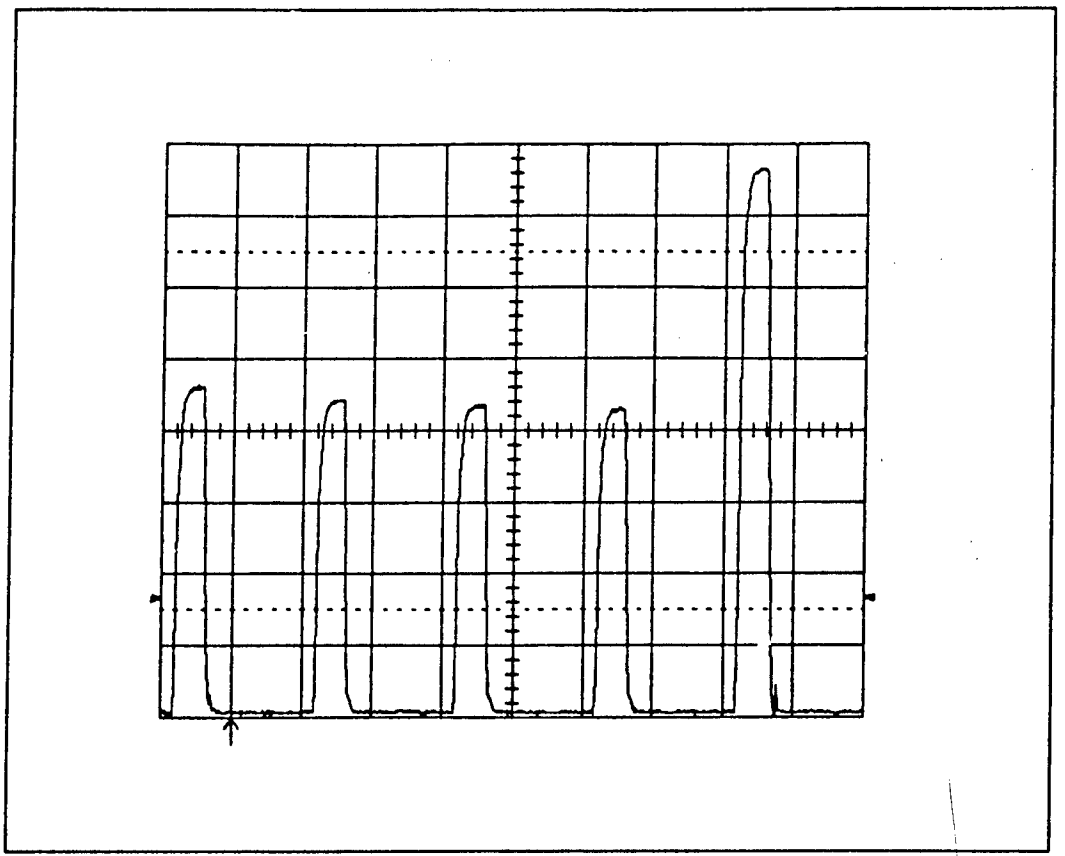

Figure 22. Oscilloscope trace of linear output from PSA using 5x compression feature on scope to show 4 gamma pulses (~4.3 V) and 1 neutron pulse (~7.6 V) (vertical scale: 1 V/div, horizontal scale: 2.5 μs/div)

Finally, the neutron/gamma discrimination window on the PSA must be set. To do this, the linear output from the PSA is used as the signal to the ADC, while the in-window

logic output is used as the gate input to the ADC. To perform this setup, the PSA, ADC, GDG, and delay amplifier must all be adjusted as part of the same process. It is necessary to send the linear output of the PSA through the delay amplifier before connecting it to the ADC, and the logic signal must be routed through the GDG before it is sent to the ADC.

First, the GDG must be set so that the logic pulse from the PSA is of the proper amplitude and duration to act as a gate for the ADC. The ADC used in this system requires that the amplitude of the gate be between +3 and +10 V and that the duration be a minimum of 1 μs. Further, the gate input must precede the triggering of the ADC's lower level discriminator (LLD) by the signal pulse by approximately 100 ns and remain until after the LLD has been triggered [25:1-6]. The GDG has three controls, the delay, amplitude, and width of the gate pulse. Set the delay to 0.1 μs, which is the minimum delay available. The amplitude and width controls must both be set using the oscilloscope, since they have no marked scales on the face of the module. The square pulse of the gate signal is set to 3.4 V, which is within the range of acceptable amplitudes. This low value is chosen because there is a large ringing at the leading edge of the gate pulse. By choosing this amplitude, the maximum amplitude of the leading edge ring is 6.4 V, which is also within the acceptable range of amplitudes. Therefore, the amplitude is in range no matter which part of the gate pulse is triggering the ADC. The width of the gate pulse is set at 3.0 V in order to comfortably meet the timing requirements for the gate.

Next, the delay setting on the delay amplifier must be set so that the PSD signal pulse falls within the gate signal. To set this control, use the oscilloscope and add delay to the signal until its leading edge falls at least 100 ns after the leading edge of the gate pulse. A setting of 0.25 μs places the leading edge of the signal 1 μs after the leading edge of the gate, while the gate continues for 0.5 μs after the signal pulse has ended. The oscilloscope trace showing the properly-set PSD signal and gate pulses is presented in Figure 23.

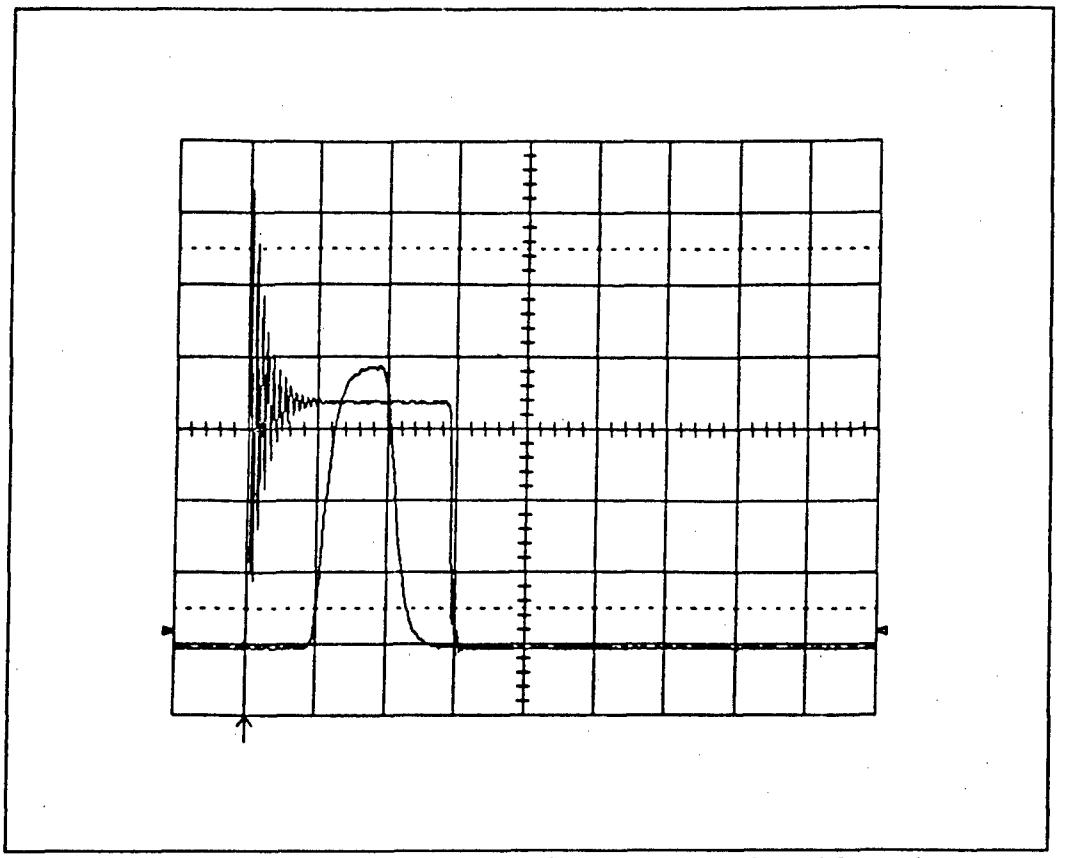

Figure 23. Oscilloscope trace showing the inputs to the ADC used for setting PSD. Large square pulse is the gate, while the smaller pulse centered in the gate is the PSD signal (vertical scale: 1 V/div, horizontal scale: 1 μs/div)

Now that the gate has been established, the discriminators on the PSA can be set. The discriminators will be set so that gamma events fall within the window, while neutron events fall above the window. The lower level discriminator is set to 0 V so that all low-amplitude pulses are counted as gamma events. Now, using the PSD spectrum on the MCA, set the coincidence control on the ADC to "coincidence" and raise the upper level discriminator of the PSA from zero until the entire gamma peak and about half of the valley is displayed on the MCA. To verify this setting, change the ADC coincidence switch to "anti-coincidence" and look at the PSD spectrum on the MCA. Now only the

neutron peak and the other half of the valley should be displayed. The optimum setting for the ULD on the PSA is 4.34 V. Looking at the oscilloscope trace of the series of linear PSA output pulses in Figure 22, one can see that, to within the uncertainty of the trace calibration and the dial setting, this discriminator level falls above the gamma pulses and below the neutron pulse.

Energy. The second part of the electronics setup, which involves the energy subsystem and part of the output subsystem, is much less complicated than the work required previously. To begin this process, the electronics must be configured back to the normal spectrometry setup shown in Figure 14. The tasks for this part of the setup are to set the amplifier, delay amplifier, ADC, and MCA such that the energy signal properly falls within the timing gate and so that the energy spectrum meets the requirements for input to the FORIST unfolding code.

First, set the input voltage discriminator on the PSA to its lowest setting, which is 0.010 V, in order to record the low-amplitude end of the spectrum. Next, the amplifier needs to be adjusted to produce a good Gaussian pulse for the energy signal. To make these adjustments, view the output of the amplifier on the oscilloscope. Now, turn off both the base line reject and delay features, since they are not needed for this application. Then set the shaping time of the pulse to 0.5 μs. Finally, set the gain to approximately 750. This gain will be adjusted later during the energy calibration of the spectrometer.

Next, connect the output of the GDG to the other input of the oscilloscope and view the PSD gate and the energy signal together so that the delay of the energy signal may be adjusted on the delay amp to meet the gating requirements of the ADC. It is found that setting the delay amp to 2.5 μs meets the requirements. The oscilloscope trace of the optimized energy signal and its PSD gate are shown in Figure 24.

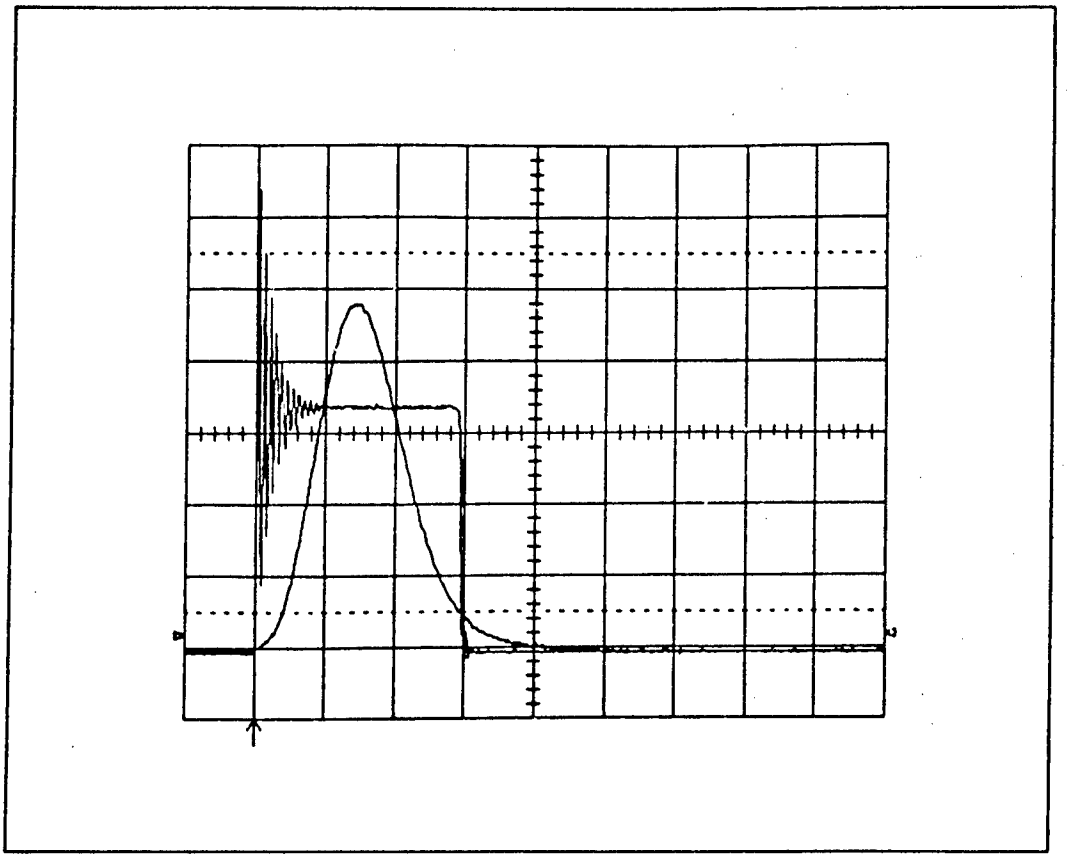

Figure 24. Oscilloscope trace of inputs to the ADC for recording energy spectra. The large square pulse is the gate produced by the PSD subsystem, while the Gaussian pulse within the gate is the signal generated by the energy subsystem (vertical scale: 1 V/div, horizontal scale: 1 μs/div)

Finally, the number of channels on the ADC needs to be set to 256, as this is the number of channels used by the ZSHIFT code to prepare the FORIST input file. Now, raise the lower level discriminator of the ADC up from zero until the dead time shown on the ADC and MCA is less than 5%. This setting is found to be at 0.22 V. Set the upper level discriminator to its maximum value, which is 10.04 V, in order to include as many of the pulses as possible in the spectrum. Now set the zero offset control to approximately 6.00. The position of this control will be finalized during the energy calibration process.

Finally, the electronics are set up and the spectrometry system is ready for use. A summary of the settings for all of the modules is given in Table 3.

Data Collection Procedure

There are three steps to be performed in the laboratory each time a data run is made with the spectrometer. These are:

1. verify the PSD discrimination point set on the PSA,
2. energy calibrate the system, and
3. take the four spectral data sets required by FORIST.

Verifying the PSD discrimination point is not a difficult task. Simply connect the electronics in the configuration of Figure 19 and view a neutron/gamma source on the MCA with the coincidence switch on the ADC set to "normal" so that both the gamma and the neutron peak are displayed. The flip the switch to "coincidence" to verify that only the gamma peak is displayed and flip the switch to "anti-coincidence" to see that only the neutron peak is displayed. Throughout the two months that this spectrometer was in constant operation, no drift in the discrimination point was seen and no corrections were needed.

The next task is to energy calibrate the system using the small ^{22}Na source (#217). To begin, the electronics must be reconfigured into their normal setup for spectrometry, as shown in Figure 14, and the settings on the modules must be in their spectrometry positions, as listed in Table 3. Set the coincidence switch on the ADC to "normal" to disable the PSD gate, since this is a gamma-only source. Then place the ^{22}Na source in contact with the detector to achieve the maximum counting rate.

Table 3. Summary of electronics settings

High Voltage Supply	
HV	-1300 V
Preamplifier	
Input Capacitance	0 pf
Delay Line Amplifier	
Fine Gain	0.3
Coarse Gain	50
Integration Time	0.25 μs
Input	positive
Pulse Shape Analyzer	
Time Range	0.4 μs
Input Discriminator	0.700 V for PSD
" "	0.010 V for spectrometry
Upper Level Discriminator	4.34 V
Lower Level Discriminator	0.00 V
Gate and Delay Generator	
Delay	0.10 μs
Amplitude	3.5 V
Width	3.0 μs
Amplifier	
Fine Gain	0.750
Coarse Gain	1000 (adjusted during runs)
Shaping Time	0.5 μs
Base Line Reject	off
Delay	out
Delay Amplifier	
Delay	1.0 μs for PSD
"	2.5 μs for spectrometry
Analog-to-Digital Converter	
Conversion Gain	1024 ch for PSD
" "	256 ch for spectrometry
Upper Level Discriminator	10.04 V
Lower Level Discriminator	0.22 V
Zero Offset	6.00
Coincidence	normal for full PSD spectrum
"	coincidence for gammas
"	anticoincidence for neutrons

The energy calibration of the system must yield four results: the gain calibrations of the spectrometer at both the high and low gain settings required for FORIST and the zero intercepts, or channel locations of zero energy, for both gain settings. FORIST requires the gain settings to be near or slightly above 0.00625 lu/ch for the high gain setting and 0.0625 lu/ch for the low gain setting, while also requiring both of the zero intercept locations to be greater than zero.

At amplifier gain settings above approximately 150, both Compton edges from the ^{22}Na source can be seen on the MCA. However, at amplifier gain settings below 150, the Compton edge of the lower-energy gamma (0.511 MeV) is no longer resolved on the MCA. Figures 25 and 26 show the measured Compton recoil electron spectra of ^{22}Na #T028 at the high (amp gain = 750) and low (amp gain = 75) gain settings used by FORIST. Because the Compton edge of the first gamma cannot be resolved at the low gain setting required by FORIST, a linear interpolation and least-squares extrapolation computer program, called CALIBER.TK has been written to calculate all of the gain and zero intercept information required by FORIST.

To use CALIBER.TK, a ^{22}Na recoil electron spectrum is recorded at each of four different amplifier gain settings, two of which correspond to the high and low gain requirements of FORIST and the other two of which fall in between. The two intermediate gain runs are required because they, along with the high gain setting, provide the three points needed for the least-squares fit which will be extrapolated to the low gain setting to find the location of the first gamma's Compton edge at low gain. For the spectrometry system constructed for this research, the following four amplifier gain settings are used. With the fine gain of the amplifier to 0.750, varying the coarse gain dial to 100, 200, 500, and 1000 results in gains of 75, 150, 325, and 750 respectively. The settings at 75 and 750 are a factor of 10 apart, as required by the low and high gain inputs for FORIST, and they also provide the necessary gain values in terms of lu/ch, as will be

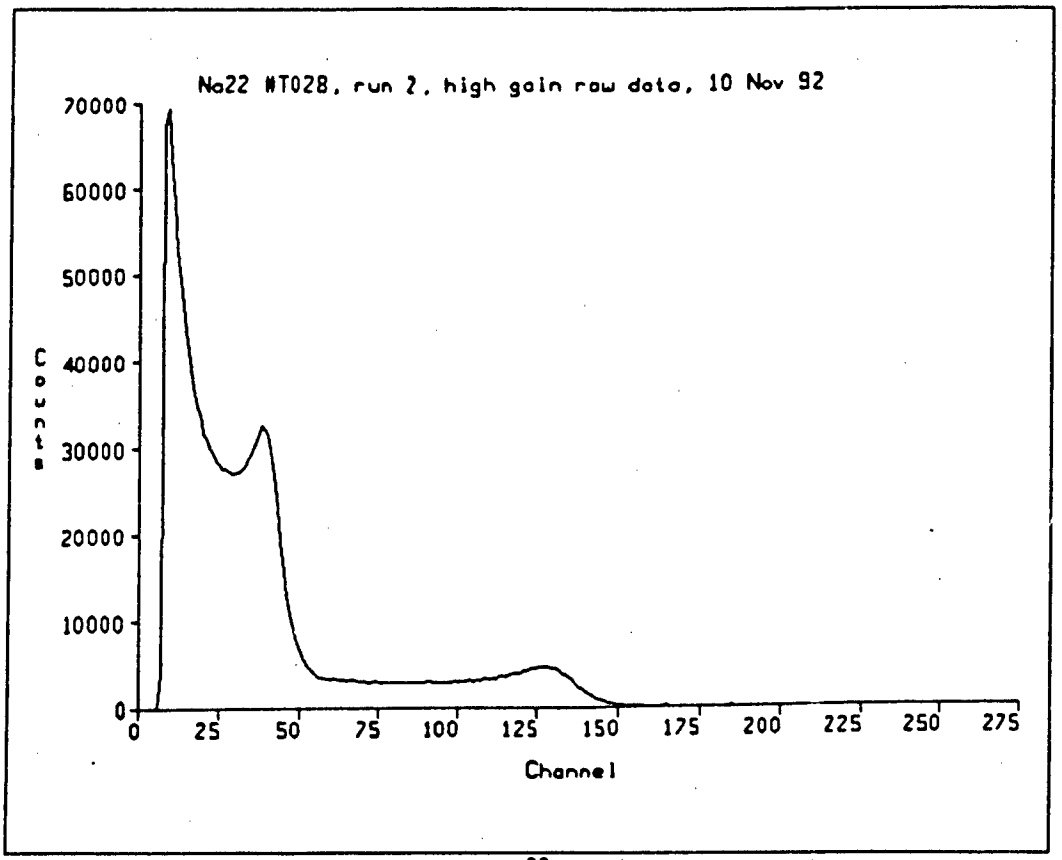

Figure 25. Laboratory measurement of ^{22}Na #T028 Compton electron spectrum at high gain setting

shown soon. The two intermediate settings at 150 and 325 each resolve both of the ^{22}Na Compton edges, so they can be used in the least-squares calculation.

The instructions for the use of CALIBER.TK are divided into 7 steps, as follows. The complete CALIBER.TK model is included in Appendix C.

First, record the four spectra described above. Use ^{22}Na source #217, placed directly on the side of the detector, and count each spectrum for 2 minutes to achieve reasonable counting statistics. Print the counts-per-channel data and locate on these print-outs the channel locatio:.s of the peaks corresponding to the two gammas

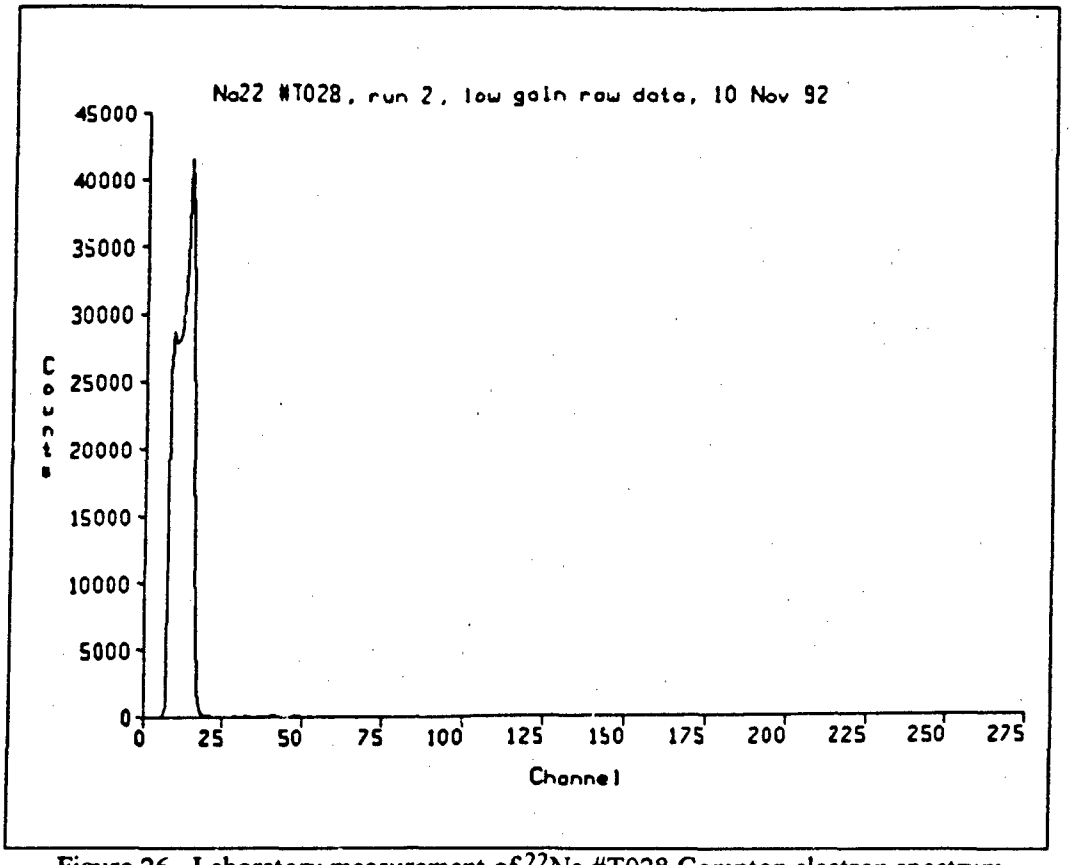

Figure 26. Laboratory measurement of ^{22}Na #T028 Compton electron spectrum at low gain setting

(with the exception of the first gamma peak in the low gain data, which is not resolved).

Second, start CALIBER.TK and display the list sheet on the screen. Fill the list called "amp_gain" with the four settings used on the amplifier, listing them from lowest to highest. Then fill the list called "peak1" with the channel locations of the three known locations of peak 1 corresponding to the three higher gain settings. Fill the "peak2" list with the channel locations of the second peak for each gain setting. Finally, fill the two lists called "PkCts1" and "PkCts2" with the counts recorded in each of the known peak locations.

Third, display the rule sheet on the screen. The rules are divided into four sections, which will be used one at a time. The first set of rules, which are labeled "find counts in 1/2 height of peaks," compute the counts in the half height location of each of the known peaks entered in the previous step. To use the first set of rules, make sure that there is an asterisk in the status column of the rule sheet next to the two rules in this section. All of the rules in the other sections should have the letter "C" next to them, indicating that they are currently canceled and will not be calculated. Now press the F10 key to solve the first set of rules. This will fill the two lists called "Cts1" and "Cts2" with the results of this calculation.

Fourth, move to the table sheet and print the three tables titled "peak_table", "pk1_cts_table", and "pk2_cts_table". These three tables, as printed by CALIBER.TK for one of the calibration runs in this research, are shown in Figure 27. Now move to the plot sheet and print the plot titled "peak_plot". This plot serves as a visual check on the data used in the calibration, as both of the gamma peak position vs. amplifier gain lines should be linear. If the plotted points do not appear linear, double-check the data entered at the beginning of this procedure and fix any errors found. The plot of this data is shown in Figure 28.

Fifth, the channel locations of the half-heights of the Compton edges must be computed using a linear interpolation routine and the results of the half-height calculation in step three. To begin this step, move to the rule sheet. Cancel the first set of rules and un-cancel the second set of rules, titled "linear interpolation routine." Now set the screen so the variable sheet and list sheet are both displayed. In the variable sheet, find the section titled "linear interpolation routine." This routine must be run seven times, once for each known peak. For each peak, enter the counts in the half-height, calculated in step three, on the input line of the variable "y3". Then look at the print-out from the MCA that contains the data for the appropriate peak and find the channels with counts immediately

Peak positions vs amp gain

Amp gain	peak 1 (ch	peak 2 (ch)
75		17
150	12	32
375	24	70
750	43	133

Peak 1: Counts in peak and 1/2 height

amp gain	peak ch	peak cts	1/2 cts
75			
150	12	27108	13554
375	24	12147	6073.5
750	43	6529	3264.5

Peak 2: Counts in peak and 1/2 height

amp gain	peak ch	peak cts	1/2 cts
75	17	7602	3801
150	32	4012	2006
375	70	1711	855.5
750	133	923	461.5

Figure 27. Three tables created by CALIBER.TK

above and below the half-height location. Enter the channel number of the channel to the left of the half-height location in the variable "x1" and enter the counts in that channel in the variable "y1". Then enter the counts in the channel immediately to the right of the half-height location in the variable "y2". Now press F9 and the linearly-interpolated location of the half-height will appear in the output column of the variable "x3". Save this

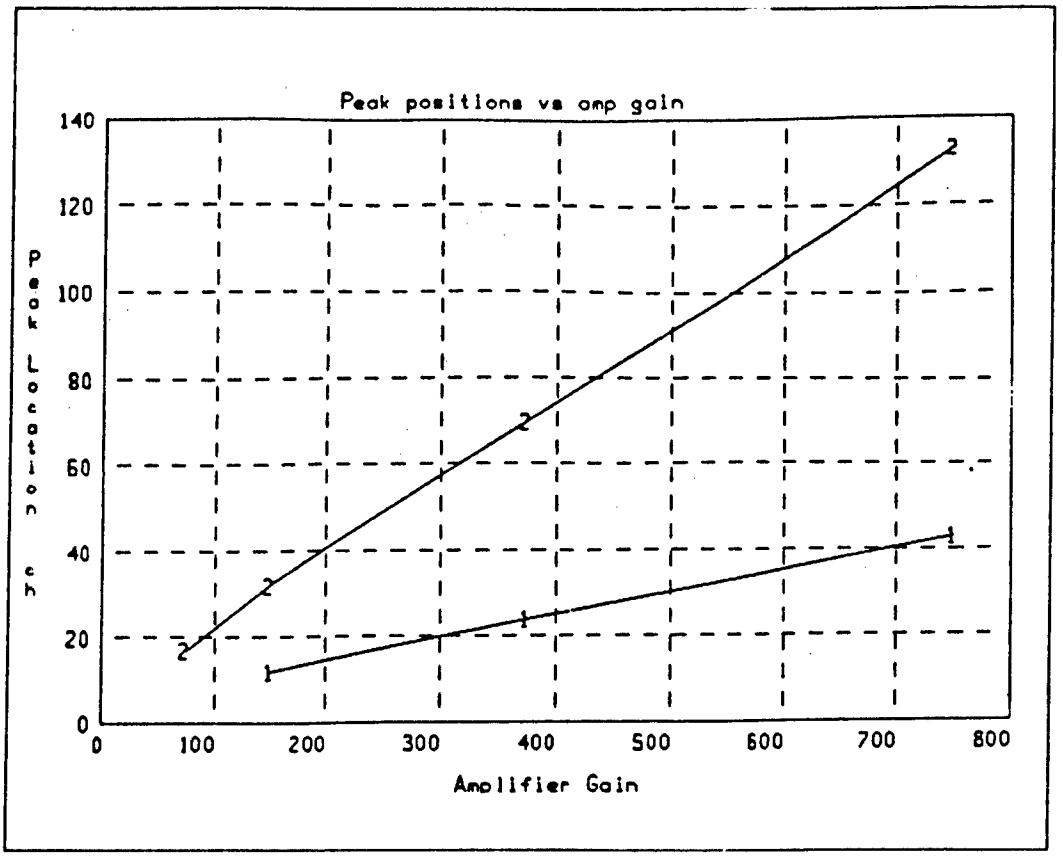

Figure 28. Plot of peak positions vs. amplifier gain to verify linearity of the data in Figure 27

result in the list sheet in either "p1_12" or "p2_12", as appropriate, and run the calculation again until the half-height locations of all seven peaks have been computed and saved.

Sixth, display both the variable sheet and the rule sheet on the screen. In the rule sheet, cancel the set of rules and un-cancel the third set of rules, titled "computation of peak 1 position using least squares fit to peak 1 data." In the variable sheet, find the section titled "peak 1 position routine" and make sure that the correct number of spectra, 4, is listed at the variable "n", and that the amplifier setting at low gain (75 for this system) is listed at the variable "x". Now press F9 and the extrapolated value for the half-height of the first peak at the low gain setting will appear in the variable sheet in the output column

for the variable "y". To verify that linearity has been preserved, copy this value into the first cell of the list "p1_12" and then move to the plot sheet and print the plot titled "gamma1_plot." This plot is shown in Figure 29.

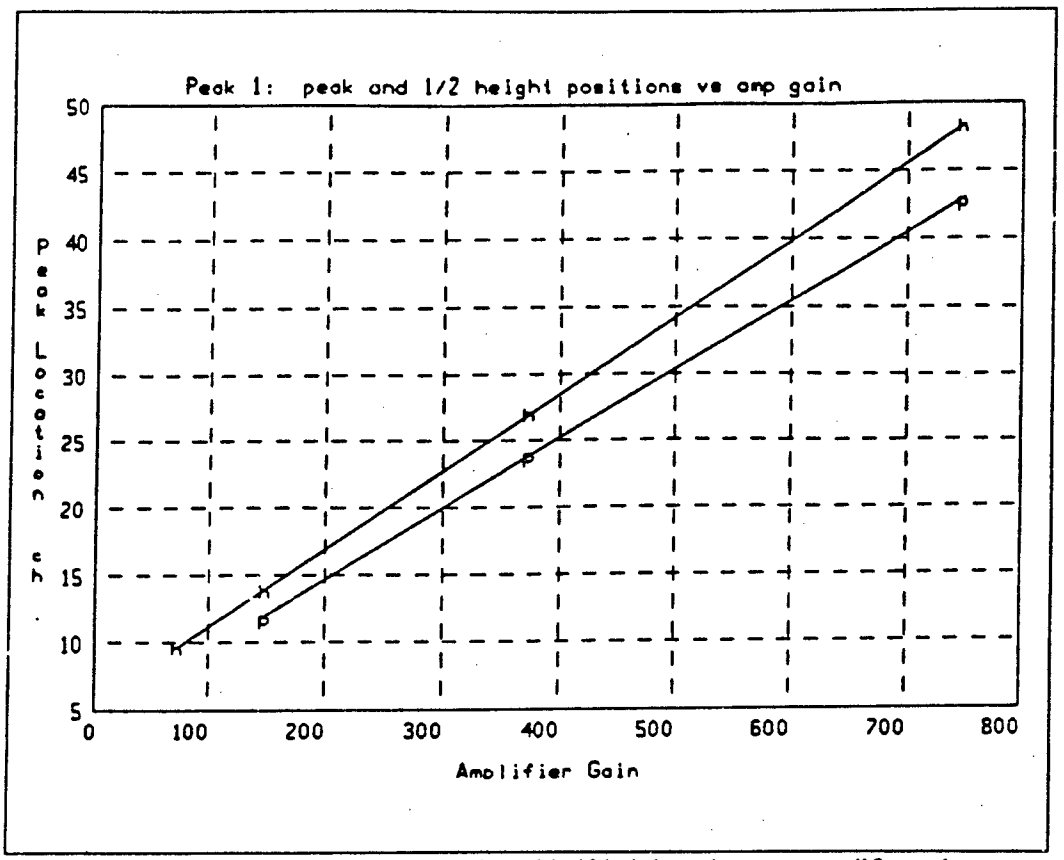

Figure 29. Plot of gamma 1 peak and half-height values vs. amplifier gain to verify linearity

Seventh, the gains and zero intercepts at the high and low gain settings can now be computed. Display the variable sheet and rule sheet on the screen. In the rule sheet cancel the third set of rules and un-cancel the fourth set of rules, titled "gain routine." In the variable sheet find the section titled "gain routine". Enter the half-height positions of

the two gammas in the high gain setting in the variables "x1_h" and "x2_h", and enter the half-height positions of the two gammas in the low gain setting in the variables "x1_l" and "x2_l". Now press F9 and the slope, y-intercept, zero-intercept, and gain (in lu/ch) will be calculated for the high and low gain settings. The part of the CALIBER.TK variable sheet which lists the answers is shown in Figure 30.

VARIABLE SHEET — For Academic Use Only

St Input	Name	Output	Unit	Comment
				-----GAIN ROUTINE----------
.341	E1		MeV	gamma1 max compton electron energy
1.062	E2		MeV	gamma2 max compton electron energy
48.388608	x1_h		ch	location of gamma1 at high gain
142.23239	x2_h		ch	location of gamma2 at high gain
	m_h	.00768298	MeV/ch	slope at high gain
	b_h	-.0307687	MeV	y-intercept at high gain
	z_h	4.0047917	ch	zero intercept at high gain (RESULT)
	G_h	.00640248	lu/ch	high gain (RESULT)
9.7522036	x1_l		ch	location of gamma1 at low gain
18.864485	x2_l		ch	location of gamma2 at low gain
	m_l	.07912398	MeV/ch	slope at low gain
	b_l	-.4306332	MeV	y-intercept at low gain
	z_l	5.4425117	ch	zero intercept at low gain (RESULT)
	G_l	.06593665	lu/ch	low gain (RESULT)

Figure 30. Part of CALIBER.TK variable sheet showing gain and zero-intercept results

FORIST requires that the resulting zero-intercepts must both be greater than zero, and that the gains must be $G_L \geq 0.0625$ lu/ch and $G_H \geq 0.00625$ lu/ch. These conditions may not be satisfied with the first calibration attempt, in which case the amplifier gains must be adjusted and the procedure repeated. Initially, this requires some trial-and-error, but once a successful calibration is made all future calibrations are much easier.

With the calibration of the spectrometry system completed, taking data is quite simple. FORIST requires that a foreground (no shadow shield) and background (with shadow shield) data run be taken at the calibrated high and low gain settings, for a total of four data runs. The four required Compton electron spectra of the PuBe #M-1170 source are shown in Figures 31 to 34, in the following order: high gain foreground, high gain background, low gain foreground, and low gain background. The foreground and background runs at each gain have the same general shape, but there are many more counts in the foreground spectra.

The counting time for these four runs must be long enough to ensure good counting statistics. For the sources used in this research, these times were 30 minutes to 2 hours for the small PuBe (#T022) source, 15 minutes for the large PuBe (#M-1170) source, and 1 hour for the large ^{22}Na (#T028) source. The four spectral data sets taken during a spectrometry data run must each be saved to disk and then converted to ASCII format using the "LOTCNV" command in the AccuSpec MCA software.

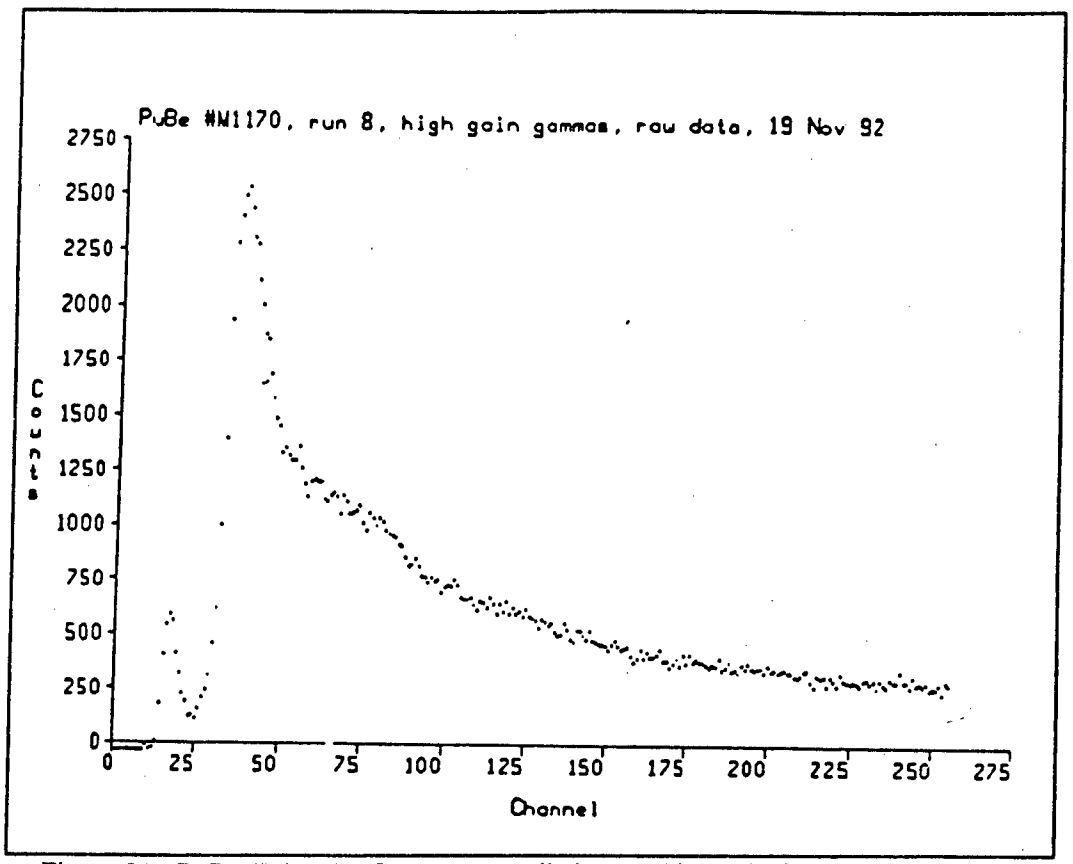

Figure 31. PuBe #M-1170 Compton recoil electron high gain foreground spectrum

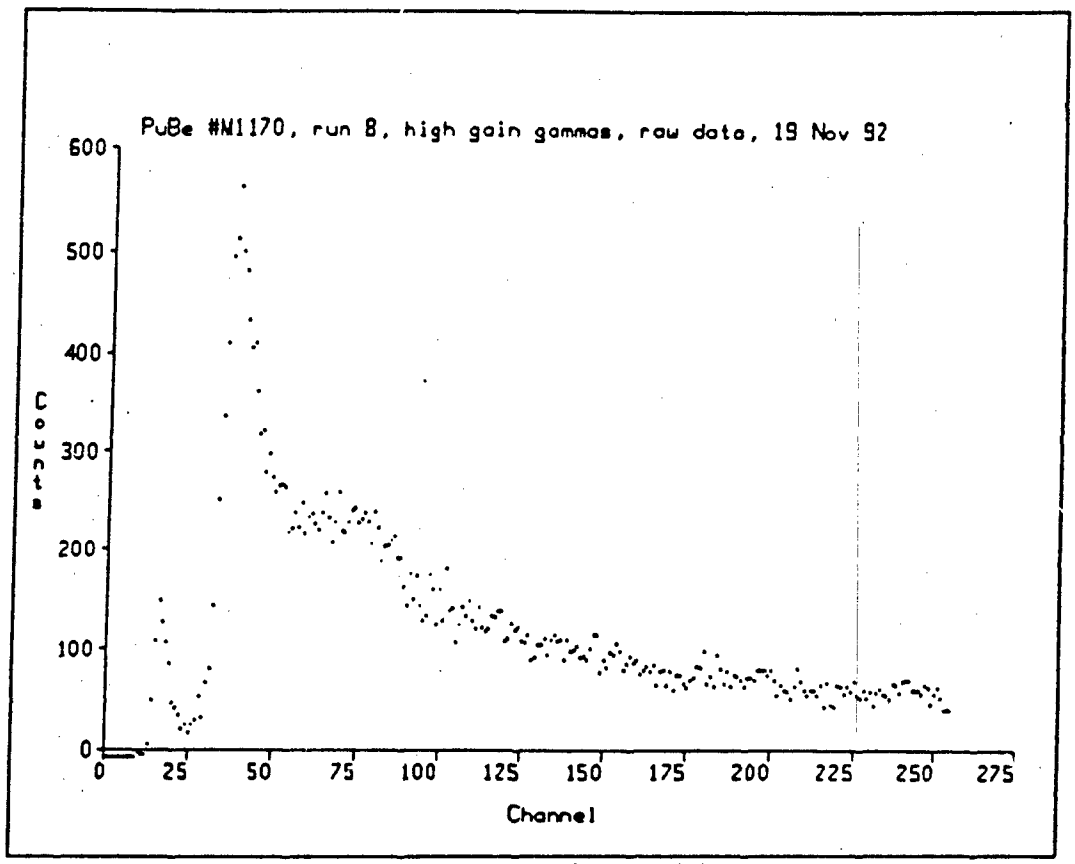

Figure 32. PuBe #M-1170 Compton recoil electron high gain background spectrum

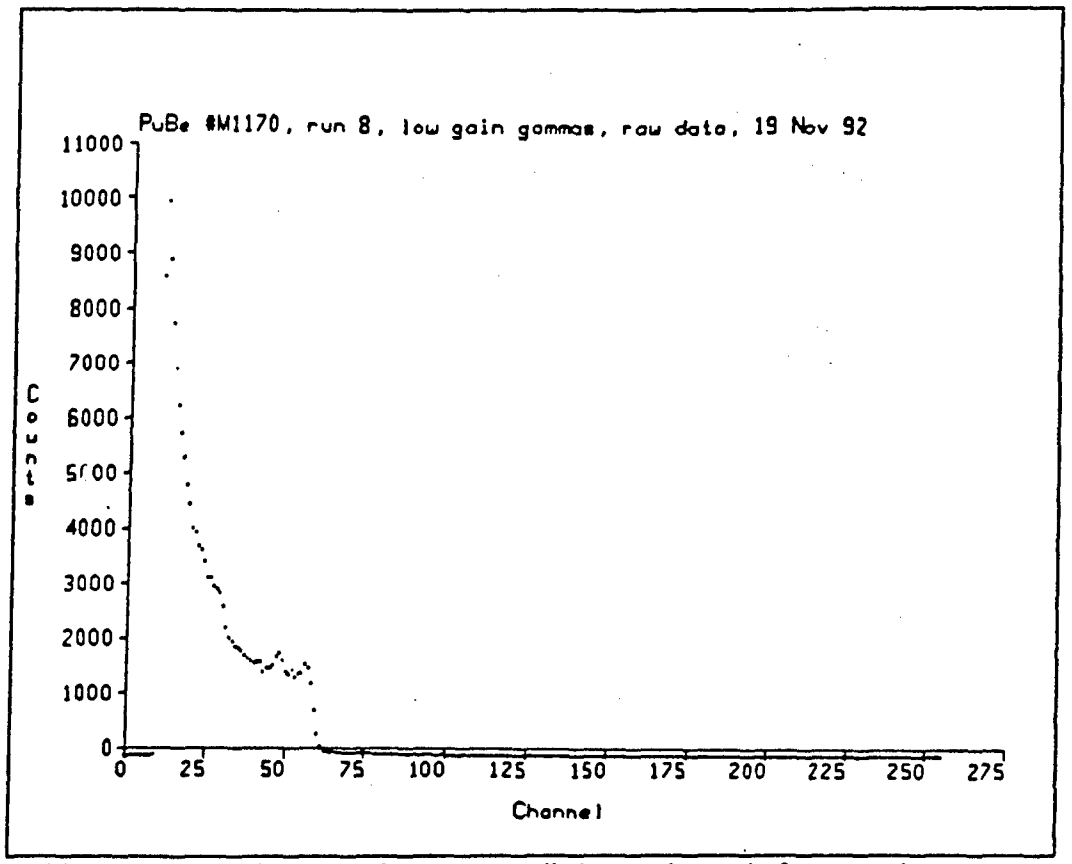

Figure 33. PuBe #M-1170 Compton recoil electron low gain foreground spectrum

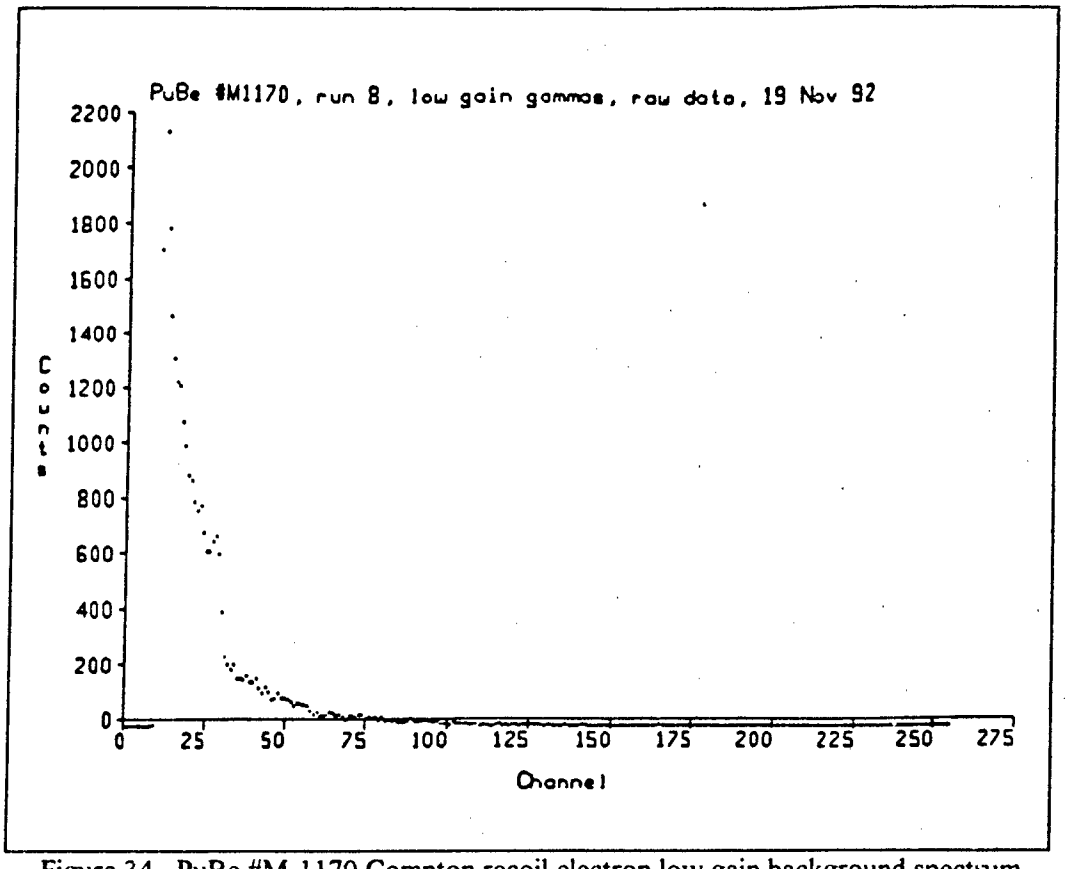

Figure 34. PuBe #M-1170 Compton recoil electron low gain background spectrum

Data Processing and Unfolding Procedure

Now that the data has been collected in the laboratory, it must be processed and unfolded to yield the spectrum of the incident radiation. The steps in this process are:

1. prepare the laboratory data for input to ZSHIFT,
2. prepare and run ZSHIFT,
3. run FORIST, and
4. plot the results from FORIST.

The first step, preparing the laboratory data for input to ZSHIFT, requires first transferring the data files from the floppy disk where they are stored in the laboratory to the mainframe account that contains ZSHIFT and FORIST. The next requirement is to modify the four ASCII-format, recoil-spectra data files so that they may be read using standard, formatted input statements in FORTRAN. The data files contain several lines of unneeded information before the spectral data, which ZSHIFT ignores. The spectral data, then, is originally formatted into rows of 8 data values, with each data value separated from its neighbors by 2 blank spaces. Since the data values contain different numbers of digits depending on their magnitudes, the effect of this format is to give the data a random look on the screen. To be read by ZSHIFT, these four spectra must be modified by hand so that the data fall into 8 columns of uniform width and spacing, a process which takes about twenty minutes.

The second step, preparing and running ZSHIFT, involves the following steps:

1. identify the four spectral data files,
2. enter the gain, zero-intercept, and counting time,
3. set the input format for the MCA data files,
4. choose the appropriate response matrix, and
5. set the desired parameters for FORIST.

Referring to the ZSHIFT computer code, contained in Appendix D, all required user-inputs and brief instructions for their use are contained on the first two pages of the code.

The first set of inputs, which identifies the spectral data files to be unfolded, requires that the user give four sets of information. First, the actual filenames of the four data files must be entered as the values "FILE(1)" through "FILE(4)". These entries are used to find and open the four data files. Second, short, 6-character titles for each of the four files must be entered in the variables "TITLE(1)" through "TITLE(4)". These titles are used to label the four spectra in some of the output generated during the data

processing and unfolding procedure. Third, longer identifiers of up to 80 characters must be entered as "IDENT(1)" through "IDENT(4)". These descriptive identifiers are also used to label the four spectra in some of the output generated during the data processing and unfolding procedure. Finally, a number to identify the laboratory data set is entered in the variable "IDENTY". This integer is used to identify the data in some of the output.

The second set of inputs gives the parameters for the experimental data. The values "ZI(1)" and "ZI(2)" contain the zero-intercepts of the high and low gain runs, respectively. The variables "HGAIN" and "LGAIN" contain the gains of the high gain and low gain spectra, in units of light units per channel. Finally the four variables "HFNORM", "HBNORM", "LFNORM", and "LBNORM" contain the counting time, in seconds, for each of the four spectra. Counting times for each set of four spectral data runs in this research were generally of equal length, but they can be of different lengths if, for instance, counting statistics on one or two of the spectra need to be improved.

The third group of inputs sets the input format for the MCA data files. The variable "M" is the number of channels in the MCA. The variable "SKIP" is a format line that tells ZSHIFT how many lines of unnecessary header information to ignore before beginning to read the spectral data. The variable "INFORM" is a format line that tells ZSHIFT the format of the spectral data in the for data files. For instance, "INFORM = '(1X,8F7.0)'" indicates that there are 8 data values on each line of data, each of which are 7 digits (including spaces) wide. It is important to verify that this format line matches the hand-modified format of the data in the four files.

The fourth input selects the response matrix that FORIST will use in the unfolding calculation. Three response matrices are currently available for FORIST. The "University of Illinois Gamma-Ray Matrix" is contained in the file "GAMMA.MAT" and should be used for all gamma unfolding runs. The "Illinois Neutron Response Matrix", stored in the file "NEUTRON.MAT" was not used during this research. Instead, the "Illinois Neutron

Response Matrix Modified Below 2.5 MeV by NEH", stored in the file "UINEUT.MAT" was used to unfold all of the neutron data. This choice was made because the low-energy modifications in "UINEUT.MAT" were made on the basis of more recent experimental data and computer modeling.

The fifth and final set of inputs to ZSHIFT allows the user to select the desired parameters for the FORIST unfolding routine. These selectable parameters are "NBITS", "STRTCH", "NPUNCH", "ITRATE", "ERRER", and "TAW". The "NBITS" parameter is the number of bits of precision of the computer on which FORIST is running, so is therefore machine-dependent. The values for several machines are listed in the ZSHIFT code. The "STRTCH" parameter is a multiplier on the Gaussian window widths used in the unfolding routine. This parameter should be near 1.0 for best results. The "NPUNCH" parameter tells FORIST which unfolded spectra to include in the output files. For this work, "NPUNCH" was always set to 3, so that the smoothed and unsmoothed spectra could both be plotted and compared against one another. The "ITRATE" parameter sets the number of smoothing iterations performed by FORIST. One smoothing iteration is usually sufficient [16:340]. The "ERRER" parameter allows the user to choose the desired statistical error, in percent, of the unfolded result. The value of this parameter is generally set at 3%. [16:341] The final parameter, "TAW", sets the constraint weight, which requires the unfolded spectrum to be "near zero", thus helping to dampen out oscillations. This parameter works best when set between 1.0 and 10.0 [14:35,82-83]. During the course of this research, the parameters "STRTCH", "ITRATE", "ERRER", and "TAW" were systematically varied in order to study their effect on the unfolded spectra. The complete set of FORIST parameters are summarized in Table 4.

Table 4. FORIST parameters for neutron and gamma unfolding

For neutron unfolding:	
NBITS	23
STRTCH	1.0
NPUNCH	3
ITRATE	1
ERRER	3
TAW	10.0
For gamma unfolding:	
NBITS	23
STRTCH	1.2
NPUNCH	3
ITRATE	1
ERRER	3
TAW	1.0

After the user has selected all of the ZSHIFT input and run ZSHIFT, two output files are generated. The first of these, called ZSHIFT.OUT, summarizes all of the input and output spectral data. This file is used for debugging ZSHIFT and is not used in the actual unfolding process. The second output file, called SPECTRA.IN, is the input file for FORIST. Samples of these two files, corresponding to the inputs contained in the ZSHIFT code in Appendix D, are located in Appendices G and H.

After the spectral data has been prepared by ZSHIFT, it is very simple to unfold it using FORIST. The FORIST code itself has no user inputs, but simply reads the SPECTRA.IN file created by ZSHIFT, along with the appropriate response matrix specified in SPECTRA.IN. FORIST generates three output files. The first of these, called FORIST.OUT, contains a great deal of information which is useful in debugging the code. The second output file, called PUNCH.OUT, is intended as an input file to a graphics routine which was not used in this research, so this file is not used in the current configuration. The third file, called TOGRAPH.OUT, is the input file to the graphics

routine, called GRAPHICS.TK, which is used in this research. Samples of FORIST.OUT and TOGRAPH.OUT, corresponding to the ZSHIFT files, are contained in Appendices I and J.

The final step in the data processing and unfolding process is to graph the data in the TOGRAPH.OUT file using the GRAPHICS.TK code. To do this, the TOGRAPH.OUT file must first be transferred from the mainframe account to a floppy disk, since the GRAPHICS.TK code runs on a personal computer. To use GRAPHICS.TK, start the program and then load the TOGRAPH.OUT data using the ASCII loading feature of TK. Now press the F10 key to convert the energy scale of the data from eV to MeV. The unfolded spectra can now be viewed by looking at the two plots in the model: the "unsmooth" plot contains the FORIST results before the smoothing routine is performed, while the "smooth" plot contains the FORIST results after one smoothing iteration. The plots should be titled and scaled appropriately before printing. If "NPUNCH" or "ITER" are changed from the recommended values of 3 and 1, GRAPHICS.TK will have to be modified accordingly.

V. Experimental Results

Now that the theory and operation of the spectrometry system have been explained, the last step is to present the laboratory results used to validate the system. These results fall into four major groups: the test of the modified FORIST code with previously-validated DT neutron data, the neutron and gamma spectra from the small PuBe source (#T022), the neutron and gamma spectra from the large PuBe source (#M1170), and the gamma spectrum from the large ^{22}Na source (#T028).

Test of Modified FORIST Code

Upon modifying the FORIST unfolding code for use on the VAX 6420 mainframe and before using the new version to unfold data taken with the newly-constructed spectrometry system, the proper functioning of the FORIST code itself needs to be verified. To make this verification, a recoil proton data set from a DT neutron generator was provided by Hartley [12:-]. This set consists of the four spectral data files required by FORIST. Additionally, the appropriate inputs to ZSHIFT, summarized in Table 5, were supplied with the data. The unfolding run yielded the neutron spectrum shown in Figure 35. The expected DT neutron spectrum for this data set, which was taken at a 135° angle with respect to the beam, is a single peak at 13.6 MeV [12:-], which is what is observed in the plot. The x-axis of the plot shows the neutron energy in MeV, while the y-axis shows the relative intensity of each data point, in units of flux per MeV. A solid line connects the data points, while vertical error bars are plotted to show the +/- uncertainty in the relative intensities.

Table 5. Inputs to ZSHIFT for FORIST verification run

Spectral Parameters:		
HGAIN	0.0064	lu/ch
LGAIN	0.0720	lu/ch
ZI(1) (high gain)	2.37	ch
ZI(2) (low gain)	3.05	ch
HFNORM	298800	
HBNORM	460000	
LFNORM	192000	
LBNORM	593000	
FORIST Parameters:		
NBITS	23	
STRTCH	1.2	
NPUNCH	3	
ITRATE	1	
ERRER	3	
TAW	1.0	

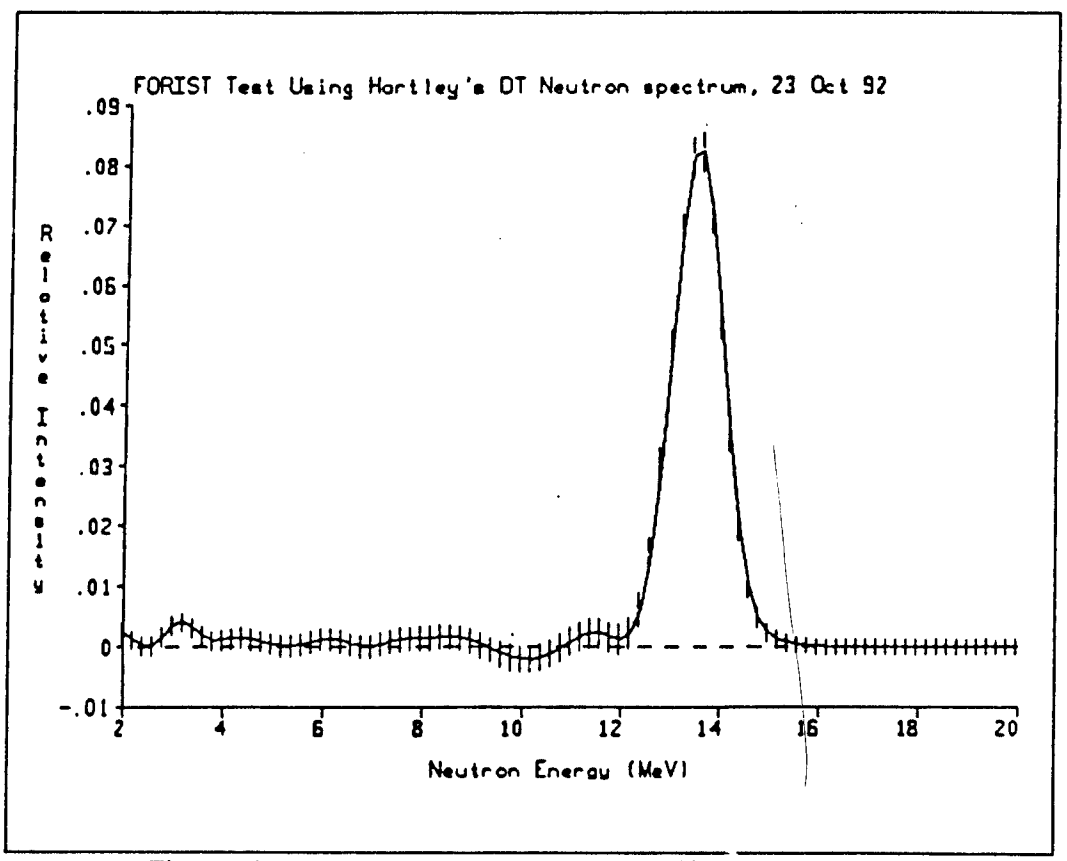

Figure 35. DT neutron spectrum used to verify correct operation of modified FORIST code

PuBe Source #T022

The recoil proton and Compton electron spectra of PuBe source #T022 were measured in the laboratory using the spectrometry system constructed for this project. They were then unfolded to yield the incident neutron and gamma spectra from the source.

The ZSHIFT input parameters for the neutron data set are given in Table 6 and the resulting unfolded PuBe neutron spectrum is shown in Figure 36. The peaks of the experimentally-determined spectrum in Figure 36 are compared with the accepted values for the PuBe peak energies [1:231] in Table 7. The agreement between the measured spectrum and the true spectrum is within the 5 - 10% uncertainty expected with the system. The unresolved peak at 1.4 MeV is not always observed in the accepted PuBe spectrum [1:341], while the observed peak at 5.3 MeV is probably an oscillation in the FORIST unfolding process. The plot in Figure 36 is the result of the 0^{th} smoothing iteration of FORIST, meaning that the spectrum has been smoothed but has not been iterated on using FORIST's "Iterated Smoothing Technique." The result generated after the first smoothing iteration was not used because FORIST interpreted most of the peaks as oscillations and tried to smooth them away.

Table 6. Inputs to ZSHIFT for PuBe #T022 neutron run

HGAIN	0.00631	lu/ch
LGAIN	0.0650	lu/ch
ZI(1) (high gain)	4.515	ch
ZI(2) (low gain)	5.580	ch
HFNORM	3600	sec
HBNORM	3600	sec
LFNORM	3600	sec
LBNORM	3600	sec

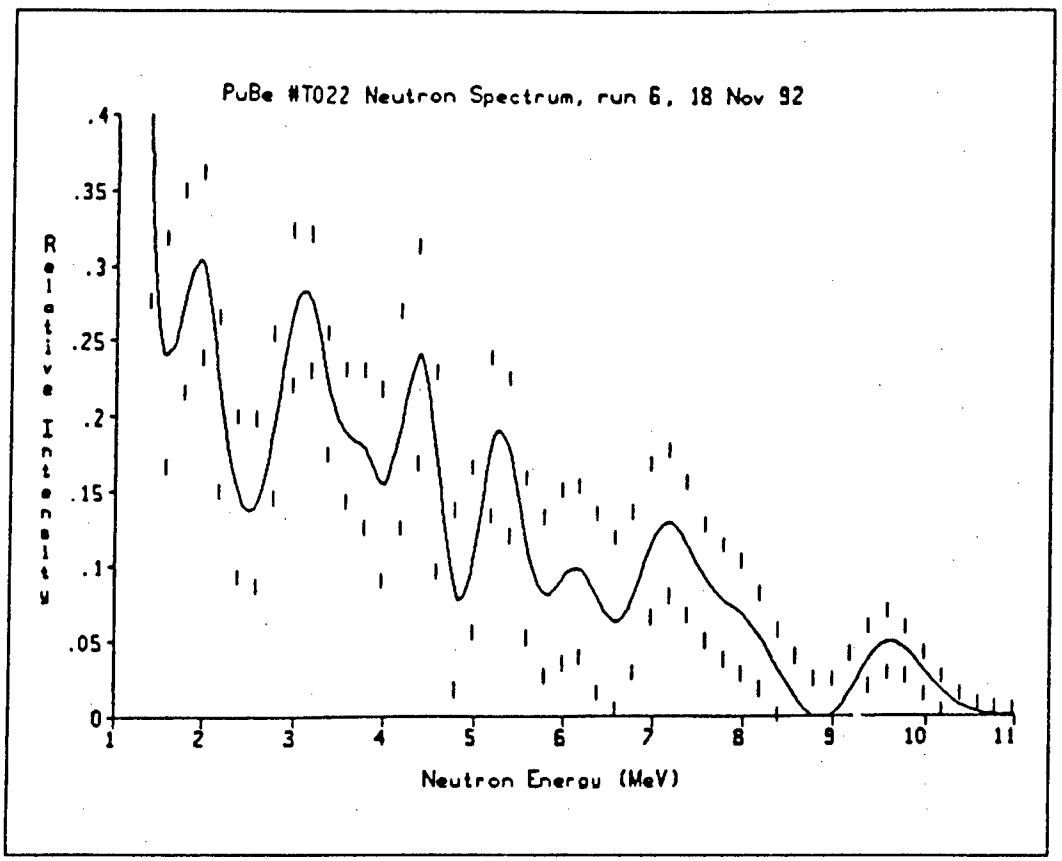

Figure 36. Experimentally-determined PuBe #T022 neutron spectrum

Table 7. Comparison of true PuBe neutron energies to measured PuBe #T022 spectrum

True Energy (MeV)	Observed Energy (MeV)	Error (%)
1.4	---	---
2.0	2.0	±0.0
3.1	3.1	±0.0
4.8	4.4	-8.3
---	5.3	---
6.6	6.2	-6.1
7.7	7.2	-6.5
9.8	9.6	-2.0

The ZSHIFT input parameters for the gamma data set are given in Table 8, while the resulting unfolded PuBe gamma spectrum is shown in Figure 37. The gamma peak of the experimental spectrum is at 4.25 MeV, while the true location of the peak is at

4.43 MeV [13:559], for an error of -4.1%, which is less than the system uncertainty of 5-10%. The results of the first smoothing iteration were used, as they gave the best resolution of the peak.

Table 8. Inputs to ZSHIFT for PuBe #T022 gamma run

HGAIN	0.00631	lu/ch
LGAIN	0.0650	lu/ch
ZI(1) (high gain)	4.515	ch
ZI(2) (low gain)	5.580	ch
HFNORM	1800	sec
HBNORM	1800	sec
LFNORM	1800	sec
LBNORM	1800	sec

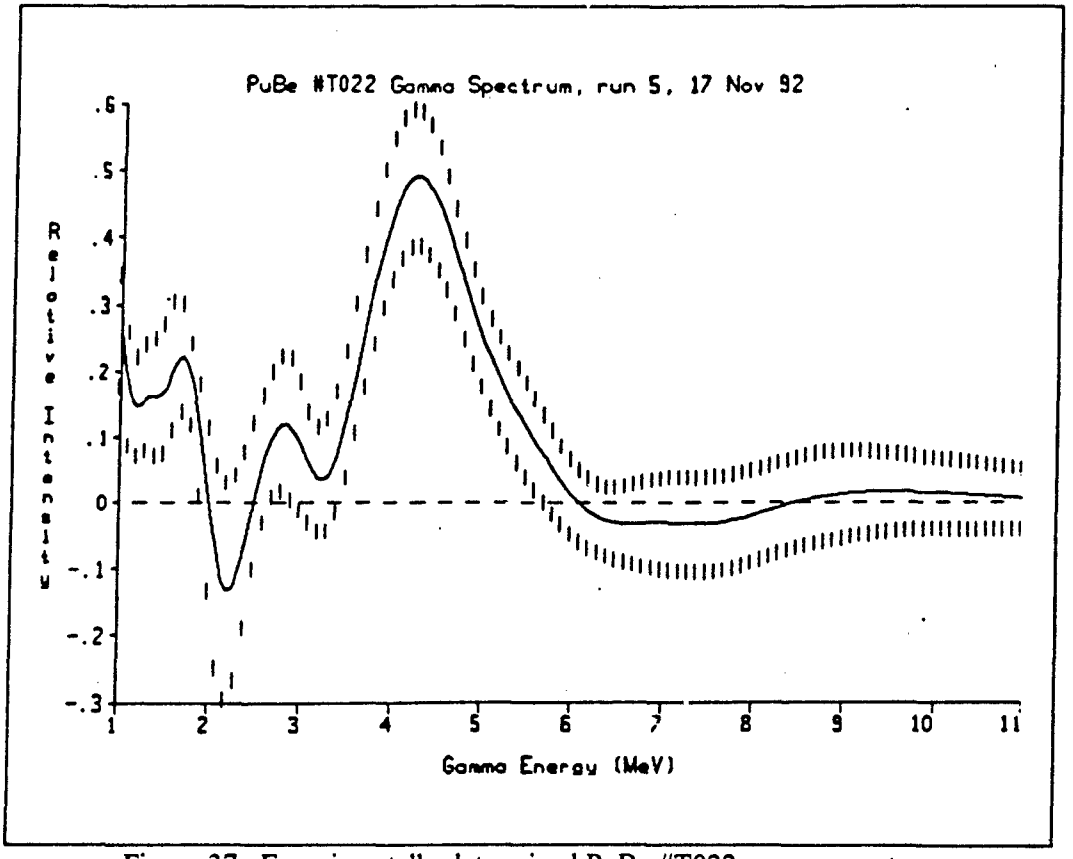

Figure 37. Experimentally-determined PuBe #T022 gamma spectrum

PuBe Source #M-1170

The recoil proton and Compton electron spectra of PuBe source #M-1170 were also measured in the laboratory and unfolded using FORIST.

The ZSHIFT input parameters for the neutron data set are given in Table 9 and the resulting unfolded PuBe neutron spectrum is shown in Figure 38. The peaks of the experimentally-determined spectrum in Figure 38 are compared with the accepted values for the PuBe peak energies [1:231] in Table 10.

Table 9. Inputs to ZSHIFT for PuBe #M-1170 neutron run

HGAIN	0.00640	lu/ch
LGAIN	0.0663	lu/ch
ZI(1) (high gain)	4.005	ch
ZI(2) (low gain)	5.509	ch
HFNORM	900	sec
HBNORM	900	sec
LFNORM	900	sec
LBNORM	900	sec

The agreement between the true and measured spectra is, again, less than the 5-10% uncertainty associated with the spectrometry system. The peak at 1.4 MeV remains unresolved, while peaks caused by FORIST oscillations show up at 4.2 and 7.2 MeV. The plot in Figure 38 is the 0^{th} smoothing iteration plot, as the peak information was smoothed out in the first smoothing iteration. Note from the error bars that even though the counting time for this spectrum was just one fourth of the counting time for the #T022 neutron spectrum, the error was smaller for the #M-1170 source. This is because the #M-1170 source was enough stronger that several times more counts were recorded in the lab, even though the counting time was much shorter.

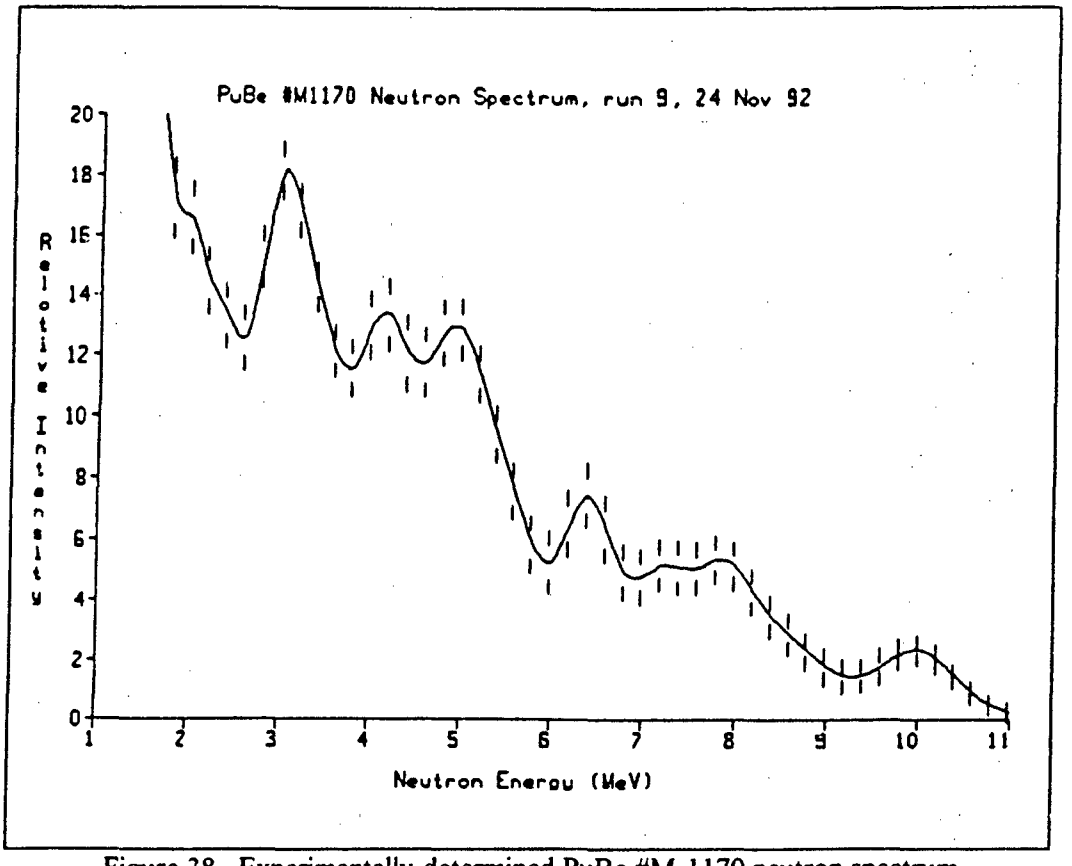

Figure 38. Experimentally-determined PuBe #M-1170 neutron spectrum

Table 10. Comparison of true PuBe neutron energies to measured PuBe #M-1170 spectrum

True Energy (MeV)	Observed Energy (MeV)	Error (%)
1.4	---	---
2.0	2.0	±0.0
3.1	3.0	-3.2
---	4.2	---
4.8	4.9	+2.1
6.6	6.4	-3.0
---	7.2	---
7.7	7.8	+1.3
9.8	10.0	+2.0

The ZSHIFT input parameters for the gamma data set are given in Table 11, while the resulting unfolded gamma spectrum is shown in Figure 39. The gamma peak of the

experimental spectrum is at 4.40 MeV, while the true location of the peak is at 4.43 MeV [13:559], for an error of -0.7%, which is again well within the uncertainty limits of the spectrometry system. The features below 3.5 MeV are FORIST oscillations. Again notice that the error bounds on the spectrum are much smaller than for the #T022 result, due to the better counting statistics. The results of the first smoothing were again used for the gamma plot.

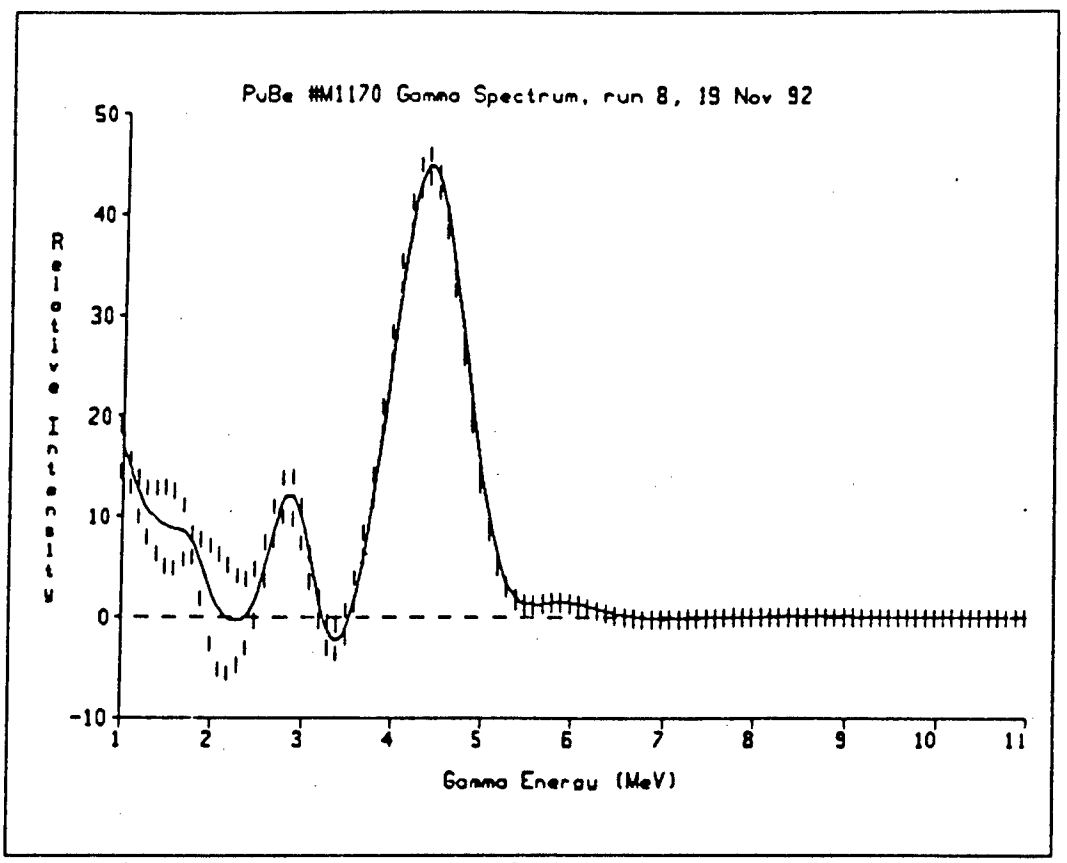

Figure 39. Experimentally-determined PuBe #M-1170 gamma spectrum

Table 11. Inputs to ZSHIFT for PuBe #M-1170 gamma run

HGAIN	0.00631	lu/ch
LGAIN	0.0650	lu/ch
ZI(1) (high gain)	4.515	ch
ZI(2) (low gain)	5.580	ch
HFNORM	1800	sec
HBNORM	1800	sec
LFNORM	1800	sec
LBNORM	1800	sec

Na-22 Source #T028

As a final check on the operation of the spectrometry system, the gamma spectrum from the large ^{22}Na source was measured and unfolded. The ZSHIFT input parameters for the run are given in Table 12, while the resulting unfolded ^{22}Na gamma spectrum is shown in Figure 40. The 0.511 MeV peak was not resolved because the FORIST gamma response matrix does not go below 0.8 MeV, but the higher-energy peak was very-well resolved. The measured energy for the second peak was 1.275 MeV, which was exactly the energy expected. The counting statistics were also very good for this run, as is shown by the very small error bars. The plot in Figure 40 is from the first smoothing iteration of FORIST, as were the other gamma results presented previously.

Table 12. Inputs to ZSHIFT for ^{22}Na #T028 gamma run

HGAIN	0.00646	lu/ch
LGAIN	0.0655	lu/ch
ZI(1) (high gain)	0.926	ch
ZI(2) (low gain)	2.180	ch
HFNORM	3600	sec
HBNORM	3600	sec
LFNORM	3600	sec
LBNORM	3600	sec

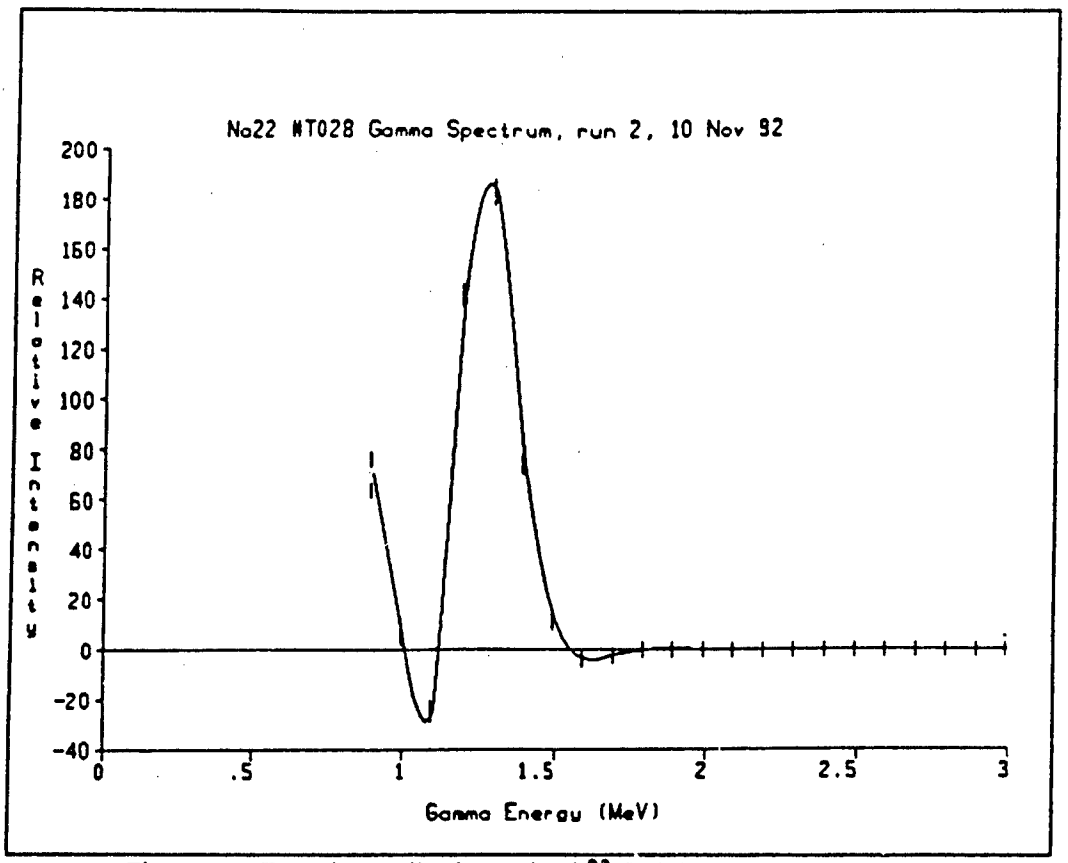

Figure 40. Experimentally-determined ^{22}Na #T028 gamma spectrum

VI. Summary and Conclusions

In summary, the goal of this thesis was to construct and test a neutron and gamma spectrometry system and to write a detailed manual for the use of this system. The detector used in the system was a xylene-based organic scintillator and the distinction between gamma and neutron events in the scintillator was made on the basis of pulse shape discrimination. The recoil proton and Compton recoil electron spectra recorded with this system were unfolded using the FORIST computer code.

This thesis first discussed the theory of pulse shape discrimination, spectrum unfolding, and energy calibration. It then described all of the apparatus used in the spectrometry system, including all of the computer software associated with the system. Then a detailed user's guide to the system was presented, from initial setup through plotting the unfolded results. Finally, the results of the tests made on the system were given.

The experimental results can be summarized in the following way. The unfolding of Hartley's DT data set verified that FORIST still produced the correct results after the modifications made to the code in order to allow it to run on the VAX 6420 mainframe. The results of the three gamma data runs (PuBe #T022, PuBe #M-1170, and ^{22}Na #T028) indicate that the spectrometry system is correctly detecting and unfolding incident gamma events. The results of the two neutron data runs (PuBe #T022 and PuBe #M-1170) also show good agreement with the accepted PuBe neutron spectrum, so the system is correctly detecting and unfolding incident neutron events, as well. The discrepancies in shape between the measured spectra and the accepted spectrum are, in all likelihood, due to the high-scattering environment in which the measurements were made.

The high scattering geometry would be much more likely to affect the neutron spectrum than the gamma spectrum.

Some further tests with other neutron sources are recommended as new sources become available. The PuBe neutron spectrum is quite complicated, so it is not the easiest source to use as an initial test for a neutron spectrometer. Better sources to use, because of their relative simplicity, would be a DT neutron generator and a ^{252}Cf spontaneous-fission source.

A better, lower-scattering geometry also should be used in future runs with this spectrometer. The room in which the thesis measurements were made was good from a standpoint of radiation safety, but the proximity of the desktop and walls made it far from optimum from a low-scattering point of view. A better setup would be to put the source, detector, and shadow shield on tripods in the center of a much larger room, in order to get as far as possible from all scattering sources.

Future work should also be done with the FORIST and ZSHIFT codes. As it currently exists at the end of this thesis, the codes run successfully on the VAX 6420 mainframe and produce an output file which can be plotted using GRAPHICS.TK. The codes have also been commented to make them easier to understand. However, it is the opinion of this author that much more work could be done with these codes, such as improving the comments, improving the logic structure, and improving the plots and data generated in the FORIST.OUT file. Especially tedious in the current setup is the need to reformat the four input spectra by hand before running ZSHIFT. Ultimately, it would be much more convenient if the FORTRAN programs could be made to run on a PC. This would allow all of the FORTRAN and TK data processing software to be located on the same machine that is used to record the MCA data in the lab. This work could even turn out to be the subject of a future thesis.

Finally, now that this spectrometry system has been constructed and tested, the Air Force Nuclear Engineering Center at the Air Force Institute of Technology has a new tool to use in future research projects. These projects could include such things as building and calibrating an associated particle system for the Center's DT neutron generator or designing the Center's new hot cell facility to handle a strong ^{252}Cf source. This spectrometry system should turn out to be a tool that will serve the Center in many different applications for years to come.

Appendix A: Equipment List

The following is a list of the equipment used to build the detector and electronic circuit for the spectrometry system.

Table 13 Equipment list

ITEM	MANUFACTURER	MODEL	ID NUMBER
Liquid Scintillator 5.0 cm diameter 5.0 cm thickness	Bicron	BC-501A	B-9599-04
Plexiglass Light Pipe 5.0 cm diameter 1.6 cm thickness	AFIT Shop	none	none
Photomultiplier Tube	Hamamatsu	R329-02	RC4765
PMT base	Ortec	265	1959
High Voltage Supply	Ortec	556	1928
Preamplifier	Ortec	113	6508
Delay Line Amplifier	Ortec	460	2014
Pulse Shape Analyzer	Ortec	458	567
Gate and Delay Generator	Ortec	416A	3639
Delay Amplifier	Ortec	427A	1272
Amplifier	Ortec	572	4716
Analog-to-Digital Converter	Nuclear Data	ND570	76-1234
Multi-Channel Analyzer	Nuclear Data	AccuSpec	Ver 01
Oscilloscope	LeCroy	9410	2435

Appendix B: The Plutonium-Beryllium Source

Two ^{239}Plutonium-^{9}Beryllium (α,n) sources were used in this research project to provide neutrons in the presence of gammas. The first was a small, 78-mCi source (Monsanto Research Corporation, #T022) in a tantalum and stainless steel cylinder with a diameter of 1.25 cm and a height of 1.40 cm. The cylinder was attached to the end of a plastic rod for handling, and the detector was placed along the axis of symmetry of the cylinder opposite to the rod. The second was a larger, 4.7-Ci source (Monsanto Research Corporation, #M-1170) in a tantalum and stainless steel cylinder with a diameter of 2.59 cm and a height of 14.02 cm [22:1]. The cylinder was attached to the end of an aluminum rod for handling, and the detector was placed perpendicular to the axis of symmetry of the cylinder.

The stable isotope of beryllium, ^{9}Be, has a relatively loosely-bound neutron (1.7 MeV binding energy). If a typical alpha particle from a radioactive decay (5-6 MeV) strikes a ^{9}Be nucleus, a neutron can be released :

$$^{4}\alpha + {}^{9}\mathrm{Be} \rightarrow {}^{12}\mathrm{C} + \mathrm{n}$$

If the beryllium is mixed with a long-lived alpha-emitting material, such as ^{239}Pu, there will be a nearly constant rate of neutron production [19:445].

However, the neutron spectrum from this source is not a simple one. Plutonium-239 can alpha decay by emitting an alpha particle with any one of several different energies. The primary energies and probabilities are 5.1554 MeV (73.3%), 5.1429 MeV (15.1%), and 5.1046 MeV (11.5%), but the range extends from 4.640 to 5.1554 MeV [21:1464]. Additionally, the product to which ^{239}Pu alpha-decays (U-235) also decays by alpha emission. A process of alpha and beta decay continues until a stable isotope of lead is reached. To further complicate the alpha emission spectrum, small

amounts of contaminant alpha activity, present in either the original sample, produced through the decay of a precursor, or produced through decay of a nuclide produced in a neutron capture reaction can influence the overall neutron yield. The isotope ^{241}Pu is particularly significant, because it beta decays with a half-life of 13.2 years to form Americium-241, which is a strong alpha-emitter. The neutron yield of this source can therefore gradually increase with time as the Am accumulates in the source. An original Pu-241 isotopic fraction of 0.7% will result in a growth rate of the neutron yield of 2% per year until an equilibrium state is reached [17:24]. The radioactive production/decay series is shown in Figure 41.

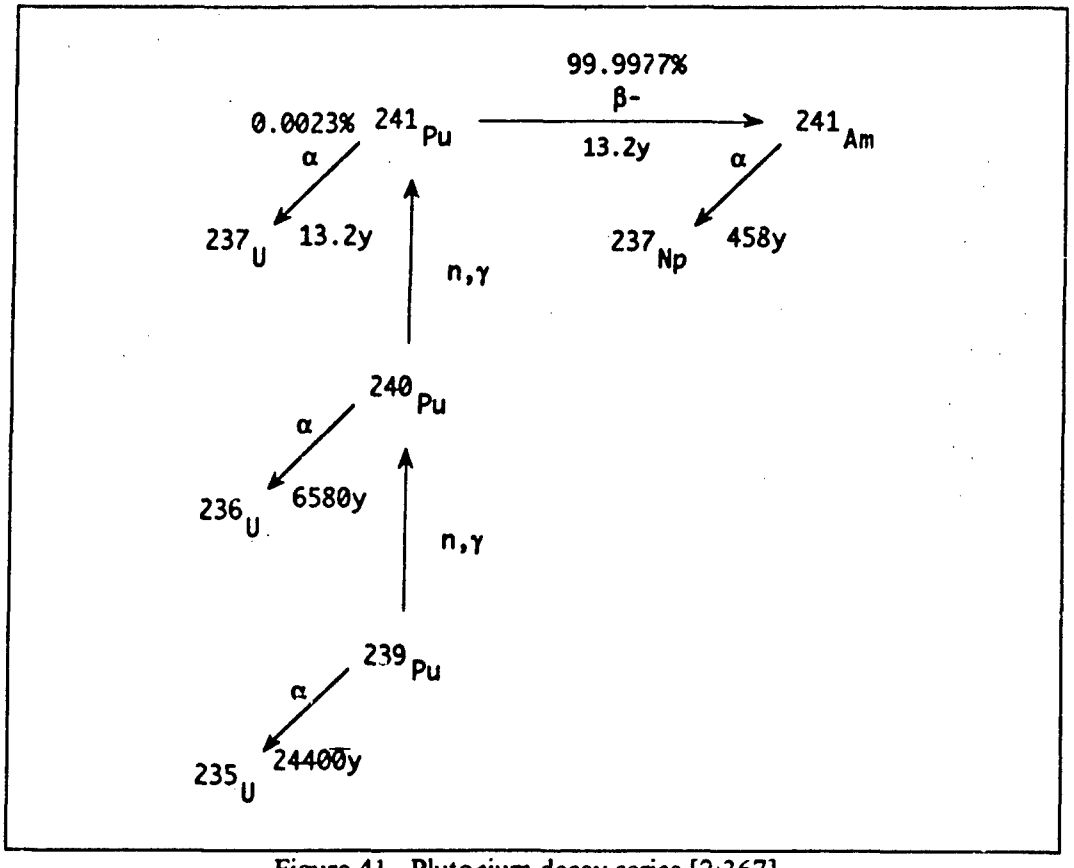

Figure 41. Plutonium decay series [2:367]

From ^{239}Pu and its products, there are alphas emitted within an approximate energy range of 1 to 6 MeV. The ^{9}Be(α,n)^{12}C reaction can leave the product carbon nucleus in its ground state or in its first or second excited states. These three states of the product carbon atom result in reaction Q-values of 5.704, 1.29, and -1.95 MeV, respectively [30:436]. Therefore, we expect to find neutrons with an energy spectrum from 0 to almost 12 MeV ($E_\alpha + Q$). The neutrons produced, then, are not monoenergetic for several reasons. These reasons are [19:445]:

1. the many different energies of the alphas produced,
2. the slowing of alphas that will occur by collision in the source material,
3. the various directions of neutron emission that can occur relative to the incoming alphas (whose directions are not known),
4. the possibility that the ^{12}C is left in one of three different energy states, and
5. the possibility that the ^{9}Be participates in a multibody breakup reaction:

$$^{4}\alpha + {}^{9}\mathrm{Be} \rightarrow {}^{4}\alpha + {}^{8}\mathrm{Be} + \mathrm{n}$$

which produces neutrons of a different energy than those from a two-body breakup [30:435].

Furthermore, once the neutrons are produced, their energies may be modified before leaving the source by one or more of the following processes [20:175]:

1. elastic scattering with materials in the source,
2. the ^{9}Be(n,2n) reaction:

$$\mathrm{n} + {}^{9}\mathrm{Be} \rightarrow {}^{8}\mathrm{Be} + \mathrm{n} + \mathrm{n}$$

3. or the ^{239}Pu(n,f) fission reaction:

$$\mathrm{n} + {}^{239}\mathrm{Pu} \rightarrow \text{fission fragments} + (1 \text{ to } 4)\ \mathrm{n}$$

Vijaya and Kumar [30:-] and Kumar and Nagarajan [20:-] calculated the theoretical neutron spectrum from a ^{9}Be(α,n) source in the following manner. The

neutron energy distributions from the $^{9}Be(\alpha,n)^{12}C$ reaction, leaving the ^{12}C in different energy states, were calculated using the equation [30:436]:

$$f_i(E_n) = N_{Be} \int_{(E_\alpha^{min})_i}^{(E_\alpha^{max})_i} \frac{1}{\varepsilon(E_\alpha)} \frac{1}{\Delta E_n'(E_\alpha)} \left[\frac{d\sigma}{d\Omega}(\Theta, E_\alpha)\right]_i dE_\alpha \qquad (14)$$

where

i = index of energy states of ^{12}C,

N_{Be} = number density of beryllium atoms in the source,

E_α^{min} = lowest value of alpha energy,

E_α^{max} = highest value of alpha energy,

$\varepsilon(E_\alpha)$ = stopping power for alpha particles of energy E_α in the source material,

$\{d\sigma/d\Omega(\Theta, E_\alpha)\}_i$ = the center-of-mass differential cross-section at alpha energy E_α and center-of-mass angle Θ for the i^{th} excitation.

The term $\Delta E_n(E_\alpha)$ is given by [30:436]:

$$\Delta E_n'(E_\alpha) = \frac{(E_\alpha M_n M_\alpha)^{1/2}}{2\pi(M_n + M_C)} \times \left\{\frac{1}{(M_n + M_C)}\left[\frac{E_\alpha M_n M_\alpha}{(M_n + M_C)} + E_\alpha(M_n - M_\alpha) + M_C Q_i\right]\right\}^{1/2} \qquad (15)$$

where M_n, M_α, and M_C are the masses of the neutron, alpha particle, and carbon atom, respectively.

The results of this calculation, $f_1(E_n)$, $f_2(E_n)$, and $f_3(E_n)$, are the neutron energy distributions from the $^{9}Be(\alpha,n)^{12}C$ reaction leaving the ^{12}C in the ground, first, and second-excited states, respectively. Similarly, the neutron energy distribution from the

multibody breakup reaction, which gives rise to a low energy neutron continuum, is computed using [30:437]:

$$f_{continuum}(E_n) = N_{Be}\int_{E_\alpha^{min}}^{E_\alpha^{max}} \frac{1}{\varepsilon(E_\alpha)}\left|\frac{d\sigma}{dE_n}(E_\alpha)\right|_{E_n} dE_\alpha \qquad (16)$$

where $|d\sigma/dE_n(E_\alpha)|_{En}$ is the energy differential cross section at bombarding energy E_α resulting in a neutron of energy E_n. The primary calculated neutron spectrum is then obtained by adding f_1, f_2, f_3, and $f_{continuum}$, as shown in Figure 42.

Modifications to the neutron spectrum caused by the three processes listed above were made to the primary spectrum with the help of a Monte Carlo code. Elastic scattering causes smearing of peaks, while the (n,2n) and (n,*f*) reactions boost the low energy part of the spectrum.

A PuBe neutron source has a neutron production rate of about $2x10^6$ neutrons per second for each Ci of ^{239}Pu [19:446], so the 78-mCi source is producing approximately $1.6x10^5$ neutrons per second, while the 4.7-Ci source is producing approximately $9.4x10^7$ neutrons per second.

In addition to producing neutrons, the PuBe source produces a significant gamma ray spectrum. These gammas result from neutron capture reactions in the heavy nuclides in the source, de-excitation of product nuclides after an alpha decay, and energetic scatters of neutrons with materials in the source and source casing. The primary gamma energy is at 4.43 MeV and is caused by the de-excitation of ^{12}C from its first excited state to its ground state after it has been produced in the $^9Be(\alpha,n)^{12}C$ reaction [13:559;21:11].

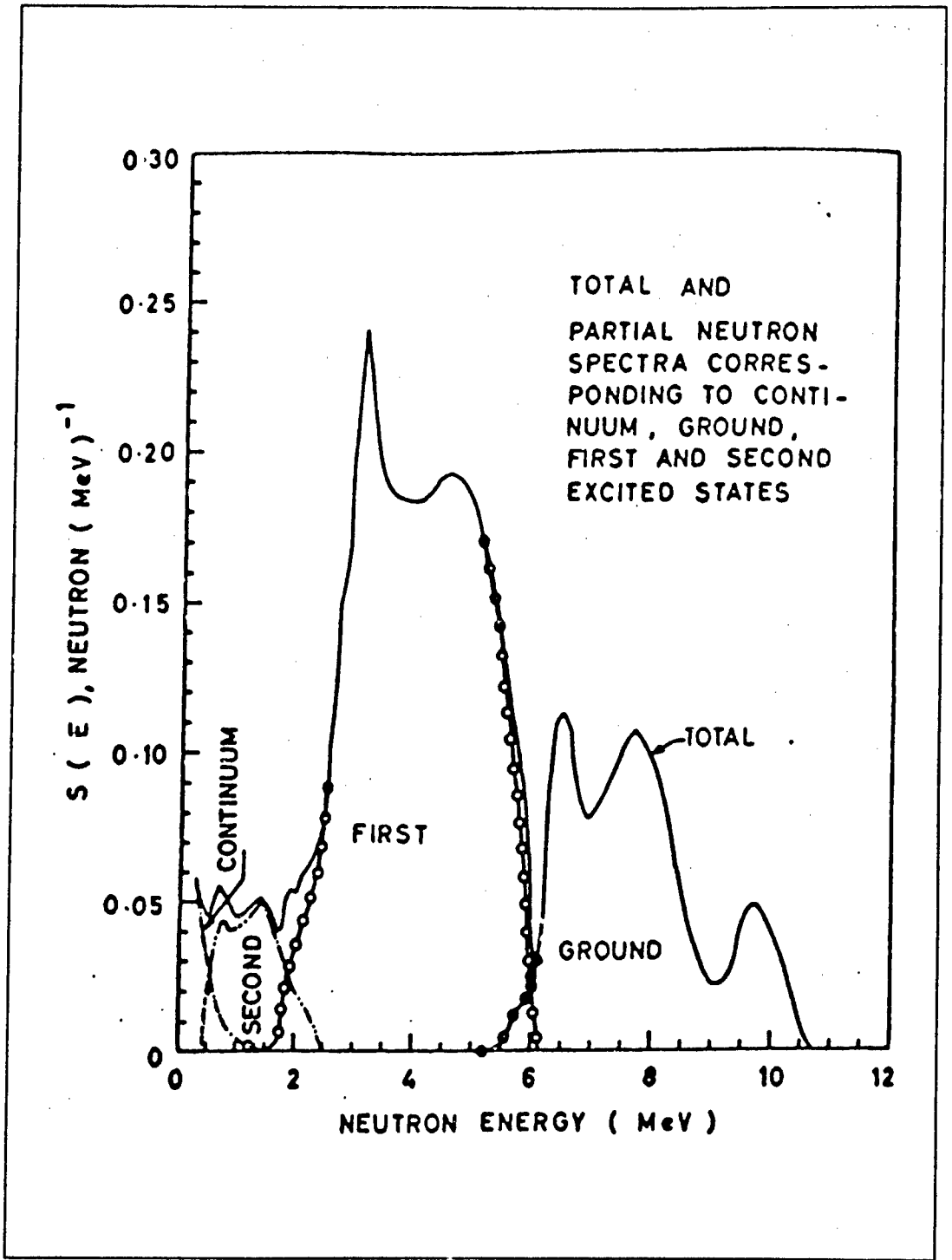

Figure 42. Theoretical spectrum of a ^{239}PuBe source showing total and partial neutron spectra corresponding to continuum, ground, first, and second excited states of ^{12}C [20:176]

Appendix C: CALIBER.TK Computer Model

VARIABLE SHEET — For Academic Use Only

St	Input	Name	Output	Unit	Comment
					Caliber.TK 7 Nov 92
					by Robert S. Pope
					A PROGRAM TO CALIBRATE THE PSD
					NEUTRON/GAMMA SPECTROMETER USING
					INFORMATION FROM THE NA-22 SOURCE
					-----CALCULATE 1/2 HEIGHT OF PEAK---
L	0	PkCts1			cts in peak 1
L	0	PkCts2			cts in peak 2
L		Cts1			cts in 1/2 height of peak 1
L		Cts2			cts in 1/2 height of peak 2
					-----LINEAR INTERPOLATION ROUTINE-----
	48	x1		ch	high point channel
	3418	y1		cts	high point counts
		x2		ch	low point channel (calc as x1 + 1)
	3023	y2		cts	low point counts
		x3		ch	desired point channel (ANSWER)
	3264.5	y3		cts	desired point counts
		m		cts/ch	slope
					-----PEAK 1 POSITION ROUTINE-----
	4	n			number of MCA spectra
	75	x			input: amp_gain = 75
		A			output from LeastSquare function
		B			output from LeastSquare function
		y		ch	desired result -- peak 1 1/2 HT
					-----GAIN ROUTINE-----------
	.341	E1		MeV	gamma1 max compton electron energy
	1.062	E2		MeV	gamma2 max compton electron energy
	48.388608	x1_h		ch	location of gamma1 at high gain
	142.23239	x2_h		ch	location of gamma2 at high gain
		m_h	.00768298	MeV/ch	slope at high gain
		b_h	-.0307687	MeV	y-intercept at high gain
		z_h	4.0047917	ch	zero intercept at high gain (RESULT)
		G_h	.00640248	lu/ch	high gain (RESULT)
	9.7522036	x1_l		ch	location of gamma1 at low gain
	18.864485	x2_l		ch	location of gamma2 at low gain
		m_l	.07912398	MeV/ch	slope at low gain
		b_l	-.4306332	MeV	y-intercept at low gain
		z_l	5.4425117	ch	zero intercept at low gain (RESULT)
		G_l	.06593665	lu/ch	low gain (RESULT)

LIST SHEET — For Academic Use Only

Name	Elements	Unit	Comment
			--INPUT THESE 5 LISTS FROM THE 22NA DATA--
amp_gain	4		ORTEC 572 Amplifier gain setting
peak1	4		channel location of peak 1
peak2	4		channel location of peak 2
PkCts1	4		counts in peak 1
PkCts2	4		counts in peak 2
			--THESE 2 LISTS ARE OUTPUT BY 1/2 HT ROUTINE--
Cts1	4		counts in 1/2 height of peak 1
Cts2	4		counts in 1/2 height of peak 2
			--FILL THESE 2 LISTS BY HAND WITH
			RESULTS OF LINEAR INTERPOLATION ROUTINE--
p1_12	4		channel location of 1/2 height of peak 1
p2_12	4		channel location of 1/2 height of peak 2

```
─────────── RULE SHEET ─────────────── For Academic Use Only
S Rule──────────────────────────────────────────────────────
  "--FIND COUNTS IN 1/2 HEIGHT OF PEAKS
* Cts1 = PkCts1 * 1/2
* Cts2 = PkCts2 * 1/2

  "--LINEAR INTERPOLATION ROUTINE
C m * (x2 - x1) = y2 - y1
C m * (x3 - x1) = y3 - y1
C x2 = x1 + 1

  "--COMPUTATION OF PEAK 1 POSITION USING LEAST SQUARES FIT TO PEAK 1 DATA
C Call LeastSquare(n;A,B)
C y = A + B*x

  "--GAIN ROUTINE
C m_h = (E2 - E1) / (x2_h - x1_h)
C b_h = E2 - m_h * x2_h
C z_h = -b_h / m_h
C G_h = 0.885 / (x2_h - z_h)

C m_l = (E2 - E1) / (x2_l - x1_l)
C b_l = E2 - m_l * x2_l
C z_l = -b_l / m_l
C G_l = 0.885 / (x2_l - z_l)

─────────── PROCEDURE FUNCTION: LeastSquare ─── For Academic Use Only
Comment:              Least Square function to calculate peak1 1/2 loc. at G_l
Parameter Variables:
Input Variables:      n
Output Variables:     A,B
S Statement─────────────────────────────────────────────────
  sumX = 0
  sumY = 0
  sumX2 = 0
  sumXY = 0
  for i = 2 to n
     sumX = sumX + 'amp_gain[i]
     sumY = sumY + 'pl_l2[i]
     sumX2 = sumX2 + ('amp_gain[i])^2
     sumXY = sumXY + 'amp_gain[i] * 'pl_l2[i]
  next i
  count = n - 1
  delta = count * sumX2 - sumX^2
  A = (sumX2 * sumY - sumX * sumXY) / delta
  B = (count * sumXY - sumX * sumY) / delta

─────────── PLOT SHEET ─────────────── For Academic Use Only
Name──────── Plot Type── Display Option── Output Device── Title──────────
peak_plot    Line chart  1.EGA                            Peak positions vs amp
gamma1_plot  Line chart  1.EGA                            Peak 1:  peak and 1/2

─────────── TABLE SHEET ─────────────── For Academic Use Only
Name──────────── Title──────────────────────────────────────
peak_table       Peak positions vs amp gain
pk1_cts_table    Peak 1:  Counts in peak and 1/2 height
pk2_cts_table    Peak 2:  Counts in peak and 1/2 height
```

Appendix D: ZSHIFT.FOR Computer Code

```
      PROGRAM ZSHIFT
C=======================================================================
C          This program creates an input file for the FORIST spectrum
C     unfolding code.  This file, called SPECTRA.IN, contains:
C       - the name of the response matrix file
C       - input parameters which govern the operation of FORIST
C       - the gain and zero shift for each spectrum
C       - the four compressed and shifted spectra.
C
C     Input files used by ZSHIFT.FOR:
C       - four files containing the MCA spectral data from the
C         laboratory
C
C     Output files created by ZSHIFT.FOR:
C       - ZSHIFT.OUT, which is intended for debugging purposes
C       - SPECTRA.IN, which is the input file for FORIST
C
C     User-inputs required by ZSHIFT.FOR:
C       - all user-inputs are in the two boxed sections below.
C         There is a section for spectral information and
C         identification and a section for FORIST parameters.
C
C     Original ZSHIFT.FOR code provided by Dr. Nolan E. Hertel.
C     Updated and modified by Robert S. Pope in November 1992.
C-----------------------------------------------------------------------
      INTEGER ERRER
      REAL LFNORM,LBNORM,LGAIN
      CHARACTER*6 TITLE
      CHARACTER*12 FILE
      CHARACTER*80 SKIP,INFORM,FMT1,FMT2,IDENT,RMATRIX
      DIMENSION Y(513),YC(513),IDENT(4),TITLE(4),FILE(4),ZI(4),SHC(4)
      OPEN (UNIT=6,FILE='ZSHIFT.OUT' ,STATUS='NEW')
      OPEN (UNIT=7,FILE='SPECTRA.IN',STATUS='NEW')
C- - - - - - - - - - - - - - - - - - - - - - - - - - - - - - - - - - - -
C     Spectrum identification and information
C
C ** Input/Output identification:
C    FILE(n) are the 4 files containing the MCA spectral data.  These
C    must be in the order:
C      1 = high gain foreground
C      2 = low gain foreground
C      3 = high gain background
C      4 = low gain background
C    TITLE(n) are the 6-character labels used in SPECTRA.IN and
C    FORIST.OUT
C    IDENT(n) are the 80-character titles used in SPECTRA.IN and
C    FORIST.OUT
C    IDENTY = the ID number of the data run
C **
      FILE(1) = 'PUBE_R9.HFN'
      FILE(2) = 'PUBE_R9.LFN'
      FILE(3) = 'PUBE_R9.HBN'
      FILE(4) = 'PUBE_R9.LBN'
      TITLE(1) = 'PB9HFN'
```

```
      TITLE(2) = 'PB9LFN'
      TITLE(3) = 'PB9HBN'
      TITLE(4) = 'PB9LBN'
      IDENT(1) = 'PuBe #M1170 run 9 neutrons hgf, 24 Nov 92'
      IDENT(2) = 'PuBe #M1170 run 9 neutrons lgf, 24 Nov 92'
      IDENT(3) = 'PuBe #M1170 run 9 neutrons hgb, 24 Nov 92'
      IDENT(4) = 'PuBe #M1170 run 9 neutrons lgb, 24 Nov 92'
      IDENTY = 9
C ** Zero intercept in channels [1=high gain, 2=low gain]:
      ZI(1) = 4.005
      ZI(2) = 5.509
C ** Gain in light units per channel:
      HGAIN = 0.00640
      LGAIN = 0.0663
C ** Normalization -- counting time in seconds for each spectrum:
      HFNORM = 000900
      HBNORM = 000900
      LFNORM = 000900
      LBNORM = 000900
C ** Format of data to be input from MCA data files:
C      SKIP = format line, one "/" for each header line to be skipped
C      INFORM = format line, each line of MCA data
C      M = Number of MCA channels in input spectra:
C **
      SKIP = '(////////////////////////////////////////////////////)'
      INFORM = '(1X,8F7.0)'
      M = 256
C ** Name of response matrix file to be used by FORIST:
C      UINEUT.MAT or NEUTRON.MAT for neutrons, GAMMA.MAT for gammas
C **
      RMATRIX = 'UINEUT.MAT'
C
C    Parameters for FORIST
C
C ** Number of bits of machine precision:
C      NBITS = 36 for CDC 1604
C      NBITS = 27 for IBM 7090
C      NBITS = 23 for VAX 6420
C      NBITS = 22 for IBM 360
C **
      NBITS=23
C ** Window width multiplier:
      STRTCH=1.0
C ** Punching option:  governs spectral data output in PUNCH.OUT
C    and TOGRAPH.OUT files from FORIST
C      0 = none
C      1 = smoothed spectrum data
C      2 = unsmoothed spectrum data
C      3 = both smoothed and unsmoothed
C **
      NPUNCH=3
C ** Number of smoothing iterations:
      ITRATE=1
C ** Desired statistical error in percent:
      ERRER=3
C ** Constraint weight:
      TAW=10.0
C- - - - - - - - - - - - - - - - - - - - - - - - - - - - - - - - - - - -
```

```
      FMT1 ='DYNMAT  1000  10  (1X,A6,I4,10F7.0)'
      FMT2 ='DYNMAT  2000  10  (1X,A6,I4,10F7.0)'
      ZI(3) = ZI(1)
      ZI(4) = ZI(2)
      SHC(1) = ZI(1) - 0.5
      SHC(2) = ZI(2) - 0.5
      SHC(3) = SHC(1)
      SHC(4) = SHC(2)
      WRITE(6,698) RMATRIX
 698  FORMAT(1X,'NAME OF RESPONSE MATRIX USED IN PROBLEM =',A80)
      WRITE(7,699) RMATRIX
 699  FORMAT(1X,A80)
      WRITE(7,700) NBITS,STRTCH,IDENTY,NPUNCH,ITRATE,ERRER,TAW
 700  FORMAT(1X,I10,F10.3,4I10,F10.4)
      WRITE(7,701) HFNORM,LFNORM
      WRITE(7,701) HBNORM,LBNORM
      WRITE(7,709) HGAIN,LGAIN
      WRITE(7,709) HGAIN,LGAIN
 701  FORMAT(1X,2F10.0)
 709  FORMAT(1X,2F10.4)
      DO 100, ITER=1,4
         OPEN (UNIT=ITER,FILE=FILE(ITER),STATUS='OLD')
         READ(ITER,SKIP)
         READ(ITER,INFORM)(Y(I),I=1,M)
         WRITE(6,601)M,ZI(ITER)
 601     FORMAT(10X,I3,1X,'CHANNEL ORIGINAL SPECTRUM'/
     +   10X,'ZERO INTERCEPT =',F7.3)
         WRITE(6,620)TITLE(ITER)
 620     FORMAT(10X,A6)
         WRITE(6,602)(Y(I),I=1,M)
         CALL SHIFTY(Y,YC,M,SHC(ITER))
         WRITE(6,603)M
         WRITE(6,602)(YC(I),I=1,M)
 602     FORMAT(8F10.0)
 603     FORMAT(10X,I3,1X,'CHANNEL ZERO-SHIFTED SPECTRUM')
         N=200
         IF(MOD(ITER,2) .NE. 0) THEN
            WRITE(7,702) FMT1
         ELSE
            WRITE(7,702) FMT2
         END IF
         WRITE(7,702) IDENT(ITER)
 702     FORMAT(1X,A80)
         DO 10 I=1,N
            Y(I)=YC(I)
  10     CONTINUE
         WRITE(6,604)
 604     FORMAT(10X,'200 CHANNEL SUMMED AND SHIFTED SPECTRUM'
     +   ,' FOR INPUT TO FORIST.FOR')
         NM=N-9
         DO 11 IB=1,NM,10
            IE=IB+9
            WRITE(6,605) TITLE(ITER),IB,(Y(I),I=IB,IE)
 605        FORMAT(1X,A6,1X,I3,1X,10F8.0)
            WRITE(7,606)TITLE(ITER),IB,(Y(I),I=IB,IE)
 606        FORMAT(1X,A6,1X,I3,10F7.0)
  11     CONTINUE
         CLOSE (ITER)
```

```
         IF(MOD(ITER,2) .EQ. 0) WRITE(7,703)
  100  CONTINUE
       WRITE(7,703)
  703  FORMAT(1X)
       CLOSE (6)
       CLOSE (7)
       STOP
       END
C=======================================================================
C                              SUBROUTINE SHIFTY
C          This routine performs a zero shift on a pulse height spectrum
C      using a linear interpolation scheme borrowed from the ALPHA-M
C      code.  The resulting spectrum is then compressed into 200 channels
C-----------------------------------------------------------------------
       SUBROUTINE SHIFTY(Y,YC,M,SHC)
       DIMENSION X(513),Y(513),XC(513),YC(513)
       NP = 0
       NP = INT(ABS(SHC)) + 1
C-----if zero intercept is positive, skip the following
       IF(SHC .LT. 0.0) THEN
          DO 10 I=1,M
             YC(I+NP) = Y(I)
    10    CONTINUE
          DO 11 I=1,NP
             YC(I)=0.0
    11    CONTINUE
          DO 12 I=1,M
             Y(I)=YC(I)
    12    CONTINUE
          SHC=SHC+1.*NP
       END IF
C-----
       DO 7 I=1,M
          XC(I)=I
          YC(I)=0.0
          X(I)=I*1.0 - SHC
    7  CONTINUE
       DO 60 I=1,M
          DO 40 J=1,M
             IF(XC(I)-X(J).EQ.0) THEN
   45           YC(I)=Y(J)
                GO TO 60
             ELSE IF(XC(I)-X(J).LT.0) THEN
   50           YC(I)=(Y(J)-Y(J-1))/(X(J)-X(J-1))
                YC(I)=Y(J-1) +YC(I)*(XC(I)-X(J-1))
                GO TO 60
             END IF
   40     CONTINUE
   60  CONTINUE
       RETURN
       END
```

Appendix E: FORIST.FOR Computer Code

```
      PROGRAM FORIST
C=======================================================================
C                    F O R I S T    ---    M A I N
C
C         A modification of the COOLC (FERDOR) unfolding code
C     by R.H. Johnson, Nuclear Engineering Program, University of
C     Illinois, 13 Feb 1975.
C         Modified by N.E. Hertel at UT Austin to read data related to
C     the response matrix and smoothing windows from tape UNIT 3.  Also
C     modified to do only one spectrum per run.
C         Modified once more by N.E. Hertel on 2 Apr 1980 to allow TAW
C     to be read in from the input data file (UNIT 5).
C         Modified by R.S. Pope at the Air Force Institute of
C     Technology in October 1992 to make the code run on the VAX and to
C     make the code FORTRAN 77 standard.  Also reorganized and better-
C     commented.
C
C     PURPOSE:
C         The FORIST code is used to unfold data from an NE-213 liquid
C     scintillator detector in order to generate the incident gamma or
C     neutron spectrum.
C
C     INPUTS:
C         All user-selectable inputs are contained in a file called
C     SPECTRA.IN, which is generated by the ZSHIFT.FOR program.  This
C     file contains the four spectra (high gain foreground, low gain
C     foreground, high gain background, and low gain background)
C     measured in the laboratory and the identification and information
C     about these spectra.  In addition, this file contains all user-
C     selectable parameters for FORIST, as well as the filename of the
C     appropriate input matrix.
C         For example, if FORIST is to unfold gammas, the two input
C     files would be:
C       - SPECTRA.IN -- the user input file
C       - GAMMA.MAT -- the response matrix for gammas
C     Details of the inputs to FORIST can be found in the ZSHIFT.FOR
C     code.
C
C     OUTPUTS:
C         The FORIST code generates four output files.  The first,
C     WORKING.IO is not intended to be read by the user.  It is simply
C     a file used during matrix manipulations in order to use less
C     memory during execution.
C         The second, FORIST.OUT, is a 25 to 30 page file which
C     contains information about the response matrix used and about the
C     input spectra.  The file then lists many of the results calculated
C     by the FORIST program during execution.  This file also contains
C     several graphs, none of which seem to be particularly useful.  The
C     best use for this file is in debugging.
C         The third file, PUNCH.OUT, contains data which can be used to
C     plot the unfolded spectrum computed by FORIST.  This particular
C     file is formatted to be read by a plotting routine on the CYBER.
C     Contact Dr. N. E. Hertel for information about this plotting
C     routine.
```

```
C          The fourth file, TOGRAPH.OUT, also contains data which can be
C     used to plot the unfolded spectrum computed by FORIST.  This file
C     was created during the 1992 modification and is meant to be read
C     by the commercially-available program "TK SOLVER!".  This file
C     contains the energy in eV, the relative counts
C     for each energy bin, and the error in the relative counts.  This
C     information is contained in single columns.  The spectral
C     information output to this file is dependent upon the punching
C     option chosen in the program ZSHIFT.FOR.  The last character of
C     each variable name in the file is an integer.  Like integers are
C     grouped together and, if there is more than one spectrum in the
C     file, the highest-valued number is the least-smoothed spectrum,
C     continuing in decending order to zero.
C
C     FOR ADDITIONAL INFORMATION:
C          "A User's Manual for COOLC and FORIST" by R. H. Johnson,
C     Purdue University, IN (1975) is available through RSIC and is
C     considered the standard manual on the FORIST code.  It develops
C     the theory nicely, but leaves much to be desired in the area of
C     actually operating the code.
C          "Construction and Testing of A Neutron and Gamma Spectrometry
C     System Using Pulse Shape Discrimination with an Organic
C     Scintillator" (AFIT/GNE/ENP/93M-6) by R. S. Pope, Air Force
C     Institute of Technology, Dayton, OH (1992) is a thesis which more
C     clearly presents the actual operation of the FORIST program and
C     associated software (ZSHFIT.FOR and TK SOLVER).
C
C-----------------------------------------------------------------------
      DIMENSION JDENT(20),IDENT(20)
      DIMENSION A(156,95),HT(156,95)
      DIMENSION B(156),S(156),UT(156),LLO(156),LUP(156)
      DIMENSION VLO(156),VUP(156),FORTE(156)
      DIMENSION W(95),Q(95),ATEMP(95),ELAB(95),X(95)
      DIMENSION PLO(111),PUP(111),WINW(111),PLAB(111),ERSAVE(111)
      DIMENSION WIND(111),ERRF(111)
      DIMENSION PLABLE(111,2)
      DIMENSION BS(156,2)
C
      COMMON A,HT
      INTEGER ERRER
      CHARACTER*80 RMATRIX
C
      EQUIVALENCE(ATEMP,X)
      EQUIVALENCE(PLABLE(1,1),PLAB(1))
      EQUIVALENCE(PLABLE(1,2),WINW(1))
      EQUIVALENCE(BS(1,1),B(1))
      EQUIVALENCE(BS(1,2),S(1))
C
      OPEN (UNIT=2,FILE='WORKING.IO' ,STATUS='NEW',FORM='UNFORMATTED')
      OPEN (UNIT=5,FILE='SPECTRA.IN' ,STATUS='OLD')
      OPEN (UNIT=6,FILE='FORIST.OUT' ,STATUS='NEW')
      OPEN (UNIT=7,FILE='PUNCH.OUT'  ,STATUS='NEW')
      OPEN (UNIT=8,FILE='TOGRAPH.OUT',STATUS='NEW')
      READ(5,113) RMATRIX
 113  FORMAT(1X,A80)
      OPEN (UNIT=3,FILE= RMATRIX     ,STATUS='OLD')
C
      KR=111
```

```
      MR = 156
      READ (3,905)   JDENT
      WRITE (6,906)  JDENT
      READ(5,903)NBITS,STRTCH,IDENTY,NPUNCH,ITRATE,ERRER,TAW
      READ(3,901)NR,NC,NW,IL
      WRITE(6,902)STRTCH,NBITS,NR,NC,NW,IDENTY,NPUNCH,ITRATE,ERRER,IL
      ITSAVE=ITRATE
      IDENTY = IDENTY - 1
      ERROR=ERRER*0.01
      CALL MATIN(FLAB,KR,NW,2)
C
C     The window width is modified by the factor STRTCH.
C
      DO   3   I = 1,NW
         WINW(I) = STRTCH * WINW(I)
         WIND(I) = WINW(I)
    3 CONTINUE
      CALL MATIN(ELAB,NC,NC,1)
      CALL AREAD(A,MR,NR,NC,NW)
      CALL BSREAD(B,S,MR,NR,NC,IDENT,LLO,LUP,VLO,VUP,FORTE,IL)
      ITRATE=ITSAVE
      DO 5 JJ=1,NW
         WINW(JJ) = WIND(JJ)
    5 CONTINUE
      IDENTY = IDENTY + 1
C
C     Calculate Q vector
C
      DO 20 J=1,NC
         Q(J)=1.0E35
         DO 20 I=1,NR
            IF(A(I,J))10,20,10
   10       QMIN=(AMAX1(B(I),0.0)+S(I))/A(I,J)
            IF(Q(J)-QMIN)20,20,15
   15       Q(J)=QMIN
   20 CONTINUE
C
C     Calculate HT and euclidean norm of HT
C
      ENORM = 0.0
      DO 25 I=1,NR
         DO 25 J=1,NC
            HT(I,J)=(Q(J)*A(I,J))/S(I)
            ENORM = ENORM+HT(I,J)**2
   25 CONTINUE
      WRITE (2) A
      BACKSPACE 2
      CALL GINV(HT,MR,NR,NC,TAW/SQRT(FLOAT(NC)),A,ATEMP)
      READ (2) A
      BACKSPACE 2
      DO 50 I=1,NR
         DO 50 J=1,NC
            HT(I,J)=(Q(J)*HT(I,J))/S(I)
   50 CONTINUE
C
C          Calculate the dual vector D.  In the FERDOR code, it is not
C     necessary to make any assumptions about the so-called true
C     solution.  However, there exist a set of coefficients,
```

```
C     D(J), J=1,NC which give teh variation of the PLO and PUP results
C     as the W(k) elements of the window matrix are varied.  These
C     coefficients are sort of a pseudo-solution.
C          Then calculate the weighted sum of the negative dual vector
C     components.  In ordinary least squares, the sum of squares of
C     residuals is minimized, but in FERDOR and additional term is
C     implied in the minimization which tends to prevent the pseudo-
C     vector from becoming negative.  If it does go negative very much,
C     it indicates that the data supplied to the problem are
C     inconsistent in the sense that no non-negative solution exists.
C     The sum of negative duals indicates the degree of inconsistency.
C     The sum should be between 0 and NC in a valid problem.
C
      ESL = 0.
      DO   110   J = 1.NC
         X(J) = 0.
         DO   104   I = 1,NR
            X(J) = X(J) + HT(I,J) * B(I)
  104    CONTINUE
         SL = X(J)/Q(J)
         PCTSL = 100. * SL
         ESL = ESL    + SL**2
  110 CONTINUE
C
C          Calculate BADJ, the adjusted B vector which is consistent
C     with the FERDOR final solution.
C          Then calculate the sum of squares of deviations (B(I)-
C     BADJ(I)), I=1,NR (weighted by 1/S(I)).  This sum is an indicator
C     of the validity o fthe input error estimates, S(I).  In an
C     ordinary least squares problem, the usm of sqauares of deviations
C     has a chi square distribution which should approximately be equal
C     to NR.  In the FERDOR formulation (which is a form of constrained
C     least squares), it is ok if the weighted sum of squares of
C     deviations is less than NR, but it indicates inconsistency if it
C     is too large.  The factor SQRT(weighted sum of squares)/NR is the
C     average factor by which the input errors need to be increased in
C     order to be consistent.
C
      WRITE (6,906) IDENT
      WRITE(6,918) TAW
      WRITE (6,911)
      ESD = 0.
      DO   120   I = 1,NR
         BADJ = 0.
         DO   114   J = 1,NC
            BADJ = BADJ + A(I,J) * X(J)
  114    CONTINUE
         DEV = (B(I) - BADJ)/S(I)
         PCTDEV = 100. * DEV
         ESD = ESD    + DEV**2
         WRITE(6,912)I,VLO(I),B(I),S(I),BADJ,PCTDEV,ESD
  120 CONTINUE
      FNC = NC
      FNR = NR
      DICA1 = SQRT(ENORM)*FNC*0.5**NBITS
      DICA2 = SQRT(ESL/FNC)
      DICA3 = SQRT(ESD/FNR)
      SUMIND = DICA1+DICA2+DICA3
```

```
      WRITE (6,913) DICA1,DICA2,DICA3,SUMIND
      WRITE(6,918) TAW
C
C     Begin window loop.
C
      IF (SUMIND .GE. 5.0) THEN
   58    WRITE (6,909)
      END IF
   59 WRITE (6,906) IDENT
      WRITE(6,918) TAW
      WRITE (6,907)
      IF (NPUNCH.EQ.1.OR.NPUNCH.EQ.3) WRITE(8,920) 'UTB',ITRATE,':'
      DO 500 K=1,NW
         CALL WREAD(W,NC,NW,K,ELAB,PLAB,WINW)
         DO 60 I=1,NR
            UT(I)=0.0
   60    CONTINUE
         DO 100 J=1,NC
            IF(W(  J))70,100,70
   70       DO 80 I=1,NR
               UT(I)=UT(I)+W(  J)*HT(I,J)
   80       CONTINUE
  100    CONTINUE
         USSUM=0.0
         UTB=0.0
         DO 150 I=1,NR
            UTB=UTB+UT(I)*B(I)
            USSUM=USSUM+(UT(I)*S(I))**2
  150    CONTINUE
         WUAQ=0.0
         DO 200 J=1,NC
            SUM=0.0
            DO 175 I=1,NR
               SUM=SUM+UT(I)*A(I,J)
  175       CONTINUE
            WUAQ=WUAQ+Q(J)*ABS(W(J)-SUM)
  200    CONTINUE
         EPSLON=SQRT(USSUM)+WUAQ
         PHIUP=UTB+EPSLON
         PHILO=UTB-EPSLON
         ERR1=SQRT(USSUM)
         ERR2=WUAQ
         WRITE (6,904) PLAB(K),K,PHILO,PHIUP,UTB,WINW(K),ERR1,ERR2
         ERSAVE(K) = EPSLON
         IF(NPUNCH.EQ.1.OR.NPUNCH.EQ.3) THEN
            WRITE(7,914)PLAB(K),K,UTB,EPSLON,IDENTY,WINW(K)
            IF (K .NE. NW) THEN
               WRITE(8,921) UTB,','
            ELSE
               WRITE(8,922) UTB
            END IF
         END IF
         PUP(K) = PHIUP
         PLO(K) = PHILO
         ERRF(K) = EPSLON / UTB
  500 CONTINUE
C
      IF(NPUNCH.EQ.1.OR.NPUNCH.EQ.3) THEN
```

```
            WRITE(8,913)
            WRITE(8,920) 'E',ITRATE,':'
            DO 600 I=1,NW-1
               WRITE(8,921) PLAB(I),','
  600       CONTINUE
            WRITE(8,922) PLAB(NW)
            WRITE(8,923)
         END IF
C
         IF(NPUNCH.EQ.1.OR.NPUNCH.EQ.3) THEN
            WRITE(8,923)
            WRITE(8,924) 'EPSLON',ITRATE,':'
            DO 601 I=1,NW-1
               WRITE(8,921) ERSAVE(I),','
  601       CONTINUE
            WRITE(8,922) ERSAVE(NW)
            WRITE(8,923)
         END IF
C
         WRITE (6,908) IDENT
         CALL PPLOT(PLO(5),137,PUP(5),137,NW-4,1,6HPLO-UP,137)
         IF(ITRATE.EQ.0) GO TO 501
         ITRATE = ITRATE - 1
         CALL SMOOTH(ERROR,ERRF,WINW,NW,WIND,PLAB)
         GO TO 59
  501    WRITE(6,908) IDENT
         CALL APLOT(PLO(5),KR,1,2,NW-4,1,2,PLAB(5),DUMMY)
         WRITE(6,915)
         DO 800 J=1,NC
            SUM1 = 0.0
            SUM2 = 0.0
            DO 700 I=1,NR
               SUM1 = SUM1 + (HT(I,J) * S(I)) ** 2
               SUM2 = SUM2 + HT(I,J) * A(I,J)
  700       CONTINUE
            ERRJ1 = SQRT(SUM1)
            DIFFR = 1.0 - SUM2
            UHAQJ = ABS(DIFFR) * Q(J)
            WRITE(6,916)J,ELAB(J),X(J),Q(J),ERRJ1,UHAQJ,IDENTY
            IF(NPUNCH.EQ.2.OR.NPUNCH.EQ.3) THEN
               WRITE(7,976)J,ELAB(J),X(J),Q(J),ERRJ1,UHAQJ,IDENTY
            END IF
  800    CONTINUE
C
         CLOSE (2)
         CLOSE (3)
         CLOSE (5)
         CLOSE (6)
         CLOSE (7)
         CLOSE (8)
C
  901    FORMAT(8I10)
  902    FORMAT(6X,'STRETCH                    =',F5.3/6X,
        +'NUMBER OF BITS          =',I5/6X,
        +'NUMBER OF ROWS          =',I5/6X,
        +'NUMBER OF COLUMNS       =',I5/6X,
        +'NUMBER OF WINDOWS       =',I5/6X,
        +'FIRST SPECTRUM NUMBER   =',I5/6X,
```

```
     +'PUNCHING OPTION        =',I5,6X,'(0/1/2/3) -- (NO PUNCHING /
     + SMOOTHED OUTPUT / UNSMOOTHED OUTPUT / BOTH)'/6X,
     +'NUMBER OF ITERATIONS   =',I5/6X,
     +'PERCENTAGE ERROR       =',I5/6X,'FIRST OVERLAP BIN      =',I5)
  903 FORMAT(1X,I10,F10.3,4I10,F10.4)
  904 FORMAT(1X,E13.3,I5,3E13.3,F7.2,2E13.3)
  905 FORMAT(20A4)
  906 FORMAT(1H1,20A4)
  907 FORMAT(6X,'ENERGY',14X,'PLO',10X,'PUP',9X,'PAVE',6X,
     +'PCT W',6X,'ERR1',9X,'ERR2',/)
  908 FORMAT(1H1,'PLO AND PUP',6X,20A4)
  909 FORMAT(1X,'****THIS IS AN INVALID RUN,....FOR DIAGNOSTIC ONLY')
  910 FORMAT(1X,I3,3E12.3,2F12.3,E12.3)
  911 FORMAT (3X,'I',6X,'VLO',10X,'B',11X,'S',9X,'BADJ',9X,
     +'PCTDEV',8X,'ESD',/)
  912 FORMAT(1X,I3,4E12.3,2F12.3)
  913 FORMAT (1H1,' INDICATOR NO. 1   =',F12.3,' (CONDITION)',//,
     +' INDICATOR NO. 2   =',F12.3,' (CONSISTENT WITH NON-NEG.)',//,
     +' INDICATOR NO. 3   =',F12.3,' (RESIDUALS)',//,
     +' SUM OF INDICATORS =',F12.3,
     +' (SHOULD BE LESS THAN 5.000 FOR VALID RUN -- SEE MANUAL)')
  914 FORMAT(10X,E10.4,I5,5X,E10.4,5X,E10.4,I5,5X,E10.4)
  915 FORMAT(1H1,8X,'J',8X,'ELAB',9X,'X',12X,'Q',9X,'ERRJ1',6X,'UHAQJ',6
     +X,'SPECTRUM NUMBER'/1H0)
  916 FORMAT(5X,I5,4X,E11.4,2X,E11.4,2X,E11.4,2X,E11.4,2X,E11.4,2X,I3)
  976 FORMAT(2X,I5,2X,E11.4,2X,E11.4,2X,E11.4,2X,E11.4,2X,E11.4,2X,I3)
  918 FORMAT('--- TAW=',F8.3,' ---',/)
  920 FORMAT(1X,A3,I1,A1)
  921 FORMAT(1X,E10.4,A1)
  922 FORMAT(1X,E10.4)
  923 FORMAT(1X)
  924 FORMAT(1X,A6,I1,A1)
C
      STOP
      END
C=======================================================================
C                          SUBROUTINE BSREAD
C     This routine assumes that B and S are contiguous in storage.
C     - IL - is the first bin of the 8-bin overlap
C-----------------------------------------------------------------------
      SUBROUTINE BSREAD(B,S,MR,NR,NC,IDENT,LLO,LUP,VLO,VUP,FORTE,IL)
C
      DIMENSION B(NR),S(NR),IDENT(20)
      DIMENSION VLO(NR),VUP(NR),LLO(NR),LUP(NR),FORTE(NR)
C
      CALL TOWCBN (B,S,NR,IDENT,LLO,LUP,VLO,VUP,FORTE)
    1 SCOFF=.01
      FUDGE=1.0
      DO 137 I=1,NR
      S(I)=AMAX1(S(I),SCOFF*B(I))
  137 CONTINUE
      COVH=B(IL)+B(IL+2)+B(IL+4)+B(IL+6)+1.E-20
      SOVH=SQRT(S(IL)**2+S(IL+2)**2+S(IL+4)**2+S(IL+6)**2)
      RERRH=SOVH/COVH
      COVL=B(IL+1)+B(IL+3)+B(IL+5)+B(IL+7)+1.E-20
      SOVL=SQRT(S(IL+1)**2+S(IL+3)**2+S(IL+5)**2+S(IL+7)**2)
      RERRL=SOVL/COVL
      FUDGE=COVL/COVH
```

```
      RELFU=ABS(1.-FUDGE)
C
C     Decide on strategy.
C
   12 IF(RERRH-RELFU)13,13,14
   13 IF(RERRL-RELFU)16,16,14
   14 FUDGE=1.0
      GO TO 34
   16 FUDGEH=1.+(COVL-COVH)/COVH*SOVL/(SOVH+SOVL)
   17 FUDGEL=1.+(COVH-COVL)/COVL*SOVH/(SOVH+SOVL)
      DO 20 I=1,IL
      B(I)=B(I)*FUDGEH
   20 S(I)=S(I)*FUDGEH
      N1=IL + 2
      N2=IL + 6
      DO 30 I=N1,N2,2
      B(I)=B(I)*FUDGEH
   30 S(I)=S(I)*FUDGEH
      N1=IL + 7
      DO 32 I=N1,NR
      B(I)=B(I)*FUDGEL
   32 S(I)=S(I)*FUDGEL
      N1=IL + 1
      N2=IL + 5
      DO 33 I=N1,N2,2
      B(I)=B(I)*FUDGEL
   33 S(I) = S(I)*FUDGEL
   90 FORMAT (1H1, 45HCOUNTS AND STANDARD DEVIATION IN GROUPED BINS
     +          ,5X,7HSCOFF =,F8.4,5X,7HFUDGE =,F8.4,5X,7HRELFU =,F8.4)
   34 WRITE (6,90)SCOFF,FUDGE,RELFU
      CALL APLOT(B,MR,1,2,NR,1,2,VLO,DUMMY)
      RETURN
      END
C=======================================================================
C                              SUBROUTINE WREAD
C-----------------------------------------------------------------------
      SUBROUTINE WREAD(W,NC,NW,NTRY,ELAB,PLAB,PCTWID)
C
      DIMENSION W(NC),PLAB(NW),PCTWID(NW),ELAB(NC)
      COMMON /STORE/ SIGJ(110)
C
      GAUSS(X) = 0.398942280414 * EXP(-0.5 * X**2)
      IF(NTRY.EQ.1) CALL WCALC(NC,NW,ELAB,PLAB,PCTWID)
      DO 10 J=1,NC
         DIFOS = ABS(ELAB(J)-PLAB(NTRY)) / SIGJ(J)
         IF(DIFOS - 5.5) 3,2,2
    2    W(J) = 0.0
         GO TO 10
    3    W(J) = 1.0E+6  * GAUSS(DIFOS) / SIGJ(J)
   10 CONTINUE
      RETURN
      END
C=======================================================================
C                              SUBROUTINE WCALC
C-----------------------------------------------------------------------
      SUBROUTINE WCALC(NC,NW,ELAB,PLAB,WINW)
C
      DIMENSION ELAB(NC),PLAB(NW),WINW(NW),I(120)
```

```
      COMMON /STORE/ SIGJ(110)
C
      DO 10 J=1,NC
         I(J) = 0
         DO 2  K=1,NW
            IF(ELAB(J) - PLAB(K)) 1,2,2
    1       I(J) = K
            GO TO 10
    2    CONTINUE
   10 CONTINUE
      DO 20 J=1,NC
      II = I(J)
      IF(II.EQ.1) GO TO 30
      IF(II.EQ.0) GO TO 40
      W = WINW(II) - (WINW(II)-WINW(II-1))*(PLAB(II)-ELAB(J))/(PLAB(II)-
     +                                              PLAB(II-1))
      GO TO 20
   30 W = WINW(1)-(WINW(2)-WINW(1))*(PLAB(1)-ELAB(J))/(PLAB(2)-PLAB(1))
      GO TO 20
   40 W = WINW(NW) + (WINW(NW)-WINW(NW-1))*(ELAB(J) -PLAB(NW)) /
     +               (PLAB(NW)-PLAB(NW-1))
   20 SIGJ(J) = (0.01 * W * ELAB(J)) / 2.35482004502
      RETURN
      END
C=======================================================================
C                          SUBROUTINE TOWCBN
C-----------------------------------------------------------------------
      SUBROUTINE TOWCBN (GC,S,NR,IDENT,LLO,LUP,VLO,VUP,FORTE)
C
      CHARACTER*6 TITLE1,TITLE2
      DIMENSION C(5000),GC(NR),S(NR),LLO(NR),LUP(NR)
      DIMENSION VLO(NR),VUP(NR),FORTE(NR)
      DIMENSION CRE(5000),BRE(5000)
      DIMENSION B(5000),UC(4),UB(4)
      DIMENSION FGAIN(4),BGAIN(4),GNOM(4)
      DIMENSION FAF(19)
      DIMENSION TITLE1(4),TITLE2(4)
      DIMENSION FBCORR(20),IDENT(20)
      EQUIVALENCE (FBCORR(1),UC(1)),(FBCORR(5),UB(1)),
     +(FBCORR(9),FGAIN(1)),(FBCORR(13),BGAIN(1)),(FBCORR(17),GNOM(1))
C
      READ (3,909) FAF
  909 FORMAT(19F4.3)
      READ (3,900) NPOINT,NGRPS,NGAIN,NPUNCH
  900 FORMAT(4I6)
      READ(5,901)(UC(I),I=1,4),(UB(I),I=1,4)
     +          ,(FGAIN(I),I=1,4),(BGAIN(I),I=1,4)
      READ(3,901)(GNOM(I),I=1,4)
  901 FORMAT(1X,4F10.0)
      CALL BINRD(NGRPS,LLO,LUP,NBINS)
      WRITE (6,400)
  400 FORMAT(1H1,'  RUN   F LIVE TIMES    B LIVE TIMES     ',
     +'F GAIN     B GAIN     NOM GAIN')
      CALL FPRINT (UC,4,4,5,3,0,1,0)
      CALL CREAD (C,5000,TITLE1,TITLE2,NERR,NPOINT,IDENT)
           DO  30  K = 1,NGAIN
           KK = 1 + K*1000
      WRITE (6,904) TITLE1(K),K
```

```
   30       CALL CPRINT (C(KK),NPOINT)
         CALL CREAD (B,5000,TITLE1,TITLE2,NERR,NPOINT,IDENT)
         DO 31 K=1,NGAIN
          KK = 1+K*1000
   26 WRITE (6,905) TITLE1(K),K
   31 CALL CPRINT(B(KK),NPOINT)
         DO 320 K=1,NGAIN
         KK = 1 + K*1000
            DO 321 I=1,NPOINT
         VVLO=FLOAT(I-1)*GNOM(K)
         VVUP=FLOAT(I)*GNOM(K)
         J = KK+I-1
         CRE(J)=REBIN(C(KK),1,NPOINT,0,FGAIN(K),1.0,VVLO,VVUP)
         BRE(J)=REBIN(B(KK),1,NPOINT,0,BGAIN(K),1.0,VVLO,VVUP)
  321    CONTINUE
  320 CONTINUE
         DO 322 K=1,NGAIN
         KK = 1+K*1000
         WRITE (6,908) TITLE1(K),K
  322 CALL CPRINT(CRE(KK),NPOINT)
         DO 323 K=1,NGAIN
         KK=1+K*1000
  325 WRITE (6,910) TITLE1(K),K
  323 CALL CPRINT(BRE(KK),NPOINT)
         DO 1999 I=1,NBINS
            GC(I)=0.0
            VAR = 0.0
            L1=LLO(I)
            L2=LUP(I)
            LL = L1/1000
            LLLO = L1 - LL*1000
            LLUP = L2 - LL*1000
            VLO(I) = FLOAT(LLLO-1)*GNOM(LL)
            VUP(I) = FLOAT(LLUP)*GNOM(LL)
            BINW = VUP(I) - VLO(I)
            DO 1998 L=L1,L2
               GC(I)=GC(I)+CRE(L)/UC(LL)-BRE(L)/UB(LL)
1998        VAR=VAR+(CRE(L)+.1)/UC(LL)**2+(BRE(L)+.1)/UB(LL)**2
            GC(I) = GC(I)/BINW
1999  S(I) = SQRT(VAR)/BINW
        DO 2 I=1,NBINS
            V=0.5*(VLO(I)+VUP(I))
            IF(V-0.10) 4,8,8
    4       IF(V-0.01) 5,  6
    5       FORTE(I) = FAF(1)
            GC(I) =0.0
            S(I) = 0.0
            GO TO 2
    8       FORTE(I) = 1.0
            GO TO 7
    6       Z = 200.0*(V-0.01)
            J=Z
            Z = Z-FLOAT(J)
            FORTE(I)=(1.0-Z)*FAF(J+1)+Z*FAF(J+2)
    7       CONTINUE
            GC(I) = GC(I)/FORTE(I)
            S(I) = S(I)/FORTE(I) + 0.2*(1.0-FORTE(I))*GC(I)
    2  CONTINUE
```

```
      WRITE (6,906) TITLE1(1)
  906 FORMAT (1H1,10X,A6,5X,19HGROUPED COUNTS/UNIT,/,1H )
      WRITE (6,401)
  401 FORMAT (1H ,6X,4HBINS,6X,6HCOUNTS,11X,5HERROR,6X,6HLOCHAN,2X,
     +6HUPCHAN,6X,7HLO P.H.,9X,7HUP P.H.,7X,6HF.A.F.)
      DO 50 I=1,NBINS
   50 WRITE (6,934) I,GC(I),S(I),LLO(I),LUP(I),VLO(I),VUP(I),FORTE(I)
  934 FORMAT (1H ,I8,2E16.5,2I8,2E16.5,F10.5)
  999 RETURN
  904 FORMAT (1H1,10X,A6,5X,28HRAW COUNTS FOREGROUND GAIN =,I2,/,1H )
  905 FORMAT (1H1,10X,A6,5X,28HRAW COUNTS BACKGROUND GAIN =,I2,/,1H )
  906 FORMAT(1H1,10X,A6,5X,30HREBIN COUNTS FOREGROUND GAIN =,I2,/,1H )
  910 FORMAT(1H1,10X,A6,5X,30HREBIN COUNTS BACKGROUND GAIN =,I2,/,1H )
      END
C=======================================================================
C                            SUBROUTINE MATIN
C     This subroutine reads data into an array.
C     A format card must precede the data, i.e. FORMAT I NN (...), with:
C        'FORMAT' in col. 1-6,
C        I = 'ROW' for row format, I = 'COL' for column format,
C        NN = number of data words per card,
C        (...) = format specification.
C     Each data card must have two index numbers indicating the matrix
C     position of the first data word.  The reading of cards is
C     completed by one blank card.  This routine has a provision for
C     changing formats in midstream.  A card with both indices negative
C     implies that a format card follows.
C-----------------------------------------------------------------------
      SUBROUTINE MATIN(A,MR,NR,NC)
C
      DIMENSION A(MR,NC),FMT(17),XLIST(78)
C
      CALL EQUIV(ICHECK,4HFORM)
      CALL EQUIV(IROW,4HROW )
      NERROR=0
      DO  4  I = 1,MR
         DO  4  J = 1,NC
    4       A(I,J) = 0.0
C  ***Read format card
    5 READ (3,900) IWORD,IROC,NN,FMT
      IF (IWORD/2-ICHECK/2) 8,10,8
    8 WRITE (6,904)
      GO TO 888
C  ***Read data card
   10 READ (3,FMT) I,J,(XLIST(K),K=1,NN)
C  ***Check for new format card
   32 IF(I)50,11,11
   50 IF(J)5,721,701
C  ***Check for blank card to end list
   11 IF (I +J)  12,888,12
   12 I = MAX0(I,1)
      J = MAX0(J,1)
      IF (IROC-IROW) 213,13,213
C *** Row format ***
   13 IF (I-NR)  14,14,701
  701 IF(NERROR-50) 702,702,10
  702 WRITE (6,901) I,J,MR,NR,NC,(XLIST(K1),K1=1,4)
      NERROR=NERROR+1
```

```
      GO TO 10
   14 DO  20  JJ = 1,NN
         JJJ = J + JJ - 1
         IF (XLIST(JJ))16,20,16
   16    IF (JJJ - NC)  17,17,703
  703    IF(NERROR-50) 704,704,10
  704    WRITE (6,902) I,JJJ,MR,NR,NC,(XLIST(K1),K1=1,4)
         NERROR=NERROR+1
         GO TO 10
   17    IF (A(I,JJJ)) 705,18,705
  705    IF(NERROR-50) 706,706,20
  706    WRITE (6,903) I,JJJ,MR,NR,NC,(XLIST(K1),K1=1,4)
         NERROR=NERROR+1
         GO TO 20
   18    A(I,JJJ) = XLIST(JJ)
   20 CONTINUE
   21 GO TO 10
C *** Column format ***
  213 IF (J-NC)  214,214,721
  721 IF(NERROR-50) 722,722,10
  722 WRITE (6,902) I,J,MR,NR,NC,(XLIST(K1),K1=1,4)
      NERROR=NERROR+1
      GO TO 10
  214 DO  220  II = 1,NN
         III = I + II - 1
         IF (XLIST(II))  216,220,216
  216    IF (III-NR)  217,217,723
  723    IF(NERROR-50) 724,724,10
  724    WRITE (6,901) III,J,MR,NR,NC,(XLIST(K1),K1=1,4)
         NERROR=NERROR+1
         GO TO 10
  217    IF (A(III,J))  725,218,725
  725    IF(NERROR-50) 726,726,220
  726    WRITE (6,903) III,J,MR,NR,NC,(XLIST(K1),K1=1,4)
         NERROR=NERROR+1
         GO TO 220
  218    A(III,J) = XLIST(II)
  220 CONTINUE
      GO TO 10
  888 RETURN
  900 FORMAT(1A4,3X,1A3,1X,I2,1X,16A4,1A2)
  901 FORMAT (22H0ILLEGAL 1ST INDEX, I=,I3,2X,2HJ=,I3,2X,3HMR=,I3,2X,
     +        3HNR=,I3,2X,3HNC=,I3,5H   **,4E12.3,3H...)
  902 FORMAT (22H0ILLEGAL 2ND INDEX, I=,I3,2X,2HJ=,I3,2X,3HMR=,I3,2X,
     +        3HNR=,I3,2X,3HNC=,I3,5H   **,4E12.3,3H...)
  903 FORMAT (22H0DUPLICATION ERROR, I=,I3,2X,2HJ=,I3,2X,3HMR=,I3,2X,
     +        3HNR=,I3,2X,3HNC=,I3,5H   **,4E12.3,3H...)
  904 FORMAT(1H0,51H***  PROGRAM EXPECTS FORMAT CARD AT THIS POINT  ***)
      END
C=======================================================================
C                          SUBROUTINE EQUIV
C-----------------------------------------------------------------------
      SUBROUTINE EQUIV(X,Y)
      X = Y
      RETURN
      END
C=======================================================================
C                          SUBROUTINE AREAD
```

```
C-----------------------------------------------------------------------
      SUBROUTINE AREAD(A,MR,NR,NC,NW)
      DIMENSION A(1)
      CALL MATIN(A,MR,NR,NC)
      RETURN
      END
C=======================================================================
C                          SUBROUTINE BINRD
C     Reads bin card(s) with (KLO(I),KUP(I),KDEL(I)),I=1,NGRPS
C     and converts to expanded bin list (LLO(J),LUP(J)),J=1,NBINS.
C     Needs NGRPS from calling program.
C     Returns LLO,LUP,NBINS.
C-----------------------------------------------------------------------
      SUBROUTINE BINRD(NGRPS,LLO,LUP,NBINS)
C
      DIMENSION LLO(7777),LUP(7777),KUP(40),KLO(40),KDEL(40)
C
C     Read binning card(s), 10 max
      READ(3,901) (KLO(I),KUP(I),KDEL(I),I=1,NGRPS)
C     Write out binning table
      WRITE (6,902)
      DO 3 M=1,NGRPS
         AUP = KUP(M)
         ALO = KLO(M)
         ADEL = KDEL(M)
         BIN = (AUP-ALO+1.0)/ADEL
         WRITE (6,903) M,KLO(M),KUP(M),KDEL(M),BIN
    3 CONTINUE
C     Convert table
      NBINS=0
      DO 20 I=1,NGRPS
         K1=KLO(I)
         K2=KUP(I)
         K3=KDEL(I)
         K3 = MAX0(K3,1)
         DO 10 K=K1,K2,K3
            NBINS=NBINS+1
            LLO(NBINS)=K
            LUP(NBINS)=K+K3-1
   10    CONTINUE
   20 CONTINUE
C     Write out computed number of bins
      WRITE (6,904) NBINS
      RETURN
  901 FORMAT(12I6)
  902 FORMAT(1H1,13HBINNING TABLE/6H0GROUP,4X,6HLOEDGE,4X,6HUPEDGE,4X,8H
     +CHAN/BIN,5X,4HBINS)
  903 FORMAT(1H ,I3,6X,I5,5X,I5,8X,I3,7X,F5.1)
  904 FORMAT(42X,4H----/25X,14HTOTAL NO. BINS,4X,I3)
      END
C=======================================================================
C                          SUBROUTINE FPRINT
C     Output routine for 1 or 2 dimensional arrays.
C
C     K  = 1, FORMAT   I12
C     K  = 2, FORMAT   F12.4
C     K  = 3, FORMAT   E12.4
C     K  = 4, FORMAT   G12.4
```

```
C     MR = first dimenstion number of array
C     L  = 0 for no column headings
C     N  = 0 for return without action
C     LL = 1 for placing fixed point numbers in G format
C
C     Compiled in FORTRAN 360 for system 360 on 25 July 1966.
C-------------------------------------------------------------------------
      SUBROUTINE FPRINT (A,MR,NR,NC,K,L,N,LL)
C
      DIMENSION A(MR,888), FMT(5), FMT3(9),FMT4(4)
      DATA  FMT/4H(I6,,4H2X, ,4H  10,4H    ,4H4)  /
      DATA  FMT3/4H   1,4H   2,4H   3,4H   4,4H   5,4H   6,4H   7,
     +  4H   8,4H   9/
      DATA  FMT4/4HI12),4HF12.,4HE12.,4HG12./
C
    4 IF (N) 1,99,1
    1 NTOU = 6
C***  Set format
      DATA FMT(3)/4H  10/
      FMT(4) = FMT4(K)
C
      JUMP = 0
   18 WRITE (NTOU,902)
   19 NFULLB =NC/10
   20 IF (NFULLB) 21,40,21
   21 NSKIP = MAX0(1,60/(NR+4))
      DO 39 M=1,NFULLB
         NC1 = 10*M - 9
         NC2 = 10*M
         GO TO 80
   37    IF (M - NSKIP*(M/NSKIP)) 39,38,39
   38    WRITE (NTOU,903)
   39 CONTINUE
   40 NCLEFT = NC - 10*NFULLB
   41 IF (NCLEFT) 42,99,42
   42 NC1 = 10*NFULLB + 1
      NC2   10*NFULLB + NCLEFT
      FMT(3) = FMT3(NCLEFT)
      JUMP = 1
   80 WRITE (NTOU,902)
      IF (L) 81,83,81
   81 WRITE (NTOU,901)((J),J=NC1,NC2)
   82 WRITE (NTOU,902)
   83 WRITE (NTOU,FMT)(I,(A(I,J),J=NC1,NC2),I=1,NR)
      IF (JUMP) 99,37,99
   99 RETURN
  901 FORMAT(1H ,3X,10I12)
  902 FORMAT(1X)
  903 FORMAT(/1H1)
      END
C=========================================================================
C                              SUBROUTINE CREAD
C     Reads spectral data from input file SPECTRA.IN.
C     Format lines in SPECTRA.IN must have the form:
C     col 1-6    DYNMAT
C     col 14-31  10 (1A6,I4,10F7.0)
C-------------------------------------------------------------------------
      SUBROUTINE CREAD (C,N,TITLE1,TITLE2,NERR,NPOINT,IDENT)
```

```
C
      CHARACTER*6 TITLE1,TITLE2
      DIMENSION C(777),CARD(20),FMT(20),IDENT(20)
      DIMENSION TITLE1(4),TITLE2(4)
C
      NERR = 0
      KK = 0
      DO 30  K = 1,N
         C(K) = 0.0
   30 CONTINUE
    1 READ (5,901) CARD(1),IREL,NWORD,(FMT(J),J=1,10)
      NCHAN = 0
      KK = KK+1
      CALL EQUIV (X,4HDYNM)
      IF (CARD(1)/2.0-X/2.0) 3,2,3
    3 CALL EQUIV(X,4H    )
      IF (CARD(1)/2.0-X/2.0) 2,88,2
    2 IF (IREL .EQ. 1000) THEN
         WRITE (6,903) CARD(1),IREL,NWORD,(FMT(J),J=1,10)
      ELSE
         WRITE(6,906) CARD(1),IREL,NWORD,(FMT(J),J=1,10)
      END IF
      READ (5,900) (IDENT(J),J=1,20)
      WRITE (6,904) (IDENT(J),J=1,20)
   10 READ(5,FMT) TITLE1(KK),IO,(CARD(J),J=1,NWORD)
      WRITE(6,905) TITLE1(KK),IO,(CARD(J),J=1,NWORD)
      TITLE2(KK)=TITLE1(KK)
      IO = IO+IREL
      DO 17   I = 1,NWORD
         NCHAN = NCHAN+1
C
C                     *
C               .....INDEX OK.....
C              NO               YES
C        ....WORD ZERO....       *
C       NO             YES     STORE
C        *              *        *
C      ALARM            *        *
C        *              *        *
C        ............CONTINUE......
C        ............CONTINUE......
C                      *
C
         II = IO + I - 1
   12    IF   (II)         14,14,13
   13    IF   (II-N)       16,16,14
   14    IF   (CARD(I))    99,17,99
   16    C(II) = CARD(I)
   17 CONTINUE
      IF (NCHAN-NPOINT) 10,1,10
   88 RETURN
   99 NERR = NERR+1
      WRITE (6,902) N,CARD
      GO TO 10
  900 FORMAT (1X,20A4)
  901 FORMAT (1X,A6,1X,I6,I3,1X,10A4)
  902 FORMAT('0','*** CREAD ERROR, N = ',I6,' CARD IS **',20 A4, '**')
  903 FORMAT (1H1,A6,2X,I6,I3,1X,10A4)
```

```
  904 FORMAT (1H ,20A4)
  905 FORMAT (1H ,1A6,1I6,10F8.0,1A6)
  906 FORMAT (1H0,A6,2X,I6,I3,1X,10A4)
      END
C=======================================================================
C                              SUBROUTINE CPRINT
C-----------------------------------------------------------------------
      SUBROUTINE CPRINT(C,NP)
C
      DIMENSION C(7777),XBUE(8),IBUE(8)
C
      TCOUNT = 0.0
      NPAGES = 1 + (NP-1)/400
      DO   10   K=1,NPAGES
         IF   (K-1)   5,5,4
    4    WRITE (6,904)
    5    NPOINT = MIN0(400,NP-(K-1)*400)
         NROWS = MIN0(NPOINT,50)
         DO 7 I=1,NROWS
            NCOLS=(NPOINT/50)+MIN0(1,(NPOINT-50*(NPOINT/50))/I)
            NCOLS = MAX0(1,NCOLS)
            DO 8 J=1,NCOLS
               NC=I+(J-1)*50+(K-1)*400
               XBUE(J)=C(NC)
               TCOUNT = TCOUNT+XBUE(J)
               IBUE(J)=NC
    8       CONTINUE
            WRITE (6,905) (IBUE(L),XBUE(L),L=1,NCOLS)
    7    CONTINUE
   10 CONTINUE
      WRITE (6,906) TCOUNT
      RETURN
  904 FORMAT(1H1)
  905 FORMAT(1H ,8(I5,F9.1,2X))
  906 FORMAT (1H0/1H0,24HTOTAL NUMBER OF COUNTS =,F12.1)
      END
C=======================================================================
C                              FUNCTION REBIN
C     The vector A gives the components fo a histogram.  The bottom
C     edge of the lower bar is a RHOLO, and the width of the bars is
C     RHODEL.  This routine adds all teh bins between VLO and VUP and
C     splits any fractional bins linearly.  For greater flexibility,
C     V = C*RHO, where C is an input parameter.
C-----------------------------------------------------------------------
      FUNCTION REBIN(A,MR,N,RHOLO,RHODEL,C,VLO,VUP)
C
      DIMENSION A(777)
C
    1 RLO=AMAX1(VLO/C,RHOLO)
    2 RUP=AMAX1(VUP/C,RHOLO)
C
   10 X1 = 2.0 + (RLO-RHOLO)/RHODEL
      I1 = X1
      I1 = MIN0(I1,N+1)
      X1 = X1-FLOAT(I1)
      X1 = AMIN1(X1,1.0)
C
   15 X2 = 1.0 + (RUP-RHOLO)/RHODEL
```

```
      I2 = X2
      I2 = MIN0(I2,N)
      X2 = X2-FLOAT(I2)
      X2 = AMIN1(X2,1.0)
C
   20 L1 = ((I1-1) - 1)*MR + 1
      L2 = (I2-1)*MR + 1
      REBIN = (1.0-X1)*A(L1) - (1.0-X2)*A(L2)
C
      IF   (I2-I1+1)   40,40,30
   30 DO 37   I = I1,I2
         L3 = (I-1)*MR + 1
         REBIN = REBIN + A(L3)
   37 CONTINUE
C
   40 RETURN
      END
C=====================================================================
C                          SUBROUTINE GINV
C          Upon entry, A = a matrix with NR rows and NC columns.
C     After the return, the original A is destroyed and the array A
C     contains the transpose of T, the transformation matrix
C     (X = T*B) which solves the pari of equations:
C          A * X = B
C     and
C          TAU  I * X = 0
C     in the least squares sense.
C          MR= 1st dimension no. of array A in the calling program.
C     TAU is a nonnegative constant which controls the error
C     propagation of the transformation matrix.  If TAU=0, then the
C     resulting transformation matrix si the ordinary least squares
C     transformation matrix (the inverse if NR=NC).  ATEMP and
C     U are used for working space by the algorithm and do not
C     necessarily contain any relevant numbers at the conclusion.
C     ATEMP must be dimensioned at least NC by the calling program.
C     U must be dimensioned at least NC*NC by the calling program.
C     TAU is a nonnegative constant which controls the error.
C     Number of multiplications = NC**2 (5/2 + 2/3 NC).
C---------------------------------------------------------------------
      SUBROUTINE GINV(A,MR,NR,NC,TAU,U,ATEMP)
C
      DIMENSION A(MR,NC),U(NC,NC),ATEMP(NC)
C
      TAUSQ = TAU ** 2
C     Place unit matrix in U
      DO 5 I=1,NC
         DO 4 J  =1,NC
    4       U(I,J) = 0.0
    5    U(I,I) = 1.0
C
C     Orthogonalize combined matrix (A above U) by Gramm-Schmidt-Hilbert
C     method with first NR rows weighted with 1 and the other NC rows
C     weighted with 1/TAU.  Then reorthogonalize to lessen
C     roundoff error.
C
      DO 20 I=1,NC
         II = I-1
         IF (II) 2,11,2
```

```
     2     DO 10 LL=1,2
              DO 10 J=1,II
                 DOT = CDOT(A(1,I),A(1,J),NR)
                 DOT2 = CDOT(U(1,I),U(1,J),J)
                 DOT = DOT + DOT2 * TAUSQ
                 CALL CLIM (U(1,I),U(1,J),DOT,J,0)
    10     CALL CLIM (A(1,I),A(1,J),DOT,NR,0)
C
C      Normalize the column *I* of the combined matrix
C
    11     DOT = 0.0
           DOT2 = 0.0
           DO 12 K = 1,NR
    12        DOT = A(K,I) * A(K,I) + DOT
           DO 14 K=1,I
    14        DOT2 = U(K,I) * U(K,I) + DOT2
           DOT = DOT + DOT2 * TAUSQ
           DOT = SQRT(DOT)
           DO 17 K=1,I
    17        U(K,I) = U(K,I)/DOT
           DO 19 K=1,NR
    19        A(K,I) = A(K,I)/DOT
    20  CONTINUE
C      Calculation of the transpose of the transformation
C      matrix T(trans.) = A + U(trans.)
C
       DO 50  I=1,NR
          DO 45  J=1,NC
             ATEMP(J) = RDOT(A(I,J),MR,U(J,J),NC,NC-J+1)
    45    CONTINUE
          DO 50 J=1,NC
             A(I,J) = ATEMP(J)
    50  CONTINUE
       RETURN
       END
C=======================================================================
C                              SUBROUTINE APLOT
C      This version plots 3 plus and 2 minus cycles on a p-log scale.
C
C      row plots:          NDC = 1
C                          NDR = first dimension of A
C                          NCR = number of rows in plot
C                          NRC = number of columns in plot
C
C      column plots:       NDC = first dimension of A
C                          NDR = 1
C                          NCR = number of columns in plot
C                          NRC = number of rows in plot
C
C      Every Nth row or column of matrix A is plotted.  NPPP specifies
C      the number of plots per page (5 max).  X is the absicsa
C      labelling array.  NT is the number of the output tape.
C-----------------------------------------------------------------------
       SUBROUTINE APLOT(A,NDC,NDR,NCR,NRC,NTH,NPPP,X,NT)
C
       DIMENSION A(777),X(333),PLOT(101),ESCALE(11),SAVE(5),SYM(5)
      +,L(5),LOC(5)
C
```

```
      BAKF(Y,F) = 0.4342944819*ALOG(Y+F)
      FORF(X,F) = 10.0**X-F
      IF(KKK-14232)10,30,10
   10 KKK=14232
      CALL EQUIV(SYM(1),1H*)
      CALL EQUIV(SYM(2),1H$)
      CALL EQUIV(SYM(3),1H=)
      CALL EQUIV(SYM(4),1H+)
      CALL EQUIV(SYM(5),1H*)
      DO 15 I=1,101
   15 CALL EQUIV(PLOT(I),1H )
      DO 20 I=1,101,10
   20 CALL EQUIV(PLOT(I),1H1)
   30 INDEX=1
      L1=1
      NPLOT=1+(NCR-1)/NTH
   40 IF(NPLOT-NPPP)42,44,44
   42 JP=NPLOT
      GO TO 46
   44 JP=NPPP
   46 NPLOT=NPLOT-NPPP
      JP1=JP+1
      AMAX=1.0E-30
      DO 60 J=1,JP
         L(J)=L1+(J-1)*NTH
         DO 60 I=1,NRC
            IJ=INDEX+NDR*(I-1)+NDC*(J-1)*NTH
            IF  (AMAX1(A(IJ),-10.0*A(IJ)) - AMAX)  60,60,50
   50       AMAX = AMAX1(A(IJ),-10.0*A(IJ))
   60 CONTINUE
      L1=L(NPPP)+NTH
      RSP = 0
      NSCALE = BAKF(AMAX,RSP)+40.95
      NSCALE=NSCALE-40
      FNSM3 = NSCALE-3
      F0 = FORF(FNSM3,RSP)
      FIX=-20*NSCALE
      FIX=FIX+101.5
      FIXN=83.0-FIX
      SCALE = NSCALE
      DO 70 I=1,11
         DIF = I-5
         ESCALE(I) = FORF(SCALE-3.+.5*ABS(DIF ),F0)
   70 ESCALE(I)=SIGN(ESCALE(I),DIF)
      IF (NDR-1) 90,90,100
   90 WRITE (6,905) (SYM(J),L(J),J=1,JP)
      WRITE (6,902)  ESCALE
      GO TO 110
  100 WRITE  (6,906) (SYM(J),L(J),J=1,JP)
      WRITE (6,903)   ESCALE
  110 DO 130 I=1,NRC
         DO 121 J=1,JP
            IJ=INDEX+NDR*(I-1)+NDC*(J-1)*NTH
            IF(A(IJ))112,114,114
  112       IJ = -20.0*BAKF(F0,-A(IJ))+FIXN
            GO TO 116
  114       IJ = 20.0*BAKF(A(IJ),F0)+FIX
  116       IF(IJ)117,117,118
```

```
  117       IJ=1
  118       IF(IJ-101)120,120,119
  119       IJ=101
  120       LOC(J)=IJ
            SAVE(J)=PLOT(IJ)
  121       PLOT(IJ)=SYM(J)
        WRITE (6,904)     I,X(I),PLOT
        DO 130 J=1,JP
           JJ=JP1-J
           IJ=LOC(JJ)
  130 PLOT(IJ)=SAVE(JJ)
      INDEX=INDEX+NPPP*NTH*NDC
      IF(NPLOT)140,140,135
  135 WRITE  (6,907)
      GO TO 40
  140 RETURN
  902 FORMAT('0',2X,'ROW',8X,5E10.1,3E10.1,3E9.1)
  903 FORMAT('0',2X,'COL',8X,5E10.1,3E10.1,3E9.1)
  904 FORMAT(' ',I3,2X,E10.3,3X,101A1)
  905 FORMAT('0',13X,5(12X,A1,' COL',I3))
  906 FORMAT('0',13X,5(12X,A1,' ROW',I3))
  907 FORMAT(1H1)
      END
C=======================================================================
C                              SUBROUTINE PPLOT
C     Line-by-line pplot.
C-----------------------------------------------------------------------
      SUBROUTINE PPLOT(V1,MR1,V2,MR2,N,NO,LABEL,NOPT)
      DIMENSION V1(MR1),V2(MR2),BUF(102)
C
C     Calculate minimum and maximum value to be plotted
C
      VMAX=-1.0E+35
      VMIN= 1.0E+35
      SUM=0.0
      DO 30 I=1,N
         IF(V1(I)-VMAX)16,16,14
   14    VMAX=V1(I)
   16    IF(V1(I)-VMIN)18,20,20
   18    VMIN=V1(I)
   20    IF(V2(I)-VMAX)24,24,22
   22    VMAX=V2(I)
   24    IF(V2(I)-VMIN)26,28,28
   26    VMIN=V2(I)
   28    SUM=SUM+ABS(V1(I)+V2(I))
   30 CONTINUE
C
C     Calculate scale factor
C
      TWON=2*N
      AVRGE=SUM/TWON
      NEXP=0
      IF(AVRGE)32,35,32
   32 NEXP=ALOG(AVRGE)*0.4342944819
   35 FEXP=10.0**NEXP
C
C     Set graph limits
C
```

```
      GRIDLO=VMIN/FEXP
      GRIDUP=VMAX/FEXP
      DELTA=(GRIDUP-GRIDLO)/100.0
C
C     Section to place zero on grid line
C
      RANGE=120.0*DELTA
      IRANGE=RANGE
      REM=RANGE-FLOAT(IRANGE)
      IF(REM)40,70,40
   40 IF(REM-0.5)50,70,60
   50 REM=0.5
      GO TO 70
   60 REM=1.0
   70 DELTA=(FLOAT(IRANGE)+REM)/100.0
      RATIO=GRIDLO/(DELTA*10.0)
      NRATIO=RATIO
      RRATIO=NRATIO
      REM=RATIO-RRATIO
      IF(REM)75,80,80
   75 RRATIO=RRATIO-1.0
   80 GRIDLO=RRATIO*DELTA*10.0
      GRIDUP=100.0*DELTA+GRIDLO
C
C     Graph is now printed, line by line
C
      WRITE (6,900) LABEL,NO,FEXP
      DO 200 M=1,N
         CALL EQUIV(BUF(1),M)
         MM1=M-1
         IF(M-N)85,140,85
   85    IF(MOD(MM1,10))90,140,90
   90    IF(MOD(MM1,10)-1)180,100,180
  100    DO 110 L1=1,101
            CALL EQUIV(BUF(L1+1),1H )
  110    CONTINUE
         DO 120 L2=1,101,10
            CALL EQUIV(BUF(L2+1),1H1)
  120    CONTINUE
         GO TO 180
  140    DO 150 L3=1,101
            CALL EQUIV(BUF(L3+1),1H-)
  150    CONTINUE
         DO 160 L4=1,101,10
            CALL EQUIV(BUF(L4+1),1H+)
  160    CONTINUE
  180    GRIDP1=V1(M)/FEXP
         JJ=(GRIDP1-GRIDLO)/DELTA+2.5
         IF(JJ-102)190,190,185
  185    JJ=102
  190    GRIDP2=V2(M)/FEXP
         LL=(GRIDP2-GRIDLO)/DELTA+2.5
         IF(LL-102)195,195,192
  192    LL=102
  195    SAVE1=BUF(JJ)
         SAVE2=BUF(LL)
         CALL EQUIV(BUF(LL),1H*)
         CALL EQUIV(BUF(JJ),1H=)
```

```
         WRITE (6,901) GRIDP1,GRIDP2,(BUF(I),I=2,102)
         BUF(JJ)=SAVE1
         BUF(LL)=SAVE2
  200 CONTINUE
C
C     Scale is now printed
C
      TEND=DELTA*10.0
      BUF(1)=GRIDLO
      DO 220 I=2,11
         II=I-1
         BUF(I)=TEND+BUF(II)
  220 CONTINUE
      WRITE (6,902) (BUF(I),I=1,11)
C
  900 FORMAT(1H0,3X,1A6,5H  NO.,I3,40X,14HSCALE FACTOR =,1PE9.1/1H0,
     +4X,1H=,6X,1H*)
  901 FORMAT(1H ,2F7.3,1X,102A1)
  902 FORMAT(11X,10(3X,F5.2,2X),1X,F5.2)
C
      RETURN
      END
C=======================================================================
C                              FUNCTION RDOT
C-----------------------------------------------------------------------
      FUNCTION RDOT (A,MA,B,MB,N)
      DIMENSION A(MA,1),B(MB,1)
      RDOT = 0.0
      DO 10 J = 1,N
   10 RDOT = RDOT + A(1,J) * B(1,J)
      RETURN
      END
C=======================================================================
C                              FUNCTION CDOT
C-----------------------------------------------------------------------
      FUNCTION CDOT (A,B,N)
      DIMENSION A(1),B(1)
      CDOT = 0.0
      DO 10 I = 1,N
   10 CDOT = CDOT + A(I) * B(I)
      RETURN
      END
C=======================================================================
C                             SUBROUTINE CLIM
C-----------------------------------------------------------------------
      SUBROUTINE CLIM (A,B,C,N,IRO)
      DIMENSION A(1),B(1)
      DO 50 J = 1,N
      IF (J-IRO) 20,50,20
   20 A(J) = A(J) - B(J) * C
   50 CONTINUE
      RETURN
      END
C=======================================================================
C                             SUBROUTINE SMOOTH
C     For each iteration, SMOOTH calculates new window widths such that
C     the final statistical error (after folding with the window
C     function) should converge to a constant specified by the user.
```

```
C-----------------------------------------------------------------------
      SUBROUTINE SMOOTH(ERROR,ERRF,WINW,NW,WIND,PLAB)
      DIMENSION WINW(NW),ERRF(NW),WIND(NW),PLAB(NW)
      DIMENSION WINDOW(130)
C
      C(ENERGY)=40.*EXP(-.08*ENERGY) + 50.*EXP(-  7*ENERGY)
C
C     For each iteration, smooth calculates new window widths such that
C     the final statistical error (after folding with the window
C     function) should converge to a constant specified by the user.
C
      ERRM = 0.08
      DO 100 J=1,NW
         ERRF(J) =ABS(ERRF(J))
         ENERGY=PLAB(J)*1.0E-6
         WMAX = 1.5 * WIND(J)
         IF(ERRF(J).GT.ERRM) GO TO 10
C
         WINDOW(J)=1/( 1/WINW(J) +(1/C(ENERGY))*ALOG(ERROR/ERRF(J)))
         GO TO 20
C
   10    WINDOW(J) = WMAX
   20    WINDOW(J) = ABS(WINDOW(J))
  100 IF(WINDOW(J).GT.WMAX) WINDOW(J)=WMAX
C
C     To prevent oscillations of the window widths, the results are
C     now smoothed with a 5-point, 1st-order least squares fit by SE15.
C
      CALL SE15(WINDOW,WINW,NW,IER)
C
      RETURN
      END
C=======================================================================
C                            SUBROUTINE SE15
C
C        PURPOSE
C           TO COMPUTE A VECTOR OF SMOOTHED FUNCTION VALUES GIVEN A
C           VECTOR OF FUNCTION VALUES WHOSE ENTRIES CORRESPOND TO
C           EQUIDISTANTLY SPACED ARGUMENT VALUES.
C
C        USAGE
C           CALL SE15(Y,Z,NDIM,IER)
C
C        DESCRIPTION OF PARAMETERS
C           Y     -  GIVEN VECTOR OF FUNCTION VALUES (DIMENSION NDIM)
C           Z     -  RESULTING VECTOR OF SMOOTHED FUNCTION VALUES
C                    (DIMENSION NDIM)
C           NDIM  -  DIMENSION OF VECTORS Y AND Z
C           IER   -  RESULTING ERROR PARAMETER
C                    IER = -1  - NDIM IS LESS THAN 5
C                    IER =  0  - NO ERROR
C
C        REMARKS
C           (1)  IF IER=-1 THERE HAS BEEN NO COMPUTATION.
C           (2)   Z CAN HAVE THE SAME STORAGE ALLOCATION AS Y.  IF Y IS
C                 DISTINCT FROM Z, THEN IT IS NOT DESTROYED.
C
C        SUBROUTINE AND FUNCTION SUBPROGRAMS REQUIRED
```

```
C            NONE
C
C         METHOD
C            IF X IS THE (SUPPRESSED) VECTOR OF ARGUMENT VALUES, THEN
C            EXCEPT AT THE POINTS X(1),X(2),X(NDIM-1) AND X(NDIM), EACH
C            SMOOTHED VALUE Z(I) IS OBTAINED BY EVALUATING AT X(I) THE
C            LEAST-SQUARES POLYNOMIAL OF DEGREE 1 RELEVANT TO THE 5
C            SUCCESSIVE POINTS (X(I+K),Y(I+K)) K = -2,-1,...,2.  (SEE
C            HILDEBRAND, F.B., INTRODUCTION TO NUMERICAL ANALYSIS,
C            MC GRAW-HILL, NEW YORK/TORONTO/LONDON, 1956, PP. 295-302.)
C-------------------------------------------------------------------------
      SUBROUTINE SE15(Y,Z,NDIM,IER)
      DIMENSION Y(NDIM),Z(NDIM)
C
C     Test of dimension
C
      IF(NDIM-5)3,1,1
C
C     Prepare loop
C
    1 A=Y(1)+Y(1)
      C=Y(2)+Y(2)
      B=.2*(A+Y(1)+C+Y(3)-Y(5))
      C=.1*(A+A+C+Y(2)+Y(3)+Y(3)+Y(4))
C
C     Start loop
C
      DO 2 I=5,NDIM
         A=B
         B=C
         C=.2*(Y(I-4)+Y(I-3)+Y(I-2)+Y(I-1)+Y(I))
    2 Z(I-4)=A
C
C     End of loop
C
C     Update last four components
C
      A=Y(NDIM)+Y(NDIM)
      A=.1*(A+A+Y(NDIM-1)+Y(NDIM-1)+Y(NDIM-1)+Y(NDIM-2)+Y(NDIM-2)
     +  +Y(NDIM-3))
      Z(NDIM-3)=B
      Z(NDIM-2)=C
      Z(NDIM-1)=A
      Z(NDIM)=A+A-C
      IER=0
      RETURN
C
C     Error exit in case NDIM is less than 5
C
    3 IER=-1
      RETURN
      END
C=========================================================================
C                              end of FORIST.FOR
C=========================================================================
```

Appendix F: GRAPHICS.TK Computer Model

VARIABLE SHEET — For Academic Use Only

St	Input	Name	Output	Unit	Comment
					Graphics.TK 23 Oct 92
					by Robert S. Pope
					A PROGRAM TO GRAPH THE RESULTS FROM
					THE FORIST UNFOLDING CODE

L	0	E1			energy - input from TOGRAPH.OUT (eV)
L		e1	0		energy - converted for x-axis (MeV)
L	0	UTB1			spectrum, unsmoothed
L	0	EPSLON1			error, unsmoothed
L		SpecUp1	0		high bound on spectrum error, unsmooth
L		SpecDn1	0		low bound on spectrum error, unsmooth
L	0	E0			energy - input from TOGRAPH.OUT (eV)
L		e0	0		energy - converted for x-axis (MeV)
L	0	UTB0			spectrum, smoothed
L	0	EPSLON0			error, smoothed
L		SpecUp0	0		high bound on spectrum error, smooth
L		SpecDn0	0		low bound on spectrum error, smooth

RULE SHEET — For Academic Use Only

S	Rule
	"Convert energy from eV to MeV
*	e1 = E1 / 1e6
*	e0 = E0 / 1e6
	"Compute error bounds on spectrum
*	SpecUp1 = UTB1 + EPSLON1
*	SpecDn1 = UTB1 - EPSLON1
*	SpecUp0 = UTB0 + EPSLON0
*	SpecDn0 = UTB0 - EPSLON0

LIST SHEET — For Academic Use Only

Name	Elements	Unit	Comment
			1. Use "/SAL" (ASCII load) command to input lists from TOGRAPH.OUT
			2. Hit F10 to create remaining lists
			3. Plot results

PLOT SHEET — For Academic Use Only

Name	Plot Type	Display Option	Output Device	Title
unsmooth1	Line chart	1.EGA		Add title
smooth0	Line chart	1.EGA		Add title

Appendix G: ZSHIFT.OUT Data File

This is the file ZSHIFT.OUT created by ZSHIFT. This file contains each of the four original spectra, the four corresponding zero-shifted spectra, and the four final 200-channel zero-shifted spectra for input to FORIST. The purpose of this file is to serve as a debugging tool for ZSHIFT. The data in this file corresponds to the other computer examples in the appendices. This file is presented in lanscape format in order to preserve the form of the actual output from ZSHIFT, which is formatted for output on a wide-carriage line printer.

NAME OF RESPONSE MATRIX USED IN PROBLEM =UINEUT.MAT
256 CHANNEL ORIGINAL SPECTRUM
ZERO INTERCEPT = 4.005
PB9HFN

1.	0.	0.	0.	0.	0.	1.	1.
0.	967.	48954.	50520.	44942.	40330.	35365.	31877.
28742.	26365.	24442.	22990.	21597.	20338.	19248.	18125.
17449.	16711.	16471.	15420.	14725.	13874.	13237.	11988.
11197.	9776.	8758.	7840.	7111.	6662.	6127.	5887.
5814.	5750.	5435.	5424.	5212.	4929.	4763.	4626.
4331.	4121.	4038.	3912.	3934.	3668.	3673.	3507.
3388.	3447.	3387.	3317.	3175.	3022.	3004.	3007.
3042.	2923.	2902.	2799.	2720.	2653.	2677.	2578.
2545.	2488.	2477.	2312.	2337.	2370.	2299.	2241.
2193.	2221.	2128.	2063.	2041.	2041.	2017.	2107.
1934.	1897.	1968.	1914.	1927.	1816.	1889.	1754.
1758.	1685.	1702.	1584.	1718.	1570.	1650.	1557.
1546.	1544.	1545.	1533.	1417.	1557.	1471.	1416.
1416.	1386.	1372.	1377.	1372.	1370.	1311.	1263.
1268.	1221.	1230.	1204.	1240.	1232.	1222.	1168.
1202.	1205.	1110.	1158.	1136.	1077.	1064.	1060.
1038.	1071.	1044.	984.	1059.	990.	1019.	975.
919.	952.	923.	947.	861.	895.	876.	898.
863.	874.	843.	860.	833.	813.	782.	808.
820.	802.	800.	723.	779.	755.	766.	746.
751.	727.	698.	741.	730.	703.	655.	668.
702.	678.	679.	711.	709.	644.	662.	614.
642.	630.	615.	602.	601.	586.	580.	595.
595.	576.	554.	621.	548.	541.	528.	533.
565.	509.	531.	520.	498.	537.	499.	487.
479.	496.	516.	503.	428.	507.	481.	431.
465.	458.	471.	473.	456.	481.	417.	386.
453.	454.	416.	443.	382.	410.	390.	398.
413.	400.	401.	398.	365.	401.	385.	371.
334.	354.	317.	327.	358.	343.	369.	365.
347.	343.	331.	363.	330.	315.	305.	314.

256 CHANNEL ZERO-SHIFTED SPECTRUM

0.	0.	1.	1.	0.	488.	25200.	49745.
47703.	42613.	37823.	33604.	30294.	27542.	25394.	23709.
22287.	20961.	19788.	18681.	17784.	17076.	16590.	15940.

15069.	14295.	13552.	12606.	11589.	10479.	9262.	8294.
7472.	6884.	6392.	6006.	5850.	5782.	5591.	5429.
5317.	5069.	4845.	4694.	4477.	4225.	4079.	3974.
3923.	3800.	3671.	3589.	3447.	3418.	3417.	3352.
3245.	3098.	3013.	3006.	3025.	2982.	2912.	2850.
2759.	2686.	2665.	2627.	2561.	2516.	2482.	2394.
2325.	2354.	2334.	2270.	2217.	2207.	2174.	2095.
2052.	2041.	2029.	2062.	2020.	1915.	1933.	1941.
1921.	1871.	1853.	1821.	1756.	1721.	1694.	1642.
1652.	1643.	1610.	1603.	1551.	1545.	1545.	1539.
1474.	1488.	1514.	1443.	1416.	1401.	1379.	1375.
1374.	1371.	1340.	1287.	1266.	1244.	1226.	1217.
1222.	1236.	1227.	1195.	1185.	1204.	1158.	1134.
1147.	1106.	1070.	1062.	1049.	1055.	1057.	1014.
1012.	1014.	1005.	997.	947.	936.	937.	935.
904.	878.	885.	887.	880.	869.	858.	852.
846.	823.	797.	795.	814.	811.	801.	761.
751.	767.	761.	756.	749.	739.	712.	720.
735.	716.	679.	662.	685.	690.	679.	695.
710.	676.	653.	638.	628.	636.	622.	608.
601.	593.	583.	588.	595.	585.	565.	588.
584.	544.	534.	531.	549.	537.	520.	525.
509.	518.	518.	493.	483.	488.	506.	509.
465.	468.	494.	456.	448.	461.	465.	472.
464.	469.	449.	401.	420.	454.	435.	430.
412.	396.	400.	394.	406.	406.	401.	399.
381.	383.	393.	378.	352.	344.	335.	322.
343.	350.	356.	367.	356.	345.	337.	347.
346.	322.	310.	310.	0.	0.	0.	0.

200 CHANNEL SUMMED AND SHIFTED SPECTRUM FOR INPUT TO FORIST.FOR

PB9HFN	1	0.	0.	1.	1.	0.	488.	25200.	49745.	47703.	42613.
PB9HFN	11	37823.	33604.	30294.	27542.	25394.	23709.	22287.	20961.	19788.	18681.
PB9HFN	21	17784.	17076.	16590.	15940.	15069.	14295.	13552.	12606.	11589.	10479.
PB9HFN	31	9262.	8294.	7472.	6884.	6392.	6006.	5850.	5782.	5591.	5429.
PB9HFN	41	5317.	5069.	4845.	4694.	4477.	4225.	4079.	3974.	3923.	3800.
PB9HFN	51	3671.	3589.	3447.	3418.	3417.	3352.	3245.	3098.	3013.	3006.
PB9HFN	61	3025.	2982.	2912.	2850.	2759.	2686.	2665.	2627.	2561.	2516.
PB9HFN	71	2482.	2394.	2325.	2354.	2334.	2270.	2217.	2207.	2174.	2095.
PB9HFN	81	2052.	2041.	2029.	2062.	2020.	1915.	1933.	1941.	1921.	1871.
PB9HFN	91	1853.	1821.	1756.	1721.	1694.	1642.	1652.	1643.	1610.	1603.

PB9HFN 101	1551.	1545.	1545.	1539.	1474.	1488.	1514.	1443.	1416.	1401.
PB9HFN 111	1379.	1375.	1374.	1371.	1340.	1287.	1266.	1244.	1226.	1217.
PB9HFN 121	1222.	1236.	1227.	1195.	1185.	1204.	1158.	1134.	1147.	1106.
PB9HFN 131	1070.	1062.	1049.	1055.	1057.	1014.	1012.	1014.	1005.	997.
PB9HFN 141	947.	936.	937.	935.	904.	878.	885.	887.	880.	869.
PB9HFN 151	858.	852.	846.	823.	797.	795.	814.	811.	801.	761.
PB9HFN 161	751.	767.	761.	756.	749.	739.	712.	[illegible]20.	735.	716.
PB9HFN 171	679.	662.	685.	690.	679.	695.	710.	676.	653.	638.
PB9HFN 181	628.	636.	622.	608.	601.	593.	583.	588.	595.	585.
PB9HFN 191	565.	588.	584.	544.	534.	531.	549.	537.	520.	525.

256 CHANNEL ORIGINAL SPECTRUM
ZERO INTERCEPT = 5.509
PB9LFN

0.	0.	0.	0.	0.	0.	0.	0.
0.	150.	21348.	22502.	19397.	17009.	14860.	13015.
11602.	10465.	9201.	8173.	7427.	6720.	6081.	5738.
5144.	4771.	4173.	3811.	3453.	3193.	2933.	2589.
2316.	2091.	1879.	1624.	1576.	1396.	1266.	1199.
1173.	1060.	965.	830.	783.	703.	656.	626.
547.	555.	455.	463.	385.	369.	348.	315.
254.	215.	193.	193.	183.	147.	123.	110.
111.	101.	90.	85.	76.	84.	77.	50.
50.	43.	39.	18.	14.	8.	5.	7.
3.	3.	2.	0.	1.	0.	0.	0.
1.	0.	0.	1.	0.	0.	0.	0.
0.	0.	0.	1.	0.	0.	0.	0.
0.	0.	0.	0.	0.	0.	0.	0.
0.	0.	0.	0.	0.	0.	0.	0.
0.	0.	0.	0.	0.	0.	0.	1.
0.	0.	0.	0.	0.	0.	0.	0.
0.	0.	0.	0.	0.	0.	0.	0.
0.	0.	0.	1.	0.	0.	0.	0.
0.	0.	0.	0.	0.	0.	0.	0.
0.	0.	0.	0.	0.	0.	0.	0.
0.	0.	0.	0.	0.	0.	0.	0.
0.	0.	0.	0.	0.	0.	0.	0.
0.	0.	0.	0.	0.	0.	0.	0.
0.	0.	0.	0.	0.	0.	0.	0.

```
      0.       0.       0.       0.       0.       0.       0.       0.
      0.       0.       0.       0.       0.       0.       0.       0.
      0.       0.       0.       0.       0.       0.       0.       0.
      0.       0.       0.       0.       0.       0.       0.       0.
      0.       0.       0.       0.       0.       0.       0.       0.
   256 CHANNEL ZERO-SHIFTED SPECTRUM
      0.       0.       0.       1.     341.   21358.   22474.   19376.
  16990.   14843.   13002.   11592.   10454.    9192.    8166.    7421.
   6714.    6078.    5733.    5141.    4766.    4170.    3808.    3451.
   3191.    2930.    2587.    2314.    2089.    1877.    1624.    1574.
   1395.    1265.    1199.    1172.    1059.     964.     830.     782.
    703.     656.     625.     547.     554.     455.     462.     385.
    369.     348.     314.     254.     215.     193.     193.     183.
    147.     123.     110.     111.     101.      90.      85.      76.
     84.      77.      50.      50.      43.      39.      18.      14.
      8.       5.       7.       3.       3.       2.       0.       1.
      0.       0.       0.       1.       0.       0.       1.       0.
      0.       0.       0.       0.       0.       0.       1.       0.
      0.       0.       0.       0.       0.       0.       0.       0.
      0.       0.       0.       0.       0.       0.       0.       0.
      0.       0.       0.       0.       0.       0.       0.       0.
      0.       0.       1.       0.       0.       0.       0.       0.
      0.       0.       0.       0.       0.       0.       0.       0.
      0.       0.       0.       0.       0.       0.       0.       0.
      0.       0.       0.       0.       0.       0.       1.       0.
      0.       0.       0.       0.       0.       0.       0.       0.
      0.       0.       0.       0.       0.       0.       0.       0.
      0.       0.       0.       0.       0.       0.       0.       0.
      0.       0.       0.       0.       0.       0.       0.       0.
      0.       0.       0.       0.       0.       0.       0.       0.
      0.       0.       0.       0.       0.       0.       0.       0.
      0.       0.       0.       0.       0.       0.       0.       0.
      0.       0.       0.       0.       0.       0.       0.       0.
      0.       0.       0.       0.       0.       0.       0.       0.
   200 CHANNEL SUMMED AND SHIFTED SPECTRUM FOR INPUT TO FORIST.FOR
PB9LFN  1       0.       0.       0.       1.     341.   21358.   22474.   19376.   16990.   14843.
```

PB9LFN	11	13002.	11592.	10454.	9192.	8166.	7421.	6714.	6078.	5733.	5141.
PB9LFN	21	4766.	4170.	3808.	3451.	3191.	2930.	2587.	2314.	2089.	1877.
PB9LFN	31	1624.	1574.	1395.	1265.	1199.	1172.	1059.	964.	830.	782.
PB9LFN	41	703.	656.	625.	547.	554.	455.	462.	385.	369.	348.
PB9LFN	51	314.	254.	215.	193.	193.	183.	147.	123.	110.	111.
PB9LFN	61	101.	90.	85.	76.	84.	77.	50.	50.	43.	39.
PB9LFN	71	18.	14.	8.	5.	7.	3.	3.	2.	0.	1.
PB9LFN	81	0.	0.	0.	1.	0.	0.	1.	0.	0.	0.
PB9LFN	91	0.	0.	0.	0.	1.	0.	0.	0.	0.	0.
PB9LFN	101	0.	0.	0.	0.	0.	0.	0.	0.	0.	0.
PB9LFN	111	0.	0.	0.	0.	0.	0.	0.	0.	0.	0.
PB9LFN	121	0.	0.	1.	0.	0.	0.	0.	0.	0.	0.
PB9LFN	131	0.	0.	0.	0.	0.	0.	0.	0.	0.	0.
PB9LFN	141	0.	0.	0.	0.	0.	0.	0.	0.	0.	0.
PB9LFN	151	1.	0.	0.	0.	0.	0.	0.	0.	0.	0.
PB9LFN	161	0.	0.	0.	0.	0.	0.	0.	0.	0.	0.
PB9LFN	171	0.	0.	0.	0.	0.	0.	0.	0.	0.	0.
PB9LFN	181	0.	0.	0.	0.	0.	0.	0.	0.	0.	0.
PB9LFN	191	0.	0.	0.	0.	0.	0.	0.	0.	0.	0.

256 CHANNEL ORIGINAL SPECTRUM
ZERO INTERCEPT = 4.005
PB9HBN

0.	0.	0.	0.	0.	0.	0.	0.
0.	308.	15377.	15743.	13633.	11695.	10112.	8706.
7427.	6651.	5924.	5251.	4710.	4252.	4024.	3729.
3446.	3267.	3044.	3007.	2690.	2462.	2395.	2310.
2066.	1943.	1740.	1556.	1492.	1427.	1308.	1248.
1217.	1155.	1005.	1056.	979.	935.	916.	837.
827.	740.	722.	745.	712.	662.	639.	653.
639.	656.	581.	544.	540.	562.	521.	490.
496.	467.	488.	449.	427.	413.	442.	378.
413.	372.	376.	360.	375.	349.	337.	355.
312.	333.	309.	294.	285.	287.	266.	248.
271.	290.	276.	262.	224.	218.	236.	219.
194.	220.	228.	203.	199.	206.	211.	181.
185.	165.	171.	160.	176.	156.	186.	148.
150.	140.	132.	136.	139.	131.	126.	132.
120.	139.	116.	117.	112.	101.	97.	126.
97.	99.	111.	104.	100.	84.	91.	90.
83.	88.	87.	86.	106.	74.	103.	98.

78.	71.	71.	88.	83.	66.	68.	62.
62.	71.	51.	62.	54.	78.	67.	84.
59.	43.	56.	67.	58.	68.	54.	55.
64.	57.	58.	57.	46.	54.	51.	40.
51.	50.	50.	34.	55.	45.	49.	51.
38.	48.	61.	33.	42.	32.	52.	40.
43.	49.	35.	31.	40.	41.	32.	42.
40.	36.	35.	32.	39.	38.	35.	36.
27.	39.	25.	29.	26.	32.	28.	40.
34.	24.	26.	25.	31.	31.	19.	24.
26.	21.	24.	23.	24.	24.	37.	22.
20.	23.	19.	24.	16.	23.	18.	22.
23.	21.	18.	22.	21.	19.	21.	15.
21.	15.	19.	17.	15.	18.	16.	16.

256 CHANNEL ZERO-SHIFTED SPECTRUM

0.	0.	0.	0.	0.	156.	7918.	15562.
14677.	12654.	10896.	9402.	8060.	7035.	6284.	5584.
4978.	4479.	4137.	3875.	3586.	3356.	3154.	3025.
2847.	2575.	2428.	2352.	2187.	2004.	1840.	1647.
1524.	1459.	1367.	1278.	1232.	1186.	1079.	1031.
1017.	957.	925.	876.	832.	783.	731.	734.
728.	687.	650.	646.	646.	648.	618.	562.
542.	551.	541.	505.	493.	481.	478.	468.
438.	420.	428.	410.	396.	392.	374.	368.
368.	362.	343.	346.	333.	323.	321.	301.
289.	286.	276.	257.	260.	281.	283.	269.
243.	221.	227.	227.	206.	207.	224.	215.
201.	203.	209.	196.	183.	175.	168.	165.
168.	166.	171.	167.	149.	145.	136.	134.
138.	135.	128.	129.	126.	130.	127.	117.
114.	106.	99.	112.	111.	98.	105.	107.
102.	92.	88.	90.	86.	86.	87.	86.
96.	90.	89.	100.	88.	74.	71.	80.
85.	74.	67.	65.	62.	67.	61.	57.
58.	66.	72.	76.	71.	51.	50.	62.
62.	63.	61.	55.	60.	60.	58.	57.
51.	50.	52.	45.	46.	50.	50.	42.
45.	50.	47.	50.	44.	43.	55.	47.
38.	37.	42.	46.	42.	46.	42.	33.
36.	41.	36.	37.	41.	38.	35.	33.

```
      36.       38.       36.       36.       31.       33.       32.       27.
      27.       29.       30.       34.       37.       29.       25.       25.
      28.       31.       25.       22.       25.       23.       23.       23.
      24.       24.       31.       29.       21.       22.       21.       22.
      20.       20.       20.       20.       25.       24.       19.       20.
      21.       20.       20.       18.       18.       18.       17.       18.
      16.       17.       17.       16.        0.        0.        0.        0.
     200 CHANNEL SUMMED AND SHIFTED SPECTRUM FOR INPUT TC FORIST.FOR
PB9HBN   1       0.        0.        0.        0.        0.      156.     7918.    15562.    14677.    12654.
PB9HBN  11   10896.     9402.     8060.     7035.     6284.     5584.     4978.     4479.     4137.     3875.
PB9HBN  21    3586.     3356.     3154.     3025.     2847.     2575.     2428.     2352.     2187.     2004.
PB9HBN  31    1840.     1647.     1524.     1459.     1367.     1278.     1232.     1186.     1079.     1031.
PB9HBN  41    1017.      957.      925.      876.      832.      783.      731.      734.      728.      687.
PB9HBN  51     650.      646.      646.      648.      618.      562.      542.      551.      541.      505.
PB9HBN  61     493.      481.      478.      468.      438.      420.      428.      410.      396.      392.
PB9HBN  71     374.      368.      368.      362.      343.      346.      333.      323.      321.      301.
PB9HBN  81     289.      286.      276.      257.      260.      281.      283.      269.      243.      221.
PB9HBN  91     227.      227.      206.      207.      224.      215.      201.      203.      209.      196.
PB9HBN 101     183.      175.      168.      165.      168.      166.      171.      167.      149.      145.
PB9HBN 111     136.      134.      138.      135.      128.      129.      126.      130.      127.      117.
PB9HBN 121     114.      106.       99.      112.      111.       98.      105.      107.      102.       92.
PB9HBN 131      88.       90.       86.       86.       87.       86.       96.       90.       89.      100.
PB9HBN 141      88.       74.       71.       80.       85.       74.       67.       65.       62.       67.
PB9HBN 151      61.       57.       58.       66.       72.       76.       71.       51.       50.       62.
PB9HBN 161      62.       63.       61.       55.       60.       60.       58.       57.       51.       50.
PB9HBN 171      52.       45.       46.       50.       50.       42.       45.       50.       47.       50.
PB9HBN 181      44.       43.       55.       47.       38.       37.       42.       46.       42.       46.
PB9HBN 191      42.       33.       36.       41.       36.       37.       41.       38.       35.       33.
     256 CHANNEL ORIGINAL SPECTRUM
     ZERO INTERCEPT =  5.509
     PB9LBN
       0.        0.        0.        0.        0.        0.        0.        0.
       0.       17.     3376.     3466.     2709.     2251.     1822.     1367.
    1132.      886.      828.      669.      559.      529.      452.      404.
     320.      274.      245.      207.      214.      184.      153.      118.
     125.       96.       84.       75.       66.       64.       47.       32.
      38.       33.       28.       34.       25.       22.       16.        7.
      16.       10.        5.       14.       10.       11.        6.        8.
       5.        6.        4.        6.        3.        4.        1.        2.
       0.        2.        1.        0.        0.        0.        2.        0.
```

0.	0.	1.	0.	0.	0.	0.	0.
0.	0.	0.	0.	0.	0.	0.	0.
0.	0.	1.	0.	0.	0.	0.	0.
0.	0.	1.	0.	0.	0.	0.	0.
0.	0.	0.	0.	0.	0.	0.	0.
0.	0.	0.	0.	0.	0.	0.	0.
0.	0.	0.	0.	0.	0.	0.	0.
0.	0.	0.	0.	0.	0.	0.	0.
0.	0.	0.	0.	0.	0.	0.	0.
0.	0.	0.	1.	0.	0.	0.	1.
0.	0.	0.	0.	0.	0.	0.	0.
0.	0.	0.	0.	0.	0.	0.	0.
0.	0.	0.	0.	0.	0.	0.	0.
0.	0.	0.	0.	0.	0.	0.	0.
0.	0.	0.	0.	0.	0.	0.	0.
0.	0.	0.	0.	0.	0.	0.	0.
0.	0.	0.	0.	0.	0.	0.	0.
0.	0.	0.	0.	0.	0.	0.	0.
0.	0.	0.	0.	0.	0.	0.	0.
0.	0.	0.	0.	0.	0.	0.	0.
0.	0.	0.	0.	0.	0.	0.	0.
0.	0.	0.	0.	0.	0.	0.	0.
0.	0.	0.	0.	0.	0.	0.	0.

256 CHANNEL ZERO-SHIFTED SPECTRUM

0.	0.	0.	0.	47.	3377.	3459.	2705.
2247.	1818.	1365.	1130.	885.	827.	668.	559.
528.	452.	403.	320.	274.	245.	207.	214.
184.	153.	118.	125.	96.	84.	75.	66.
64.	47.	52.	38.	33.	28.	34.	25.
22.	16.	7.	16.	10.	5.	14.	10.
11.	6.	8.	5.	6.	4.	6.	3.
4.	1.	2.	0.	2.	1.	0.	0.
0.	2.	0.	0.	0.	1.	0.	0.
0.	0.	0.	0.	0.	0.	0.	0.
0.	0.	0.	0.	0.	1.	0.	0.
0.	0.	0.	0.	0.	1.	0.	0.
0.	0.	0.	0.	0.	0.	0.	0.
0.	0.	0.	0.	0.	0.	0.	0.
0.	0.	0.	0.	0.	0.	0.	0.
0.	0.	0.	0.	0.	0.	0.	0.

0.	0.	0.	0.	0.	0.	0.	0.
0.	0.	0.	0.	0.	0.	1.	0.
0.	0.	1.	0.	0.	0.	0.	0.
0.	0.	0.	0.	0.	0.	0.	0.
0.	0.	0.	0.	0.	0.	0.	0.
0.	0.	0.	0.	0.	0.	0.	0.
0.	0.	0.	0.	0.	0.	0.	0.
0.	0.	0.	0.	0.	0.	0.	0.
0.	0.	0.	0.	0.	0.	0.	0.
0.	0.	0.	0.	0.	0.	0.	0.
0.	0.	0.	0.	0.	0.	0.	0.
0.	0.	0.	0.	0.	0.	0.	0.
0.	0.	0.	0.	0.	0.	0.	0.
0.	0.	0.	0.	0.	0.	0.	0.
0.	0.	0.	0.	0.	0.	0.	0.
0.	0.	0.	0.	0.	0.	0.	0.

200 CHANNEL SUMMED AND SHIFTED SPECTRUM FOR INPUT TO FORIST.FOR

PB9LBN	1	0.	0.	0.	0.	47.	3377.	3459.	2705.	2247.	1818.
PB9LBN	11	1365.	1130.	885.	827.	668.	559.	528.	452.	403.	320.
PB9LBN	21	274.	245.	207.	214.	184.	153.	118.	125.	96.	84.
PB9LBN	31	75.	66.	64.	47.	52.	38.	33.	28.	34.	25.
PB9LBN	41	22.	16.	7.	16.	10.	5.	14.	10.	11.	6.
PB9LBN	51	8.	5.	6.	4.	6.	3.	4.	1.	2.	0.
PB9LBN	61	2.	1.	0.	0.	0.	2.	0.	0.	0.	1.
PB9LBN	71	0.	0.	0.	0.	0.	0.	0.	0.	0.	1.
PB9LBN	81	0.	0.	0.	0.	0.	1.	0.	0.	0.	0.
PB9LBN	91	0.	0.	0.	1.	0.	0.	0.	0.	0.	0.
PB9LBN	101	0.	0.	0.	0.	0.	0.	0.	0.	0.	0.
PB9LBN	111	0.	0.	0.	0.	0.	0.	0.	0.	0.	0.
PB9LBN	121	0.	0.	0.	0.	0.	0.	0.	0.	0.	0.
PB9LBN	131	0.	0.	0.	0.	0.	0.	0.	0.	0.	0.
PB9LBN	141	0.	0.	1.	0.	0.	0.	1.	0.	0.	0.
PB9LBN	151	0.	0.	0.	0.	0.	0.	0.	0.	0.	0.
PB9LBN	161	0.	0.	0.	0.	0.	0.	0.	0.	0.	0.
PB9LBN	171	0.	0.	0.	0.	0.	0.	0.	0.	0.	0.
PB9LBN	181	0.	0.	0.	0.	0.	0.	0.	0.	0.	0.
PB9LBN	191	0.	0.	0.	0.	0.	0.	0.	0.	0.	0.

Appendix H: SPECTRA.IN Data File

The following is the data file called SPECTRA.IN, which is created by ZSHIFT to be the input file for FORIST. This version of the file corresponds to the other computer files contained in the appendices. The format of this file is important and must be maintained if FORIST is to be able to read the file properly. The page breaks of this file have been included so that the output would fit into the format of the thesis. In the acutal file, there are no blank lines between the pages.

```
UINEUT.MAT
        23     1.000         9         3         1         3   10.0000
     900.       900.
     900.       900.
   0.0064     0.0663
   0.0064     0.0663
DYNMAT  1000  10  (1X,A6,I4,10F7.0)
PuBe #M1170 run 9 neutrons hgf, 24 Nov 92
PB9HFN   1     0.      0.      1.      1.      0.    488. 25200. 49745. 47703. 42613.
PB9HFN  11 37823. 33604. 30294. 27542. 25394. 23709. 22287. 20961. 19788. 18681.
PB9HFN  21 17784. 17076. 16590. 15940. 15069. 14295. 13552. 12606. 11589. 10479.
PB9HFN  31  9262.  8294.  7472.  6884.  6392.  6006.  5850.  5782.  5591.  5429.
PB9HFN  41  5317.  5069.  4845.  4694.  4477.  4225.  4079.  3974.  3923.  3800.
PB9HFN  51  3671.  3589.  3447.  3418.  3417.  3352.  3245.  3098.  3013.  3006.
PB9HFN  61  3025.  2982.  2912.  2850.  2759.  2686.  2665.  2627.  2561.  2516.
PB9HFN  71  2482.  2394.  2325.  2354.  2334.  2270.  2217.  2207.  2174.  2095.
PB9HFN  81  2052.  2041.  2029.  2062.  2020.  1915.  1933.  1941.  1921.  1871.
PB9HFN  91  1853.  1821.  1756.  1721.  1694.  1642.  1652.  1643.  1610.  1603.
PB9HFN 101  1551.  1545.  1545.  1539.  1474.  1488.  1514.  1443.  1416.  1401.
PB9HFN 111  1379.  1375.  1374.  1371.  1340.  1287.  1266.  1244.  1226.  1217.
PB9HFN 121  1222.  1236.  1227.  1195.  1185.  1204.  1158.  1134.  1147.  1106.
PB9HFN 131  1070.  1062.  1049.  1055.  1057.  1014.  1012.  1014.  1005.   997.
PB9HFN 141   947.   936.   937.   935.   904.   878.   885.   887.   880.   869.
PB9HFN 151   858.   852.   846.   823.   797.   795.   814.   811.   801.   761.
PB9HFN 161   751.   767.   761.   756.   749.   739.   712.   720.   735.   716.
PB9HFN 171   679.   662.   685.   690.   679.   695.   710.   676.   653.   638.
PB9HFN 181   628.   636.   622.   608.   601.   593.   583.   588.   595.   585.
PB9HFN 191   565.   588.   584.   544.   534.   531.   549.   537.   520.   525.
DYNMAT  2000  10  (1X,A6,I4,10F7.0)
PuBe #M1170 run 9 neutrons lgf, 24 Nov 92
PB9LFN   1     0.      0.      0.      1.    341. 21358. 22474. 19376. 16990. 14843.
PB9LFN  11 13002. 11592. 10454.  9192.  8166.  7421.  6714.  6078.  5733.  5141.
PB9LFN  21  4766.  4170.  3808.  3451.  3191.  2930.  2587.  2314.  2089.  1877.
PB9LFN  31  1624.  1574.  1395.  1265.  1199.  1172.  1059.   964.   830.   782.
PB9LFN  41   703.   656.   625.   547.   554.   455.   462.   385.   369.   348.
PB9LFN  51   314.   254.   215.   193.   193.   183.   147.   123.   110.   111.
PB9LFN  61   101.    90.    85.    76.    84.    77.    50.    50.    43.    39.
PB9LFN  71    18.    14.     8.     5.     7.     3.     3.     2.     0.     1.
PB9LFN  81     0.     0.     0.     1.     0.     0.     1.     0.     0.     0.
PB9LFN  91     0.     0.     0.     0.     1.     0.     0.     0.     0.     0.
```

```
PB9LFN 101      0.      0.      0.      0.      0.      0.      0.      0.      0.      0.
PB9LFN 111      0.      0.      0.      0.      0.      0.      0.      0.      0.      0.
PB9LFN 121      0.      0.      1.      0.      0.      0.      0.      0.      0.      0.
PB9LFN 131      0.      0.      0.      0.      0.      0.      0.      0.      0.      0.
PB9LFN 141      0.      0.      0.      0.      0.      0.      0.      0.      0.      0.
PB9LFN 151      1.      0.      0.      0.      0.      0.      0.      0.      0.      0.
PB9LFN 161      0.      0.      0.      0.      0.      0.      0.      0.      0.      0.
PB9LFN 171      0.      0.      0.      0.      0.      0.      0.      0.      0.      0.
PB9LFN 181      0.      0.      0.      0.      0.      0.      0.      0.      0.      0.
PB9LFN 191      0.      0.      0.      0.      0.      0.      0.      0.      0.      0.

DYNMAT  1000  10  (1X,A6,I4,10F7.0)
PuBe #M1170 run 9 neutrons hgb, 24 Nov 92
PB9HBN    1     0.      0.      0.      0.      0.    156.   7918.  15562.  14677.  12654.
PB9HBN   11 10896.   9402.   8060.   7035.   6284.   5584.   4978.   4479.   4137.   3875.
PB9HBN   21  3586.   3356.   3154.   3025.   2847.   2575.   2428.   2352.   2187.   2004.
PB9HBN   31  1840.   1647.   1524.   1459.   1367.   1278.   1232.   1186.   1079.   1031.
PB9HBN   41  1017.    957.    925.    876.    832.    783.    731.    734.    728.    687.
PB9HBN   51   650.    646.    646.    648.    618.    562.    542.    551.    541.    505.
PB9HBN   61   493.    481.    478.    468.    438.    420.    428.    410.    396.    392.
PB9HBN   71   374.    368.    368.    362.    343.    346.    333.    323.    321.    301.
PB9HBN   81   289.    286.    276.    257.    260.    281.    283.    269.    243.    221.
PB9HBN   91   227.    227.    206.    207.    224.    215.    201.    203.    209.    196.
PB9HBN  101   183.    175.    168.    165.    168.    166.    171.    167.    149.    145.
PB9HBN  111   136.    134.    138.    135.    128.    129.    126.    130.    127.    117.
PB9HBN  121   114.    106.     99.    112.    111.     98.    105.    107.    102.     92.
PB9HBN  131    88.     90.     86.     86.     87.     86.     96.     90.     89.    100.
PB9HBN  141    88.     74.     71.     80.     85.     74.     67.     65.     62.     67.
PB9HBN  151    61.     57.     58.     66.     72.     76.     71.     51.     50.     62.
PB9HBN  161    62.     63.     61.     55.     60.     60.     58.     57.     51.     50.
PB9HBN  171    52.     45.     46.     50.     50.     42.     45.     50.     47.     50.
PB9HBN  181    44.     43.     55.     47.     38.     37.     42.     46.     42.     46.
PB9HBN  191    42.     33.     36.     41.     36.     37.     41.     38.     35.     33.
DYNMAT  2000  10  (1X,A6,I4,10F7.0)
PuBe #M1170 run 9 neutrons lgb, 24 Nov 92
PB9LBN    1     0.      0.      0.      0.     47.   3377.   3459.   2705.   2247.   1818.
PB9LBN   11  1365.   1130.    885.    827.    668.    559.    528.    452.    403.    320.
PB9LBN   21   274.    245.    207.    214.    184.    153.    118.    125.     96.     84.
PB9LBN   31    75.     66.     64.     47.     52.     38.     33.     28.     34.     25.
PB9LBN   41    22.     16.      7.     16.     10.      5.     14.     10.     11.      6.
```

PB9LBN 51	8.	5.	6.	4.	6.	3.	4.	1.	2.	0.
PB9LBN 61	2.	1.	0.	0.	0.	2.	0.	0.	0.	1.
PB9LBN 71	0.	0.	0.	0.	0.	0.	0.	0.	0.	0.
PB9LBN 81	0.	0.	0.	0.	0.	1.	0.	0.	0.	0.
PB9LBN 91	0.	0.	0.	1.	0.	0.	0.	0.	0.	0.
PB9LBN 101	0.	0.	0.	0.	0.	0.	0.	0.	0.	0.
PB9LBN 111	0.	0.	0.	0.	0.	0.	0.	0.	0.	0.
PB9LBN 121	0.	0.	0.	0.	0.	0.	0.	0.	0.	0.
PB9LBN 131	0.	0.	0.	0.	0.	0.	0.	0.	0.	0.
PB9LBN 141	0.	0.	1.	0.	0.	0.	1.	0.	0.	0.
PB9LBN 151	0.	0.	0.	0.	0.	0.	0.	0.	0.	0.
PB9LBN 161	0.	0.	0.	0.	0.	0.	0.	0.	0.	0.
PB9LBN 171	0.	0.	0.	0.	0.	0.	0.	0.	0.	0.
PB9LBN 181	0.	0.	0.	0.	0.	0.	0.	0.	0.	0.
PB9LBN 191	0.	0.	0.	0.	0.	0.	0.	0.	0.	0.

Appendix I: FORIST.OUT Data File

This appendix contains the output file from FORIST, called FORIST.OUT, as well as a key to the information that is contained on each page of this output file. Because the output file is meant to be printed on a wide-carriage printer, FORIST.OUT is presented in lanscape format. To correspond with the key, page number headings have been added to indicate the beginning of each page. The page-by-page key to this output file, which is presented in Table 14, has been adapted from Johnson.
[15:16-18]

Table 14. Description of contents of FORIST.OUT file

Page Number	Description
1	Title or response matrix, FORIST input parameters
2	Binning table
3	Normalizations, gains, and nominal gains
4	Foreground data, high and low gain
5	Rearranged high-gain foreground data
6	Rearranged low-gain foreground data
7	Background data, high and low gain
8	Rearranged high-gain background data
9	Rearranged low-gain background data
10	Rebinned high-gain foreground data
11	Rebinned low-gain foreground data
12	Rebinned high-gain background data
13	Rebinned low-gain background data
14-15	Summary of binned input: COUNTS: grouped counts/light unit/second ERROR: statistical error in COUNTS LOCHAN: lower channel of bin UPCHAN: upper channel of bin LO P. H.: lower pulse height boundary of bin UP P. H.: upper pulse height boundary of bin F.A.F.: Forte Acceptance Factor

Table 14. (continued)

Page Number	Description
16-17	Overlap parameters SCOFF, FUDGE, and REFLU Plot of binned counts and errors
18-19	Binned input adjusted for smooth overlap; chi-square test I: bin number VLO: lower pulse height boundary of bin B: COUNTS adjusted for smooth overlap S: ERROR adjusted for smooth overlap BADJ: refolded vector PCTDEV: relative error, in percent ESD: estimated standard deviation
20	Indicators for valid problem 1: matrix inversion accuracy 2: consistency with non-negativity 3: chi-square consistency
21-22	Unfolded solution summary ("zeroth" smoothing iteration) ENERGY: energies, in eV PLO: lower bound (-1 std. dev.) of unfolded spectrum PUP: upper bound (+1 std dev.) of unfolded spectrum PAVE: unfolded spectrum, in neutrons/cm^2-sec-MeV PCT W: window width, in percent ERR1: statistical error in PAVE ERR2: numerical error in PAVE
23-24	Pseudo-semilog plot of PLO and PUP for "0th" smoothing iteration
25-26	Unfolded solution summary (first smoothing iteration)
27-28	Pseudo-semilog plot of PLO and PUP for first smoothing iteration
29-30	Linear plot of PLO and PUP for final smoothing iteration
31-32	Summary of unfolded solution before smoothing ELAB: energies, in eV X: solution vector Q: weak upper bound for X ERRJ1: statistical error in X UHAQJ: numerical error in X

The file FORIST.OUT corresponding to the rest of the code examples in the apendices will now be presented in its entirety.

Page 1:

THE ILLINOIS NEUTRON RESPONSE MATRIX MODIFIED BY NEH BELOW 2.5 MEV

STRETCH	=1.000	
NUMBER OF BITS	= 23	
NUMBER OF ROWS	= 113	
NUMBER OF COLUMNS	= 81	
NUMBER OF WINDOWS	= 109	
FIRST SPECTRUM NUMBER	= 9	
PUNCHING OPTION	= 3	(0/1/2/3) -- (NO PUNCHING / SMOOTHED OUTPUT / UNSMOOTHED OUTPUT / BOTH)
NUMBER OF ITERATIONS	= 1	
PERCENTAGE ERROR	= 3	
FIRST OVERLAP BIN	= 24	

Page 2:

BINNING TABLE

GROUP	LOEDGE	UPEDGE	CHAN/BIN	BINS
1	1009	1016	2	4.0
2	1017	1022	3	2.0
3	1023	1026	4	1.0
4	1027	1036	5	2.0
5	1037	1048	6	2.0
6	1049	1062	7	2.0
7	1063	1078	8	2.0
8	1079	1150	9	8.0
9	1151	1160	10	1.0
10	2016	2016	1	1.0
11	1161	1170	10	1.0
12	2017	2017	1	1.0
13	1171	1180	10	1.0
14	2018	2018	1	1.0
15	1181	1190	10	1.0
16	2019	2040	1	22.0
17	2041	2100	2	30.0
18	2101	2178	3	26.0
19	2179	2198	4	5.0
		TOTAL NO. BINS		113

Page 3:

RUN	F LIVE TIMES	B LIVE TIMES	F GAIN	B GAIN	NOM GAIN
1	0.9000E+03	0.9000E+03	0.6400E-02	0.6400E-02	0.6250E-02
2	0.9000E+03	0.9000E+03	0.6630E-01	0.6630E-01	0.6250E-01
3	0.0000E+00	0.0000E+00	0.0000E+00	0.0000E+00	0.0000E+00
4	0.0000E+00	0.0000E+00	0.0000E+00	0.0000E+00	0.0000E+00

Page 4:

```
DYNMAT    1000 10  (1X,A6,I4,10F7.0)
PuBe #M1170 run 9 neutrons hgf, 24 Nov 92
PB9HFN     1      0.      0.      1.      1.      0.    488.  25200.  49745.  47703.  42613.
PB9HFN    11  37823.  33604.  30294.  27542.  25394.  23709.  22287.  20961.  19788.  18681.
PB9HFN    21  17784.  17076.  16590.  15940.  15069.  14295.  13552.  12606.  11589.  10479.
PB9HFN    31   9262.   8294.   7472.   6884.   6392.   6006.   5850.   5782.   5591.   5429.
PB9HFN    41   5317.   5069.   4845.   4694.   4477.   4225.   4079.   3974.   3923.   3800.
PB9HFN    51   3671.   3589.   3447.   3418.   3417.   3352.   3245.   3098.   3013.   3006.
PB9HFN    61   3025.   2982.   2912.   2850.   2759.   2686.   2665.   2627.   2561.   2516.
PB9HFN    71   2482.   2394.   2325.   2354.   2334.   2270.   2217.   2207.   2174.   2095.
PB9HFN    81   2052.   2041.   2029.   2062.   2020.   1915.   1933.   1941.   1921.   1871.
PB9HFN    91   1853.   1821.   1756.   1721.   1694.   1642.   1652.   1643.   1610.   1603.
PB9HFN   101   1551.   1545.   1545.   1539.   1474.   1488.   1514.   1443.   1416.   1401.
PB9HFN   111   1379.   1375.   1374.   1371.   1340.   1287.   1266.   1244.   1226.   1217.
PB9HFN   121   1222.   1236.   1227.   1195.   1185.   1204.   1158.   1134.   1147.   1106.
PB9HFN   131   1070.   1062.   1049.   1055.   1057.   1014.   1012.   1014.   1005.    997.
PB9HFN   141    947.    936.    937.    935.    904.    878.    885.    887.    880.    869.
PB9HFN   151    858.    852.    846.    823.    797.    795.    814.    811.    801.    761.
PB9HFN   161    751.    767.    761.    756.    749.    739.    712.    720.    735.    716.
PB9HFN   171    679.    662.    685.    690.    679.    695.    710.    676.    653.    638.
PB9HFN   181    628.    636.    622.    608.    601.    593.    583.    588.    595.    585.
PB9HFN   191    565.    588.    584.    544.    534.    531.    549.    537.    520.    525.

DYNMAT    2000 10  (1X,A6,I4,10F7.0)
PuBe #M1170 run 9 neutrons lgf, 24 Nov 92
PB9LFN     1      0.      0.      0.      1.    341.  21358.  22474.  19376.  16990.  14843.
PB9LFN    11  13002.  11592.  10454.   9192.   8166.   7421.   6714.   6078.   5733.   5141.
PB9LFN    21   4766.   4170.   3808.   3451.   3191.   2930.   2587.   2314.   2089.   1877.
PB9LFN    31   1624.   1574.   1395.   1265.   1199.   1172.   1059.    964.    830.    782.
PB9LFN    41    703.    656.    625.    547.    554.    455.    462.    385.    369.    348.
```

PB9LFN	51	314.	254.	215.	193.	193.	183.	147.	123.	110.	111.
PB9LFN	61	101.	90.	85.	76.	84.	77.	50.	50.	43.	39.
PB9LFN	71	18.	14.	8.	5.	7.	3.	3.	2.	0.	1.
PB9LFN	81	0.	0.	0.	1.	0.	0.	1.	0.	0.	0.
PB9LFN	91	0.	0.	0.	0.	1.	0.	0.	0.	0.	0.
PB9LFN	101	0.	0.	0.	0.	0.	0.	0.	0.	0.	0.
PB9LFN	111	0.	0.	0.	0.	0.	0.	0.	0.	0.	0.
PB9LFN	121	0.	0.	1.	0.	0.	0.	0.	0.	0.	0.
PB9LFN	131	0.	0.	0.	0.	0.	0.	0.	0.	0.	0.
PB9LFN	141	0.	0.	0.	0.	0.	0.	0.	0.	0.	0.
PB9LFN	151	1.	0.	0.	0.	0.	0.	0.	0.	0.	0.
PB9LFN	161	0.	0.	0.	0.	0.	0.	0.	0.	0.	0.
PB9LFN	171	0.	0.	0.	0.	0.	0.	0.	0.	0.	0.
PB9LFN	181	0.	0.	0.	0.	0.	0.	0.	0.	0.	0.
PB9LFN	191	0.	0.	0.	0.	0.	0.	0.	0.	0.	0.

Page 5:

PB9HFN RAW COUNTS FOREGROUND GAIN = 1

1	0.0	51	3671.0	101	1551.0	151	858.0
2	0.0	52	3589.0	102	1545.0	152	852.0
3	1.0	53	3447.0	103	1545.0	153	846.0
4	1.0	54	3418.0	104	1539.0	154	823.0
5	0.0	55	3417.0	105	1474.0	155	797.0
6	488.0	56	3352.0	106	1488.0	156	795.0
7	25200.0	57	3245.0	107	1514.0	157	814.0
8	49745.0	58	3098.0	108	1443.0	158	811.0
9	47703.0	59	3013.0	109	1416.0	159	801.0
10	42613.0	60	3006.0	110	1401.0	160	761.0
11	37823.0	61	3025.0	111	1379.0	161	751.0
12	33604.0	62	2982.0	112	1375.0	162	767.0
13	30294.0	63	2912.0	113	1374.0	163	761.0
14	27542.0	64	2850.0	114	1371.0	164	756.0
15	25394.0	65	2759.0	115	1340.0	165	749.0
16	23709.0	66	2686.0	116	1287.0	166	739.0
17	22287.0	67	2665.0	117	1266.0	167	712.0
18	20961.0	68	2627.0	118	1244.0	168	720.0
19	19788.0	69	2561.0	119	1226.0	169	735.0

20	18681.0	70	2516.0	120	1217.0	170	716.0
21	17784.0	71	2482.0	121	1222.0	171	679.0
22	17076.0	72	2394.0	122	1236.0	172	662.0
23	16590.0	73	2325.0	123	1227.0	173	685.0
24	15940.0	74	2354.0	124	1195.0	174	690.0
25	15069.0	75	2334.0	125	1185.0	175	679.0
26	14295.0	76	2270.0	126	1204.0	176	695.0
27	13552.0	77	2217.0	127	1158.0	177	710.0
28	12606.0	78	2207.0	128	1134.0	178	676.0
29	11589.0	79	2174.0	129	1147.0	179	653.0
30	10479.0	80	2095.0	130	1106.0	180	638.0
31	9262.0	81	2052.0	131	1070.0	181	628.0
32	8294.0	82	2041.0	132	1062.0	182	636.0
33	7472.0	83	2029.0	133	1049.0	183	622.0
34	6884.0	84	2062.0	134	1055.0	184	608.0
35	6392.0	85	2020.0	135	1057.0	185	601.0
36	6006.0	86	1915.0	136	1014.0	186	593.0
37	5850.0	87	1933.0	137	1012.0	187	583.0
38	5782.0	88	1941.0	138	1014.0	188	588.0
39	5591.0	89	1921.0	139	1005.0	189	595.0
40	5429.0	90	1871.0	140	997.0	190	585.0
41	5317.0	91	1853.0	141	947.0	191	565.0
42	5069.0	92	1821.0	142	936.0	192	588.0
43	4845.0	93	1756.0	143	937.0	193	584.0
44	4694.0	94	1721.0	144	935.0	194	544.0
45	4477.0	95	1694.0	145	904.0	195	534.0
46	4225.0	96	1642.0	146	878.0	196	531.0
47	4079.0	97	1652.0	147	885.0	197	549.0
48	3974.0	98	1643.0	148	887.0	198	537.0
49	3923.0	99	1610.0	149	880.0	199	520.0
50	3800.0	100	1603.0	150	869.0	200	525.0

TOTAL NUMBER OF COUNTS = 895699.0

Page 6:

PB9LFN RAW COUNTS FOREGROUND GAIN = 2

1	0.0	51	314.0	101	0.0	151	1.0
2	0.0	52	254.0	102	0.0	152	0.0
3	0.0	53	215.0	103	0.0	153	0.0
4	1.0	54	193.0	104	0.0	154	0.0
5	341.0	55	193.0	105	0.0	155	0.0
6	21358.0	56	183.0	106	0.0	156	0.0
7	22474.0	57	147.0	107	0.0	157	0.0
8	19376.0	58	123.0	108	0.0	158	0.0
9	16990.0	59	110.0	109	0.0	159	0.0
10	14843.0	60	111.0	110	0.0	160	0.0
11	13002.0	61	101.0	111	0.0	161	0.0
12	11592.0	62	90.0	112	0.0	162	0.0
13	10454.0	63	85.0	113	0.0	163	0.0
14	9192.0	64	76.0	114	0.0	164	0.0
15	8166.0	65	84.0	115	0.0	165	0.0
16	7421.0	66	77.0	116	0.0	166	0.0
17	6714.0	67	50.0	117	0.0	167	0.0
18	6078.0	68	50.0	118	0.0	168	0.0
19	5733.0	69	43.0	119	0.0	169	0.0
20	5141.0	70	39.0	120	0.0	170	0.0
21	4766.0	71	18.0	121	0.0	171	0.0
22	4170.0	72	14.0	122	0.0	172	0.0
23	3808.0	73	8.0	123	1.0	173	0.0
24	3451.0	74	5.0	124	0.0	174	0.0
25	3191.0	75	7.0	125	0.0	175	0.0
26	2930.0	76	3.0	126	0.0	176	0.0
27	2587.0	77	3.0	127	0.0	177	0.0
28	2314.0	78	2.0	128	0.0	178	0.0
29	2089.0	79	0.0	129	0.0	179	0.0
30	1877.0	80	1.0	130	0.0	180	0.0
31	1624.0	81	0.0	131	0.0	181	0.0
32	1574.0	82	0.0	132	0.0	182	0.0
33	1395.0	83	0.0	133	0.0	183	0.0
34	1265.0	84	1.0	134	0.0	184	0.0
35	1199.0	85	0.0	135	0.0	185	0.0
36	1172.0	86	0.0	136	0.0	186	0.0

37	1059.0	87	1.0	137	0.0	187	0.0
38	964.0	88	0.0	138	0.0	188	0.0
39	830.0	89	0.0	139	0.0	189	0.0
40	782.0	90	0.0	140	0.0	190	0.0
41	703.0	91	0.0	141	0.0	191	0.0
42	656.0	92	0.0	142	0.0	192	0.0
43	625.0	93	0.0	143	0.0	193	0.0
44	547.0	94	0.0	144	0.0	194	0.0
45	554.0	95	1.0	145	0.0	195	0.0
46	455.0	96	0.0	146	0.0	196	0.0
47	462.0	97	0.0	147	0.0	197	0.0
48	385.0	98	0.0	148	0.0	198	0.0
49	369.0	99	0.0	149	0.0	199	0.0
50	348.0	100	0.0	150	0.0	200	0.0

TOTAL NUMBER OF COUNTS = 229631.0

Page 7:

```
DYNMAT    1000 10  (1X,A6,I4,10F7.0)
PuBe #M1170 run 9 neutrons hgb, 24 Nov 92
PB9HBN     1      0.      0.      0.      0.      0.    156.   7918.  15562.  14677.  12654.
PB9HBN    11  10896.   9402.   8060.   7035.   6284.   5584.   4978.   4479.   4137.   3875.
PB9HBN    21   3586.   3356.   3154.   3025.   2847.   2575.   2428.   2352.   2187.   2004.
PB9HBN    31   1840.   1647.   1524.   1459.   1367.   1278.   1232.   1186.   1079.   1031.
PB9HBN    41   1017.    957.    925.    876.    832.    783.    731.    734.    728.    687.
PB9HBN    51    650.    646.    646.    648.    618.    562.    542.    551.    541.    505.
PB9HBN    61    493.    481.    478.    468.    438.    420.    428.    410.    396.    392.
PB9HBN    71    374.    368.    368.    362.    343.    346.    333.    323.    321.    301.
PB9HBN    81    289.    286.    276.    257.    260.    281.    283.    269.    243.    221.
PB9HBN    91    227.    227.    206.    207.    224.    215.    201.    203.    209.    196.
PB9HBN   101    183.    175.    168.    165.    168.    166.    171.    167.    149.    145.
PB9HBN   111    136.    134.    138.    135.    128.    129.    126.    130.    127.    117.
PB9HBN   121    114.    106.     99.    112.    111.     98.    105.    107.    102.     92.
PB9HBN   131     88.     90.     86.     86.     87.     86.     96.     90.     89.    100.
PB9HBN   141     88.     74.     71.     80.     85.     74.     67.     65.     62.     67.
PB9HBN   151     61.     57.     58.     66.     72.     76.     71.     51.     50.     62.
PB9HBN   161     62.     63.     61.     55.     60.     60.     58.     57.     51.     50.
PB9HBN   171     52.     45.     46.     50.     50.     42.     45.     50.     47.     50.
```

```
PB9HBN   181     44.     43.     55.     47.     38.     37.     42.     46.     42.     46.
PB9HBN   191     42.     33.     36.     41.     36.     37.     41.     38.     35.     33.

DYNMAT    2000 10  (1X,A6,I4,10F7.0)
PuBe #M1170 run 9 neutrons lgb, 24 Nov 92
PB9LBN     1      0.      0.      0.      0.     47.   3377.   3459.   2705.   2247.   1818.
PB9LBN    11   1365.   1130.    885.    827.    668.    559.    528.    452.    403.    320.
PB9LBN    21    274.    245.    207.    214.    184.    153.    118.    125.     96.     84.
PB9LBN    31     75.     66.     64.     47.     52.     38.     33.     28.     34.     25.
PB9LBN    41     22.     16.      7.     16.     10.      5.     14.     10.     11.      6.
PB9LBN    51      8.      5.      6.      4.      6.      3.      4.      1.      2.      0.
PB9LBN    61      2.      1.      0.      0.      0.      2.      0.      0.      0.      1.
PB9LBN    71      0.      0.      0.      0.      0.      0.      0.      0.      0.      0.
PB9LBN    81      0.      0.      0.      0.      0.      1.      0.      0.      0.      0.
PB9LBN    91      0.      0.      0.      1.      0.      0.      0.      0.      0.      0.
PB9LBN   101      0.      0.      0.      0.      0.      0.      0.      0.      0.      0.
PB9LBN   111      0.      0.      0.      0.      0.      0.      0.      0.      0.      0.
PB9LBN   121      0.      0.      0.      0.      0.      0.      0.      0.      0.      0.
PB9LBN   131      0.      0.      0.      0.      0.      0.      0.      0.      0.      0.
PB9LBN   141      0.      0.      1.      0.      0.      0.      1.      0.      0.      0.
PB9LBN   151      0.      0.      0.      0.      0.      0.      0.      0.      0.      0.
PB9LBN   161      0.      0.      0.      0.      0.      0.      0.      0.      0.      0.
PB9LBN   171      0.      0.      0.      0.      0.      0.      0.      0.      0.      0.
PB9LBN   181      0.      0.      0.      0.      0.      0.      0.      0.      0.      0.
PB9LBN   191      0.      0.      0.      0.      0.      0.      0.      0.      0.      0.
```

Page 8:

```
        PB9HBN      RAW COUNTS BACKGROUND GAIN = 1

  1       0.0     51    650.0    101    183.0    151     61.0
  2       0.0     52    646.0    102    175.0    152     57.0
  3       0.0     53    646.0    103    168.0    153     58.0
  4       0.0     54    648.0    104    165.0    154     66.0
  5       0.0     55    618.0    105    168.0    155     72.0
  6     156.0     56    562.0    106    166.0    156     76.0
  7    7918.0     57    542.0    107    171.0    157     71.0
  8   15562.0     58    551.0    108    167.0    158     51.0
  9   14677.0     59    541.0    109    149.0    159     50.0
```

10	12654.0	60	505.0	110	145.0	160	62.0
11	10896.0	61	493.0	111	136.0	161	62.0
12	9402.0	62	481.0	112	134.0	162	63.0
13	8060.0	63	478.0	113	138.0	163	61.0
14	7035.0	64	468.0	114	135.0	164	55.0
15	6284.0	65	438.0	115	128.0	165	60.0
16	5584.0	66	420.0	116	129.0	166	60.0
17	4978.0	67	428.0	117	126.0	167	58.0
18	4479.0	68	410.0	118	130.0	168	57.0
19	4137.0	69	396.0	119	127.0	169	51.0
20	3875.0	70	392.0	120	117.0	170	50.0
21	3586.0	71	374.0	121	114.0	171	52.0
22	3356.0	72	368.0	122	106.0	172	45.0
23	3154.0	73	368.0	123	99.0	173	46.0
24	3025.0	74	362.0	124	112.0	174	50.0
25	2847.0	75	343.0	125	111.0	175	50.0
26	2575.0	76	346.0	126	98.0	176	42.0
27	2428.0	77	333.0	127	105.0	177	45.0
28	2352.0	78	323.0	128	107.0	178	50.0
29	2187.0	79	321.0	129	102.0	179	47.0
30	2004.0	80	301.0	130	92.0	180	50.0
31	1840.0	81	289.0	131	88.0	181	44.0
32	1647.0	82	286.0	132	90.0	182	43.0
33	1524.0	83	276.0	133	86.0	183	55.0
34	1459.0	84	257.0	134	86.0	184	47.0
35	1367.0	85	260.0	135	87.0	185	38.0
36	1278.0	86	281.0	136	86.0	186	37.0
37	1232.0	87	283.0	137	96.0	187	42.0
38	1186.0	88	269.0	138	90.0	188	46.0
39	1079.0	89	243.0	139	89.0	189	42.0
40	1031.0	90	221.0	140	100.0	190	46.0
41	1017.0	91	227.0	141	88.0	191	42.0
42	957.0	92	227.0	142	74.0	192	33.0
43	925.0	93	206.0	143	71.0	193	36.0
44	876.0	94	207.0	144	80.0	194	41.0
45	832.0	95	224.0	145	85.0	195	36.0
46	783.0	96	215.0	146	74.0	196	37.0
47	731.0	97	201.0	147	67.0	197	41.0
48	734.0	98	203.0	148	65.0	198	38.0
49	728.0	99	209.0	149	62.0	199	35.0

50	687.0	100	196.0	150	67.0	200	33.0

TOTAL NUMBER OF COUNTS = 191780.0

Page 9:

PB9LBN RAW COUNTS BACKGROUND GAIN = 2

1	0.0	51	8.0	101	0.0	151	0.0
2	0.0	52	5.0	102	0.0	152	0.0
3	0.0	53	6.0	103	0.0	153	0.0
4	0.0	54	4.0	104	0.0	154	0.0
5	47.0	55	6.0	105	0.0	155	0.0
6	3377.0	56	3.0	106	0.0	156	0.0
7	3459.0	57	4.0	107	0.0	157	0.0
8	2705.0	58	1.0	108	0.0	158	0.0
9	2247.0	59	2.0	109	0.0	159	0.0
10	1818.0	60	0.0	110	0.0	160	0.0
11	1365.0	61	2.0	111	0.0	161	0.0
12	1130.0	62	1.0	112	0.0	162	0.0
13	885.0	63	0.0	113	0.0	163	0.0
14	827.0	64	0.0	114	0.0	164	0.0
15	668.0	65	0.0	115	0.0	165	0.0
16	559.0	66	2.0	116	0.0	166	0.0
17	528.0	67	0.0	117	0.0	167	0.0
18	452.0	68	0.0	118	0.0	168	0.0
19	403.0	69	0.0	119	0.0	169	0.0
20	320.0	70	1.0	120	0.0	170	0.0
21	274.0	71	0.0	121	0.0	171	0.0
22	245.0	72	0.0	122	0.0	172	0.0
23	207.0	73	0.0	123	0.0	173	0.0
24	214.0	74	0.0	124	0.0	174	0.0
25	184.0	75	0.0	125	0.0	175	0.0
26	153.0	76	0.0	126	0.0	176	0.0
27	118.0	77	0.0	127	0.0	177	0.0
28	125.0	78	0.0	128	0.0	178	0.0
29	96.0	79	0.0	129	0.0	179	0.0
30	84.0	80	0.0	130	0.0	180	0.0
31	75.0	81	0.0	131	0.0	181	0.0

32	66.0	82	0.0	132	0.0	182	0.0
33	64.0	83	0.0	133	0.0	183	0.0
34	47.0	84	0.0	134	0.0	184	0.0
35	52.0	85	0.0	135	0.0	185	0.0
36	38.0	86	1.0	136	0.0	186	0.0
37	33.0	87	0.0	137	0.0	187	0.0
38	28.0	88	0.0	138	0.0	188	0.0
39	34.0	89	0.0	139	0.0	189	0.0
40	25.0	90	0.0	140	0.0	190	0.0
41	22.0	91	0.0	141	0.0	191	0.0
42	16.0	92	0.0	142	0.0	192	0.0
43	7.0	93	0.0	143	1.0	193	0.0
44	16.0	94	1.0	144	0.0	194	0.0
45	10.0	95	0.0	145	0.0	195	0.0
46	5.0	96	0.0	146	0.0	196	0.0
47	14.0	97	0.0	147	1.0	197	0.0
48	10.0	98	0.0	148	0.0	198	0.0
49	11.0	99	0.0	149	0.0	199	0.0
50	6.0	100	0.0	150	0.0	200	0.0

TOTAL NUMBER OF COUNTS = 23118.0

Page 10:

PB9HBN REBIN COUNTS FOREGROUND GAIN = 1

1	0.0	51	3732.1	101	1583.6	151	865.2
2	0.0	52	3610.2	102	1568.0	152	863.1
3	0.9	53	3522.8	103	1535.0	153	854.8
4	1.0	54	3400.6	104	1511.3	154	844.3
5	0.1	55	3345.6	105	1508.8	155	835.7
6	419.4	56	3337.2	106	1505.7	156	830.0
7	21134.3	57	3293.8	107	1470.9	157	818.8
8	44552.2	58	3204.9	108	1446.0	158	796.0
9	46967.8	59	3078.2	109	1464.7	159	777.8
10	42687.9	60	2974.9	110	1448.6	160	781.1
11	38059.2	61	2938.4	111	1398.4	161	794.3
12	33904.1	62	2945.9	112	1377.2	162	790.0
13	30514.9	63	2931.6	113	1360.4	163	775.0

14	27735.0	64	2877.1	114	1345.4	164	741.6
15	25503.6	65	2814.2	115	1342.5	165	735.5
16	23745.7	66	2742.0	116	1341.0	166	748.4
17	22297.9	67	2663.0	117	1330.9	167	742.7
18	20998.1	68	2614.5	118	1296.2	168	737.8
19	19819.0	69	2588.0	119	1252.4	169	731.0
20	18736.1	70	2541.7	120	1232.2	170	721.3
21	17787.7	71	2485.9	121	1211.9	171	695.3
22	17024.2	72	2446.4	122	1196.0	172	703.1
23	16451.7	73	2398.4	123	1189.1	173	717.3
24	15916.8	74	2319.6	124	1194.7	174	700.2
25	15205.7	75	2277.5	125	1206.4	175	666.0
26	14413.5	76	2294.5	126	1196.8	176	648.2
27	13687.1	77	2266.8	127	1166.7	177	666.1
28	12909.2	78	2207.7	128	1157.2	178	673.1
29	11984.8	79	2163.6	129	1175.8	179	665.3
30	10987.8	80	2151.1	130	1131.9	180	675.6
31	9900.6	81	2115.0	131	1108.6	181	690.1
32	8802.9	82	2042.5	132	1119.2	182	668.4
33	7913.3	83	2003.3	133	1083.9	183	643.8
34	7177.4	84	1992.8	134	1049.2	184	627.4
35	6634.3	85	1981.7	135	1038.2	185	616.4
36	6181.9	86	2013.7	136	1026.5	186	618.4
37	5844.5	87	1973.3	137	1029.1	187	612.5
38	5705.5	88	1874.2	138	1031.8	188	599.1
39	5630.1	89	1886.6	139	1000.3	189	589.7
40	5449.8	90	1894.8	140	988.8	190	582.5
41	5297.4	91	1878.2	141	989.7	191	573.9
42	5188.5	92	1833.8	142	984.2	192	571.8
43	4950.2	93	1812.4	143	976.3	193	577.6
44	4733.2	94	1784.1	144	942.4	194	576.5
45	4588.7	95	1728.0	145	918.2	195	562.7
46	4383.9	96	1688.6	146	914.6	196	561.1
47	4145.7	97	1661.0	147	913.9	197	572.7
48	3998.2	98	1617.7	148	896.6	198	555.9
49	3894.0	99	1610.3	149	869.6	199	527.9
50	3838.6	100	1607.4	150	860.8	200	520.5

TOTAL NUMBER OF COUNTS = 893203.1

Page 11:

PB9LBN REBIN COUNTS FOREGROUND GAIN = 2

1	0.0	51	361.7	101	0.7	151	0.0
2	0.0	52	347.4	102	0.0	152	0.0
3	0.0	53	328.1	103	0.0	153	0.0
4	0.8	54	297.3	104	0.0	154	0.0
5	243.5	55	245.1	105	0.0	155	0.0
6	14110.9	56	208.6	106	0.0	156	0.0
7	20802.1	57	186.6	107	0.0	157	0.0
8	19508.4	58	181.9	108	0.0	158	0.0
9	17110.2	59	175.8	109	0.0	159	0.0
10	15099.8	60	152.3	110	0.0	160	0.8
11	13312.0	61	126.5	111	0.0	161	0.2
12	11816.6	62	110.1	112	0.0	162	0.0
13	10637.5	63	104.1	113	0.0	163	0.0
14	9605.5	64	101.3	114	0.0	164	0.0
15	8521.2	65	92.2	115	0.0	165	0.0
16	7636.2	66	83.8	116	0.0	166	0.0
17	6977.5	67	78.7	117	0.0	167	0.0
18	6329.2	68	72.5	118	0.0	168	0.0
19	5749.8	69	78.9	119	0.0	169	0.0
20	5435.1	70	72.6	120	0.0	170	0.0
21	4933.0	71	47.5	121	0.0	171	0.0
22	4569.2	72	47.1	122	0.0	172	0.0
23	4086.5	73	41.4	123	0.0	173	0.0
24	3704.9	74	37.5	124	0.0	174	0.0
25	3387.3	75	22.0	125	0.0	175	0.0
26	3120.7	76	14.4	126	0.0	176	0.0
27	2890.0	77	9.7	127	0.0	177	0.0
28	2626.5	78	6.0	128	0.0	178	0.0
29	2346.5	79	5.7	129	0.0	179	0.0
30	2118.2	80	4.9	130	0.5	180	0.0
31	1921.9	81	2.8	131	0.5	181	0.0
32	1727.4	82	2.5	132	0.0	182	0.0
33	1525.5	83	1.4	133	0.0	183	0.0
34	1474.6	84	0.2	134	0.0	184	0.0
35	1315.0	85	0.8	135	0.0	185	0.0
36	1193.3	86	0.0	136	0.0	186	0.0

37	1134.5	87	0.0	137	0.0	187	0.0
38	1108.1	88	0.0	138	0.0	188	0.0
39	1018.4	89	0.9	139	0.0	189	0.0
40	931.1	90	0.1	140	0.0	190	0.0
41	821.6	91	0.0	141	0.0	191	0.0
42	754.0	92	0.7	142	0.0	192	0.0
43	694.9	93	0.3	143	0.0	193	0.0
44	640.2	94	0.0	144	0.0	194	0.0
45	605.4	95	0.0	145	0.0	195	0.0
46	560.8	96	0.0	146	0.0	196	0.0
47	517.8	97	0.0	147	0.0	197	0.0
48	497.6	98	0.0	148	0.0	198	0.0
49	430.3	99	0.0	149	0.0	199	0.0
50	425.2	100	0.3	150	0.0	200	0.0

TOTAL NUMBER OF COUNTS = 229631.0

Page 12:

PP9HBN REBIN COUNTS BACKGROUND GAIN = 1

1	0.0	51	677.9	101	202.0	151	64.5
2	0.0	52	642.0	102	196.2	152	62.2
3	0.0	53	631.7	103	183.8	153	62.6
4	0.0	54	630.9	104	174.2	154	63.1
5	0.0	55	632.3	105	167.1	155	56.1
6	134.1	56	612.2	106	162.5	156	56.0
7	6640.9	57	566.3	107	162.6	157	59.2
8	13943.2	58	536.0	108	163.1	158	66.2
9	14498.9	59	534.9	109	164.3	159	71.4
10	12784.1	60	532.1	110	165.3	160	73.0
11	11052.7	61	507.8	111	155.9	161	64.8
12	9566.8	62	486.6	112	144.0	162	49.6
13	8248.5	63	475.2	113	138.4	163	51.0
14	7182.4	64	468.2	114	132.2	164	60.5
15	6383.1	65	462.0	115	132.1	165	60.7
16	5699.2	66	443.4	116	133.9	166	61.3
17	5088.6	67	420.0	117	130.0	167	59.1
18	4572.9	68	413.4	118	125.2	168	54.0

19	4184.3	69	411.1	119	125.3	169	58.6
20	3900.9	70	395.4	120	123.8	170	58.6
21	3637.4	71	385.4	121	126.5	171	56.6
22	3390.5	72	377.2	122	122.6	172	55.7
23	3184.2	73	363.5	123	113.9	173	50.0
24	3023.6	74	359.4	124	110.6	174	48.9
25	2880.4	75	357.9	125	103.0	175	50.6
26	2674.0	76	349.4	126	97.3	176	44.7
27	2460.7	77	335.5	127	109.4	177	44.8
28	2345.0	78	335.7	128	108.4	178	48.2
29	2244.0	79	323.7	129	95.7	179	48.8
30	2081.4	80	315.2	130	102.4	180	42.6
31	1912.2	81	311.4	131	104.4	181	43.3
32	1748.6	82	293.0	132	100.0	182	47.6
33	1580.5	83	282.1	133	90.8	183	46.7
34	1475.1	84	279.0	134	86.4	184	48.0
35	1408.3	85	269.4	135	87.6	185	44.8
36	1321.1	86	251.0	136	84.6	186	42.3
37	1241.9	87	253.9	137	84.0	187	49.4
38	1198.1	88	273.6	138	84.8	188	49.0
39	1149.0	89	276.2	139	84.2	189	40.8
40	1050.7	90	263.9	140	91.2	190	36.6
41	1006.3	91	240.2	141	89.6	191	38.8
42	992.2	92	218.7	142	87.2	192	43.0
43	934.6	93	220.7	143	94.0	193	43.0
44	903.6	94	221.7	144	90.2	194	42.8
45	857.0	95	205.4	145	77.5	195	43.2
46	814.9	96	201.9	146	70.5	196	37.4
47	768.5	97	214.5	147	74.3	197	33.4
48	719.1	98	212.4	148	80.8	198	37.0
49	716.4	99	200.4	149	77.4	199	38.4
50	711.8	100	197.6	150	68.9	200	35.5

TOTAL NUMBER OF COUNTS = 191607.6

Page 13:

PB9LBN REBIN COUNTS BACKGROUND GAIN = 2

1	0.0	51	9.5	101	0.0	151	0.3
2	0.0	52	10.3	102	0.0	152	0.7
3	0.0	53	5.7	103	0.0	153	0.0
4	0.0	54	7.5	104	0.0	154	0.0
5	33.5	55	5.0	105	0.0	155	0.1
6	2229.1	56	5.5	106	0.0	156	0.9
7	3232.5	57	4.2	107	0.0	157	0.0
8	2852.5	58	5.1	108	0.0	158	0.0
9	2328.2	59	3.8	109	0.0	159	0.0
10	1935.1	60	3.4	110	0.0	160	0.0
11	1546.4	61	2.3	111	0.0	161	0.0
12	1213.4	62	1.4	112	0.0	162	0.0
13	1002.8	63	1.1	113	0.0	163	0.0
14	822.8	64	0.7	114	0.0	164	0.0
15	757.3	65	1.6	115	0.0	165	0.0
16	620.7	66	0.7	116	0.0	166	0.0
17	526.2	67	0.0	117	0.0	167	0.0
18	497.7	68	0.0	118	0.0	168	0.0
19	428.5	69	0.1	119	0.0	169	0.0
20	384.3	70	1.9	120	0.0	170	0.0
21	313.8	71	0.0	121	0.0	171	0.0
22	267.7	72	0.0	122	0.0	172	0.0
23	238.5	73	0.0	123	0.0	173	0.0
24	207.2	74	0.8	124	0.0	174	0.0
25	199.1	75	0.2	125	0.0	175	0.0
26	186.4	76	0.0	126	0.0	176	0.0
27	159.4	77	0.0	127	0.0	177	0.0
28	130.4	78	0.0	128	0.0	178	0.0
29	113.6	79	0.0	129	0.0	179	0.0
30	109.7	80	0.0	130	0.0	180	0.0
31	87.8	81	0.0	131	0.0	181	0.0
32	77.7	82	0.0	132	0.0	182	0.0
33	69.7	83	0.0	133	0.0	183	0.0
34	62.1	84	0.0	134	0.0	184	0.0
35	60.3	85	0.0	135	0.0	185	0.0
36	44.4	86	0.0	136	0.0	186	0.0

37	48.7	87	0.0	137	0.0	187	0.0
38	37.5	88	0.0	138	0.0	188	0.0
39	32.0	89	0.0	139	0.0	189	0.0
40	27.6	90	0.0	140	0.0	190	0.0
41	30.3	91	0.8	141	0.0	191	0.0
42	26.7	92	0.2	142	0.0	192	0.0
43	22.0	93	0.0	143	0.0	193	0.0
44	17.9	94	0.0	144	0.0	194	0.0
45	11.3	95	0.0	145	0.0	195	0.0
46	9.9	96	0.0	146	0.0	196	0.0
47	13.2	97	0.0	147	0.0	197	0.0
48	8.2	98	0.0	148	0.0	198	0.0
49	6.4	99	0.3	149	0.0	199	0.0
50	12.7	100	0.7	150	0.0	200	0.0

TOTAL NUMBER OF COUNTS = 23118.0

Page 14:

PB9HBN GROUPED COUNTS/UNIT

BINS	COUNTS	ERROR	LOCHAN	UPCHAN	LO P.H.	UP P.H.	F.A.F.
1	0.12529E+05	0.14657E+04	1009	1010	0.50000E-01	0.62500E-01	0.44250
2	0.63719E+04	0.39937E+03	1011	1012	0.62500E-01	0.75000E-01	0.71625
3	0.41631E+04	0.97789E+02	1013	1014	0.75000E-01	0.87500E-01	0.91425
4	0.33137E+04	0.21068E+02	1015	1016	0.87500E-01	0.10000E+00	0.99700
5	0.29197E+04	0.16440E+02	1017	1019	0.10000E+00	0.11875E+00	1.00000
6	0.25256E+04	0.15047E+02	1020	1022	0.11875E+00	0.13750E+00	1.00000
7	0.22322E+04	0.12070E+02	1023	1026	0.13750E+00	0.16250E+00	1.00000
8	0.17218E+04	0.94416E+01	1027	1031	0.16250E+00	0.19375E+00	1.00000
9	0.10374E+04	0.74789E+01	1032	1036	0.19375E+00	0.22500E+00	1.00000
10	0.78452E+03	0.59078E+01	1037	1042	0.22500E+00	0.26250E+00	1.00000
11	0.64599E+03	0.52836E+01	1043	1048	0.26250E+00	0.30000E+00	1.00000
12	0.52573E+03	0.43980E+01	1049	1055	0.30000E+00	0.34375E+00	1.00000
13	0.45708E+03	0.40596E+01	1056	1062	0.34375E+00	0.38750E+00	1.00000
14	0.40630E+03	0.35320E+01	1063	1070	0.38750E+00	0.43750E+00	1.00000
15	0.35184E+03	0.32631E+01	1071	1078	0.43750E+00	0.48750E+00	1.00000
16	0.31325E+03	0.28637E+01	1079	1087	0.48750E+00	0.54375E+00	1.00000
17	0.28164E+03	0.26871E+01	1088	1096	0.54375E+00	0.60000E+00	1.00000

18	0.24602E+03	0.24949E+01	1097	1105	0.60000E+00	0.65625E+00	1.00000
19	0.22576E+03	0.23545E+01	1106	1114	0.65625E+00	0.71250E+00	1.00000
20	0.20264E+03	0.22109E+01	1115	1123	0.71250E+00	0.76875E+00	1.00000
21	0.18817E+03	0.21081E+01	1124	1132	0.76875E+00	0.82500E+00	1.00000
22	0.16700E+03	0.19775E+01	1133	1141	0.82500E+00	0.88125E+00	1.00000
23	0.14925E+03	0.18739E+01	1142	1150	0.88125E+00	0.93750E+00	1.00000
24	0.13565E+03	0.16776E+01	1151	1160	0.93750E+00	0.10000E+01	1.00000
25	0.12472E+03	0.16154E+01	2016	2016	0.93750E+00	0.10000E+01	1.00000
26	0.12337E+03	0.15998E+01	1161	1170	0.10000E+01	0.10625E+01	1.00000
27	0.11469E+03	0.15400E+01	2017	2017	0.10000E+01	0.10625E+01	1.00000
28	0.11234E+03	0.15192E+01	1171	1180	0.10625E+01	0.11250E+01	1.00000
29	0.10367E+03	0.14689E+01	2018	2018	0.10625E+01	0.11250E+01	1.00000
30	0.10311E+03	0.14550E+01	1181	1190	0.11250E+01	0.11875E+01	1.00000
31	0.94601E+02	0.13974E+01	2019	2019	0.11250E+01	0.11875E+01	1.00000
32	0.89793E+02	0.13562E+01	2020	2020	0.11875E+01	0.12500E+01	1.00000
33	0.82118E+02	0.12877E+01	2021	2021	0.12500E+01	0.13125E+01	1.00000
34	0.76472E+02	0.12364E+01	2022	2022	0.13125E+01	0.13750E+01	1.00000
35	0.68409E+02	0.11692E+01	2023	2023	0.13750E+01	0.14375E+01	1.00000
36	0.62182E+02	0.11120E+01	2024	2024	0.14375E+01	0.15000E+01	1.00000
37	0.56679E+02	0.10647E+01	2025	2025	0.15000E+01	0.15625E+01	1.00000
38	0.52164E+02	0.10224E+01	2026	2026	0.15625E+01	0.16250E+01	1.00000
39	0.48544E+02	0.98175E+00	2027	2027	0.16250E+01	0.16875E+01	1.00000
40	0.44375E+02	0.93348E+00	2028	2028	0.16875E+01	0.17500E+01	1.00000
41	0.39696E+02	0.88180E+00	2029	2029	0.17500E+01	0.18125E+01	1.00000
42	0.35708E+02	0.83917E+00	2030	2030	0.18125E+01	0.18750E+01	1.00000
43	0.32607E+02	0.79702E+00	2031	2031	0.18750E+01	0.19375E+01	1.00000
44	0.29329E+02	0.75536E+00	2032	2032	0.19375E+01	0.20000E+01	1.00000
45	0.25880E+02	0.71009E+00	2033	2033	0.20000E+01	0.20625E+01	1.00000
46	0.25111E+02	0.69695E+00	2034	2034	0.20625E+01	0.21250E+01	1.00000
47	0.22306E+02	0.65936E+00	2035	2035	0.21250E+01	0.21875E+01	1.00000
48	0.20424E+02	0.62549E+00	2036	2036	0.21875E+01	0.22500E+01	1.00000
49	0.19302E+02	0.61156E+00	2037	2037	0.22500E+01	0.23125E+01	1.00000
50	0.19032E+02	0.60177E+00	2038	2038	0.23125E+01	0.23750E+01	1.00000
51	0.17536E+02	0.57623E+00	2039	2039	0.23750E+01	0.24375E+01	1.00000
52	0.16063E+02	0.55050E+00	2040	2040	0.24375E+01	0.25000E+01	1.00000
53	0.13499E+02	0.35921E+00	2041	2042	0.25000E+01	0.26250E+01	1.00000
54	0.11514E+02	0.32965E+00	2043	2044	0.26250E+01	0.27500E+01	1.00000
55	0.10178E+02	0.30634E+00	2045	2046	0.27500E+01	0.28750E+01	1.00000
56	0.88353E+01	0.28628E+00	2047	2048	0.28750E+01	0.30000E+01	1.00000
57	0.74342E+01	0.26293E+00	2049	2050	0.30000E+01	0.31250E+01	1.00000

Page 15:

58	0.61277E+01	0.24005E+00	2051	2052	0.31250E+01	0.32500E+01	1.00000
59	0.54419E+01	0.22467E+00	2053	2054	0.32500E+01	0.33750E+01	1.00000
60	0.39401E+01	0.19161E+00	2055	2056	0.33750E+01	0.35000E+01	1.00000
61	0.31927E+01	0.17287E+00	2057	2058	0.35000E+01	0.36250E+01	1.00000
62	0.28522E+01	0.16285E+00	2059	2060	0.36250E+01	0.37500E+01	1.00000
63	0.20709E+01	0.13790E+00	2061	2062	0.37500E+01	0.38750E+01	1.00000
64	0.18101E+01	0.12807E+00	2063	2064	0.38750E+01	0.40000E+01	1.00000
65	0.15432E+01	0.11882E+00	2065	2066	0.40000E+01	0.41250E+01	1.00000
66	0.13436E+01	0.10943E+00	2067	2068	0.41250E+01	0.42500E+01	1.00000
67	0.13287E+01	0.11025E+00	2069	2070	0.42500E+01	0.43750E+01	1.00000
68	0.84062E+00	0.86646E-01	2071	2072	0.43750E+01	0.45000E+01	1.00000
69	0.69479E+00	0.79545E-01	2073	2074	0.45000E+01	0.46250E+01	1.00000
70	0.32166E+00	0.54120E-01	2075	2076	0.46250E+01	0.47500E+01	1.00000
71	0.13894E+00	0.35589E-01	2077	2078	0.47500E+01	0.48750E+01	1.00000
72	0.94198E-01	0.29477E-01	2079	2080	0.48750E+01	0.50000E+01	1.00000
73	0.47508E-01	0.21326E-01	2081	2082	0.50000E+01	0.51250E+01	1.00000
74	0.14091E-01	0.12524E-01	2083	2084	0.51250E+01	0.52500E+01	1.00000
75	0.72398E-02	0.97958E-02	2085	2086	0.52500E+01	0.53750E+01	1.00000
76	0.00000E+00	0.56218E-02	2087	2088	0.53750E+01	0.55000E+01	1.00000
77	0.88889E-02	0.10517E-01	2089	2090	0.55000E+01	0.56250E+01	1.00000
78	-0.24266E-02	0.12964E-01	2091	2092	0.56250E+01	0.57500E+01	1.00000
79	0.24266E-02	0.72921E-02	2093	2094	0.57500E+01	0.58750E+01	1.00000
80	0.00000E+00	0.56218E-02	2095	2096	0.58750E+01	0.60000E+01	1.00000
81	0.00000E+00	0.56218E-02	2097	2098	0.60000E+01	0.61250E+01	1.00000
82	-0.65024E-02	0.11482E-01	2099	2100	0.61250E+01	0.62500E+01	1.00000
83	0.43349E-02	0.68380E-02	2101	2103	0.62500E+01	0.64375E+01	1.00000
84	0.00000E+00	0.45902E-02	2104	2106	0.64375E+01	0.66250E+01	1.00000
85	0.00000E+00	0.45902E-02	2107	2109	0.66250E+01	0.68125E+01	1.00000
86	0.00000E+00	0.45902E-02	2110	2112	0.68125E+01	0.70000E+01	1.00000
87	0.00000E+00	0.45902E-02	2113	2115	0.70000E+01	0.71875E+01	1.00000
88	0.00000E+00	0.45902E-02	2116	2118	0.71875E+01	0.73750E+01	1.00000
89	0.00000E+00	0.45902E-02	2119	2121	0.73750E+01	0.75625E+01	1.00000
90	0.00000E+00	0.45902E-02	2122	2124	0.75625E+01	0.77500E+01	1.00000
91	0.00000E+00	0.45902E-02	2125	2127	0.77500E+01	0.79375E+01	1.00000
92	0.32535E-02	0.63522E-02	2128	2130	0.79375E+01	0.81250E+01	1.00000
93	0.26724E-02	0.60751E-02	2131	2133	0.81250E+01	0.83125E+01	1.00000
94	0.00000E+00	0.45902E-02	2134	2136	0.83125E+01	0.85000E+01	1.00000
95	0.00000E+00	0.45902E-02	2137	2139	0.85000E+01	0.86875E+01	1.00000

96	0.00000E+00	0.45902E-02	2140	2142	0.86875E+01	0.88750E+01	1.00000
97	0.00000E+00	0.45902E-02	2143	2145	0.88750E+01	0.90625E+01	1.00000
98	0.00000E+00	0.45902E-02	2146	2148	0.90625E+01	0.92500E+01	1.00000
99	-0.20466E-02	0.57619E-02	2149	2151	0.92500E+01	0.94375E+01	1.00000
100	-0.38791E-02	0.66376E-02	2152	2154	0.94375E+01	0.96250E+01	1.00000
101	-0.59259E-02	0.74958E-02	2155	2157	0.96250E+01	0.98125E+01	1.00000
102	0.49160E-02	0.70853E-02	2158	2160	0.98125E+01	0.10000E+02	1.00000
103	0.10099E-02	0.52014E-02	2161	2163	0.10000E+02	0.10188E+02	1.00000
104	0.00000E+00	0.45902E-02	2164	2166	0.10188E+02	0.10375E+02	1.00000
105	0.00000E+00	0.45902E-02	2167	2169	0.10375E+02	0.10563E+02	1.00000
106	0.00000E+00	0.45902E-02	2170	2172	0.10563E+02	0.10750E+02	1.00000
107	0.00000E+00	0.45902E-02	2173	2175	0.10750E+02	0.10938E+02	1.00000
108	0.00000E+00	0.45902E-02	2176	2178	0.10938E+02	0.11125E+02	1.00000
109	0.00000E+00	0.39752E-02	2179	2182	0.11125E+02	0.11375E+02	1.00000
110	0.00000E+00	0.39752E-02	2183	2186	0.11375E+02	0.11625E+02	1.00000
111	0.00000E+00	0.39752E-02	2187	2190	0.11625E+02	0.11875E+02	1.00000
112	0.00000E+00	0.39752E-02	2191	2194	0.11875E+02	0.12125E+02	1.00000
113	0.00000E+00	0.39752E-02	2195	2198	0.12125E+02	0.12375E+02	1.00000

Page 16:

COUNTS AND STANDARD DEVIATION IN GROUPED BINS SCOFF = 0.0100 FUDGE = 0.9225 RELFU = 0.0775

ROW		* COL 1 -0.1E+05	-0.3E+04	-0.9E+03	$ COL 2 -0.2E+03	0.0E+00	0.2E+03	0.9E+03	0.3E+04	0.1E+05	0.3E+05	0.1E+06
1	0.500E-01	1	1	1	1	1	1	1 $	1	1 *	1	1
2	0.625E-01	1	1	1	1	1	1 $	1	1 *	1	1	1
3	0.750E-01	1	1	1	1	1 $	1	1	1 *	1	1	1
4	0.875E-01	1	1	1	1	1 $	1	1	*	1	1	1
5	0.100E+00	1	1	1	1	1 $	1	1	*1	1	1	1
6	0.119E+00	1	1	1	1	1 $	1	1	* 1	1	1	1
7	0.138E+00	1	1	1	1	1 $	1	1	* 1	1	1	1
8	0.163E+00	1	1	1	1	1$	1	1	* 1	1	1	1
9	0.194E+00	1	1	1	1	1$	1	1*	1	1	1	1
10	0.225E+00	1	1	1	1	1$	1	*1	1	1	1	1
11	0.263E+00	1	1	1	1	1$	1	* 1	1	1	1	1
12	0.300E+00	1	1	1	1	$	1	* 1	1	1	1	1
13	0.344E+00	1	1	1	1	$	1	* 1	1	1	1	1
14	0.388E+00	1	1	1	1	$	1	* 1	1	1	1	1
15	0.438E+00	1	1	1	1	$	1	* 1	1	1	1	1
16	0.488E+00	1	1	1	1	$	1	* 1	1	1	1	1
17	0.544E+00	1	1	1	1	$	1*	1	1	1	1	1
18	0.600E+00	1	1	1	1	$	1*	1	1	1	1	1
19	0.656E+00	1	1	1	1	$	*	1	1	1	1	1
20	0.713E+00	1	1	1	1	$	*1	1	1	1	1	1

21	0.769E+00	1	1	1	1	$	1	1	1	1	1	1
22	0.825E+00	1	1	1	1	$	1	1	1	1	1	1
23	0.881E+00	1	1	1	1	$	1	1	1	1	1	1
24	0.938E+00	1	1	1	1	$	1	1	1	1	1	1
25	0.938E+00	1	1	1	1	$	1	1	1	1	1	1
26	0.100E+01	1	1	1	1	$	1	1	1	1	1	1
27	0.100E+01	1	1	1	1	$	1	1	1	1	1	1
28	0.106E+01	1	1	1	1	$	1	1	1	1	1	1
29	0.106E+01	1	1	1	1	$	1	1	1	1	1	1
30	0.113E+01	1	1	1	1	$	1	1	1	1	1	1
31	0.113E+01	1	1	1	1	$	1	1	1	1	1	1
32	0.119E+01	1	1	1	1	$	1	1	1	1	1	1
33	0.125E+01	1	1	1	1	$	1	1	1	1	1	1
34	0.131E+01	1	1	1	1	$	1	1	1	1	1	1
35	0.138E+01	1	1	1	1	$	1	1	1	1	1	1
36	0.144E+01	1	1	1	1	$	1	1	1	1	1	1
37	0.150E+01	1	1	1	1	$	1	1	1	1	1	1
38	0.156E+01	1	1	1	1	$	1	1	1	1	1	1
39	0.163E+01	1	1	1	1	$	1	1	1	1	1	1
40	0.169E+01	1	1	1	1	$	1	1	1	1	1	1
41	0.175E+01	1	1	1	1	$	1	1	1	1	1	1
42	0.181E+01	1	1	1	1	$	1	1	1	1	1	1
43	0.188E+01	1	1	1	1	$	1	1	1	1	1	1
44	0.194E+01	1	1	1	1	$	1	1	1	1	1	1
45	0.200E+01	1	1	1	1	$	1	1	1	1	1	1
46	0.206E+01	1	1	1	1	$	1	1	1	1	1	1
47	0.213E+01	1	1	1	1	$	1	1	1	1	1	1
48	0.219E+01	1	1	1	1	$	1	1	1	1	1	1
49	0.225E+01	1	1	1	1	$	1	1	1	1	1	1
50	0.231E+01	1	1	1	1	$	1	1	1	1	1	1
51	0.238E+01	1	1	1	1	$	1	1	1	1	1	1
52	0.244E+01	1	1	1	1	$	1	1	1	1	1	1
53	0.250E+01	1	1	1	1	$	1	1	1	1	1	1
54	0.263E+01	1	1	1	1	$	1	1	1	1	1	1
55	0.275E+01	1	1	1	1	$	1	1	1	1	1	1

Page 17:

56	0.288E+01	1	1	1	1	$	1	1	1	1	1	1
57	0.300E+01	1	1	1	1	$	1	1	1	1	1	1
58	0.313E+01	1	1	1	1	$	1	1	1	1	1	1
59	0.325E+01	1	1	1	1	$	1	1	1	1	1	1
60	0.338E+01	1	1	1	1	$	1	1	1	1	1	1
61	0.350E+01	1	1	1	1	$	1	1	1	1	1	1
62	0.363E+01	1	1	1	1	$	1	1	1	1	1	1
63	0.375E+01	1	1	1	1	$	1	1	1	1	1	1
64	0.388E+01	1	1	1	1	$	1	1	1	1	1	1
65	0.400E+01	1	1	1	1	$	1	1	1	1	1	1
66	0.413E+01	1	1	1	1	$	1	1	1	1	1	1

67	0.425E+C1	1	1	1	1	$	1	1	1	1	1	1
68	0.438E+C1	1	1	1	1	$	1	1	1	1	1	1
69	0.450E+01	1	1	1	1	$	1	1	1	1	1	1
70	0.463E+01	1	1	1	1	$	1	1	1	1	1	1
71	0.475E+01	1	1	1	1	$	1	1	1	1	1	1
72	0.488E+01	1	1	1	1	$	1	1	1	1	1	1
73	0.500E+01	1	1	1	1	$	1	1	1	1	1	1
74	0.513E+01	1	1	1	1	$	1	1	1	1	1	1
75	0.525E+01	1	1	1	1	$	1	1	1	1	1	1
76	0.538E+01	1	1	1	1	$	1	1	1	1	1	1
77	0.550E+01	1	1	1	1	$	1	1	1	1	1	1
78	0.563E+01	1	1	1	1	$	1	1	1	1	1	1
79	0.575E+01	1	1	1	1	$	1	1	1	1	1	1
80	0.588E+01	1	1	1	1	$	1	1	1	1	1	1
81	0.600E+01	1	1	1	1	$	1	1	1	1	1	1
82	0.613E+01	1	1	1	1	$	1	1	1	1	1	1
83	0.625E+01	1	1	1	1	$	1	1	1	1	1	1
84	0.644E+01	1	1	1	1	$	1	1	1	1	1	1
85	0.663E+01	1	1	1	1	$	1	1	1	1	1	1
86	0.681E+01	1	1	1	1	$	1	1	1	1	1	1
87	0.700E+01	1	1	1	1	$	1	1	1	1	1	1
88	0.719E+01	1	1	1	1	$	1	1	1	1	1	1
89	0.738E+C1	1	1	1	1	$	1	1	1	1	1	1
90	0.756E+01	1	1	1	1	$	1	1	1	1	1	1
91	0.775E+01	1	1	1	1	$	1	1	1	1	1	1
92	0.794E+01	1	1	1	1	$	1	1	1	1	1	1
93	0.813E+01	1	1	1	1	$	1	1	1	1	1	1
94	0.831E+01	1	1	1	1	$	1	1	1	1	1	1
95	0.850E+01	1	1	1	1	$	1	1	1	1	1	1
96	0.869E+01	1	1	1	1	$	1	1	1	1	1	1
97	0.888E+01	1	1	1	1	$	1	1	1	1	1	1
98	0.906E+01	1	1	1	1	$	1	1	1	1	1	1
99	0.925E+01	1	1	1	1	$	1	1	1	1	1	1
100	0.944E+01	1	1	1	1	$	1	1	1	1	1	1
101	0.963E+01	1	1	1	1	$	1	1	1	1	1	1
102	0.981E+01	1	1	1	1	$	1	1	1	1	1	1
103	0.100E+02	1	1	1	1	$	1	1	1	1	1	1
104	0.102E+02	1	1	1	1	$	1	1	1	1	1	1
105	0.104E+02	1	1	1	1	$	1	1	1	1	1	1
106	0.106E+02	1	1	1	1	$	1	1	1	1	1	1
107	0.108E+02	1	1	1	1	$	1	1	1	1	1	1
108	0.109E+02	1	1	1	1	$	1	1	1	1	1	1
109	0.111E+02	1	1	1	1	$	1	1	1	1	1	1
110	0.114E+02	1	1	1	1	$	1	1	1	1	1	1
111	0.116E+02	1	1	1	1	$	1	1	1	1	1	1
112	0.119E+02	1	1	1	1	$	1	1	1	1	1	1
113	0.121E+02	1	1	1	1	$	1	1	1	1	1	1

Page 18:

PuBe #M1170 run 9 neutrons lgb, 24 Nov 92
--- TAW= 10.000 ---

I	VLO	B	S	BADJ	PCTDEV	ESD
1	0.500E-01	0.121E+05	0.141E+04	0.121E+05	0.191	0.000
2	0.625E-01	0.613E+04	0.384E+03	0.613E+04	0.934	0.000
3	0.750E-01	0.400E+04	0.941E+02	0.400E+04	1.051	0.000
4	0.875E-01	0.319E+04	0.319E+02	0.319E+04	-1.520	0.000
5	0.100E+00	0.281E+04	0.281E+02	0.281E+04	2.508	0.001
6	0.119E+00	0.243E+04	0.243E+02	0.243E+04	-2.348	0.002
7	0.138E+00	0.215E+04	0.215E+02	0.215E+04	0.905	0.002
8	0.163E+00	0.166E+04	0.166E+02	0.166E+04	1.074	0.002
9	0.194E+00	0.998E+03	0.998E+01	0.998E+03	-0.947	0.002
10	0.225E+00	0.755E+03	0.755E+01	0.755E+03	0.055	0.002
11	0.263E+00	0.621E+03	0.621E+01	0.621E+03	1.121	0.002
12	0.300E+00	0.506E+03	0.506E+01	0.506E+03	-3.128	0.003
13	0.344E+00	0.440E+03	0.440E+01	0.439E+03	8.997	0.011
14	0.388E+00	0.391E+03	0.391E+01	0.392E+03	-21.037	0.055
15	0.438E+00	0.338E+03	0.338E+01	0.337E+03	36.465	0.188
16	0.488E+00	0.301E+03	0.301E+01	0.303E+03	-52.904	0.468
17	0.544E+00	0.271E+03	0.271E+01	0.269E+03	71.820	0.984
18	0.600E+00	0.237E+03	0.240E+01	0.239E+03	-78.637	1.602
19	0.656E+00	0.217E+03	0.226E+01	0.215E+03	93.290	2.473
20	0.713E+00	0.195E+03	0.213E+01	0.197E+03	-96.410	3.402
21	0.769E+00	0.181E+03	0.203E+01	0.180E+03	71.054	3.907
22	0.825E+00	0.161E+03	0.190E+01	0.161E+03	-41.477	4.079
23	0.881E+00	0.144E+03	0.180E+01	0.143E+03	5.012	4.082
24	0.938E+00	0.130E+03	0.161E+01	0.130E+03	24.635	4.142
25	0.938E+00	0.130E+03	0.168E+01	0.130E+03	-2.171	4.143
26	0.100E+01	0.119E+03	0.154E+01	0.119E+03	-38.740	4.293
27	0.100E+01	0.120E+03	0.161E+01	0.119E+03	20.518	4.335
28	0.106E+01	0.108E+03	0.146E+01	0.108E+03	7.172	4.340
29	0.106E+01	0.108E+03	0.153E+01	0.108E+03	9.785	4.350
30	0.113E+01	0.992E+02	0.140E+01	0.992E+02	-1.351	4.350
31	0.113E+01	0.987E+02	0.146E+01	0.992E+02	-38.122	4.495
32	0.119E+01	0.936E+02	0.141E+01	0.927E+02	68.542	4.965
33	0.125E+01	0.856E+02	0.134E+01	0.866E+02	-68.580	5.435

34	0.131E+01	0.797E+02	0.129E+01	0.791E+02	48.352	5.669
35	0.138E+01	0.713E+02	0.122E+01	0.717E+02	-25.865	5.736
36	0.144E+01	0.648E+02	0.116E+01	0.649E+02	-0.646	5.736
37	0.150E+01	0.591E+02	0.111E+01	0.589E+02	22.659	5.787
38	0.156E+01	0.544E+02	0.107E+01	0.547E+02	-32.742	5.895
39	0.163E+01	0.506E+02	0.102E+01	0.504E+02	17.954	5.927
40	0.169E+01	0.463E+02	0.973E+00	0.461E+02	14.557	5.948
41	0.175E+01	0.414E+02	0.920E+00	0.416E+02	-19.876	5.988
42	0.181E+01	0.372E+02	0.875E+00	0.375E+02	-26.291	6.057
43	0.188E+01	0.340E+02	0.831E+00	0.336E+02	50.002	6.307
44	0.194E+01	0.306E+02	0.788E+00	0.304E+02	24.564	6.367
45	0.200E+01	0.270E+02	0.740E+00	0.278E+02	-109.119	7.558
46	0.206E+01	0.262E+02	0.727E+00	0.255E+02	88.786	8.346
47	0.213E+01	0.233E+02	0.688E+00	0.233E+02	-8.910	8.354
48	0.219E+01	0.213E+02	0.652E+00	0.213E+02	-5.154	8.357
49	0.225E+01	0.201E+02	0.638E+00	0.203E+02	-31.892	8.458
50	0.231E+01	0.198E+02	0.628E+00	0.197E+02	30.142	8.549
51	0.238E+01	0.183E+02	0.601E+00	0.183E+02	2.966	8.550
52	0.244E+01	0.168E+02	0.574E+00	0.167E+02	15.006	8.573
53	0.250E+01	0.141E+02	0.375E+00	0.142E+02	-38.557	8.721
54	0.263E+01	0.120E+02	0.344E+00	0.119E+02	43.996	8.915
55	0.275E+01	0.106E+02	0.319E+00	0.107E+02	-30.284	9.006

Page 19:

56	0.288E+01	0.921E+01	0.299E+00	0.920E+01	3.497	9.008
57	0.300E+01	0.775E+01	0.274E+00	0.768E+01	26.691	9.079
58	0.313E+01	0.639E+01	0.250E+00	0.651E+01	-48.790	9.317
59	0.325E+01	0.567E+01	0.234E+00	0.555E+01	54.286	9.612
60	0.338E+01	0.411E+01	0.200E+00	0.415E+01	-20.511	9.654
61	0.350E+01	0.333E+01	0.180E+00	0.343E+01	-54.573	9.952
62	0.363E+01	0.297E+01	0.170E+00	0.279E+01	107.100	11.099
63	0.375E+01	0.216E+01	0.144E+00	0.224E+01	-59.359	11.451
64	0.388E+01	0.189E+01	0.134E+00	0.186E+01	17.156	11.480
65	0.400E+01	0.161E+01	0.124E+00	0.163E+01	-15.269	11.504
66	0.413E+01	0.140E+01	0.114E+00	0.144E+01	-32.028	11.606
67	0.425E+01	0.139E+01	0.115E+00	0.123E+01	137.308	13.492
68	0.438E+01	0.877E+00	0.904E-01	0.997E+00	-133.239	15.267
69	0.450E+01	0.725E+00	0.830E-01	0.637E+00	105.913	16.389

70	0.463E+01	0.335E+00	0.564E-01	0.336E+00	-0.314	16.389
71	0.475E+01	0.145E+00	0.371E-01	0.175E+00	-80.923	17.044
72	0.488E+01	0.982E-01	0.307E-01	0.810E-01	55.991	17.357
73	0.500E+01	0.496E-01	0.222E-01	0.385E-01	49.981	17.607
74	0.513E+01	0.147E-01	0.131E-01	0.171E-01	-18.798	17.642
75	0.525E+01	0.755E-02	0.102E-01	0.684E-02	6.955	17.647
76	0.538E+01	0.000E+00	0.586E-02	0.248E-02	-42.313	17.826
77	0.550E+01	0.927E-02	0.110E-01	0.100E-02	75.363	18.394
78	0.563E+01	-0.253E-02	0.135E-01	0.645E-03	-23.490	18.449
79	0.575E+01	0.253E-02	0.760E-02	0.574E-03	25.727	18.515
80	0.588E+01	0.000E+00	0.586E-02	0.511E-03	-8.710	18.523
81	0.600E+01	0.000E+00	0.586E-02	0.456E-03	-7.772	18.529
82	0.613E+01	-0.678E-02	0.120E-01	0.420E-03	-60.142	18.891
83	0.625E+01	0.452E-02	0.713E-02	0.368E-03	58.232	19.230
84	0.644E+01	0.000E+00	0.479E-02	0.310E-03	-6.484	19.234
85	0.663E+01	0.000E+00	0.479E-02	0.232E-03	-4.848	19.236
86	0.681E+01	0.000E+00	0.479E-02	0.174E-03	-3.633	19.238
87	0.700E+01	0.000E+00	0.479E-02	0.126E-03	-2.641	19.238
88	0.719E+01	0.000E+00	0.479E-02	0.146E-03	-3.055	19.239
89	0.738E+01	0.000E+00	0.479E-02	0.239E-03	-4.995	19.242
90	0.756E+01	0.000E+00	0.479E-02	0.394E-03	-8.240	19.249
91	0.775E+01	0.000E+00	0.479E-02	0.546E-03	-11.414	19.262
92	0.794E+01	0.339E-02	0.662E-02	0.674E-03	41.038	19.430
93	0.813E+01	0.279E-02	0.634E-02	0.633E-03	33.999	19.546
94	0.831E+01	0.000E+00	0.479E-02	0.474E-03	-9.911	19.555
95	0.850E+01	0.000E+00	0.479E-02	0.222E-03	-4.639	19.558
96	0.869E+01	0.000E+00	0.479E-02	-0.553E-04	1.155	19.558
97	0.888E+01	0.000E+00	0.479E-02	-0.317E-03	6.628	19.562
98	0.906E+01	0.000E+00	0.479E-02	-0.547E-03	11.432	19.575
99	0.925E+01	-0.213E-02	0.601E-02	-0.667E-03	-24.426	19.635
100	0.944E+01	-0.405E-02	0.692E-02	-0.675E-03	-48.686	19.872
101	0.963E+01	-0.618E-02	0.782E-02	-0.548E-03	-72.047	20.391
102	0.981E+01	0.513E-02	0.739E-02	-0.382E-03	74.547	20.947
103	0.100E+02	0.105E-02	0.542E-02	-0.194E-03	22.993	21.000
104	0.102E+02	0.000E+00	0.479E-02	-0.515E-04	1.076	21.000
105	0.104E+02	0.000E+00	0.479E-02	0.195E-04	-0.408	21.000
106	0.106E+02	0.000E+00	0.479E-02	0.383E-04	-0.801	21.000
107	0.108E+02	0.000E+00	0.479E-02	0.330E-04	-0.689	21.000
108	0.109E+02	0.000E+00	0.479E-02	0.228E-04	-0.476	21.000
109	0.111E+02	0.000E+00	0.415E-02	0.160E-04	-0.385	21.000

110	0.114E+02	0.000E+00	0.415E-02	0.127E-04	-0.305	21.000
111	0.116E+02	0.000E+00	0.415E-02	0.975E-05	-0.235	21.000
112	0.119E+02	0.000E+00	0.415E-02	0.623E-05	-0.150	21.000
113	0.121E+02	0.000E+00	0.415E-02	0.350E-05	-0.084	21.000

Page 20:

```
 INDICATOR NO. 1   =       0.013 (CONDITION)
 INDICATOR NO. 2   =       0.177 (CONSISTENT WITH NON-NEG.)
 INDICATOR NO. 3   =       0.431 (RESIDUALS)
 SUM OF INDICATORS =       0.620 (SHOULD BE LESS THAN 5.000 FOR VALID --- TAW=  10.000 ---
RUN -- SEE MANUAL)
```

Page 21:

PuBe #M1170 run 9 neutrons lgb, 24 Nov 92
--- TAW= 10.000 ---

ENERGY		PLO	PUP	PAVE	PCT W	ERR1	ERR2
0.200E+06	1	-0.172E+37	0.172E+37	0.731E+07	46.00	0.215E+08	0.172E+37
0.400E+06	2	-0.546E+33	0.546E+33	0.469E+06	37.00	0.133E+07	0.546E+33
0.600E+06	3	-0.195E+04	0.256E+04	0.306E+03	33.00	0.125E+03	0.213E+04
0.800E+06	4	0.415E+02	0.678E+02	0.546E+02	30.00	0.330E+01	0.985E+01
0.100E+07	5	0.529E+02	0.712E+02	0.621E+02	28.00	0.197E+01	0.716E+01
0.120E+07	6	0.784E+02	0.904E+02	0.844E+02	26.00	0.159E+01	0.440E+01
0.140E+07	7	0.341E+02	0.389E+02	0.365E+02	24.00	0.119E+01	0.125E+01
0.160E+07	8	0.223E+02	0.264E+02	0.243E+02	22.00	0.112E+01	0.908E+00
0.180E+07	9	0.171E+02	0.194E+02	0.182E+02	21.00	0.982E+00	0.188E+00
0.200E+07	10	0.162E+02	0.182E+02	0.172E+02	20.00	0.888E+00	0.117E+00
0.220E+07	11	0.139E+02	0.157E+02	0.148E+02	19.00	0.803E+00	0.947E-01
0.240E+07	12	0.126E+02	0.143E+02	0.134E+02	18.30	0.730E+00	0.118E+00
0.260E+07	13	0.118E+02	0.134E+02	0.126E+02	17.80	0.710E+00	0.127E+00
0.280E+07	14	0.145E+02	0.161E+02	0.153E+02	17.00	0.697E+00	0.886E-01
0.300E+07	15	0.175E+02	0.189E+02	0.182E+02	16.30	0.646E+00	0.706E-01
0.320E+07	16	0.162E+02	0.175E+02	0.169E+02	16.00	0.585E+00	0.665E-01
0.340E+07	17	0.137E+02	0.149E+02	0.143E+02	15.50	0.546E+00	0.400E-01
0.360E+07	18	0.115E+02	0.128E+02	0.122E+02	15.00	0.586E+00	0.499E-01
0.380E+07	19	0.109E+02	0.123E+02	0.116E+02	14.50	0.622E+00	0.905E-01

0.400E+07	20	0.121E+02	0.139E+02	0.130E+02	14.00	0.748E+00	0.130E+00
0.420E+07	21	0.124E+02	0.143E+02	0.133E+02	13.80	0.801E+00	0.162E+00
0.440E+07	22	0.110E+02	0.131E+02	0.121E+02	13.30	0.815E+00	0.207E+00
0.460E+07	23	0.109E+02	0.127E+02	0.118E+02	13.00	0.768E+00	0.146E+00
0.480E+07	24	0.119E+02	0.136E+02	0.128E+02	12.80	0.709E+00	0.141E+00
0.500E+07	25	0.121E+02	0.136E+02	0.128E+02	12.60	0.636E+00	0.133E+00
0.520E+07	26	0.107E+02	0.121E+02	0.114E+02	12.20	0.605E+00	0.945E-01
0.540E+07	27	0.872E+01	0.101E+02	0.942E+01	12.00	0.578E+00	0.117E+00
0.560E+07	28	0.687E+01	0.826E+01	0.757E+01	11.90	0.568E+00	0.124E+00
0.580E+07	29	0.513E+01	0.655E+01	0.584E+01	11.60	0.576E+00	0.134E+00
0.600E+07	30	0.446E+01	0.607E+01	0.526E+01	11.50	0.583E+00	0.221E+00
0.620E+07	31	0.568E+01	0.736E+01	0.652E+01	11.20	0.592E+00	0.246E+00
0.640E+07	32	0.663E+01	0.824E+01	0.743E+01	11.00	0.584E+00	0.218E+00
0.660E+07	33	0.551E+01	0.720E+01	0.635E+01	10.80	0.578E+00	0.264E+00
0.680E+07	34	0.424E+01	0.560E+01	0.492E+01	10.70	0.514E+00	0.166E+00
0.700E+07	35	0.411E+01	0.546E+01	0.478E+01	10.50	0.494E+00	0.181E+00
0.720E+07	36	0.455E+01	0.577E+01	0.516E+01	10.30	0.466E+00	0.147E+00
0.740E+07	37	0.441E+01	0.575E+01	0.508E+01	10.20	0.471E+00	0.199E+00
0.760E+07	38	0.444E+01	0.570E+01	0.507E+01	10.10	0.446E+00	0.185E+00
0.780E+07	39	0.479E+01	0.592E+01	0.535E+01	10.00	0.410E+00	0.155E+00
0.800E+07	40	0.457E+01	0.571E+01	0.514E+01	9.80	0.397E+00	0.173E+00
0.820E+07	41	0.375E+01	0.484E+01	0.430E+01	9.70	0.373E+00	0.170E+00
0.840E+07	42	0.301E+01	0.393E+01	0.347E+01	9.60	0.309E+00	0.150E+00
0.860E+07	43	0.241E+01	0.334E+01	0.287E+01	9.50	0.319E+00	0.150E+00
0.880E+07	44	0.192E+01	0.270E+01	0.231E+01	9.40	0.258E+00	0.133E+00
0.900E+07	45	0.139E+01	0.219E+01	0.179E+01	9.30	0.273E+00	0.130E+00
0.920E+07	46	0.112E+01	0.183E+01	0.148E+01	9.20	0.239E+00	0.116E+00
0.940E+07	47	0.115E+01	0.183E+01	0.149E+01	9.10	0.217E+00	0.124E+00
0.960E+07	48	0.144E+01	0.217E+01	0.181E+01	9.00	0.230E+00	0.138E+00
0.980E+07	49	0.194E+01	0.247E+01	0.221E+01	8.90	0.168E+00	0.997E-01
0.100E+08	50	0.208E+01	0.262E+01	0.235E+01	8.80	0.164E+00	0.109E+00
0.102E+08	51	0.181E+01	0.231E+01	0.206E+01	8.70	0.158E+00	0.944E-01
0.104E+08	52	0.129E+01	0.166E+01	0.147E+01	8.60	0.108E+00	0.764E-01
0.106E+08	53	0.737E+00	0.105E+01	0.893E+00	8.50	0.857E-01	0.708E-01
0.108E+08	54	0.370E+00	0.606E+00	0.488E+00	8.40	0.687E-01	0.494E-01
0.110E+08	55	0.168E+00	0.344E+00	0.256E+00	8.30	0.451E-01	0.429E-01

Page 22:

0.112E+08	56	0.543E-01	0.207E+00	0.131E+00	8.20	0.339E-01	0.427E-01
0.114E+08	57	0.194E-02	0.124E+00	0.628E-01	8.10	0.251E-01	0.358E-01
0.116E+08	58	-0.146E-01	0.677E-01	0.266E-01	8.00	0.155E-01	0.257E-01
0.118E+08	59	-0.227E-01	0.416E-01	0.946E-02	8.00	0.100E-01	0.221E-01
0.120E+08	60	-0.272E-01	0.330E-01	0.293E-02	8.00	0.811E-02	0.220E-01
0.122E+08	61	-0.283E-01	0.304E-01	0.103E-02	8.00	0.718E-02	0.222E-01
0.124E+08	62	-0.274E-01	0.287E-01	0.655E-03	8.00	0.677E-02	0.213E-01
0.126E+08	63	-0.258E-01	0.271E-01	0.689E-03	8.00	0.670E-02	0.198E-01
0.128E+08	64	-0.259E-01	0.275E-01	0.837E-03	8.00	0.665E-02	0.201E-01
0.130E+08	65	-0.236E-01	0.256E-01	0.101E-02	8.00	0.649E-02	0.181E-01
0.132E+08	66	-0.257E-01	0.280E-01	0.114E-02	8.00	0.630E-02	0.206E-01
0.134E+08	67	-0.242E-01	0.266E-01	0.117E-02	8.00	0.618E-02	0.192E-01
0.136E+08	68	-0.238E-01	0.259E-01	0.104E-02	8.00	0.613E-02	0.187E-01
0.138E+08	69	-0.247E-01	0.263E-01	0.763E-03	8.00	0.610E-02	0.194E-01
0.140E+08	70	-0.238E-01	0.245E-01	0.345E-03	8.00	0.606E-02	0.181E-01
0.142E+08	71	-0.244E-01	0.241E-01	-0.169E-03	8.00	0.603E-02	0.182E-01
0.144E+08	72	-0.248E-01	0.233E-01	-0.726E-03	8.00	0.602E-02	0.180E-01
0.146E+08	73	-0.253E-01	0.227E-01	-0.126E-02	8.00	0.603E-02	0.180E-01
0.148E+08	74	-0.269E-01	0.235E-01	-0.171E-02	8.00	0.605E-02	0.192E-01
0.150E+08	75	-0.283E-01	0.243E-01	-0.197E-02	8.00	0.605E-02	0.203E-01
0.152E+08	76	-0.280E-01	0.241E-01	-0.195E-02	8.00	0.603E-02	0.200E-01
0.154E+08	77	-0.280E-01	0.248E-01	-0.160E-02	8.00	0.605E-02	0.203E-01
0.156E+08	78	-0.270E-01	0.252E-01	-0.899E-03	8.00	0.614E-02	0.199E-01
0.158E+08	79	-0.261E-01	0.262E-01	0.829E-04	8.00	0.629E-02	0.199E-01
0.160E+08	80	-0.265E-01	0.289E-01	0.121E-02	8.00	0.649E-02	0.212E-01
0.162E+08	81	-0.251E-01	0.298E-01	0.233E-02	8.00	0.671E-02	0.208E-01
0.164E+08	82	-0.275E-01	0.341E-01	0.329E-02	8.00	0.692E-02	0.239E-01
0.166E+08	83	-0.266E-01	0.345E-01	0.399E-02	8.00	0.712E-02	0.234E-01
0.168E+08	84	-0.279E-01	0.366E-01	0.435E-02	8.00	0.731E-02	0.249E-01
0.170E+08	85	-0.283E-01	0.370E-01	0.435E-02	8.00	0.745E-02	0.252E-01
0.172E+08	86	-0.296E-01	0.376E-01	0.398E-02	8.00	0.754E-02	0.260E-01
0.174E+08	87	-0.314E-01	0.379E-01	0.323E-02	8.00	0.755E-02	0.271E-01
0.176E+08	88	-0.306E-01	0.350E-01	0.217E-02	8.00	0.751E-02	0.253E-01
0.178E+08	89	-0.331E-01	0.349E-01	0.892E-03	8.00	0.746E-02	0.265E-01
0.180E+08	90	-0.325E-01	0.316E-01	-0.434E-03	8.00	0.746E-02	0.246E-01
0.182E+08	91	-0.337E-01	0.304E-01	-0.163E-02	8.00	0.753E-02	0.245E-01
0.184E+08	92	-0.348E-01	0.297E-01	-0.252E-02	8.00	0.766E-02	0.246E-01
0.186E+08	93	-0.356E-01	0.295E-01	-0.301E-02	8.00	0.782E-02	0.247E-01

0.188E+08	94	-0.382E-01	0.320E-01	-0.308E-02	8.00	0.798E-02	0.271E-01
0.190E+08	95	-0.370E-01	0.315E-01	-0.280E-02	8.00	0.815E-02	0.261E-01
0.192E+08	96	-0.389E-01	0.343E-01	-0.227E-02	8.00	0.836E-02	0.283E-01
0.194E+08	97	-0.390E-01	0.357E-01	-0.166E-02	8.00	0.859E-02	0.288E-01
0.196E+08	98	-0.372E-01	0.351E-01	-0.107E-02	8.00	0.882E-02	0.273E-01
0.198E+08	99	-0.378E-01	0.366E-01	-0.583E-03	8.00	0.899E-02	0.282E-01
0.200E+08	100	-0.360E-01	0.356E-01	-0.238E-03	8.00	0.902E-02	0.268E-01
0.202E+08	101	-0.353E-01	0.353E-01	-0.266E-04	8.00	0.884E-02	0.265E-01
0.204E+08	102	-0.352E-01	0.354E-01	0.794E-04	8.00	0.844E-02	0.268E-01
0.206E+08	103	-0.315E-01	0.318E-01	0.116E-03	8.00	0.789E-02	0.238E-01
0.208E+08	104	-0.306E-01	0.308E-01	0.115E-03	8.00	0.739E-02	0.233E-01
0.210E+08	105	-0.286E-01	0.288E-01	0.101E-03	8.00	0.716E-02	0.215E-01
0.212E+08	106	-0.252E-01	0.254E-01	0.869E-04	8.00	0.729E-02	0.180E-01
0.214E+08	107	-0.226E-01	0.227E-01	0.780E-04	8.00	0.764E-02	0.150E-01
0.216E+08	108	-0.220E-01	0.222E-01	0.736E-04	8.00	0.793E-02	0.142E-01
0.218E+08	109	-0.227E-01	0.228E-01	0.710E-04	8.00	0.789E-02	0.149E-01

Page 23:

PLO AND PUP Puße #M1170 run 9 neutrons lgb, 24 Nov 92

PLO- NO. 1 SCALE FACTOR = 1.0E+00

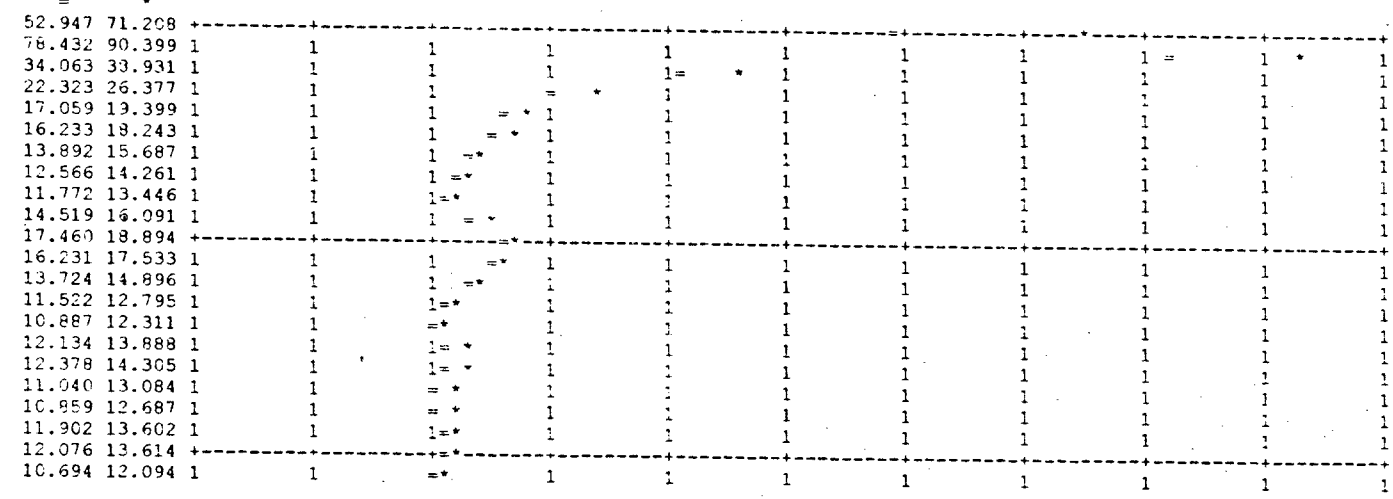

```
 8.722 10.113 1          1          =*1          1          1          1          1          1          1          1          1
 6.875  9.259 1          1            = *1       1          1          1          1          1          1          1          1
 5.131  6.549 1          1         =*    1       1          1          1          1          1          1          1          1
 4.459  6.068 1          1         = *   1       1          1          1          1          1          1          1          1
 5.681  7.356 1          1           = * 1       1          1          1          1          1          1          1          1
 6.631  8.235 1          1             = 1       1          1          1          1          1          1          1          1
 5.511  7.196 1          1           = *   1       1          1          1          1          1          1          1          1
 4.243  5.602 1          1         =*      1       1          1          1          1          1          1          1          1
 4.108  5.458 +----------+---=*-----+-------+-------+-------+-------+-------+-------+-------+-------+-------+-------+-------+
 4.547  5.772 1          1         =*      1       1          1          1          1          1          1          1          1
 4.413  5.754 1          1         =*      1       1          1          1          1          1          1          1          1
 4.439  5.701 1          1         =*      1       1          1          1          1          1          1          1          1
 4.788  5.917 1          1         =*      1       1          1          1          1          1          1          1          1
 4.571  5.713 1          1         =*      1       1          1          1          1          1          1          1          1
 3.754  4.841 1          1       =*        1       1          1          1          1          1          1          1          1
 3.012  3.929 1          1       =*        1       1          1          1          1          1          1          1          1
 2.406  3.343 1          1     =*          1       1          1          1          1          1          1          1          1
 1.921  2.704 1          1     =           1       1          1          1          1          1          1          1          1
 1.385  2.192 +----------+=*--------------+-------+-------+-------+-------+-------+-------+-------+-------+-------+-------+
 1.122  1.833 1          1=*             1       1          1          1          1          1          1          1          1
 1.150  1.833 1          1=*             1       1          1          1          1          1          1          1          1
 1.438  2.173 1          1=*             1       1          1          1          1          1          1          1          1
 1.938  2.474 1          1 =             1       1          1          1          1          1          1          1          1
 2.079  2.625 1          1 =             1       1          1          1          1          1          1          1          1
 1.807  2.313 1          1 =             1       1          1          1          1          1          1          1          1
 1.290  1.660 1          1=*             1       1          1          1          1          1          1          1          1
 0.737  1.050 1          1=              1       1          1          1          1          1          1          1          1
 0.370  0.606 1          =*              1       1          1          1          1          1          1          1          1
 0.166  0.344 +----------=--------------+-------+-------+-------+-------+-------+-------+-------+-------+-------+-------+
 0.054  0.207 1          =               1       1          1          1          1          1          1          1          1
 0.002  0.124 1          =               1       1          1          1          1          1          1          1          1
-0.015  0.068 1          =               1       1          1          1          1          1          1          1          1
-0.023  0.042 1          =               1       1          1          1          1          1          1          1          1
```

Page 24:

```
-0.027  0.033 1          =               1       1          1          1          1          1          1          1          1
-0.028  0.030 1          =               1       1          1          1          1          1          1          1          1
-0.027  0.029 1          =               1       1          1          1          1          1          1          1          1
-0.026  0.027 1          =               1       1          1          1          1          1          1          1          1
-0.026  0.028 1          =               1       1          1          1          1          1          1          1          1
-0.024  0.026 +----------=--------------+-------+-------+-------+-------+-------+-------+-------+-------+-------+-------+
-0.026  0.028 1          =               1       1          1          1          1          1          1          1          1
-0.024  0.027 1          =               1       1          1          1          1          1          1          1          1
-0.024  0.026 1          =               1       1          1          1          1          1          1          1          1
-0.025  0.026 1          =               1       1          1          1          1          1          1          1          1
-0.024  0.024 1          =               1       1          1          1          1          1          1          1          1
-0.024  0.024 1          =               1       1          1          1          1          1          1          1          1
-0.025  0.023 1          =               1       1          1          1          1          1          1          1          1
```

```
-0.025  0.023 1         =         1         1         1         1         1         1         1         1         1
-0.027  0.023 1         =         1         1         1         1         1         1         1         1         1
-0.028  0.024 +---------=---------+---------+---------+---------+---------+---------+---------+---------+---------+
-0.028  0.024 1         =         1         1         1         1         1         1         1         1         1
-0.028  0.025 1         =         1         1         1         1         1         1         1         1         1
-0.027  0.025 1         =         1         1         1         1         1         1         1         1         1
-0.026  0.026 1         =         1         1         1         1         1         1         1         1         1
-0.027  0.029 1         =         1         1         1         1         1         1         1         1         1
-0.025  0.030 1         =         1         1         1         1         1         1         1         1         1
-0.028  0.034 1         =         1         1         1         1         1         1         1         1         1
-0.027  0.035 1         =         1         1         1         1         1         1         1         1         1
-0.028  0.037 1         =         1         1         1         1         1         1         1         1         1
-0.028  0.037 +---------=---------+---------+---------+---------+---------+---------+---------+---------+---------+
-0.030  0.038 1         =         1         1         1         1         1         1         1         1         1
-0.031  0.038 1         =         1         1         1         1         1         1         1         1         1
-0.031  0.035 1         =         1         1         1         1         1         1         1         1         1
-0.033  0.035 1         =         1         1         1         1         1         1         1         1         1
-0.032  0.032 1         =         1         1         1         1         1         1         1         1         1
-0.034  0.030 1         =         1         1         1         1         1         1         1         1         1
-0.035  0.030 1         =         1         1         1         1         1         1         1         1         1
-0.036  0.030 1         =         1         1         1         1         1         1         1         1         1
-0.036  0.032 1         =         1         1         1         1         1         1         1         1         1
-0.037  0.031 +---------=---------+---------+---------+---------+---------+---------+---------+---------+---------+
-0.039  0.034 1         =         1         1         1         1         1         1         1         1         1
-0.039  0.036 1         =         1         1         1         1         1         1         1         1         1
-0.037  0.035 1         =         1         1         1         1         1         1         1         1         1
-0.038  0.037 1         =         1         1         1         1         1         1         1         1         1
-0.036  0.036 1         =         1         1         1         1         1         1         1         1         1
-0.035  0.035 1         =         1         1         1         1         1         1         1         1         1
-0.035  0.035 1         =         1         1         1         1         1         1         1         1         1
-0.032  0.032 1         =         1         1         1         1         1         1         1         1         1
-0.031  0.031 1         =         1         1         1         1         1         1         1         1         1
-0.029  0.029 +---------=---------+---------+---------+---------+---------+---------+---------+---------+---------+
-0.025  0.025 1         =         1         1         1         1         1         1         1         1         1
-0.023  0.023 1         =         1         1         1         1         1         1         1         1         1
-0.022  0.022 1         =         1         1         1         1         1         1         1         1         1
-0.023  0.023 +---------=---------+---------+---------+---------+---------+---------+---------+---------+---------+
          *****       0.00      10.90     21.80     32.70     43.60     54.50     65.40     76.30     87.20     98.10
```

Page 25:

PuBe #M1170 run 9 neutrons lgb, 24 Nov 92
--- TAW= 10.000 ---

ENERGY		PLO	PUP	PAVE	PCT W	ERR1	ERR2
0.200E+06	1	-0.128E+37	0.128E+37	0.791E+07	65.10	0.232E+08	0.128E+37

0.400E+06	2	-0.186E+35	0.186E+35	0.196E+07	58.65	0.571E+07	0.186E+35
0.600E+06	3	-0.608E+05	0.639E+05	0.154E+04	52.20	0.270E+04	0.596E+05
0.800E+06	4	0.143E+02	0.158E+03	0.863E+02	46.20	0.839E+01	0.636E+02
0.100E+07	5	0.605E+02	0.649E+02	0.627E+02	42.30	0.691E+00	0.150E+01
0.120E+07	6	0.673E+02	0.703E+02	0.688E+02	39.00	0.679E+00	0.820E+00
0.140E+07	7	0.405E+02	0.457E+02	0.431E+02	36.24	0.520E+00	0.211E+01
0.160E+07	8	0.249E+02	0.271E+02	0.260E+02	33.45	0.440E+00	0.635E+00
0.180E+07	9	0.199E+02	0.202E+02	0.195E+02	31.10	0.398E+00	0.245E+00
0.200E+07	10	0.164E+02	0.172E+02	0.168E+02	29.29	0.383E+00	0.376E-01
0.220E+07	11	0.144E+02	0.152E+02	0.148E+02	28.03	0.370E+00	0.401E-01
0.240E+07	12	0.130E+02	0.138E+02	0.134E+02	26.23	0.373E+00	0.331E-01
0.260E+07	13	0.131E+02	0.140E+02	0.135E+02	24.32	0.398E+00	0.387E-01
0.280E+07	14	0.150E+02	0.159E+02	0.155E+02	22.47	0.400E+00	0.419E-01
0.300E+07	15	0.169E+02	0.178E+02	0.174E+02	20.67	0.385E+00	0.388E-01
0.320E+07	16	0.167E+02	0.175E+02	0.171E+02	19.31	0.393E+00	0.383E-01
0.340E+07	17	0.147E+02	0.155E+02	0.151E+02	19.10	0.373E+00	0.277E-01
0.360E+07	18	0.128E+02	0.135E+02	0.131E+02	19.60	0.341E+00	0.240E-01
0.380E+07	19	0.118E+02	0.125E+02	0.121E+02	20.14	0.318E+00	0.207E-01
0.400E+07	20	0.117E+02	0.124E+02	0.121E+02	20.54	0.322E+00	0.259E-01
0.420E+07	21	0.119E+02	0.127E+02	0.123E+02	20.46	0.337E+00	0.310E-01
0.440E+07	22	0.119E+02	0.126E+02	0.123E+02	20.07	0.328E+00	0.263E-01
0.460E+07	23	0.119E+02	0.125E+02	0.122E+02	19.51	0.313E+00	0.285E-01
0.480E+07	24	0.118E+02	0.125E+02	0.121E+02	18.93	0.301E+00	0.330E-01
0.500E+07	25	0.114E+02	0.121E+02	0.117E+02	18.54	0.285E+00	0.397E-01
0.520E+07	26	0.105E+02	0.111E+02	0.108E+02	18.21	0.270E+00	0.329E-01
0.540E+07	27	0.907E+01	0.964E+01	0.935E+01	17.85	0.261E+00	0.280E-01
0.560E+07	28	0.765E+01	0.821E+01	0.793E+01	17.66	0.254E+00	0.262E-01
0.580E+07	29	0.659E+01	0.716E+01	0.687E+01	17.46	0.247E+00	0.391E-01
0.600E+07	30	0.607E+01	0.664E+01	0.636E+01	17.16	0.239E+00	0.449E-01
0.620E+07	31	0.599E+01	0.651E+01	0.625E+01	16.83	0.232E+00	0.310E-01
0.640E+07	32	0.595E+01	0.647E+01	0.621E+01	16.56	0.227E+00	0.322E-01
0.660E+07	33	0.572E+01	0.625E+01	0.599E+01	16.26	0.223E+00	0.436E-01
0.680E+07	34	0.536E+01	0.586E+01	0.561E+01	15.99	0.212E+00	0.403E-01
0.700E+07	35	0.506E+01	0.551E+01	0.528E+01	15.75	0.200E+00	0.244E-01
0.720E+07	36	0.491E+01	0.533E+01	0.512E+01	15.54	0.190E+00	0.234E-01
0.740E+07	37	0.485E+01	0.529E+01	0.507E+01	15.33	0.183E+00	0.339E-01
0.760E+07	38	0.481E+01	0.523E+01	0.502E+01	15.12	0.177E+00	0.339E-01
0.780E+07	39	0.468E+01	0.507E+01	0.487E+01	14.94	0.169E+00	0.285E-01
0.800E+07	40	0.438E+01	0.476E+01	0.457E+01	14.76	0.163E+00	0.292E-01
0.820E+07	41	0.393E+01	0.429E+01	0.411E+01	14.58	0.154E+00	0.258E-01

0.840E+07	42	0.338E+01	0.372E+01	0.355E+01	14.40	0.143E+00	0.280E-01
0.860E+07	43	0.283E+01	0.314E+01	0.298E+01	14.25	0.133E+00	0.211E-01
0.880E+07	44	0.235E+01	0.264E+01	0.249E+01	14.10	0.124E+00	0.203E-01
0.900E+07	45	0.199E+01	0.226E+01	0.213E+01	13.95	0.116E+00	0.223E-01
0.920E+07	46	0.178E+01	0.204E+01	0.191E+01	13.80	0.107E+00	0.215E-01
0.940E+07	47	0.171E+01	0.195E+01	0.183E+01	13.65	0.988E-01	0.222E-01
0.960E+07	48	0.173E+01	0.195E+01	0.184E+01	13.50	0.910E-01	0.207E-01
0.980E+07	49	0.176E+01	0.197E+01	0.186E+01	13.35	0.833E-01	0.216E-01
0.100E+08	50	0.171E+01	0.191E+01	0.181E+01	13.20	0.772E-01	0.232E-01
0.102E+08	51	0.155E+01	0.174E+01	0.164E+01	13.05	0.724E-01	0.200E-01
0.104E+08	52	0.129E+01	0.145E+01	0.137E+01	12.90	0.649E-01	0.185E-01
0.106E+08	53	0.968E+00	0.112E+01	0.104E+01	12.75	0.541E-01	0.203E-01
0.108E+08	54	0.666E+00	0.788E+00	0.727E+00	12.60	0.430E-01	0.181E-01
0.110E+08	55	0.420E+00	0.514E+00	0.467E+00	12.45	0.336E-01	0.135E-01

Page 26:

0.112E+08	56	0.239E+00	0.319E+00	0.279E+00	12.30	0.257E-01	0.146E-01
0.114E+08	57	0.123E+00	0.190E+00	0.156E+00	12.18	0.193E-01	0.139E-01
0.116E+08	58	0.565E-01	0.109E+00	0.830E-01	12.09	0.142E-01	0.122E-01
0.118E+08	59	0.195E-01	0.640E-01	0.418E-01	12.03	0.102E-01	0.120E-01
0.120E+08	60	0.218E-03	0.398E-01	0.200E-01	12.00	0.741E-02	0.124E-01
0.122E+08	61	-0.795E-02	0.263E-01	0.916E-02	12.00	0.589E-02	0.112E-01
0.124E+08	62	-0.125E-01	0.207E-01	0.414E-02	12.00	0.529E-02	0.113E-01
0.126E+08	63	-0.151E-01	0.192E-01	0.203E-02	12.00	0.510E-02	0.120E-01
0.128E+08	64	-0.150E-01	0.175E-01	0.124E-02	12.00	0.499E-02	0.112E-01
0.130E+08	65	-0.153E-01	0.172E-01	0.980E-03	12.00	0.488E-02	0.114E-01
0.132E+08	66	-0.145E-01	0.162E-01	0.873E-03	12.00	0.474E-02	0.106E-01
0.134E+08	67	-0.153E-01	0.168E-01	0.778E-03	12.00	0.462E-02	0.114E-01
0.136E+08	68	-0.153E-01	0.165E-01	0.615E-03	12.00	0.452E-02	0.114E-01
0.138E+08	69	-0.147E-01	0.155E-01	0.377E-03	12.00	0.446E-02	0.106E-01
0.140E+08	70	-0.153E-01	0.154E-01	0.773E-04	12.00	0.442E-02	0.109E-01
0.142E+08	71	-0.153E-01	0.147E-01	-0.255E-03	12.00	0.440E-02	0.106E-01
0.144E+08	72	-0.155E-01	0.144E-01	-0.576E-03	12.00	0.438E-02	0.105E-01
0.146E+08	73	-0.161E-01	0.145E-01	-0.839E-03	12.00	0.437E-02	0.109E-01
0.148E+08	74	-0.164E-01	0.144E-01	-0.997E-03	12.00	0.436E-02	0.111E-01
0.150E+08	75	-0.168E-01	0.148E-01	-0.101E-02	12.00	0.435E-02	0.114E-01
0.152E+08	76	-0.164E-01	0.147E-01	-0.851E-03	12.00	0.435E-02	0.112E-01
0.154E+08	77	-0.158E-01	0.147E-01	-0.521E-03	12.00	0.438E-02	0.109E-01

0.156E+08	78	-0.155E-01	0.154E-01	-0.394E-04	12.00	0.444E-02	0.110E-01
0.158E+08	79	-0.150E-01	0.161E-01	0.551E-03	12.00	0.454E-02	0.110E-01
0.160E+08	80	-0.150E-01	0.174E-01	0.119E-02	12.00	0.466E-02	0.116E-01
0.162E+08	81	-0.152E-01	0.188E-01	0.180E-02	12.00	0.479E-02	0.122E-01
0.164E+08	82	-0.154E-01	0.201E-01	0.231E-02	12.00	0.493E-02	0.128E-01
0.166E+08	83	-0.164E-01	0.217E-01	0.267E-02	12.00	0.505E-02	0.140E-01
0.168E+08	84	-0.169E-01	0.226E-01	0.283E-02	12.00	0.515E-02	0.146E-01
0.170E+08	85	-0.173E-01	0.228E-01	0.277E-02	12.00	0.521E-02	0.149E-01
0.172E+08	86	-0.177E-01	0.227E-01	0.249E-02	12.00	0.524E-02	0.149E-01
0.174E+08	87	-0.178E-01	0.218E-01	0.203E-02	12.00	0.525E-02	0.145E-01
0.176E+08	88	-0.183E-01	0.211E-01	0.143E-02	12.00	0.523E-02	0.145E-01
0.178E+08	89	-0.178E-01	0.193E-01	0.755E-03	12.00	0.522E-02	0.134E-01
0.180E+08	90	-0.183E-01	0.184E-01	0.720E-04	12.00	0.522E-02	0.131E-01
0.182E+08	91	-0.184E-01	0.173E-01	-0.555E-03	12.00	0.524E-02	0.126E-01
0.184E+08	92	-0.190E-01	0.169E-01	-0.107E-02	12.00	0.530E-02	0.127E-01
0.186E+08	93	-0.199E-01	0.170E-01	-0.144E-02	12.00	0.539E-02	0.131E-01
0.188E+08	94	-0.209E-01	0.176E-01	-0.165E-02	12.00	0.549E-02	0.138E-01
0.190E+08	95	-0.222E-01	0.188E-01	-0.171E-02	12.00	0.560E-02	0.149E-01
0.192E+08	96	-0.222E-01	0.189E-01	-0.163E-02	12.00	0.569E-02	0.149E-01
0.194E+08	97	-0.227E-01	0.198E-01	-0.146E-02	12.00	0.576E-02	0.155E-01
0.196E+08	98	-0.228E-01	0.204E-01	-0.122E-02	12.00	0.578E-02	0.158E-01
0.198E+08	99	-0.220E-01	0.201E-01	-0.965E-03	12.00	0.573E-02	0.153E-01
0.200E+08	100	-0.210E-01	0.196E-01	-0.715E-03	12.00	0.561E-02	0.147E-01
0.202E+08	101	-0.202E-01	0.192E-01	-0.493E-03	12.00	0.543E-02	0.143E-01
0.204E+08	102	-0.184E-01	0.178E-01	-0.310E-03	12.00	0.522E-02	0.129E-01
0.206E+08	103	-0.170E-01	0.167E-01	-0.172E-03	12.00	0.501E-02	0.118E-01
0.208E+08	104	-0.159E-01	0.158E-01	-0.728E-04	12.00	0.487E-02	0.110E-01
0.210E+08	105	-0.146E-01	0.145E-01	-0.792E-05	12.00	0.482E-02	0.973E-02
0.212E+08	106	-0.135E-01	0.136E-01	0.310E-04	12.00	0.485E-02	0.872E-02
0.214E+08	107	-0.121E-01	0.122E-01	0.515E-04	12.00	0.494E-02	0.719E-02
0.216E+08	108	-0.124E-01	0.126E-01	0.598E-04	12.00	0.500E-02	0.750E-02
0.218E+08	109	-0.125E-01	0.127E-01	0.608E-04	12.00	0.499E-02	0.761E-02

Page 27:

PLO AND PUP PuBe #M1170 run 9 neutrons lgb, 24 Nov 92

PLO- NO. 1 SCALE FACTOR = 1.0E+00

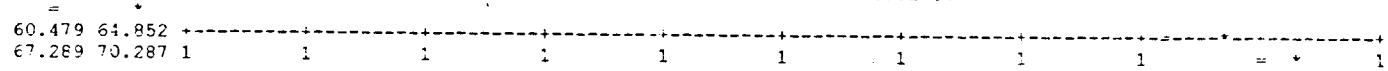

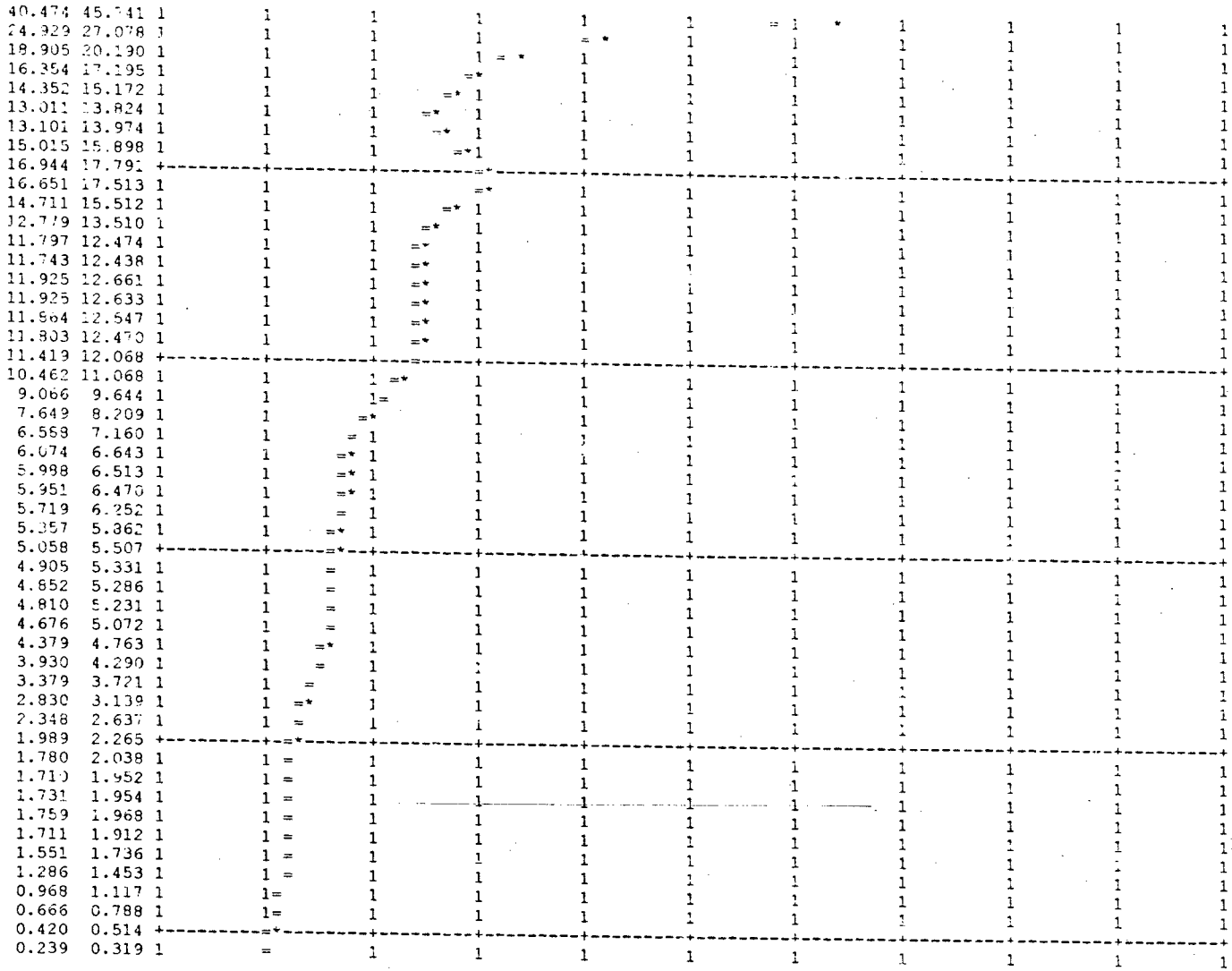

0.123	0.190	1	=	1	1	1	1	1	1	1	1	1
0.057	0.109	1	=	1	1	1	1	1	1	1	1	1
0.020	0.054	1	=	1	1	1	1	1	1	1	1	1

Page 28:

0.000	0.040	1	=	1	1	1	1	1	1	1	1	1
-0.009	0.026	1	=	1	1	1	1	1	1	1	1	1
-0.012	0.021	1	=	1	1	1	1	1	1	1	1	1
-0.015	0.019	1	=	1	1	1	1	1	1	1	1	1
-0.015	0.017	1	=	1	1	1	1	1	1	1	1	1
-0.015	0.017	+	=	+	+	+	+	+	+	+	+	+
-0.014	0.016	1	=	1	1	1	1	1	1	1	1	1
-0.015	0.017	1	=	1	1	1	1	1	1	1	1	1
-0.015	0.017	1	=	1	1	1	1	1	1	1	1	1
-0.015	0.015	1	=	1	1	1	1	1	1	1	1	1
-0.015	0.015	1	=	1	1	1	1	1	1	1	1	1
-0.015	0.015	1	=	1	1	1	1	1	1	1	1	1
-0.016	0.014	1	=	1	1	1	1	1	1	1	1	1
-0.016	0.014	1	=	1	1	1	1	1	1	1	1	1
-0.016	0.014	1	=	1	1	1	1	1	1	1	1	1
-0.017	0.015	+	=	+	+	+	+	+	+	+	+	+
-0.016	0.015	1	=	1	1	1	1	1	1	1	1	1
-0.016	0.015	1	=	1	1	1	1	1	1	1	1	1
-0.016	0.015	1	=	1	1	1	1	1	1	1	1	1
-0.015	0.016	1	=	1	1	1	1	1	1	1	1	1
-0.015	0.017	1	=	1	1	1	1	1	1	1	1	1
-0.015	0.018	1	=	1	1	1	1	1	1	1	1	1
-0.015	0.020	1	=	1	1	1	1	1	1	1	1	1
-0.016	0.022	1	=	1	1	1	1	1	1	1	1	1
-0.017	0.023	1	=	1	1	1	1	1	1	1	1	1
-0.017	0.023	+	=	+	+	+	+	+	+	+	+	+
-0.018	0.023	1	=	1	1	1	1	1	1	1	1	1
-0.018	0.022	1	=	1	1	1	1	1	1	1	1	1
-0.018	0.021	1	=	1	1	1	1	1	1	1	1	1
-0.018	0.019	1	=	1	1	1	1	1	1	1	1	1
-0.018	0.018	1	=	1	1	1	1	1	1	1	1	1
-0.018	0.017	1	=	1	1	1	1	1	1	1	1	1
-0.019	0.017	1	=	1	1	1	1	1	1	1	1	1
-0.020	0.017	1	=	1	1	1	1	1	1	1	1	1
-0.021	0.018	1	=	1	1	1	1	1	1	1	1	1
-0.022	0.019	+	=	+	+	+	+	+	+	+	+	+
-0.022	0.019	1	=	1	1	1	1	1	1	1	1	1
-0.023	0.020	1	=	1	1	1	1	1	1	1	1	1
-0.023	0.020	1	=	1	1	1	1	1	1	1	1	1
-0.022	0.020	1	=	1	1	1	1	1	1	1	1	1
-0.021	0.020	1	=	1	1	1	1	1	1	1	1	1
-0.020	0.019	1	=	1	1	1	1	1	1	1	1	1
-0.018	0.018	1	=	1	1	1	1	1	1	1	1	1

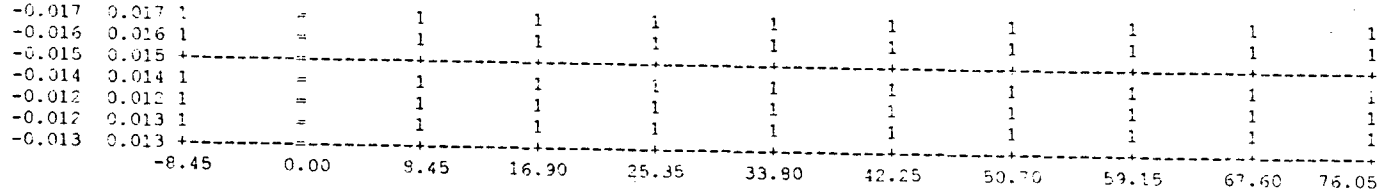

Page 29:

PLO AND PUP PuBe #M1170 run 9 neutrons lgb, 24 Nov 92

* COL 1 $ COL 2

ROW		-0.1E+02	-0.3E+01	-0.9E+00	-0.2E+00	0.0E+00	0.2E+00	0.9E+00	0.3E+01	0.1E+02	0.3E+02	0.1E+03
1	0.100E+07	1	1	1	1	1	1	1	1	1	1	$ 1
2	0.120E+07	1	1	1	1	1	1	1	1	1	1	$ 1
3	0.140E+07	1	1	1	1	1	1	1	1	1	1	$ 1
4	0.160E+07	1	1	1	1	1	1	1	1	1	1 *$	1
5	0.180E+07	1	1	1	1	1	1	1	1	1	*$1	1
6	0.200E+07	1	1	1	1	1	1	1	1	1 $	1	1
7	0.220E+07	1	1	1	1	1	1	1	1	1 *$	1	1
8	0.240E+07	1	1	1	1	1	1	1	1	1 *$	1	1
9	0.260E+07	1	1	1	1	1	1	1	1	1 *$	1	1
10	0.280E+07	1	1	1	1	1	1	1	1	1 *$	1	1
11	0.300E+07	1	1	1	1	1	1	1	1	1 $	1	1
12	0.320E+07	1	1	1	1	1	1	1	1	1 $	1	1
13	0.340E+07	1	1	1	1	1	1	1	1	1 *$	1	1
14	0.360E+07	1	1	1	1	1	1	1	1	1 *$	1	1
15	0.380E+07	1	1	1	1	1	1	1	1	1 *$	1	1
16	0.400E+07	1	1	1	1	1	1	1	1	1 $	1	1
17	0.420E+07	1	1	1	1	1	1	1	1	1*$	1	1
18	0.440E+07	1	1	1	1	1	1	1	1	1 $	1	1
19	0.460E+07	1	1	1	1	1	1	1	1	1 $	1	1
20	0.480E+07	1	1	1	1	1	1	1	1	1 $	1	1
21	0.500E+07	1	1	1	1	1	1	1	1	1 $	1	1
22	0.520E+07	1	1	1	1	1	1	1	1	1*$	1	1
23	0.540E+07	1	1	1	1	1	1	1	1	*$	1	1
24	0.560E+07	1	1	1	1	1	1	1	1	*$	1	1
25	0.580E+07	1	1	1	1	1	1	1	1	$ 1	1	1
26	0.600E+07	1	1	1	1	1	1	1	1	$ 1	1	1
27	0.620E+07	1	1	1	1	1	1	1	1	*$ 1	1	1
28	0.640E+07	1	1	1	1	1	1	1	1	$ 1	1	1
29	0.660E+07	1	1	1	1	1	1	1	1	$ 1	1	1
30	0.680E+07	1	1	1	1	1	1	1	1	*$ 1	1	1
31	0.700E+07	1	1	1	1	1	1	1	1	*$ 1	1	1
32	0.720E+07	1	1	1	1	1	1	1	1	*$ 1	1	1
33	0.740E+07	1	1	1	1	1	1	1	1	*$ 1	1	1
34	0.760E+07	1	1	1	1	1	1	1	1	*$ 1	1	1
35	0.780E+07	1	1	1	1	1	1	1	1	$ 1	1	1

36	0.800E+07	1	1	1	1	1	1	1	1 *$	1	1	1
37	0.820E+07	1	1	1	1	1	1	1	1 *$	1	1	1
38	0.840E+07	1	1	1	1	1	1	1	1*$	1	1	1
39	0.860E+07	1	1	1	1	1	1	1	*$	1	1	1
40	0.880E+07	1	1	1	1	1	1	1	*$1	1	1	1
41	0.900E+07	1	1	1	1	1	1	1 *$	1	1	1	1
42	0.920E+07	1	1	1	1	1	1	1 * $	1	1	1	1
43	0.940E+07	1	1	1	1	1	1	1 *$	1	1	1	1
44	0.960E+07	1	1	1	1	1	1	1 *$	1	1	1	1
45	0.980E+07	1	1	1	1	1	1	1 *$	1	1	1	1
46	0.100E+08	1	1	1	1	1	1	1 *$	1	1	1	1
47	0.102E+08	1	1	1	1	1	1	1 *$	1	1	1	1
48	0.104E+08	1	1	1	1	1	1	1 *$	1	1	1	1
49	0.106E+08	1	1	1	1	1	1	1*$	1	1	1	1
50	0.108E+08	1	1	1	1	1	1	*$1	1	1	1	1
51	0.110E+08	1	1	1	1	1	1 * $	1	1	1	1	1
52	0.112E+08	1	1	1	1	1	1*$	1	1	1	1	1
53	0.114E+08	1	1	1	1	1 * $1	1	1	1	1	1	1
54	0.116E+08	1	1	1	1	1 * $	1	1	1	1	1	1
55	0.118E+08	1	1	1	1	1 * $	1	1	1	1	1	1

Page 30:

56	0.120E+08	1	1	1	1	* $	1	1	1	1	1	1
57	0.122E+08	1	1	1	1	*1 $	1	1	1	1	1	1
58	0.124E+08	1	1	1	1	*1 $	1	1	1	1	1	1
59	0.126E+08	1	1	1	1	*1 $	1	1	1	1	1	1
60	0.128E+08	1	1	1	1	*1$	1	1	1	1	1	1
61	0.130E+08	1	1	1	1	*1$	1	1	1	1	1	1
62	0.132E+08	1	1	1	1	*1$	1	1	1	1	1	1
63	0.134E+08	1	1	1	1	*1$	1	1	1	1	1	1
64	0.136E+08	1	1	1	1	*1$	1	1	1	1	1	1
65	0.138E+08	1	1	1	1	*1$	1	1	1	1	1	1
66	0.140E+08	1	1	1	1	*1$	1	1	1	1	1	1
67	0.142E+08	1	1	1	1	*1$	1	1	1	1	1	1
68	0.144E+08	1	1	1	1	*1$	1	1	1	1	1	1
69	0.146E+08	1	1	1	1	*1$	1	1	1	1	1	1
70	0.148E+08	1	1	1	1	*1$	1	1	1	1	1	1
71	0.150E+08	1	1	1	1	*1$	1	1	1	1	1	1
72	0.152E+08	1	1	1	1	*1$	1	1	1	1	1	1
73	0.154E+08	1	1	1	1	*1$	1	1	1	1	1	1
74	0.156E+08	1	1	1	1	*1$	1	1	1	1	1	1
75	0.158E+08	1	1	1	1	*1$	1	1	1	1	1	1
76	0.160E+08	1	1	1	1	*1$	1	1	1	1	1	1
77	0.162E+08	1	1	1	1	*1$	1	1	1	1	1	1
78	0.164E+08	1	1	1	1	*1 $	1	1	1	1	1	1
79	0.166E+08	1	1	1	1	*1 $	1	1	1	1	1	1
80	0.168E+08	1	1	1	1	*1 $	1	1	1	1	1	1
81	0.170E+08	1	1	1	1	*1 $	1	1	1	1	1	1

82	0.172E+08	1	1	1	1	*1 $	1	1	1	1	1	1
83	0.174E+08	1	1	1	1	*1 $	1	1	1	1	1	1
84	0.176E+08	1	1	1	1	*1 $	1	1	1	1	1	1
85	0.178E+08	1	1	1	1	*1 $	1	1	1	1	1	1
86	0.180E+08	1	1	1	1	*1$	1	1	1	1	1	1
87	0.182E+08	1	1	1	1	*1$	1	1	1	1	1	1
88	0.184E+08	1	1	1	1	* 1$	1	1	1	1	1	1
89	0.186E+08	1	1	1	1	* 1$	1	1	1	1	1	1
90	0.188E+08	1	1	1	1	* 1$	1	1	1	1	1	1
91	0.190E+08	1	1	1	1	* 1$	1	1	1	1	1	1
92	0.192E+08	1	1	1	1	* 1 $	1	1	1	1	1	1
93	0.194E+08	1	1	1	1	* 1 $	1	1	1	1	1	1
94	0.196E+08	1	1	1	1	* 1 $	1	1	1	1	1	1
95	0.198E+08	1	1	1	1	* 1 $	1	1	1	1	1	1
96	0.200E+08	1	1	1	1	* 1 $	1	1	1	1	1	1
97	0.202E+08	1	1	1	1	* 1 $	1	1	1	1	1	1
98	0.204E+08	1	1	1	1	*1$	1	1	1	1	1	1
99	0.206E+08	1	1	1	1	*1$	1	1	1	1	1	1
100	0.208E+08	1	1	1	1	*1$	1	1	1	1	1	1
101	0.210E+08	1	1	1	1	*1$	1	1	1	1	1	1
102	0.212E+08	1	1	1	1	*1$	1	1	1	1	1	1
103	0.214E+08	1	1	1	1	*1$	1	1	1	1	1	1
104	0.216E+08	1	1	1	1	*1$	1	1	1	1	1	1
105	0.218E+08	1	1	1	1	*1$	1	1	1	1	1	1

Page 31:

J	ELAB	X	Q	ERRJ1	UHAQJ	SPECTRUM NUMBER
1	0.2010E+06	0.0000E+00	0.1000E+36	0.0000E+00	0.1000E+36	9
2	0.2313E+06	0.0000E+00	0.1000E+36	0.0000E+00	0.1000E+36	9
3	0.2615E+06	0.1917E+07	0.1282E+09	0.5638E+07	0.1088E+09	9
4	0.2918E+06	0.1751E+06	0.1171E+08	0.5150E+06	0.9942E+07	9
5	0.3220E+06	0.1812E+05	0.1126E+07	0.4367E+05	0.9662E+06	9
6	0.3483E+06	0.2941E+04	0.1723E+06	0.5910E+04	0.1490E+06	9
7	0.3745E+06	0.6359E+03	0.3434E+05	0.9615E+03	0.2999E+05	9
8	0.4008E+06	0.1661E+03	0.8796E+04	0.1800E+03	0.7765E+04	9
9	0.4270E+06	0.7028E+02	0.2799E+04	0.4032E+02	0.2495E+04	9
10	0.4745E+06	0.2394E+02	0.6094E+03	0.2707E+02	0.5342E+03	9
11	0.5220E+06	0.1659E+02	0.2299E+03	0.2235E+02	0.1723E+03	9
12	0.5695E+06	0.1817E+02	0.1322E+03	0.1425E+02	0.7449E+02	9
13	0.6170E+06	0.2059E+02	0.9860E+02	0.6703E+01	0.4070E+02	9
14	0.6888E+06	0.5455E+01	0.6609E+02	0.6874E+01	0.1579E+02	9
15	0.7605E+06	0.3144E+01	0.5193E+02	0.6978E+01	0.8393E+01	9

16	0.8323E+06	0.8198E+01	0.4705E+02	0.5312E+01	0.4883E+01	9
17	0.9040E+06	-0.6027E+01	0.4466E+02	0.2860E+01	0.7201E+01	9
18	0.9793E+06	-0.3204E+01	0.4587E+02	0.2329E+01	0.1483E+02	9
19	0.1055E+07	0.1416E+02	0.4742E+02	0.3082E+01	0.1599E+02	9
20	0.1130E+07	0.1776E+02	0.4915E+02	0.3012E+01	0.8697E+01	9
21	0.1205E+07	0.3906E+01	0.5177E+02	0.2589E+01	0.7033E+01	9
22	0.1307E+07	-0.1885E+01	0.3994E+02	0.2490E+01	0.1292E+02	9
23	0.1409E+07	0.8318E+01	0.3733E+02	0.2323E+01	0.1172E+02	9
24	0.1511E+07	0.2006E+01	0.3472E+02	0.1923E+01	0.4884E+01	9
25	0.1613E+07	0.2458E+01	0.3345E+02	0.1544E+01	0.9028E+00	9
26	0.1768E+07	0.1569E+01	0.3194E+02	0.1327E+01	0.1368E+00	9
27	0.1923E+07	0.5189E+01	0.2987E+02	0.1404E+01	0.9818E-01	9
28	0.2078E+07	0.7129E-01	0.3004E+02	0.1361E+01	0.8099E-01	9
29	0.2233E+07	0.4233E+01	0.3061E+02	0.1009E+01	0.4211E-01	9
30	0.2484E+07	0.2924E+01	0.3115E+02	0.7400E+00	0.2184E-01	9
31	0.2736E+07	0.2681E+01	0.3281E+02	0.7555E+00	0.2153E-01	9
32	0.2987E+07	0.5990E+01	0.3361E+02	0.7681E+00	0.2172E-01	9
33	0.3238E+07	0.3533E+01	0.3364E+02	0.7609E+00	0.2129E-01	9
34	0.3488E+07	0.4020E+01	0.3159E+02	0.7384E+00	0.2138E-01	9
35	0.3737E+07	0.1520E+01	0.3048E+02	0.9890E+00	0.3998E-01	9
36	0.3987E+07	0.3729E+01	0.2980E+02	0.1601E+01	0.1091E+00	9
37	0.4236E+07	0.4255E+01	0.2962E+02	0.3217E+01	0.4580E+00	9
38	0.4407E+07	0.4648E+00	0.2890E+02	0.4672E+01	0.1018E+01	9
39	0.4578E+07	0.1794E+01	0.2729E+02	0.4773E+01	0.1146E+01	9
40	0.4748E+07	0.2029E+01	0.2579E+02	0.4393E+01	0.1017E+01	9
41	0.4919E+07	0.3761E+01	0.2456E+02	0.3076E+01	0.5113E+00	9
42	0.5194E+07	0.3459E+01	0.2168E+02	0.1938E+01	0.2253E+00	9
43	0.5468E+07	0.1663E+01	0.1950E+02	0.1867E+01	0.2335E+00	9
44	0.5743E+07	0.3358E+01	0.1666E+02	0.2005E+01	0.3225E+00	9
45	0.6017E+07	-0.2153E+01	0.1592E+02	0.2430E+01	0.5191E+00	9
46	0.6272E+07	0.4455E+01	0.1494E+02	0.2910E+01	0.8369E+00	9
47	0.6527E+07	0.2494E+01	0.1480E+02	0.3033E+01	0.9536E+00	9
48	0.6782E+07	-0.7391E+00	0.1292E+02	0.2772E+01	0.9326E+00	9
49	0.7037E+07	0.1358E+01	0.1181E+02	0.2637E+01	0.9373E+00	9
50	0.7285E+07	0.3624E+01	0.1118E+02	0.2617E+01	0.9924E+00	9
51	0.7533E+07	-0.2575E+01	0.1035E+02	0.2497E+01	0.9814E+00	9
52	0.7781E+07	0.4436E+01	0.9270E+01	0.2235E+01	0.8438E+00	9
53	0.8029E+07	0.7702E+00	0.8132E+01	0.1382E+01	0.3441E+00	9
54	0.8522E+07	0.1797E+01	0.5638E+01	0.6354E+00	0.9722E-01	9
55	0.9015E+07	0.6644E+00	0.3903E+01	0.5225E+00	0.9382E-01	9

56	0.9507E+07	0.4137E+00	0.3104E+01	0.4483E+00	0.8814E-01	9
57	0.1000E+08	0.1896E+01	0.2332E+01	0.3134E+00	0.6006E-01	9

Page 32:

58	0.1050E+08	0.2821E+00	0.6842E+00	0.1506E+00	0.5488E-01	9
59	0.1099E+08	0.7453E-01	0.1612E+00	0.5226E-01	0.3833E-01	9
60	0.1149E+08	-0.5817E-03	0.2919E-01	0.8770E-02	0.2071E-01	9
61	0.1198E+08	0.3789E-03	0.1728E-01	0.4902E-02	0.1303E-01	9
62	0.1249E+08	0.1472E-03	0.1674E-01	0.4612E-02	0.1212E-01	9
63	0.1299E+08	0.5267E-03	0.1715E-01	0.4834E-02	0.1168E-01	9
64	0.1350E+08	0.8894E-03	0.1753E-01	0.4974E-02	0.1187E-01	9
65	0.1401E+08	0.3339E-03	0.1706E-01	0.4863E-02	0.1164E-01	9
66	0.1452E+08	-0.4981E-03	0.1723E-01	0.4763E-02	0.1206E-01	9
67	0.1503E+08	-0.1462E-02	0.1805E-01	0.4974E-02	0.1280E-01	9
68	0.1554E+08	-0.1726E-02	0.1857E-01	0.4804E-02	0.1358E-01	9
69	0.1606E+08	0.9234E-03	0.1974E-01	0.4892E-02	0.1461E-01	9
70	0.1649E+08	0.2157E-02	0.2091E-01	0.4961E-02	0.1578E-01	9
71	0.1693E+08	0.2473E-02	0.2215E-01	0.5402E-02	0.1677E-01	9
72	0.1737E+08	0.2545E-02	0.2344E-01	0.5456E-02	0.1800E-01	9
73	0.1781E+08	0.1184E-02	0.2482E-01	0.5797E-02	0.1891E-01	9
74	0.1833E+08	-0.3050E-02	0.2669E-01	0.6486E-02	0.1976E-01	9
75	0.1886E+08	-0.3106E-02	0.2871E-01	0.6880E-02	0.2141E-01	9
76	0.1938E+08	-0.9987E-04	0.3078E-01	0.7693E-02	0.2296E-01	9
77	0.1991E+08	0.3240E-03	0.3318E-01	0.8129E-02	0.2463E-01	9
78	0.2038E+08	0.1398E-03	0.3534E-01	0.8208E-02	0.2626E-01	9
79	0.2096E+08	-0.5538E-04	0.3755E-01	0.7951E-02	0.2792E-01	9
80	0.2133E+08	-0.1138E-04	0.3976E-01	0.7283E-02	0.2737E-01	9
81	0.2181E+08	0.1399E-03	0.3915E-01	0.1250E-01	0.2021E-01	9

Appendix J: TOGRAPH.OUT Data File

The file TOGRAPH.OUT is generated by FORIST and is used as the data input to the graphing routine GRAPHICS.TK. This file contains, for each iteration of FORIST, the unfolded spectrum (UTBx), the energy scale of the unfolded spectrum (Ex), and the uncertainty in the unfolded spectrum (EPSLONx). The "x" in each variable name is an integer which begins with its largest value corresponding to the unsmoothed spectrum and decreases by one with each smoothing iteration until zero is reached. If FORIST is run in its ususal mode with one smoothing iteration (ITER=1), there will be a total of six data lists in this file. The lists in this file correspond to the computer examples in the other appendices.

This data file is created by FORIST to be in the format required by TK Solver Plus. Each data set begins with the name of the variable, which is followed by a colon. The data is then listed one point at a time with a comma following each data point but the last.

```
UTB1:
0.7308E+07,
0.4685E+06,
0.3055E+03,
0.5461E+02,
0.6208E+02,
0.8442E+02,
0.3650E+02,
0.2435E+02,
0.1823E+02,
0.1724E+02,
0.1479E+02,
0.1341E+02,
0.1261E+02,
0.1530E+02,
0.1818E+02,
0.1688E+02,
0.1431E+02,
0.1216E+02,
0.1160E+02,
0.1301E+02,
0.1334E+02,
```

0.1206E+02,
0.1177E+02,
0.1275E+02,
0.1285E+02,
0.1139E+02,
0.9418E+01,
0.7567E+01,
0.5840E+01,
0.5264E+01,
0.6518E+01,
0.7433E+01,
0.6354E+01,
0.4922E+01,
0.4783E+01,
0.5160E+01,
0.5083E+01,
0.5070E+01,
0.5353E+01,
0.5142E+01,
0.4297E+01,
0.3470E+01,
0.2874E+01,
0.2312E+01,
0.1788E+01,
0.1477E+01,
0.1491E+01,
0.1806E+01,
0.2206E+01,
0.2352E+01,
0.2060E+01,
0.1475E+01,
0.8933E+00,
0.4878E+00,
0.2557E+00,
0.1309E+00,
0.6284E-01,
0.2656E-01,
0.9459E-02,
0.2929E-02,
0.1027E-02,
0.6551E-03,
0.6889E-03,
0.8372E-03,
0.1011E-02,
0.1143E-02,
0.1168E-02,
0.1045E-02,
0.7632E-03,
0.3447E-03,
-.1690E-03,
-.7258E-03,
-.1264E-02,

-.1709E-02,
-.1969E-02,
-.1954E-02,
-.1600E-02,
-.8990E-03,
0.8292E-04,
0.1214E-02,
0.2332E-02,
0.3292E-02,
0.3987E-02,
0.4353E-02,
0.4354E-02,
0.3976E-02,
0.3229E-02,
0.2165E-02,
0.8916E-03
- 433?E-03,
- 1627E-02
- 2521E-02
- 3012E-02,
- 3082E-02
- 2795E-02,
- 2274E-02,
- 1658E-02,
- 1068E-02,
- 5834E-03,
- 2381E-03,
- 2659E-04,
0.7935E-04,
0.1157E-03,
0.1150E-03,
0.1009E-03,
0.8693E-04,
0.7799E-04,
0.7363E-04,
0.7096E-04

E1:
0.2000E+06,
0.4000E+06,
0.6000E+06,
0.8000E+06,
0.1000E+07,
0.1200E+07,
0.1400E+07,
0.1600E+07,
0.1800E+07,
0.2000E+07,
0.2200E+07,
0.2400E+07,
0.2600E+07,
0.2800E+07,

0.3000E+07,
0.3200E+07,
0.3400E+07,
0.3600E+07,
0.3800E+07,
0.4000E+07,
0.4200E+07,
0.4400E+07,
0.4600E+07,
0.4800E+07,
0.5000E+07,
0.5200E+07,
0.5400E+07,
0.5600E+07,
0.5800E+07,
0.6000E+07,
0.6200E+07,
0.6400E+07,
0.6600E+07,
0.6800E+07,
0.7000E+07,
0.7200E+07,
0.7400E+07,
0.7600E+07,
0.7800E+07,
0.8000E+07,
0.8200E+07,
0.8400E+07,
0.8600E+07,
0.8800E+07,
0.9000E+07,
0.9200E+07,
0.9400E+07,
0.9600E+07,
0.9800E+07,
0.1000E+08,
0.1020E+08,
0.1040E+08,
0.1060E+08,
0.1080E+08,
0.1100E+08,
0.1120E+08,
0.1140E+08,
0.1160E+08,
0.1180E+08,
0.1200E+08,
0.1220E+08,
0.1240E+08,
0.1260E+08,
0.1280E+08,
0.1300E+08,
0.1320E+08,

0.1340E+08,
0.1360E+08,
0.1380E+08,
0.1400E+08,
0.1420E+08,
0.1440E+08,
0.1460E+08,
0.1480E+08,
0.1500E+08,
0.1520E+08,
0.1540E+08,
0.1560E+08,
0.1580E+08,
0.1600E+08,
0.1620E+08,
0.1640E+08,
0.1660E+08,
0.1680E+08,
0.1700E+08,
0.1720E+08,
0.1740E+08,
0.1760E+08,
0.1780E+08,
0.1800E+08,
0.1820E+08,
0.1840E+08,
0.1860E+08,
0.1880E+08,
0.1900E+08,
0.1920E+08,
0.1940E+08,
0.1960E+08,
0.1980E+08,
0.2000E+08,
0.2020E+08,
0.2040E+08,
0.2060E+08,
0.2080E+08,
0.2100E+08,
0.2120E+08,
0.2140E+08,
0.2160E+08,
0.2180E+08

EPSLON1:
0.1723E+37,
0.5460E+33,
0.2256E+04,
0.1316E+02,
0.9130E+01,
0.5984E+01,

0.2434E+01,
0.2027E+01,
0.1170E+01,
0.1005E+01,
0.8976E+00,
0.8473E+00,
0.8373E+00,
0.7859E+00,
0.7169E+00,
0.6510E+00,
0.5861E+00,
0.6361E+00,
0.7125E+00,
0.8774E+00,
0.9633E+00,
0.1022E+01,
0.9139E+00,
0.8501E+00,
0.7687E+00,
0.6996E+00,
0.6954E+00,
0.6924E+00,
0.7092E+00,
0.8047E+00,
0.8376E+00,
0.8022E+00,
0.8425E+00,
0.6792E+00,
0.6750E+00,
0.6127E+00,
0.6705E+00,
0.6312E+00,
0.5646E+00,
0.5708E+00,
0.5434E+00,
0.4584E+00,
0.4684E+00,
0.3916E+00,
0.4032E+00,
0.3553E+00,
0.3411E+00,
0.3675E+00,
0.2680E+00,
0.2729E+00,
0.2526E+00,
0.1849E+00,
0.1565E+00,
0.1181E+00,
0.8805E-01,
0.7660E-01,
0.6090E-01,
0.4116E-01,

0.3211E-01,
0.3011E-01,
0.2937E-01,
0.2809E-01,
0.2646E-01,
0.2670E-01,
0.2462E-01,
0.2688E-01,
0.2539E-01,
0.2487E-01,
0.2549E-01,
0.2415E-01,
0.2424E-01,
0.2403E-01,
0.2401E-01,
0.2520E-01,
0.2631E-01,
0.2604E-01,
0.2636E-01,
0.2608E-01,
0.2615E-01,
0.2772E-01,
0.2746E-01,
0.3083E-01,
0.3055E-01,
0.3221E-01,
0.3266E-01,
0.3358E-01,
0.3465E-01,
0.3281E-01,
0.3397E-01,
0.3205E-01,
0.3206E-01,
0.3226E-01,
0.3256E-01,
0.3507E-01,
0.3425E-01,
0.3661E-01,
0.3739E-01,
0.3613E-01,
0.3721E-01,
0.3580E-01,
0.3531E-01,
0.3528E-01,
0.3166E-01,
0.3069E-01,
0.2870E-01,
0.2530E-01,
0.2263E-01,
0.2208E-01,
0.2278E-01

UTB0:
0.7906E+07,
0.1957E+07,
0.1538E+04,
0.8627E+02,
0.6267E+02,
0.6879E+02,
0.4311E+02,
0.2600E+02,
0.1955E+02,
0.1677E+02,
0.1476E+02,
0.1342E+02,
0.1354E+02,
0.1546E+02,
0.1737E+02,
0.1708E+02,
0.1511E+02,
0.1314E+02,
0.1214E+02,
0.1209E+02,
0.1229E+02.
0.1228E+02.
0.1221E+02,
0.1214E+02,
0.1174E+02,
0.1076E+02,
0.9355E+01,
0.7929E+01,
0.6874E+01,
0.6358E+01,
0.6251E+01,
0.6211E+01,
0.5985E+01,
0.5609E+01,
0.5282E+01,
0.5118E+01,
0.5069E+01,
0.5021E+01,
0.4874E+01,
0.4571E+01,
0.4110E+01,
0.3550E+01,
0.2984E+01,
0.2493E+01,
0.2127E+01,
0.1909E+01,
0.1831E+01,
0.1843E+01,
0.1864E+01,
0.1812E+01,
0.1644E+01,

0.1369E+01,
0.1043E+01,
0.7269E+00,
0.4669E+00,
0.2788E+00,
0.1564E+00,
0.8297E-01,
0.4179E-01,
0.2000E-01,
0.9155E-02,
0.4139E-02,
0.2027E-02,
0.1239E-02,
0.9799E-03,
0.8789E-03,
0.7777E-03,
0.6151E-03,
0.3774E-03,
0.7735E-04,
-.2546E-03,
-.5763E-03,
-.8394E-03,
-.9967E-03,
-.1009E-02,
-.8514E-03,
-.5214E-03,
-.3944E-04,
0.5507E-03,
0.1187E-02,
0.1798E-02,
0.2313E-02,
0.2671E-02,
0.2829E-02,
0.2768E-02,
0.2492E-02,
0.2030E-02,
0.1430E-02,
0.7554E-03,
0.7199E-04,
-.5551E-03,
-.1072E-02,
-.1444E-02,
-.1655E-02,
-.1710E-02,
-.1633E-02,
-.1458E-02,
-.1223E-02,
-.9650E-03,
-.7146E-03,
-.4925E-03,
-.3105E-03,
-.1715E-03,

-.7283E-04,
-.7920E-05,
0.3101E-04,
0.5148E-04,
0.5982E-04,
0.6079E-04

E0:
0.2000E+06,
0.4000E+06,
0.6000E+06,
0.8000E+06,
0.1000E+07,
0.1200E+07,
0.1400E+07,
0.1600E+07,
0.1800E+07,
0.2000E+07,
0.2200E+07,
0.2400E+07,
0.2600E+07,
0.2800E+07,
0.3000E+07,
0.3200E+07,
0.3400E+07,
0.3600E+07,
0.3800E+07,
0.4000E+07,
0.4200E+07,
0.4400E+07,
0.4600E+07,
0.4800E+07,
0.5000E+07,
0.5200E+07,
0.5400E+07,
0.5600E+07,
0.5800E+07,
0.6000E+07,
0.6200E+07,
0.6400E+07,
0.6600E+07,
0.6800E+07,
0.7000E+07,
0.7200E+07,
0.7400E+07,
0.7600E+07,
0.7800E+07,
0.8000E+07,
0.8200E+07,
0.8400E+07,
0.8600E+07,
0.8800E+07,

0.9000E+07,
0.9200E+07,
0.9400E+07,
0.9600E+07,
0.9800E+07,
0.1000E+08,
0.1020E+08,
0.1040E+08,
0.1060E+08,
0.1080E+08,
0.1100E+08,
0.1120E+08,
0.1140E+08,
0.1160E+08,
0.1180E+08,
0.1200E+08,
0.1220E+08,
0.1240E+08,
0.1260E+08,
0.1280E+08.
0.1300E+08,
0.1320E+08,
0.1340E+08,
0.1360E+08,
0.1380E+08,
0.1400E+08.
0.1420E+08,
0.1440E+08,
0.1460E+08,
0.1480E+08,
0.1500E+08,
0.1520E+08,
0.1540E+08,
0.1560E+08,
0.1580E+08,
0.1600E+08,
0.1620E+08,
0.1640E+08,
0.1660E+08,
0.1680E+08,
0.1700E+08,
0.1720E+08,
0.1740E+08,
0.1760E+08,
0.1780E+08,
0.1800E+08,
0.1820E+08,
0.1840E+08,
0.1860E+08,
0.1880E+08,
0.1900E+08,
0.1920E+08,

0.1940E+08,
0.1960E+08,
0.1980E+08,
0.2000E+08,
0.2020E+08,
0.2040E+08,
0.2060E+08,
0.2080E+08,
0.2100E+08,
0.2120E+08,
0.2140E+08,
0.2160E+08,
0.2180E+08

EPSLON0:
0.1279E+37,
0.1859E+35,
0.6230E+05,
0.7196E+02,
0.2186E+01,
0.1499E+01,
0.2633E+01,
0.1075E+01,
0.6427E+00,
0.4206E+00,
0.4103E+00,
0.4061E+00,
0.4365E+00,
0.4416E+00,
0.4233E+00,
0.4313E+00,
0.4007E+00,
0.3653E+00,
0.3389E+00,
0.3475E+00,
0.3682E+00,
0.3540E+00,
0.3415E+00,
0.3336E+00,
0.3247E+00,
0.3031E+00,
0.2890E+00,
0.2801E+00,
0.2858E+00,
0.2842E+00,
0.2628E+00,
0.2596E+00,
0.2562E+00,
0.2527E+00,
0.2242E+00,
0.2130E+00,

0.2170E+00,
0.2108E+00,
0.1980E+00,
0.1918E+00,
0.1801E+00,
0.1713E+00,
0.1541E+00,
0.1[illegible]E+00,
0.1380E+00,
0.1288E+00,
0.1210E+00,
0.1116E+00,
0.1049E+00,
0.1003E+00,
0.9234E-01,
0.8336E-01,
0.7439E-01,
0.6111E-01,
0.4711E-01,
0.4030E-01,
0.3319E-01,
0.2643E-01,
0.2226E-01,
0.1978E-01,
0.1710E-01,
0.1659E-01,
0.1713E-01,
0.1624E-01,
0.1624E-01,
0.1534E-01,
0.1603E-01,
0.1589E-01,
0.1511E-01,
0.1536E-01,
0.1500E-01,
0.1493E-01,
0.1530E-01,
0.1543E-01,
0.1577E-01,
0.1558E-01,
0.1525E-01,
0.1548E-01,
0.1555E-01,
0.1621E-01,
0.1697E-01,
0.1774E-01,
0.1905E-01,
0.1974E-01,
0.2004E-01,
0.2018E-01,
0.1978E-01,
0.1968E-01,

0.1859E-01,
0.1835E-01,
0.1783E-01,
0.1796E-01,
0.1848E-01,
0.1926E-01,
0.2046E-01,
0.2057E-01,
0.2128E-01,
0.2159E-01,
0.2103E-01,
0.2032E-01,
0.1973E-01,
0.1814E-01,
0.1682E-01,
0.1583E-01,
0.1455E-01,
0.1358E-01,
0.1213E-01,
0.1250E-01,
0.1260E-01

Bibliography

1. Anderson, M. E. and R. A. Neff. "Neutron Energy Spectra of Different Size ^{239}PuBe(α,n) Sources," Nuclear Instruments and Methods, 99: 231-235 (1972).

2. Benedict, M., T. H. Figford, and H. Levi. Nuclear Chemical Engineering (Second Edition). New York: McGraw-Hill, 1981.

3. Bicron Corporation. "BC-501A Liquid Scintillator Data Sheet," Newbury, Ohio, 1990.

4. Brooks, F. D. "Development of Organic Scintillators," Nuclear Instruments and Methods, 162: 477-505 (1979).

5. Brunfelter, B., J. Kockum and H. O. Zetterstrom. "Unscrambling of Proton Recoil Spectra," Nuclear Instruments and Methods, 40: 84-88 (1966).

6. Burrus, W. R. and V. V. Verbinski. "Fast-neutron Spectroscopy with Thick Organic Scintillators," Nuclear Instruments and Methods, 67: 181-196 (1969).

7. Cherubini, R. *et al.* "Gamma Calibration of Organic Scintillators," Nuclear Instruments and Methods in Physics Research, A281: 349-352 (1989).

8. Cross, William G. and Harry Ing. "Neutron Spectroscopy" in The Dosimetry of Ionizing Radiation, Volume 2, edited by Kenneth R. Kase. Orlando: Academic Press, 1987.

9. EG&G ORTEC. Model 458 Pulse Shape Analyzer Operating and Service Manual. Oak Ridge, Tennessee, 1970.

10. EG&G ORTEC. Model 460 Delay Line Amplifier Operating and Service Manual. Oak Ridge, Tennessee, 1971.

11. Hamamatsu. Photomultiplier Tubes. Bridgewater, New Jersey, 1988.

12. Hartley, Richard S., Proffessor of Nuclear Engineering, Air Force Institute of Technology. Computer disk containing raw data for DT neutrons .

13. Ingersoll, D. T. and B. W. Wehring. "Gamma-ray Pulse-height Response of an NE-213 Scintillation Detector," Nuclear Instruments and Methods, 147: 551-561 (1977).

14. Ingersoll, Daniel Thomas. Integral Testing of Neutron Cross Sections Using Simultaneous Neutron and Gamma-ray Measurements. PhD Thesis. University of Illinois at Urbana-Champaign, Champaign, Illinois, 1977.

15. Johnson, R. H. A User's Manual for COOLC and FORIST. West Lafayette, Indiana: Purdue University, 1975.

16. Johnson, R. H. *et al.* "NE-213 Neutron Spectrometry System for Measurements from 1.0 to 20 MeV," Nuclear Instruments and Methods, 145: 337-346 (1977).

17. Knoll, Glenn F. Radiation Detection and Measurement (Second Edition). New York: John Wiley & Sons, 1989.

18. Knox, H. H. and T. G. Miller. "A Technique for Determining Bias Settings for Organic Scintillators," Nuclear Instruments and Methods, 101: 519-525 (1972).

19. Krane, Kenneth S. Introductory Nuclear Physics. New York: John Wiley & Sons, 1988.

20. Kumar, Arun and P. S. Nagarajan. "Neutron Spectra of ^{239}Pu-Be Neutron Sources," Nuclear Instruments and Methods, 140: 175-179 (1977).

21. Lederer, C. Michael and Virginia S. Shirley. Table of Isotopes (Seventh Edition). New York: John Wiley & Sons, 1978.

22. Monsanto Research Corporation. "Shipping Data, Plutonium Neutron Source (#M-1170)," Miamisburg, Ohio: Mound Laboratory, 1962.

23. Murphie, William Edward. Measured Neutron and Gamma-ray Spectra in a Tissue-equivalent Liquid Irradiated with 14-MeV Neutrons. MS Thesis. The University of Texas at Austin, Austin, Texas, 1980.

24. Naqvi, A. A. *et al.* "Energy Resolution Tests of 125-mm Diameter Cylindrical NE-213 Detector Using Monoenergetic Gamma Rays," Nuclear Instruments and Methods in Physics Research, A306: 267-271 (1991).

25. Nuclear Data Inc. Hardware Instruction Manual ND570/ND571/ND575 ADC 07-0037. Schaumburg, Illinois, 1987.

26. Radiation Shielding Information Center. "FORIST: FERDOR with Optimized Resolution Using an Iterative Smoothing Technique. Neutron Spectrum Unfolding Code," RSIC Computer Code Collection, PSR-92, Oak Ridge National Laboratory, Oak Ridge, Tennessee, 1984.

27. RCA. RCA Photomultipliers. Lancaster, Pennsylvania, 1984.

28. Universal Technical Systems, Inc. TK Solver Plus. Rockford, Illinois, 1989.

29. Verbinski, V. V. *et al.* "Calibration of an Organic Scintillator for Neutron Spectrometry," Nuclear Instruments and Methods, 65: 8-25 (1968)

30. Vijaya, A. D. and Arun Kumar. "The Neutron Spectrum of Am-Be Neutron Sources," Nuclear Instruments and Methods, 111: 435-440 (1973).

Vita

Second Lieutenant Robert S. Pope was born on 2 March 1969 in Crawfordsville, Indiana. He graduated from Clare High School in Clare, Michigan in 1987 and attended Michigan State University, graduating with honors with a Bachelor of Science in Physics in June 1991. While at Michigan State University, he participated in the Air Force ROTC program, graduating from the program as a Distinguished Graduate and receiving his commission. In August 1991, as his first assignment in the Air Force, Lt. Pope entered the nuclear engineering program at the Air Force Institute of Technology.

Permanent Address: 210 Wilcox Pkwy.
Clare, MI 48617

REPORT DOCUMENTATION PAGE

Form Approved
OMB No. 0704-0188

1. AGENCY USE ONLY (Leave blank)	2. REPORT DATE	3. REPORT TYPE AND DATES COVERED
	March 1993	Master's Thesis

4. TITLE AND SUBTITLE

Construction and Testing of a Neutron and Gamma Spectrometry System Using Pulse Shape Discrimination with an Organic Scintillator

5. FUNDING NUMBERS

6. AUTHOR(S)

Robert S. Pope, 2Lt, USAF

7. PERFORMING ORGANIZATION NAME(S) AND ADDRESS(ES)

Air Force Institute of Technology, WPAFB OH 45433-6853

8. PERFORMING ORGANIZATION REPORT NUMBER

AFIT/GNE/ENP/93M-06

9. SPONSORING/MONITORING AGENCY NAME(S) AND ADDRESS(ES)

Capt Praminko
AL/OEBD
2402 E Drive
Brooks AFB, TX 78235-5114

10. SPONSORING/MONITORING AGENCY REPORT NUMBER

11. SUPPLEMENTARY NOTES

12a. DISTRIBUTION/AVAILABILITY STATEMENT

Approved for public release; distribution unlimited

12b. DISTRIBUTION CODE

13. ABSTRACT *(Maximum 200 words)*

The goal of this thesis was to construct and test a neutron detector to measure the energy spectrum of 1 to 14-MeV neutrons in the presence of gammas. A spectrometer based on the process of pulse shape discrimination (PSD) was constructed, in which the scintillator NE-213 was used. The primary neutron/gamma sources used were 78-mCi and 4.7-Ci ^{239}PuBe sources, while 4.7-μCi and 97.6-μCi ^{22}Na gamma sources were used for energy calibration and additional testing of the detector. Proton recoil spectra and Compton electron spectra were unfolded with the neutron and gamma unfolding code FORIST to generate the incident neutron and gamma spectra, respectively. FORIST, which was written for a CDC computer, was modified to run on a VAX 6420. The experimental spectra were compared to those in the literature. The locations of the peaks in the ^{239}PuBe spectrum agreed with the literature to within 8.3%, the ^{239}PuBe gamma spectrum agreed to within 0.7%, while the ^{22}Na gamma spectrum agreed exactly. Uncertainties in the detection system and unfolding procedure are on the order of 5-10%.This thesis is intended to be a summary of the relevant literature and a user's guide to the PSD spectrometer.

14. SUBJECT TERMS	15. NUMBER OF PAGES
Neutron Unfolding Code, Gamma Spectrometry, Neutron Spectrometry Pulse Shape Discrimination	206
	16. PRICE CODE

17. SECURITY CLASSIFICATION OF REPORT	18. SECURITY CLASSIFICATION OF THIS PAGE	19. SECURITY CLASSIFICATION OF ABSTRACT	20. LIMITATION OF ABSTRACT
Unclassified	Unclassified	Unclassified	UL